2023

Soil and Wastewater Properties that Influence the Uptake of Anti(retro)viral Pharmaceuticals in Plants

Akenga, Preston Chebai

UNIVERSITY OF
PLYMOUTH

SOIL AND WASTEWATER PROPERTIES THAT INFLUENCE THE UPTAKE OF ANTI(RETRO)VIRAL PHARMACEUTICALS IN PLANTS

by

PRESTON CHEBAI AKENGA

A thesis submitted to the University of Plymouth

in partial fulfilment for the degree of

DOCTOR OF PHILOSOPHY

School of Geography, Earth and Environmental Sciences

September 2022

Acknowledgement

Author's Declaration

At no time during the registration for the degree of Doctor of Philosophy has the author been registered for any other University award without the prior agreement of the Doctoral College Quality Sub-Committee.

Work submitted for this research degree at the University of Plymouth has not formed part of any other degree either at the University of Plymouth or at another establishment.

Publications

Akenga, P., Gachanja, A., Fitzsimons, M.F., Tappin, A., Comber, S., 2021. *Uptake, Accumulation and Impact of Antiretroviral and Antiviral Pharmaceutical Compounds in Lettuce*. Sci. Total Environ. 766, 144499. https://doi.org/10.1016/j.scitotenv.2020.144499

Oral presentations

Akenga, P., Fitzsimons, M.F & Comber, S. *Evidence of In-plant metabolism of Anti(retro)viral pharmaceuticals*, SETAC EUROPE virtual conference, 3rd -6th May 2021.

Akenga, P., Fitzsimons, M.F & Comber, S. *Impact of wastewater matrix on uptake of Anti(retro)viral pharmaceuticals in plants,* Biogeochemistry Research Centre Annual Christmas Conference, Coxside Marine Station, Plymouth - 15th December 2021

Akenga, P., Fitzsimons, M.F & Comber, S. *Uptake of Antiviral Pharmaceutical Compounds in Lettuce,* EnvChem2020, Joint RSC/SETAC UK Branch, Chemistry of the Whole Environment Research (virtual)*,* 10th July 2020.

Akenga, P., Fitzsimons, M.F & Comber, S, *Modification and optimization of QuEChERS for the extraction of selected antiviral pharmaceutical compounds in plant matrices*, 10th Annual Conference of the Biogeochemistry Research, Coxside Marine Station, University of Plymouth 11th December 2019.

Akenga, P, *Assessment of Antiviral Pharmaceutical Uptake in Plants Irrigated with Wastewaters*, Postgraduate Research Showcase 17th June 2019, University of Plymouth

Word count of the main body of the thesis: 42390

Signed

Date   20th September 2022

Abstract

Soil and wastewater properties that influence the uptake of anti(retro)viral pharmaceuticals in plants- Preston Chebai Akenga

This study evaluated the fate of anti(retro)viral (ARVDs) pharmaceutical compounds in the wastewater-soil-plant-human continuum. Wastewater frequently contains pharmaceutical micropollutants. A cause to worry is the potential uptake and bioaccumulation of these biologically active contaminants via the plant's roots into the edible tissues, posing a health threat to non-target consumers. Presently, the influence of the wastewater and soil parameters (pH, soil organic matter, dissolved organic carbon) on the uptake patterns of the (ARVDs) pharmaceutical compounds is unclear. Hydroponic and pot-soil experiments were utilized to assess the ARVD accumulation in lettuce (*Lactuca sativa*). Spiked freshwater (stored rainwater) and synthetic wastewater (adopted as a surrogate for actual wastewater) were used as irrigation agents. The OECD 106 adsorption/desorption protocols were used to determine the binding potential of the ARVD molecules to the soil sorbent. ARVD solutes and associated metabolites were separated, detected, and quantified using a liquid chromatograph- a high-resolution mass spectrometer. ARVD accumulation in the lettuce positively correlated with molecule lipophilicity, whereby solutes with log $K_{ow} > 1$ were detected in soils and the exposed lettuce. In contrast, solutes with log $K_{ow} < 1$ neither accumulated in the soils nor the lettuce. The mean accumulation of ARVDs in lettuce grown in low organic, sandy soils was eight times higher (323 ng g^{-1}) than in lettuce grown in organic-rich soils (39 ng g^{-1}). While wastewater independently reduced accumulation in lettuce by 37-97 % in aqueous-based experiments, in synthetic wastewater-irrigated soils, accumulation was six times higher (310 ng g^{-1}) than in freshwater-irrigated soils (52 ng g^{-1}). Nevirapine was identified as a priority contaminant since it accumulated in the edible tissues of lettuce. Nonetheless, its accumulation was 2000 times below the daily dietary intake limits. Irrigation using ARVD-contaminated wastewater enhances the accumulation of organic micropollutants in plants

Table of Contents

List of Figures

List of Tables

List of appendices

List of frequently used abbreviations

ACV	Acyclovir
AmFo	Ammonium formate solvent
ARVD	Anti(retro)viral pharmaceuticals
COD	Chemical oxygen demand
DDI	Daily dietary intake
DMSO	Dimethylsulfoxide
DOC	Dissolved organic carbon
EFV	Efavirenz
EIC	Extracted ion chromatogram
ESI+	Positive electrospray ionization
ESI-	**Negative electrospray ionization**
FA-	Formic acid
FW	Freshwater
HLB	Hydrophilic/lipophilic balanced cartridges
HPW	High purity water
HRMS	High-resolution mass spectrometry
LMIC	Low to middle-income countries
LVD	Lamivudine
MC	Moisture content
MDD	Maximum daily dose
MeCN	Acetonitrile
MeOH	Methanol
MP	Mobile phases
MS/MS	Tandem mass spectrometry
MWHC	Maximum water holding capacity
NVP	Nevirapine
OSV	Oseltamivir

PCP's	Personal care products
PLWHIV	People living with HIV and AIDs
Pos-neg	Positive and negative switching
qqqMS	Triple quadrupole mass spectrometer
RPLC-ESI/MS	Reversed-phase liquid chromatography- electrospray ionization-mass spectrometry
RWW	Reclaimed wastewater
SFW	Spiked fresh water
SP	Stationary phase
SPM	Suspended particulate material
STWW	Spiked treated wastewater
SW	Synthetic wastewater
TN	Total Nitrogen
TWW	Treated wastewater
UPLC-QqQ	Ultra high-pressure liquid chromatography, triple quadrupole
US-FDA	United States Food Drug Administration
NSAIDs	Nonsteroidal anti-inflammatory drugs

Chapter 1 Introduction
The fate of pharmaceuticals in agroecosystems

Overview

This chapter first collates identified research gaps and recommendations that merit further research in wastewater reuse practices in agroecosystems and then describes the rationale for selecting topical areas of interest. Most notable was that, despite the high frequency and concentration levels of anti(retro)viral drugs (ARVDs) measured in surface and wastewaters (a source of these contaminants to agroecosystems), less is known of their fate. This review further highlights the physical-chemical processes and environmental properties that attenuate pharmaceutical molecules within the soil and wastewater environment, consequently impacting the availability of the molecule to plant roots. It also describes the general uptake mechanisms of organic contaminants in plants.

1.1 Introduction

In agriculture, soil moisture and nutrients are essential for plant growth. For this reason, agriculture is continually searching for innovative methods to supply these two critical components (Cogger et al., 2013). The practice of irrigation using wastewater (treated or untreated) and amending soils with biosolids has been embraced and has contributed to increased crop yields (Ilias et al., 2014; Oron et al., 2014). It has helped conserve dwindling freshwater resources and ensure that food production is not compromised due to severe weather conditions or competition from industrial, municipal, or domestic needs (Jaramillo and Restrepo, 2017; Ofori et al., 2021).

Pharmaceuticals are sometimes referred to as emerging pollutants (EPs) since they have recently become ubiquitous in the environment. These EPs have been prevalent in

agroecosystems since they were introduced into the market but may not have been detected due to limitations in analytical capability (Geissen et al., 2015). They are also not routinely monitored due to the insufficiency of environmental quality standards. Irrigation with pharmaceutical-contaminated wastewater is the main pathway for introducing these micropollutants into agroecosystems in developing countries (Kasprzyk-Hordern et al., 2008; Tasho and Cho, 2016 Ben Mordechay et al., 2018).

Most pharmaceutical molecules are non-volatile and polar, with ionizable functional groups. Thus, plant root uptake represents an important potential pathway (Miller et al., 2015). A concern about these molecules is their potential accumulation in terrestrial or aquatic plants, posing a risk to non-target receptors such as humans and animals at higher trophic levels in the food chain (Rodriguez-Eugenio et al., 2018). Although some pharmaceuticals are not persistent, they are pseudo-persistent, i.e. their continuous discharge into the agroecosystems may negate any degradation losses so that their environmental concentrations continue to rise (Mira et al.2003). One challenge is that accurately elucidating their fate in wastewater-irrigated agroecosystems is not straightforward since the molecules are co-introduced with the wastewater matrix, which further complex the pharmaceutical-soil interaction processes in the soil (Maoz and Chefetz, 2010; Carter et al., 2019).

Proof that ingestion of wastewater-irrigated food crops exposes humans to the exogenous chemicals was confirmed when healthy individuals (previously not under any medical prescription) ingested carbamazepine, an anticonvulsant drug, from wastewater-irrigated fresh produce. The parent molecule and its two associated metabolites were measured in the collected urine at 25 ng L^{-1} (Paltiel et al., 2016). Such data informs the urgency to assess the fate of a wider variety of these organic micropollutants in agroecosystems, particularly their

interaction and accumulation tendencies and their acute or chronic effects on the receptors.

Moreover, acquired data may help design appropriate wastewater reuse policies for

agriculture since most existing water guidelines rarely account for the presence of

pharmaceuticals and the potential risk they may pose to human and ecosystem health via this

source (Carter et al., 2019).

The present study is intertwined with the overarching theme of agriculture, environmental

sustainability, water, food security, and the reuse of natural resources. A concept that falls

under the United Nations Sustainability goals addresses the theme of 'Sustainable Food and

Agriculture (United Nations, 2015). Similarly, the study aligns with Food Agricultural

Organization's (FAO) conceptual framework (FAO, 2012) that addresses food security under

water scarcity conditions in agriculture.

Figure 1.1 shows a schematic diagram of the research questions general outline of this
research.

General outline of the thesis

Chapter 2

i. How do varying mobile phases (acidic and alkaline), and stationary phases (C18 and hexyl-phenyl) impact the chromatographic separation of ARVD compounds?

Chapter 1

i. **Introduction/literature review**
What are the knowledge gaps in the emerging issue of contamination/pollution of agroecosystems with pharmaceuticals micropollutants?

Chapter 3

i. Do leafy vegetables uptake and bioaccumulate ARVD molecules into their tissues?
ii. What is the correlation between bioaccumulation and physical-chemical characteristic of ARVD molecules
iii. Does the bioaccumulated ARVD molecule induce observable toxic effects in plants?

ARVD spiked nutrient solution

Lid
O2
H2O

Hydroponics

Chapter 4

i. Do plants biotransform accumulated ARVD molecules?
ii. Is single-stage mass spectrometry a viable tool to investigate in-plant pharmaceutical biotransformation?

AB
enzymes
A+OH
B+OH

LC-HRMS

Antivirals contaminated wastewater

irrigation

Chapter 7

i. Does irrigation with wastewater influence the bioavailability of the micropollutants in the plants and soil ?
ii. Is the priority pharmaceutical pollutant a health risk to the contaminated plants' exposed receptors (consumers)?

Pot trials (soil)

Chapter 6

i. What are the sorption/desorption tendencies of ARVDs in soils based on the soil's organic matter , pH, sand, and silt content?

Batch sorption experiments

Chapter 5

i. What is the magnitude of binding of ARVD molecules to wastewater constituents, i.e. to DOM and SPM?
ii. How do wastewater constituents impact the uptake of ARVDs in an aquatic-only environment?

Figure 1.1. Schematic diagram of the general outline of this research

1.2 Existing knowledge gaps in wastewater irrigation practices in agroecosystems

Intensive utilization of wastewater in agriculture has generated significant interest in understanding the fate of wastewater-borne chemicals in agroecosystems. Accordingly, several reviews have concurrently collated information outlining the extent of understanding and identifying information gaps that merit further investigations in the pharmaceutical wastewater-soil-receptor topical issue. Table 1.1 highlights information gaps and opportunities for further research extracted from several recent reviews.

Carter et al., (2019) ranked some of the knowledge gaps according to the level of information available for each process ('highly', 'moderately', or 'poorly' knowledgeable). The knowledge gaps were further categorized in a Sources-Pathways-Receptors (S-P-R) component format. In the framework, 'reclaimed wastewater' for an example of a 'source' component that introduced pharmaceuticals to agroecosystems. 'Receptors' were humans, wildlife, livestock, terrestrial plants or aquatic animals. At the same time, receptors were classified as potential secondary pathways of exposure. For example, exposure to humans or animals is via consuming contaminated crops. There was a 'high' level of understanding of only five processes in the 'source' component. The depth of knowledge of the 'pathways' and 'receptor' components was found insufficient hence the components were classified as 'moderately' or 'poorly' understood. Accordingly, to further understand the fate of organic contaminants in agroecosystems, the present study selected topical areas from the 'moderately' knowledgeable areas of interest from

Table 1.1. Knowledge gaps and topical areas recommended for further investigations in pharmaceutical-wastewater-soil-receptor studies

Study keywords	Existing research gaps/Future recommendations		Study
Antibiotics Accumulation Human health risks Antibiotic-resistant genes Uptake Reclaimed wastewater	i.	Carry out field-based studies to measure uptake of contaminants of emerging concern in fully characterized soils, using actual wastewater	(Christou et al., 2017a)
	ii.	Monitor pharmaceutical transformation products in reclaimed wastewater and soils and their potential for uptake.	
	iii.	Obtain public health risks data from field-based studies that utilized reclaimed wastewater (RWW) for irrigation.	
	iv.	Evaluate the effect of chemical mixtures rather than single molecules	
	v.	Monitor phytotoxic and other stress-related phenomena in the plants exposed to the pharmaceutical xenobiotics.	
	vi.	Develop standardized protocols for the analyses of pharmaceutical molecules in essential matrices.	
Contaminants of emerging concern Recycled water Plant uptake Exposure Health risks	i.	Review and prioritize contaminants of emerging concern for future evaluation	(Shi et al., 2022)
	ii.	Evaluate uptake of pharmaceuticals under field conditions	
	iii.	Assess uptake differences among different plant types	
	iv.	Assess potential risks due to pharmaceutical mixtures and metabolites	
	v.	Assessment of the long-term ecotoxicological risks to agroecosystems from contaminants of emerging concern	
Pharmaceuticals Environment Soil Plants Accumulation	i.	Measure data on bioaccumulation of pharmaceuticals in organisms/receptors in the higher trophic chain is scarce	(Gworek et al., 2021)
	ii.	Evaluate the health risks for individuals consuming contaminated plants	

Croplands Antibiotics, Plants, PCPs, Reclaimed wastewater irrigation Soil	i. Evaluate the chronic effects pharmaceuticals at environmentally relevant concentrations on terrestrial organisms, soil fauna and crops ii. Investigate the nature and amount of unidentified PPCPs transformation products iii. Evaluate the influence of individual soil components, i.e. soil organic matter, clay content, and pH, in altering PPCPs toxicity iv. Assess potential ecotoxicological effects of PPCPS on groundwater at environmentally relevant concentrations	Qin et al., 2015)
Veterinary antibiotics, Agricultural soils, Manure fertilization, Fate and ecotoxicity, Antibiotic resistance, Future research strategies	i. Identify pharmaceutical bioactive biotransformation products in agroecosystems ii. Evaluate the long-term environmental effects of veterinary antibiotics in different soil types iii. Determine safe environmental levels of veterinary antibiotics for manure, soil, water and plants that will render no risk for purposes of setting policy-level standards	Kuppusamy et al., 2018)
Endocrine disruptors Emerging contaminants Soil amendment	i. Human risk exposure data is still insufficient ii. Absence of antiviral uptake data iii. Determination of potential health risks from emerging contaminants metabolites iv. Insufficient data on plant uptake of PPCPs from overhead irrigation and leaves	Keerthanan et al., 2021)

Contaminants of emerging concern, Food crops, Biochar, Phyto-uptake Engineered nanomaterials	i. Estimate risk quotient from actual environment data to accurately assess potential risks ii. Assess the robustness of the developed analytical techniques for pharmaceutical measurements iii. Development of biosensors	(Pullagurala et al., 2018)
PPCPs Biotransformation Wastewater irrigation Soil Food chain	i. There is insufficient information on potential transformation products ii. The extent to which soil properties influence the transportation and rate photodegradation of pharmaceutical molecules is unclear	(Zhang et al., 2021)
Antibiotics Persistence Bioaccumulation, Translocation Edible crop human exposure	i. Use of radiolabelled compounds rather than unlabelled compounds in degradation studies ii. Undertake accumulation and translocation mechanisms in plants under field conditions iii. Carry out chronic phytotoxicity testing of antibiotics in plants iv. Carry out further experiments to understand the behaviour of and fate of pharmaceuticals in soil v. Investigate on transformation and metabolites of antibiotics in plants	(Pan and Chu, 2017)

While it would have been more beneficial to look into the least explored areas ('poorly understood'), most were not practically feasible with available resources (e.g. the acute or chronic impact on wildlife from consuming pasture in pharmaceutical-contaminated grazing lands).

1.3 Topical areas selected for further study

Discussion about the topical areas selected for further study is presented in subsections 1.3.1 to 1.3.5. The rationale for choosing the molecule of interest and the appropriate detection and quantification techniques is presented. The plant exposure experimental protocols and their associated significances used to determine the extent of pharmaceutical accumulation and associated uptake mechanisms in soil and aquatic environments are provided. Factors that impact the binding potential of the pharmaceutical to the wastewater and soil matrix are also discussed.

1.3.1 Pharmaceutical molecule of interest

Fate data on most pharmaceuticals is still lacking. Approximately one-third of the 1500 pharmaceutical molecules currently in use have been identified in wastewater effluent (Guo et al., 2016). As listed in the keywords column in, the fate of antibiotics has preferentially been investigated, driven by antimicrobial resistance concerns. However, Keerthanan et al. (2021) call explicitly for investigations of the fate of the ARVD therapeutic class of pharmaceuticals in agroecosystems. Again, notable in Table 1.2 is the limited of ARVD data in soil and plant matrices.

Table 1.2 Summary data on the fate of different therapeutic classes of pharmaceuticals in the various environmental compartments (extracted from Carter et al., 2019).

Therapeutic Class	Reclaimed wastewater	Soil	Surface	Groundwater	Plants
Analgesic	✓	✓	✓	✓	✓
Antibiotic	✓	✓	✓	✓	✓
Antidepressant	✓	✓	✓	✓	✓
Antidiabetic	✓	✓	✓	✓	✓
Antiviral	✓	?	✓	✓	?
Antiepileptic	✓	✓	✓	✓	✓
Antihypertensive	✓	✓	✓	✓	✓
Antipsychotic	✓	✓	✓	✓	✓

Table 1.2 highlights some eight classes of pharmaceuticals of interest. It is essential to mention that frequently consumed pharmaceuticals have the highest potential to be detected in the environment and therefore are of greatest concern.

A list of the top 100 frequently consumed pharmaceuticals was collated by Patel et al., (2019). Pharmaceutical molecules of interest that warrant future investigation include corticosteroids, beta-blockers, lipid-lowering agents, antihistamines, antifungals and opioids. Antimalarials are another class of priority pharmaceuticals, especially in tropical countries such as Kenya (K'oreje et al., 2016).

1.3.1.1 Spatial occurrence of ARVDs

There exist regional monitoring priorities and preferences in pharmaceutical analyses. For example, antibiotics are commonly analyzed in the Asia-pacific region, analgesics in Eastern Europe, and a wide range of pharmaceuticals in Western Europe (Aus der Beek et al., 2016). A global sampling campaign covering 104 countries revealed that heavily pharmaceutical-contaminated water samples had originated from low-to-middle-income countries (LMIC). A

probable indicator of the extent of surface water pollution due to lack of adequate sewage treatment in the LMIC, a region that initially had received little or no pharmaceutical monitoring attention (Wilkinson et al., 2022). Nevertheless, Africa-based current literature is addressing the question of the occurrence of pharmaceuticals, particularly the ARVDs, in the aquatic environment (Wood et al., 2017; Rimayi et al., 2018; Madikizela et al., 2020; Adeola et al., 2021; Adeola and Forbes, 2022; Fekadu et al., 2019; Madikizela et al., 2020, 2017; Mlunguza et al., 2020a; Ngumba et al., 2020; Rimayi et al., 2018; Wood et al., 2017; Adeola et al., 2021; Adeola and Forbes, 2022).

Of the 19.8 million people under antiretroviral therapy (ART) in 2017, more than three-quarters (78 %) resided in Sub-Saharan Africa. While this class of drug significantly improved the quality of life and life expectancy of people living with HIV (PLWHIV), its inability to destroy the HIV-1 virus necessitates lifelong antiretroviral therapy (Nakagawa et al., 2013; Rwagitinywa et al., 2018; Leen and Bulteel, 2019) giving rise to environmental contamination stemming from the continued elimination from the human system. Indeed, ARVD contamination is more of a spatial problem fueled by antiretroviral use.

Figure 1.2 shows higher ARVD concentrations in Africa compared with Europe and Asia. The mean ARVD concentrations in Africa were > 1000 ng L^{-1}, while the nearest concentrations from other regions were five times lower.
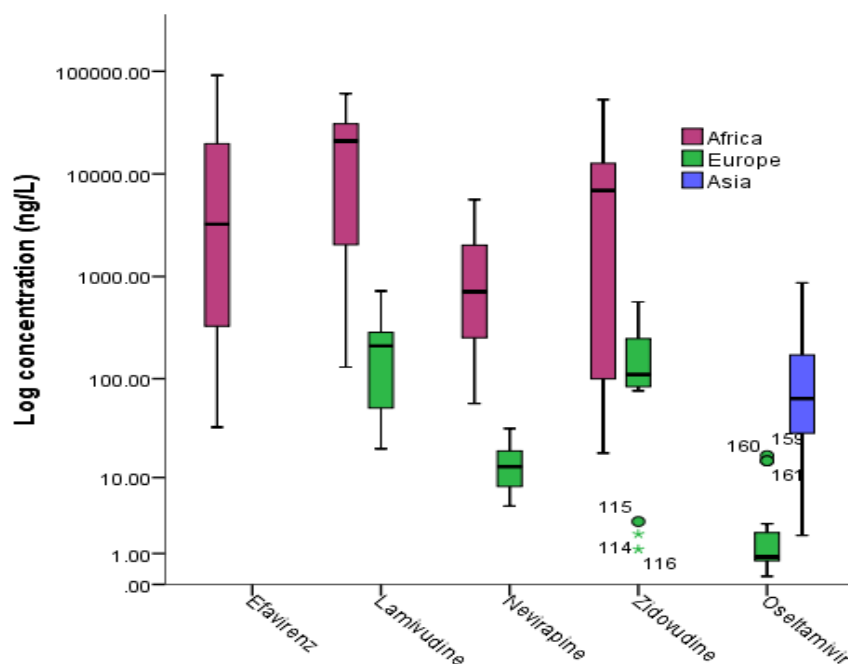
Figure 1.2. Box plots comparing concentrations of five ARVDs in freshwater and wastewater environments in Africa, Europe and Asia.

In Sub-Saharan Africa, due to limited wastewater treatment infrastructure, most of its wastewater goes untreated and is intensively used for irrigation in urban and peri-urban zones in major cities such as Nairobi in Kenya, and Dakar-Senegal (Rodriguez-Eugenio et al., 2018; UNU-INWEH, 2019), further compounding the contamination menace.

However, global happenings such as the occurrence of the COVID-19 pandemic will, in the foreseeable future, potentially will propel antiviral molecule contamination into a universal problem. In Europe, for example, reports highlighted an upsurge in antiviral compounds in the aquatic environment following the COVID-19 pandemic. In Greece, a wastewater-based epidemiological tool used to estimate drug consumption patterns revealed an increase of up to 170 % of antiviral compounds in wastewater between 2019 (pre-pandemic) to 2020 (pandemic year) (Galani et al., 2021), likely from the increase in consumption of antiviral pharmaceutical products In 2022, according to the EU's Global Drought Observatory, Europe

experienced one of its severest droughts in 500 years, creating unprecedented stress on surface water reservoirs (BBC, 2022). In the long run, such persistent dry weather conditions will compel the reuse of the contaminated wastewater for irrigation in agriculture, introducing the molecules into agroecosystems in the continent. Hence the urgency to understand the fate of ARVDs in terrestrial and aquatic environments

1.3.2 Analytical methods

Current methods used to analyse pharmaceutical molecules in environmental matrices are not standardized. (Christou et al., 2017b). Frequently sample preparation protocols, including extraction, separation, and detection for ARVD analyses not specific. These protocols are designed to analyse a wide range of physically and chemically varying pharmaceutical molecules, resulting in high detection limits which compromise estimation of potential risks (Geissen et al., 2015). For this reason, Pullagurala et al. (2018) and Carter et al., (2019) recommended the development of robust analytical methods for analyses of pharmaceutical residues, preferably using novel approaches such as high-resolution mass spectrometry. In response to this call, this research focussed on one aspect of method development, optimization of chromatographic conditions, i.e, selection of appropriate mobile and stationary phases to analyze a mixture of acidic and basic ARVDs in complex environmental matrices. .

Analytical approaches for analysing pharmaceutical compounds usually are dictated by the low concentrations of these contaminants in environmental samples. Due to severe matrix interferences, pharmaceutical contaminants in complex and heterogenous environmental compartments are primarily analysed using hyphenated techniques, i.e., separative accompanied by appropriate detection methods (Duarte and Duarte, 2020). Given that most

pharmaceutical molecules are ionizable, polar and non-volatile, liquid chromatography coupled with mass spectrometry is the main analytical instrument used to measure these molecules (Al-Farsi et al., 2017; Nannou et al., 2020). Liquid chromatography, combined with electrospray ionization (ESI), is preferentially used over gas chromatography. MS systems with ESI provide better sensitivity than atmospheric pressure chemical ionization for most pharmaceuticals (Meng et al., 2021). Other analytical methods, e.g. titrimetric, potentiometric, UV-vis spectrophotometry, and microbiological assays, exist; however, they are prescribed for the assay of bulk drug materials (Siddiqui et al., 2017).

The high-resolution mass spectrometry approach (HRMS) (which was employed in the present study) is the most advanced of the mass spectrometric systems. Its most significant advantage compared to other mass spectrometry systems like conventional tandem mass spectrometry (MS/MS) is that it assigns accurate molecular masses. It provides the highest possible precision of *m/z* measurements, which is especially important when analysing analytes in a complex matrix. HRMS typically delivers a resolution (30,000-70,000 FWHM twenty times greater than conventional quadrupole or linear ion trap mass spectrometers. Additionally, HRMS is ideal even for untargeted analysis in identifying metabolites (Kuchař et al., 2016; Meng et al., 2021). In HRMS, the ions introduced by the electrospray in the mass analyzer are trapped in an ultra-high vacuum. The detector picks the current of the ions, and the signal is Fourier transformed to yield high-resolution mass spectra (Eliuk and Makarov, 2015)

1.3.3 Uptake of ARVD pharmaceuticals in plants

Uptake and accumulation data of a majority of therapeutic classes of pharmaceuticals is available, except for ARVDs, as shown in Table 1.2. Given the high ARVD occurrence levels in

African surface and wastewater streams, as discussed in Section 1.3.1.1, reusing these contaminated waters in soil amendment would contaminate agroecosystems. Hence the need to assess the uptake tendencies of ARVDs in plants. Uptake of xenobiotics predominantly occurs via the roots, and the processes can either be a compound active or passive process. The former relies on the characteristic of the contaminant, whereas the passive process depends on the prevailing weather conditions that affect the transpiration stream (Kumar and Gupta, 2016). For example, elevated temperatures and low humidity favour increased evapotranspiration and, consequently, higher rates of uptake and translocation in the plant (Kumar and Gupta, 2016). The physiological nature of the plant, duration of exposure and the xenobiotic concentration in the exposure medium also significantly influence the magnitude of uptake (Bartrons and Peñuelas, 2017a; Bartrons and Peñuelas, 2017b; Christou et al., 2019a).

In addition to evaluating the of uptake of a particular contaminant, further recommends monitoring phytotoxic and other stress-related phenomena on the receptor plants. It also calls for developing appropriate models to describe uptake since current models are either too simplistic or data-intensive (Bartrons and Peñuelas, 2017a; Hurtado et al., 2017).

The nature of an organic contaminant significantly determines its magnitude of accumulation in plant tissues. For example, the non-steroidal anti-inflammatory drug (NSAIDs), carbamazepine, (log 2.45(K_{ow} 2.45) and lamotrigine (K_{ow} 2.57), all which exhibit mid-hydrophobicity, accumulated in vegetables at concentrations one order higher than the concentrations of similar nonionic molecules of lower hydrophobicity, i.e. sulfapyridine (antibiotic) (K_{ow} 0.35) and caffeine (stimulant) (K_{ow} 0.07) (Goldstein et al., 2014).

While hydroponic-based uptake experiments do not mimic actual field conditions, they contribute toward the rapid elucidation of uptake mechanisms and identify priority pollutants. Therefore, investigations should be conducted in well-characterized soil at environmentally realistic concentrations. For example, in Wu et al. (2015), the bioconcentration factors (BCFs) in hydroponics were as high as 840 L kg^{-1}, while in soil-based experiments, they were as low as background to 40 L kg^{-1} for the same compounds. Indicating that not all contaminant was available for uptake in the soil. The uptake experiments in this research were first performed in hydroponics (Chapter 3), then upscaled to a synthetic wastewater-only environment and then in well-characterized soils irrigated with contaminated synthetic wastewater, and will be discussed in Chapter 5 and Chapter 7, respectively.

1.3.4 In-plant pharmaceutical biotransformation biotransformation

After permeating the root, xenobiotics may be biotransformed by the plant enzymes into a more hydrophilic molecule, reducing its accumulation (Dudley et al., 2019 Sun et al., 2019). Natural biodegradation of xenobiotics in plants depends on the availability of enzymes and has not been studied for a wide range of emerging pollutants, including ARVDs (Geissen et al., 2015). In plants, biotransformation involves the combination of the transformed molecules with natural molecules such as sugars and amino acids, then catalyzed by enzymes (Wu et al., 2021). It is important to note that, as with the parent molecule, metabolites may be a potential risk to the exposed receptors in the food chain (Celiz et al., 2009) hence the need to analyze their occurrence in matrices of concern. As revealed in

Table **1.1**, the most consistent proposal from more than half of the reviews was for investigations into the biotransformation of pharmaceuticals in agroecosystems. Little is known about in-plant biotransformation processes, metabolic reactions and resulting metabolite products because the processes are plant and compound-specific (Shi et al., 2022).Nonetheless, in-plant biotransformation of several pharmaceuticals, including ibuprofen and diclofenac, which formed glycoside conjugates in a carrot cell structure, has been reported (Wu et al., 2016)

Concerning extraction and detection methods, absence of targeted extraction approaches haspartly fuelled the scarcity of metabolite data. For this reason, it is beneficial if extraction methods for the parent molecules simultaneously extract associated metabolites to enhance laboratory throughput. Initially, existing conventional detection methods focussed only on a *priori* select chemicals i.e. targeted chemicals. Currently, advanced mass spectrometric techniques permit full scan screening capability, allowing retrieval of many transformation products (Geissen et al., 2015). The present research describes the identification and semi-quantification of in-plant ARVD transformation products in Chapter 4.

1.3.5 Soil and wastewater properties impacting the availability of pharmaceuticals to plant roots

Lessof pharmaceutical molecule behaviour is known in soil-plant agroecosystems (Madikizela et al., 2020; Shi et al., 2022). At the same time, establishing 'normal contaminant concentrations' in soils is vague since these molecules do not occur naturally in the environment; hence, any concentration is considered a potential risk (Rodriguez-Eugenio et al., 2018). There is hardly any information on the fate of ARVDs in the terrestrial environment (Madikizela et al., 2020). Once deposited in agricultural soils, most organic contaminants are involved in several interrelated processes, including sorption and degradation. Sorption is

predominantly determines the molecules' mobility and their availability for uptake (Paz et al., 2016 ;Shi et al., 2022).

For this reason, Kuppusamy et al. (2018) recommended assessing the long-term environmental effects of veterinary antibiotics in different soil types. Consequently, the environmental impacts of other pharmaceutical molecules, including ARVDs, should be evaluated. Carter et al. (2019) reported on the scarcity of information regarding these molecules' interactions with soil. The present study contributes to this information gap by evaluating the short-term binding tendencies of ARVDs in two soil types in Chapter 6. While in soils, the distribution and transformation of these organic xenobiotics are mainly impacted by the soil's organic matter (SOM), dissolved organic matter (DOM), pH and soil salinity (Wauchope et al., 2002; Müller et al., 2007). The introduction of wastewater (via irrigation), which by itself is a complex matrix consisting of organic suspended material, effluent dissolved organic matter, bacteria and minerals (Jaramillo and Restrepo, 2017; Ofori et al., 2021), modifies the existing processes further enhancing the complexity of their fate in agroecosystems (Peña et al., 2020).

1.3.5.1 Soil organic matter (SOM)

SOM is a critical organic sink for organic contaminants. It controls the extent of sorption by either decreasing or increasing the mass of molecules available for uptake by controlling the amount of contaminant interacting with the root of a plant. For this reason, the only fraction available for uptake is the molecule dissolved in the soil pore water (Miller et al., 2015). This partitioning between the molecule and solid sorbent is described by the soil-water partitioning coefficient, K_d or the organic carbon-normalized sorption coefficient, K_{oc} (Kodešová et al., 2015; Peña et al., 2020).

The presence of strongly sorbing material in soils, e.g. biochars, increases the soil's cumulative binding potential to organic micropollutants, further limiting plant uptake. For example, carbamazepine partitioned to biochar-amended soils three times higher than in the unamended soils, effectively reducing its uptake in ryegrass by between 17-64 % (Williams et al., 2015a). Similarly, soil column experiments revealed reduced mobility with increased SOM (Chefetz et al., 2008).

A key characteristic of SOM is that its charge is pH-dependent, and a vital sink for ionizable organic contaminants. It contains several –COOH groups which deprotonate at the 5-8 pH range (typical for most agricultural soils). For the polar and ionizable molecules, other interactions beyond usual hydrophobic interactions, e.g. hydrogen bonding, cation exchanges, protonation, and surface complexations, are involved (Williams et al., 2015a The higher SOM is present in the soil, the higher the soil's tendency to sorb positively charged ions (Neuman, 2017)

1.3.5.2 Effluent Dissolved organic matter (DOM$_{EF}$)

Due to the complex nature of the effluent wastewater matrix, its reuse impacts the fate of pesticides added to soils for pest control (Peña et al., 2020). Similarly, DOM$_{EF}$ influences the fate of pharmaceuticals in soil and the resultant uptake in receptors, e.g. plant or soil fauna (Michael-Kordatou et al., 2015). The dissolved organic carbon either enhances or reduces the mobility of organic contaminants in soils (Ding et al., 2011; Haham et al., 2012), influencing plant uptake. DOM$_{EF}$ may facilitate the movement of organic molecules within the soils by forming soluble complexes with the contaminants or competing for sorption sites on soil particles. For example, competition for active sites in the bulk of soil particles was noted between carbonyl and phenol moieties of DOM and sulfapyridine (Haham et al., 2012). Also,

sometimes, DOM sorbs to soil particles and together with the SOM, they enhance the binding association with the contaminants (Haham et al., 2012). Interestingly, the sorptive tendencies of the same organic contaminant may behave differently depending on the concentration and composition of the DOM (Peña et al., 2020).

1.3.5.3 Wastewater solution chemistry

The varying pH of wastewater affects the mobility of most pharmaceuticals by inducing the dissociation of their functional groups (Borgman and Chefetz, 2013). Increase in wastewater pH enhanced the transport of sulphonamide antibiotics due to the increase in the negatively charged sulphonamide species (Kurwadkar et al., 2011). On the other hand, increasing the alkalinity of soil columns packed with sandy soil increased the acidic naproxen's mobility due to the carboxylic group's deprotonation (Schaffer et al., 2012).

1.3.5.4 Degradation in soils
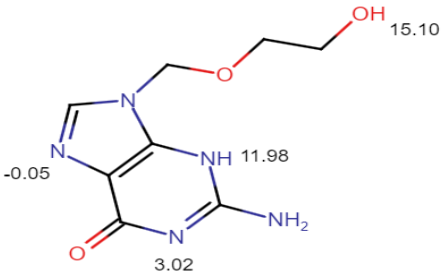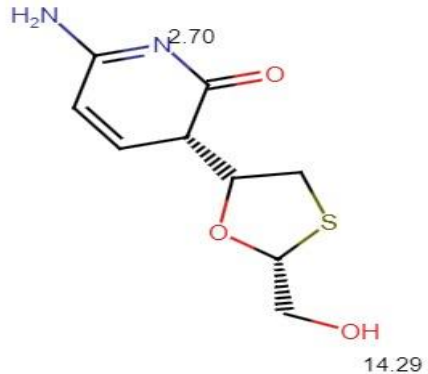
As mentioned earlier, the utilization of wastewater in agroecosystems can modify soil properties influencing the vulnerability of organic contaminants to degradation. Wastewater introduces microorganisms that are exogenous to the soils, thereby contributing to biodegradation or inhibiting the functions of the previously endogenous bacteria community (Peña et al., 2020). In soil systems, degradation of organic contaminants is largely biotic influenced, driven by the soil microbial community and activity. Chemical and photochemical processes mediate abiotic decay. The resulting abiotic and biotic transformation may alter the contaminant concentration available for uptake in the amended soils.

1.4 ARVD selection criteria

Since the most significant ARVD burden exists in Sub-Saharan Africa, as described in section 1.3.1.1, molecules of interest for further study were selected from amongst the commonly prescribed antiretrovirals from Kenya's Ministry of Health ART protocols (The star, 2018). Five ARVD drugs were selected, covering the antiretroviral (nevirapine, lamivudine, efavirenz) and antiviral (acyclovir and oseltamivir) classes of pharmaceuticals. The pharmacology (typical dosage, excretion levels and associated side effects) are shown in Physical-Chemical characteristics

The variation in the physicochemical characteristics of the selected molecules is shown in Table 1.3. The behaviour of the pharmaceuticals depend on their physical-chemical characteristics, such as the octanol-water partitioning (K_{ow}), dissociation constant (pK_a), soil partition coefficient (K_d), and solubility. The selected ARVD compounds were within the small organic molecule region extending from 200 - 400 g mol^{-1}. Acyclovir and lamivudine exhibited exceptionally high water solubility, 9.0 and 13.8 mg mL^{-1}, respectively, which was several magnitudes higher than nevirapine and efavirenz, 0.19 mg mL^{-1} and 9.3×10^{-5} mg mL^{-1} respectively.

Table 1.3. Physical and chemical structures of selected ARVDs (integers within the structures denote the acidic/basic protons)

ARVD	Molecular structure	MW[a] (g mol^{-1})	Solubility [a] (mg mL^{-1})	Log K$_{ow}$[a]	Acid/basic characteristics	pKa
Acyclovir (ACV) C$_8$H$_{11}$N$_5$O$_3$		225.208	9.0	-1	Amphoteric (weakly basic)	Basic 3.02 Acidic 11.9
Lamivudine (LVD) (C$_8$H$_{11}$N$_3$O$_3$S)		229.25	13.8	-1	Weak base	2.7

Oseltamivir **(OSV)** ($C_{16}H_{28}N_2O_4$)		312.40	0.811	1.16	Weak acid
Nevirapine **(NVP)** ($C_{15}H_{14}N_4O$)		266.29	0.191	2.4	Amphoteric/ weakly basic	3.2
Efavirenz **(EFV)** ($C_{14}H_9ClF_3NO_2$)		315.67	0.0[a] 9.3E^{-5} [b]	4.5	Weak acid	12.52

a (ChemAxon, 2021)

1.4.1 Acid and base characteristics of select ARVD compounds

Understanding the acid-base characteristics of the ARVDs facilitates the rationalization of their behaviour in the mobile phase during analyses. The strength of a weakly acid or weakly base molecule depends on its ability to lose or gain protons. Sometimes the designation of pK_a does not categorically differentiate proton loss from acid or a conjugate acid of a base (whereby the conjugate acid is protonated salt forms of the corresponding bases) (Gallicano and Kashuba, 2000). Herein, pK_a was used to describe the acid-base nature of the ARVDs, in relation present functional groups in the molecules.

Weakly acidic -molecules are compounds with functional groups whose protons can easily be deprotonated. Lamivudine is weakly basic with a pK_a value of 2.7. Nevirapine has a pK_a value of 3.2. This value may suggest a moderately strongly acidic molecule, but nevirapine has only a single acidic proton and three basic nitrogen atoms. Therefore, the acidic pK_a reflects the deprotonation of one of these centres, which is consistent with NVP's high solubility at pH > 3 (ChemAxon, 2021) Acyclovir is amphoteric. It has two basic nitrogen atoms, one singly acidic proton and one acidic hydroxyl oxygen atom. It has two pK_a values, a basic 3.02 and an acidic pKa value is 11.9. Acyclovir is amphoteric with weakly acid and weakly basic groups (Susantakumar et al., 2011; Shamshina et al., 2017). Efavirenz is weakly acidic molecule. It has the strongest basic pK_a of -1.49, which is highly unlikely in the actual environment. Therefore, the strongest acidic pK_a of 12.52, which is probable, shows the alkaline strength required to abstract the hydrogen from the single basic nitrogen. Oseltamivir has two acidicprotons. The pK_a values of 9.26 and 14.03 reflect the acidic strength required for deprotonation.

1.5 Research Aims and objectives

1.5.1 Research aim

The overall aim of the present study was to investigate the the fate of anti(retro)viral pharmaceuticals in the soil, wastewater and plant matrices irrigated agroecosystems.

1.5.1.1 Specific research objectives

The specific research objectives and the chapters wherein they were discussed are listed below:

i.   To review knowledge on pharmaceutical contamination of agroecosystems to identify existing research gaps in RWW irrigation practices that merit further research (Chapter 1).

ii. To develop and optimize a selective chromatographic analytical method for separating differing ARVDs characteristically by evaluating the influence of eluent and stationary phases (Chapter 2).

iii. To evaluate the magnitude and mechanism of uptake of selected ARVDs in lettuce using hydroponics (Chapter 3)

iv. To investigate in-plant biotransformation of accumulated ARVD molecules in lettuce plants (Chapter 4)

v.   To assess the impact of wastewater matrix on the uptake of ARVDs in plants in a wastewater-only environment (Chapter 5).

vi. To assess the sorption/desorption characteristic of ARVDs in soils using freshwater and synthetic wastewater (Chapter 6).

vii. To measure the magnitude of uptake in lettuce following irrigation with ARVD-contaminated synthetic wastewater in a controlled soil-plant system (Chapter 7).

Chapter 2 : Materials and methods

Selection of chromatographic conditions for the analyses of antiviral compounds using LC-HRMS

Overview

A stepwise procedure for identifying optimum mobile and stationary phase conditions for separating the select anti(retro)viral compounds (ARVDs) is described herein. Summarily, the selectivity of seven eluents of varying pH and two characteristically differing stationary phases, C18 and phenyl-hexyl, were evaluated, particularly concerning signal response and resolution. A higher signal response was obtained from alkaline eluents (pH > 8) eluents than from low pH (pH < 7) eluents across all molecules. The signal response from the two stationary phases was not noticeably different; however, a better resolution was obtained from the phenyl-hexyl column.

2.1 Introduction

The analyst must accurately separate and measure an ever-increasing number of organic and ionizable compounds that are physically and chemically unique and accumulate in complex matrices. Reversed-phase liquid chromatography-electrospray ionization-mass spectrometry (RPLC-ESI-MS) is the technique of choice for such analyses. RPLC-ESI-MS is capable of separating, detecting and analyzing small molecules *(m/z < 400)* such as pharmaceuticals and metabolites due to its specificity, sensitivity and the provision of crucial structural information (Henriksen et al., 2005). During method optimization, the large diversity in the choice of experimental conditions, including stationary phases (SP), mobile phases (MP), organic modifiers, analyte concentration, mobile phase additive, flowrate and solution pH (Kamel et al., 1999), usually present a method development selection challenge to the analyst. ARVDs, for example, contain different functional groups with divergent pKa values, which induces

varied signal responses and analyte resolution challenges (Prasse et al., 2010). Such differences may demand custom-made protocols for individual molecule analyses, an approach which reduces sample throughput (Henriksen et al., 2005).

Optimization influences selectivity, sensitivity, and resolution and is achieved by adjusting the pH of the organic or aqueous eluents by incorporating additives (pH modifiers and buffers). Eluent composition influences the formation of ions in solution, which impacts the detection and sensitivity of mass -spectrometers (Heinisch and Rocca, 2004; Li et al., 2010; Rainville et al., 2012). Correcting for low sensitivity in the mass spectrometer either demands adjustment of the structure of the solute or modification of the eluent. Of the two alternatives, eluent adjustment is more feasible than molecule derivatization, underscoring additives' significance during analyses (Gao et al., 2005).

Organic modifiers in reverse-phase chromatography negate the de-wetting effect that arises from strongly aqueous eluents. De-wetting induces poor retention, reproducibility, and low selectivity (McCalley, 2010a). Methanol (MeOH) and acetonitrile (MeCN) are preferentially employed as organic modifiers for LC-MS detection. The two modifiers are distinct. While MeOH is a protic solvent with dissociable hydrogens and can undergo hydrogen-bonding through the O-H group, MeCN is an aprotic solvent (contains no dissociable hydrogen) (Boyes and Dong, 2018).

Since more than 70 % of pharmaceutical molecules are weak bases and approximately 20 % are weakly acidic (McCalley, 2010b), most pharmaceutical analyses use mobile phases in the pH 2-4 range (Dong, 2006; Dong and Boyes, 2018). These low pH solutions facilitate the ionization of the basic molecules in the mass spectrometer and limit the dissolution of the silica backbone in conventional SPs (Espada and Rivera-Sagredo, 2003; Tan and Fanaras,

2019). However, these acidic mobile phases have limitations, such as weak retention of analytes in the stationary phase, generation of peak shape with poor asymmetry-primarily peak tailing, low resolution, and low loading capacity (McCalley, 2010b; Voisin et al., 2012). Similarly, in the analyses of ARVDs, most reported research confirms the preferential utilization of acidic conditions (Table 2.1). There is little information on the analyses of ARVDs using an alkaline mobile phase, only a few, such as Zhang et al. (2009), resolved entecavir (anti-hepatitis B) using alkaline eluent.

Despite the considerable diversity of experimental conditions, keeping the final selection practically feasible is desirable. For this reason, modern trends and best selection practices advocate for the reduction or non-incorporation of additives in the mobile phases, simpler binary mixtures, and linear eluent gradients (Boyes and Dong, 2018).

The objective of this study was to evaluate the influence of eluent composition and the type of stationary phase in the analyses of acidic and basic ARVDs described in section 0 by considering the compound resolution and the generated analyte signal response and consequently select the most appropriate mobile phase and stationary phase for ARVD analyses

Table 2.1 Recent studies on analyses of ARVDs molecules on various matrices (unless specified, 0.1 % FA was prepared in H_2O)

ARVD	Matrix	Stationary phase Column dimension (particle size μm x ID mm x length mm)	Mobile phase	pH range carbon loading Endcapping	mass analyser/ ionization source	Reference
Tenofovir, lamivudine and nevirapine	Human hair	Platsil ODS C18 (5 μm	A:2 mM Ammonium acetate B:MeOH:H_2O (80:20)	1-11	qqqMS/ ESI+	(Wu et al., 2018)
Amantadine, rimantadine, oseltamivir, oseltamivir carboxylate, memantine, arbidol, and moroxydine acyclovir, ganciclovir, famciclovir, penciclovir, ribavirin	Chicken muscle	Agilent SB-Aq C18 1.8×3× 100,	A:0.1 % FA B: MeOH	1-8	qqqMS/ ESI+	(Mu et al., 2016)
Dolutegravir, Elvitegravir Cobicistat	Human plasma	X-Bridge C18 2.1× 50	A:0.1 % FA B:MeOH in H_2O (80:20)		qqqMS/ ESI+	(Penchala et al., 2016)
Emtricitabine, tenofovir disoproxil efavirenz	Aqueous samples and plants	Luna Omega C18 column 3×4.6×50	A:0.1 % FA B:0.1 % FA in MeCN		HRMS/ ESI+	(Mlunguza et al., 2020b)

Compound	Matrix	Column	Mobile phase		Detection	Reference
Simeprevir, daclatasvir, sofosbuvir	Human plasma	MassTox TDM MasterColumn A (50×2 mm)	A:0.1 % FA B:0.1% FA in MeOH		qqqMS/ ESI+	(Ferrari et al., 2019)
Nevirapine, efavirenz and lopinavir	Human blood	Kinetex F5 100 Å (2.6×2.1×50)	A:0.1 % FA B: 0.1 % FA in MeOH		qqqMS/ ESI+ & posneg switch	(Duthaler et al., 2017)
Dolutegravir, elvitegravir rilpivirine, Tipranavir Nevirapine,Nelfinavir Etravirine, Maraviroc Indinavir, Efavirenz	Human plasma	Acquity UPLC HSS T3 1.3×2.1×150	A: 0.05 % FA B: 0.05 % formic acid in MeCN		qqqMS/ ESI+ for all ARVD ESI- for EFV only	(Simiele et al., 2017)
Tenofovir Efavirenz	Biological tissues	Mediterranean Sea C18 2.1×100 mm, 3 µm	A: 0.1 % FA B: 0.1 % FA in MeCN		qqqMS/ ESI+ for tenofovir ESI- for efavirenz	(Barreiros et al., 2017)
Tenofovir, emtricitabine, dolutegravir	Human tissue	XBridge C18 , 5 µm	A: H2O B: 0.1 % FA in MeCN		qqqMS/ ESI+	(Patel et al., 2019)
Umifenovir (Arbidol)	wastewater	Nucleodur PFP column 50×2.1 mm, 1.8 µm	A:0.1 % FA B: MeOH	1-9 endcapped	HRMS/ ESI+	(Ul'yanovskii et al., 2022)
Efavirenz, lamivudine nevirapine	Aqueous sample	Hypersil gold 50×2.1 mm, 1.9 µm	A: 0.1 % FA B: 0.1 % FA in MeOH	1-11	HRMS/ ESI+& ESI-	(K'oreje et al., 2018a)

Atazanavir, efavirenz, lopinavir nevirapine abacavir, lamivudine zidovudine	Wastewater	Hypersil Gold C18 50×2.1 mm, 1.9 µm	A: 0.1 % FA B: 0.1 % FA in MeCN	1-11	qqqMS/ ESI+	(Abafe et al., 2018)
Nevirapine, Efavirenz	wastewater	HSS T3 150 ×2.1 mm, 1.8 µm	A:0.1 % FA B: Acetonitrile		qqqMS/ ESI+ & ESI-	(Mosekiemang et al., 2019a)
Nevirapine, Efavirenz	Aqueous sample	Acquity UPLC, BEH shield 150 ×2.1 mm, 1.7 µm	A: 0.1 % FA B:0.1 % FA in MeCN		qqqMS/ ESI+ & ESI-	(Adeola et al., 2021)

2.2 Materials and method

2.2.1 Instrumentation

Separation, characterisation, identification and quantitation of the ARVDs compounds was carried out using a hybrid quadrupole-Orbitrap High-Resolution Accurate Mass-Mass Spectrometer coupled with a Liquid Chromatography system (LC/HRAM-MS). The system was a Dionex U3000 HPLC reverse phase liquid chromatography system coupled with Q Exactive Focus Orbitrap mass spectrometer (resolution 70,000 @ m/z 200) that was fitted with a heated electrospray ionisation source (HESI, Thermo Scientific, Hemel Hempstead, UK).

2.2.2 Preparation of standards

Individual ARVD stock standards were prepared on a weight basis in either MeOH or dimethyl sulfoxide (DMSO). A mixture of the particular ARVDs stock was prepared in 30 % MeOH in high-purity water (HPW, 18.2 MΩ cm resistivity). Working solutions were prepared in the 1-100 µg L^{-1} concentration range. All stock solutions and associated dilutions were stored in amber-coloured vials at 4 °C.

2.2.3 Mobile phase and column selection

The present research followed the standard convention that mobile phase A refers to the aqueous fraction, and mobile phase B is the organic modifier. Method optimization was systematically conducted by running the test eluents and recording the generated analyte signal responses. The seven eluents under investigation are shown in Table 2.2 and were prepared by dissolution or mixing the selected additive in high-purity water. Appropriate pH adjustment was performed with either 0.1 M ammonia solution (NH$_4$OH) or 0.1 M formic acid solution. The pH range of the seven mobile phases A eluent was from 2.6 to 10.8. In the present study, the mobile phase pH referred to the pH of the aqueous eluent only, not the

apparent pH. Contamination was prevented by measuring the pH eluent as an aliquot in a separate vial. The vial's content was after that discarded to avoid contamination from the pH probe's tip. The apparent pH (pH of the binary mixture) is often not expected to differ from the aqueous eluent pH. For example, in (Kamel et al., 1999), the pH of the mixture of several aqueous and organic modifiers (MeOH) eluents mixed in equal portions did not differ by more than ± 0.2 pH units from the initial aqueous eluent pH. In this study, additives were only added to the aqueous eluent.

Table 2.2. Aqueous mobile phases evaluated during method development

Mobile Phase	pH
0.1 % formic acid (FA) in H_2O	2.6
0.1 % ammonia (NH_3) in H_2O + 0.1 % formic acid (FA) in H_2O, (pH unadjusted), (1:1, v/v)	4.2
10 mM Ammonium formate (formate (AmFo) (pH unadjusted)	6.3
Pure LC-MS water	7.2
10 mM Ammonium formate (adjusted with NH_4 solution)	8.4
0.1 % Ammonia in H_2O + 0.1 % formic acid in H_2O (adjusted by NH_4 solution)	8.4
0.1 % ammonia in H_2O	10.8

Five µL of a 50 µg L^{-1} ARVD mix standard was injected into the LC-HRMS and eluted with the test eluents, and the generated ESI chromatographic signal response was observed. The eluent that induced the highest signal response (ion count) with the adequate resolution was selected for the subsequent optimization steps. The organic modifier was selected after identifying the appropriate aqueous mobile phase. Column performance between the C18 and phenyl-hexyl stationary phases, whose characteristics are described in section 2.2.4, was evaluated by assessing each column's resolution, retention times, peak shape, and signal-to-noise ratio. The ionisation mode was selected by evaluating the signal response obtained

under positive (ESI+), negative (ESI-) and signal switching modes. While the buffer concentration, column temperature and gradient profile parameters may also impact the signal response, they are less critical (Ruta et al., 2012) and were not tested. The mass spectrometric conditions shown in Table 2.3 were kept constant.

An ideal approach to evaluate the selectivity of the eluents and electrospray response would have been through a direct infusion of the analyte in the eluent into the mass spectrometer bypassing the column, an approach used by Kamel et al. (1999) and Erb and Oberacher, (2014). However, such an approach is devoid of stationary phase contribution. Given that in actual analysis, the eluent permeates through the column, it was necessary to have the column affixed to accurately collate the cumulative impact of the mobile phase and stationary towards the ARVD compounds.

The analyte solutions were infused into the chromatographic system as a 'clean solvent' rather than a matrix. The assumption was that the responses observed would be replicated when the analyte was in the matrix. This approach was taken because the entire study consisted of three separate matrices (soil, wastewater, and plant tissue). It was not feasible to replicate analytical runs under these different matrices. Nonetheless, calibrations and recoveries were performed and calculated during the individual experiments with the appropriate matrix Detailed information on extraction recoveries and method optimization data is presented in the method sections of the preceding chapters.

Table 2.3. Chromatographic and mass spectrometric operating conditions

Operating Parameter	Operating Value
Column temperature	50 ^{0}C
Mobile phase components	A=various additives in water, B=MeOH or MeCN
Mobile phase flowrate	500 µL min^{-1}
Injector volume	5 µL
Scanning range	100- 1500 m/z
Scan type	Full scan
Ionization	ESI positive and negative
MS drying gas	Nitrogen,
Nebulizing pressure	60 psi
Spray voltage	3.5 Kv
Resolution	70000
AGC target	1e6
Capillary temperature	325 °C
Auxiliary gas heater	425 °C

The positive and negative ion spectra were obtained from the protonated [M+H]$^+$ and deprotonated [M-H]$^-$ molecular adducts shown in Table 2.4.

Table 2.4. Monoisotopic mass and molecular adducts of ARVDs

ARVD	[M]	[M+H]$^+$	[M+NH$_4$]$^+$	[M-H]$^-$
Acyclovir	225.08619	226.09347	243.12002	224.07891
Lamivudine	229.05211	230.05939	247.08594	228.04483
Oseltamivir	312.20491	313.21218	330.23873	311.19763
Nevirapine	266.11676	267.12404	284.15059	265.10948
Efavirenz	315.02739	316.03467	333.06122	314.02011

The signal-to-noise ratio (S/N) and peak widths were obtained from the peak detection algorithm within the Mass Lynx Freestyle vs 4.5 software.

Peak tailing and fronting were measured by determining the peak asymmetry factor, A_s, estimated using Equation (2.1

$$A_s = \frac{b}{a} \qquad\qquad (2.1)$$

Where a was the distance from the peak's leading edge to the midpoint (perpendicular to the peak's highest point) and b was the distance from the peak midpoint to the trailing edge of the peak measured at 10 % height.

The resolution, R_s, a measure of the quality of separation between peaks, was determined using Equation 2.2.

$$R_s = (t_{R2} - t_{R1})/(1.7 \times 0.5 \times (w_1 + w_2) \qquad\qquad (2.2)$$

Where t_1 and t_2 are the retention times of the two peaks, and w_1 and w_2 are the widths of the peaks at half height.

Column efficiency was presented as the number of theoretical plates per column, as shown in Equation (2.3)

$$N = 5.54(t_R / w_{0.5})^2 \qquad\qquad (2.3)$$

Where t_R is the retention time of the analyte of interest and $w_{0.5}$ is the width of the peak at half height.

2.2.4 Characteristics of the selected stationary phases

The separation efficiency of two encapsulated columns, a C18 and phenyl-hexyl type, whose characteristics are listed in Table 2.5 and illustrated in Figure 2.1, were evaluated. The phenyl-hexyl stationary phase had the aromatic phenyl group and the hexyl carbon chain embedded in its surface. Correspondingly, the phenyl-hexyl had a lower carbon content than the C18 column. The two stationary phases demonstrated selectivity over a wide pH range (1.5-11.0).

Table 2.5: Characteristics of selected stationary phases

Column name	Functional group	Particle size (µm)	Pore size (Å)	Carbon content (%)
C18	Octadecyl encapsulated	2.5	95	7.0
Phenyl-Hexyl	Phenyl-Hexyl	2.5	95	4.6

The column encapsulation (Figure 2.1) increases the silica surface's ligand coverage, minimizing the leaching of unbonded silanol groups at high pH.
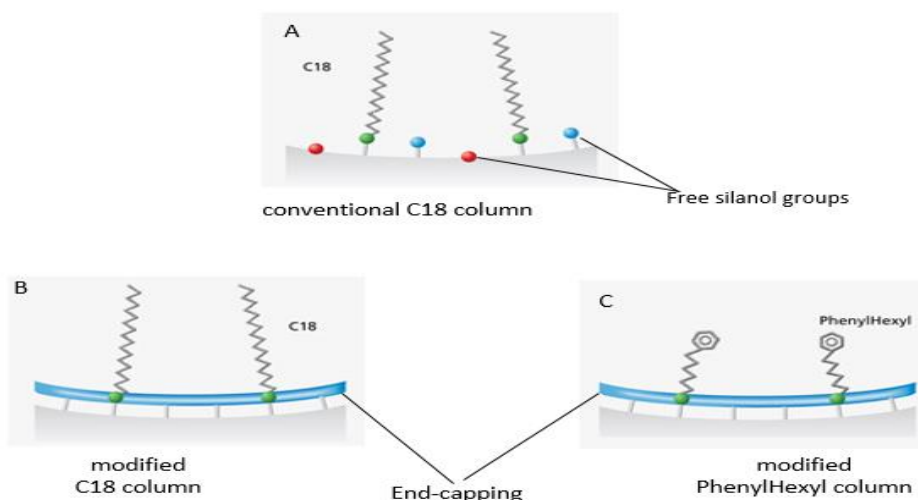
Figure 2.1. Encapsulation of the stationary phases (Main sketches obtained from www.ace-hplc.com)

2.2.5 Data analyses

Chromatographic and mass spectral data were obtained from Mass Lynx Freestyle vs 4.5 software. The generated data were visually and arithmetically evaluated by interpreting the mass spectral resolutions and retention time of individual ARVDs. Results were presented as extracted ion chromatograms (EICs) and as graphs of ion intensities of the EICs as a function of the mobile phase or stationary phase.

2.3 Results and discussion

2.3.1 ARVD ESI ion count signal response

The cumulative signal response (across the two stationary phases) obtained from the test eluents is shown in Figure 2.2.
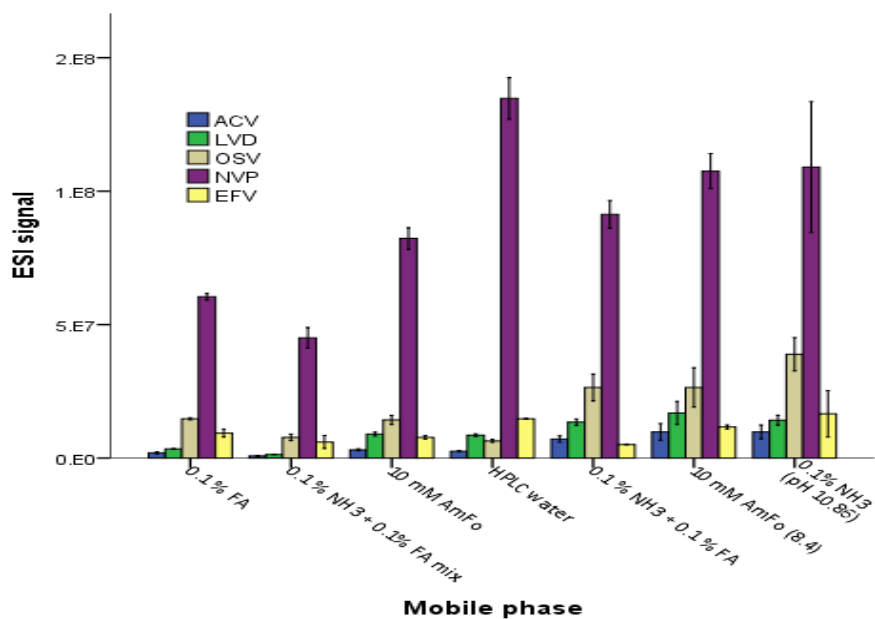
Figure 2.2. The cumulative mean ion count signal response of the ARVDs from the seven aqueous eluents across the two stationary phases (n=3 ± SD)
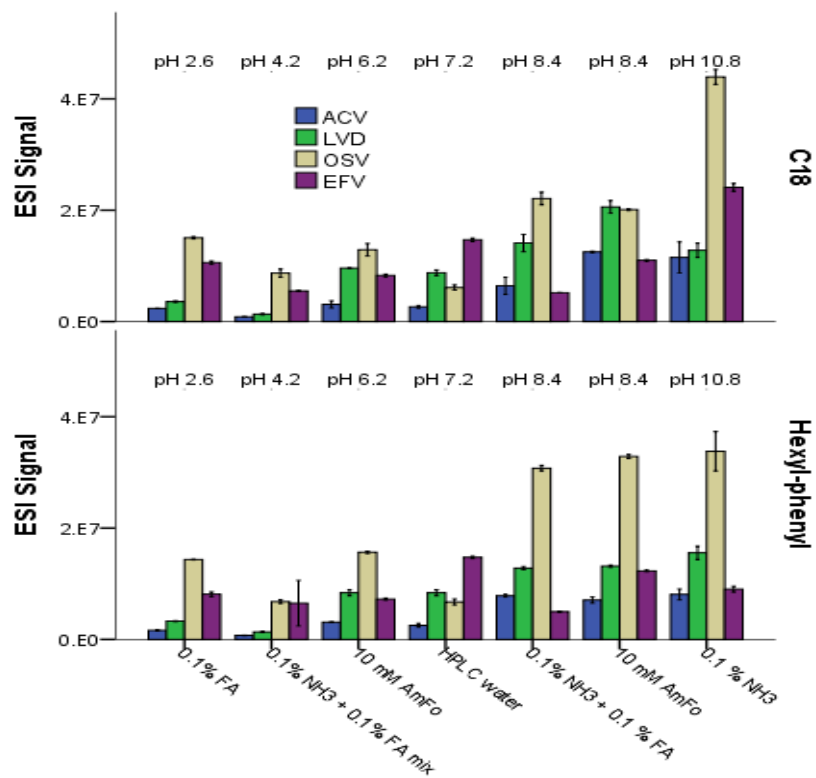
Figure 2.3. ARVD signal response ion count (excluding NVP) was obtained from each mobile phase for the two stationary phases (n=3 ± SD).
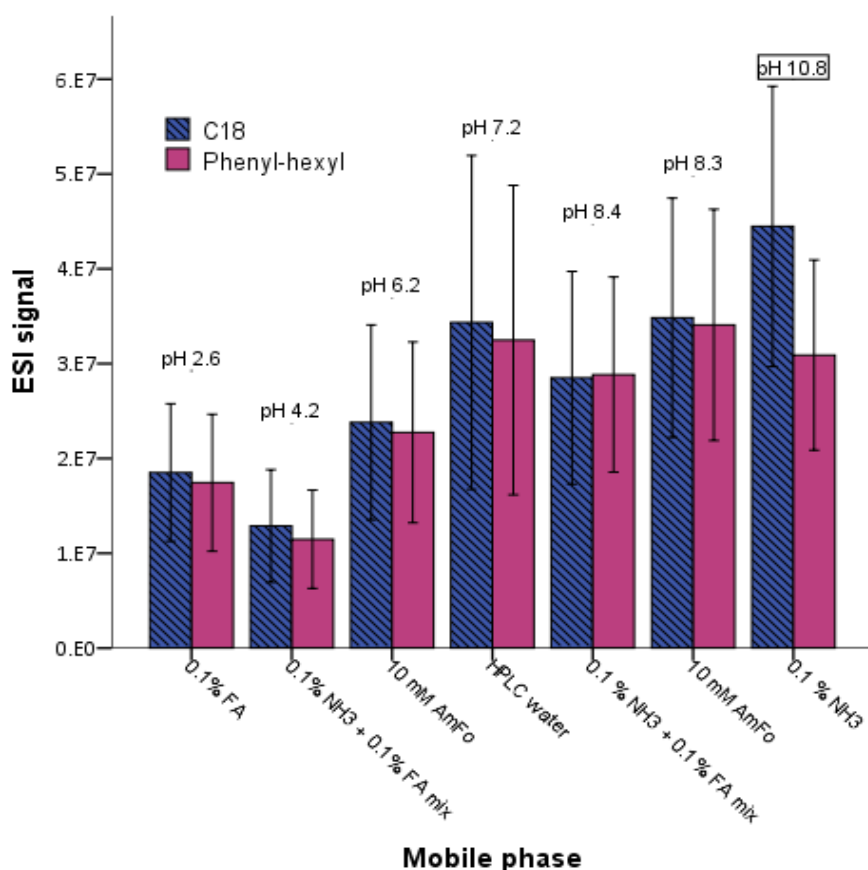
Figure 2.4. ESI ion count signal response (cumulative signal response for all analytes) between the C18 and phenyl-hexyl stationary phases (n=3 ± SD)

Figure 2.2 shows that NVP exhibited a signal approximately three orders of magnitude higher relative to the other ARVD molecules across the seven mobile phases A. For this reason, Figure 2.3 was constructed excluding NVP to illustrate better the signal response variation between the remaining four ARVDs. In general, a satisfactory total ion current (TIC) signal response> 1E6 (above the automatic gain control count (AGC) for all molecules. The measured signal strength for the remaining ARVDs was OSV > EFV > LVD > ACV. The acidic OSV and EFV signal was approximately two times higher than the weakly basic LVD and ACV. However, it is likely that the hydrophilic nature of ACV and LVD predominantly contributed to their lower signal rather than their weakly basic nature. According to Kamel et al. (1999), the more hydrophobic a molecule, the higher the signal response expected.

The cumulative signal response from the C18 SP was 6.5 % higher than the signal from the phenyl-hexyl stationary phase (Figure 2.4). Nonetheless, the variation was not significantly different (p=0.66).

Concerning the individual eluents, the 0.1 % NH_3 (pH 10.8) mobile phase yielded the highest signal response, which was 2.5 times higher than the 0.1 % FA (pH 2.6) and five times higher than the lowest signal obtained from the 0.1 % NH_3 + FA mix (pH 4.2) eluent. The descending signal strength from the eluents was such that 0.1 % NH_3 (pH 10.8) > 10mM AmFo (pH 8.4) > 0.1 % NH_3 +0.1% FA (pH 8.45) > 10 mM AmFo (pH 6.3) > ultrapure H_2O (pH 7.2) > 0.1% FA (pH 2.6) > 0.1 % NH_3 +0.1% FA (pH 4.2). Generally, a higher ESI ion count signal response was obtained by the alkaline mobile phases with pH > 8. The response was approximately two times greater than the signal generated by eluents with pH ≤ 7.0.

2.3.2 Mobile and stationary phase separation efficiency (resolution)

After establishing the signal responses generated by the mobile phase A in the two columns, the separation (resolution) of the individual ARVDs in each column under the different eluents were assessed. The ARVDs should have been late-appearing (later than the solvent front of the mobile phase) within the run time rather than early-appearing, especially for the hydrophilic ARVDs. Usually, shorter retention times are desirable in chromatography, leading to shorter runtimes and, thus, higher sample throughput. In this study, the total chromatographic analysis time was 10 minutes. This terminology will be used in the remaining sections.

2.3.2.1 Selectivity in a neutral environment (ultra-pure water, pH 7.2)

Figure 2.5 A and B are the EIC showing the separation achieved by unmodified ultrapure H_2O (pH 7.2).
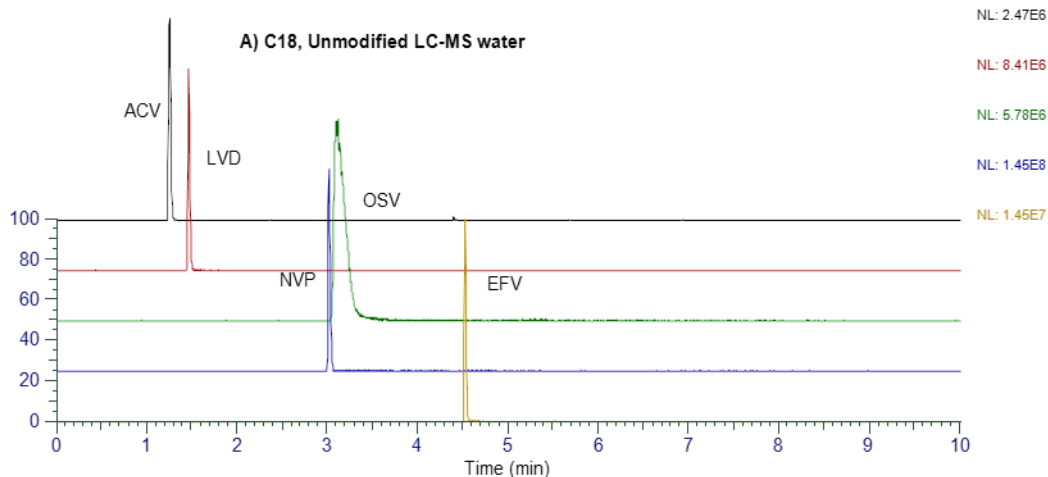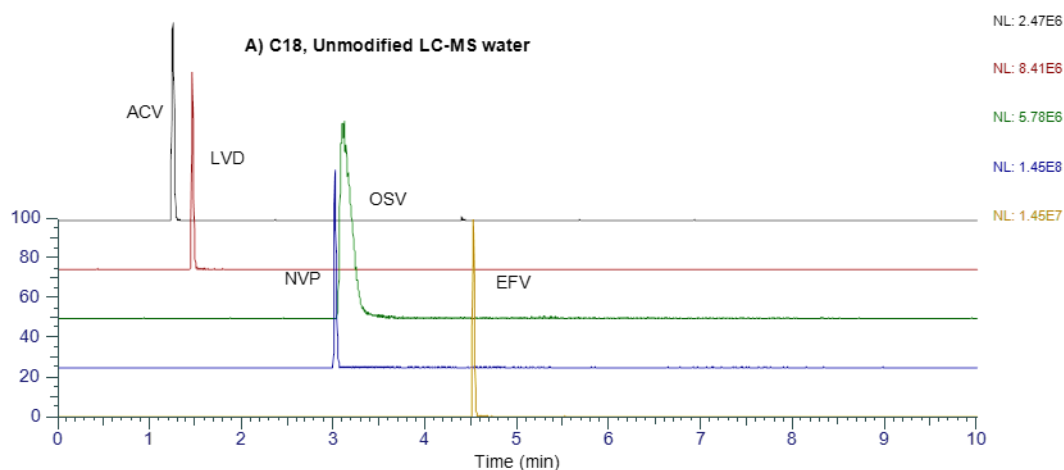
Figure 2.5. Separation of the 5 ARVDs in (A) C18 and (B) Phenyl-hexyl with unmodified LC-MS water, pH 7.2.

Separation of the ARVDs in the C18 column, Figure 2.5 A, showed impeded separation between NVP-OSV. Moreover, OSV in both columns exhibited tailing tendencies, indicating a > 1 peak asymmetry factor, i.e., 2.5 and 2.2 in the C18 and phenyl-hexyl columns, respectively. Usually, a fronting peak exhibits an A_s value of < 1, while a tailing peak has an A_s value of > 1 (Pápai and Pap, 2002). For a symmetrical peak, the value is 1. The higher the A_s value, the lesser the symmetry. Therefore the A_s > 2 obtained from the ultra-pure water mobile phase were undesirable and could lead to compromised quantification.

2.3.2.2 Selectivity in acidic environment (pH 2.6)
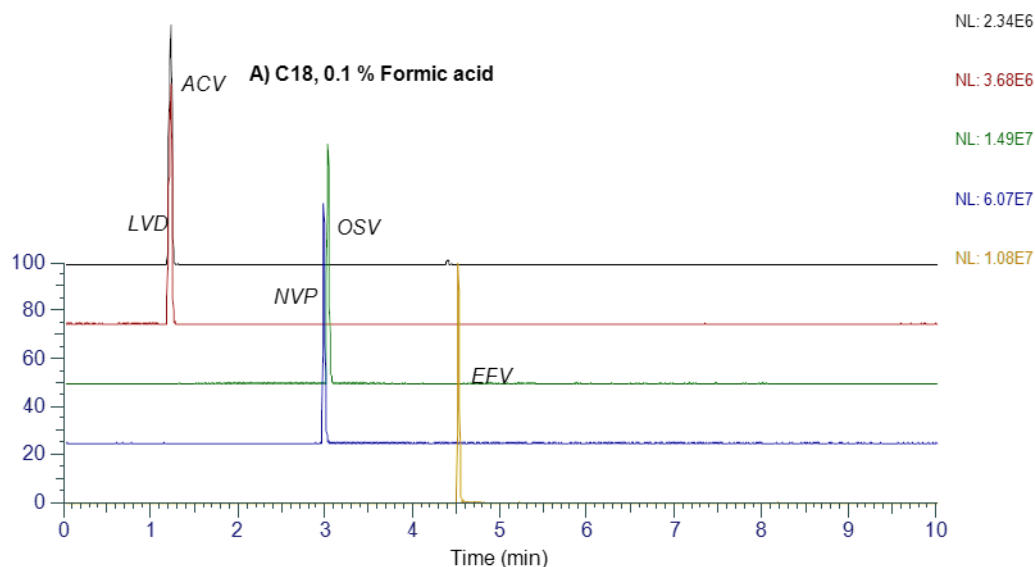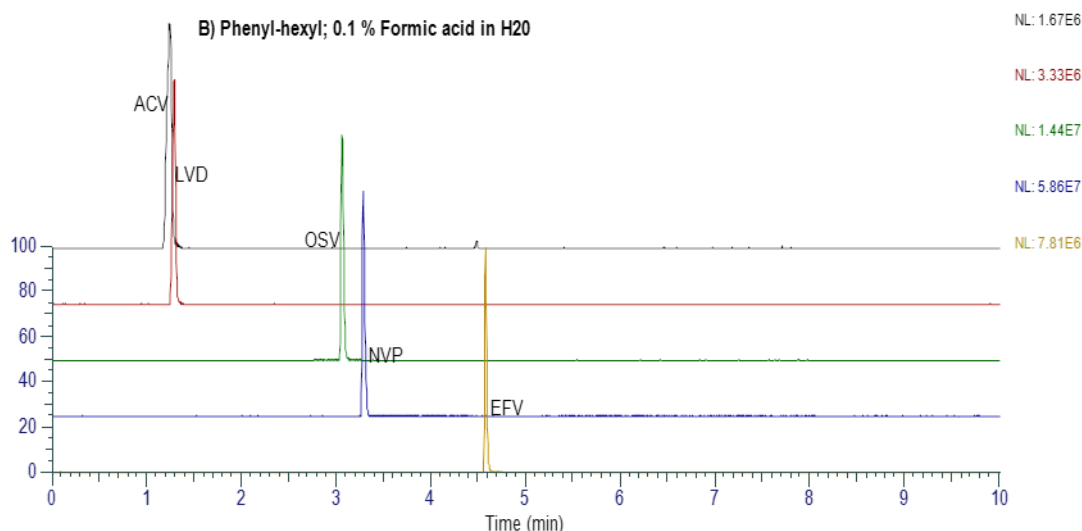
Figure 2.6. Separation of 5 ARVDs in (A) C18 and (B) phenyl-hexyl as stationary phases in 0.1 % formic acid.

The C18 column in Figure 2.6 A showed inadequate separation between two sets of adjacent (in terms of retention time) ARVDs, i.e. ACV-LVD and OSV-NVP, exhibiting some co-elution tendency. Similarly, the separation of adjacent ACV-LVD in the phenyl-hexyl column Figure 2.6 B was inadequate. Interestingly, 0.1 % FA, a low pH eluent, is extensively used elsewhere as an additive of choice, as indicated in Table 2.1.

2.3.2.3 Selectivity in basic pH environment (pH 8.4 -10.4)

The separation of the ARVDs under three alkaline eluents was evaluated.
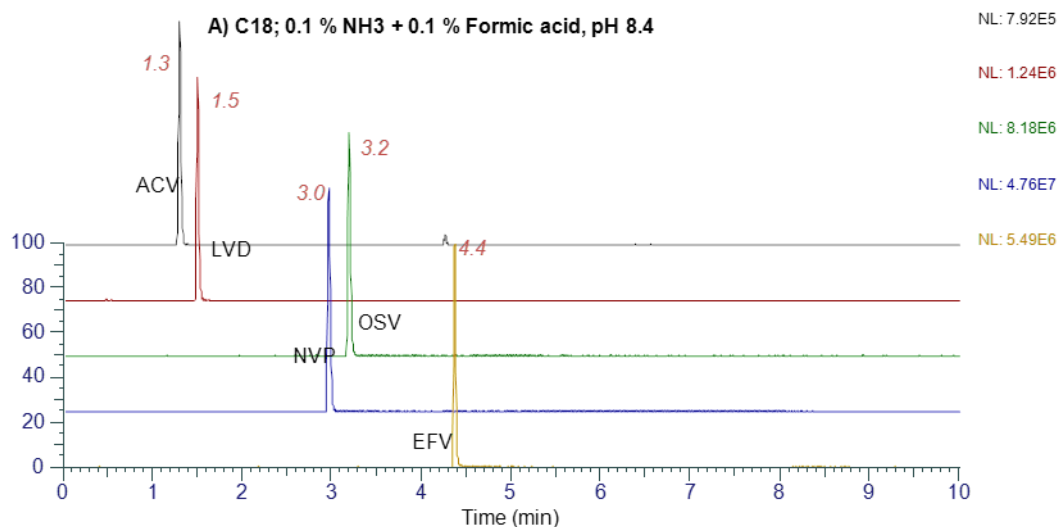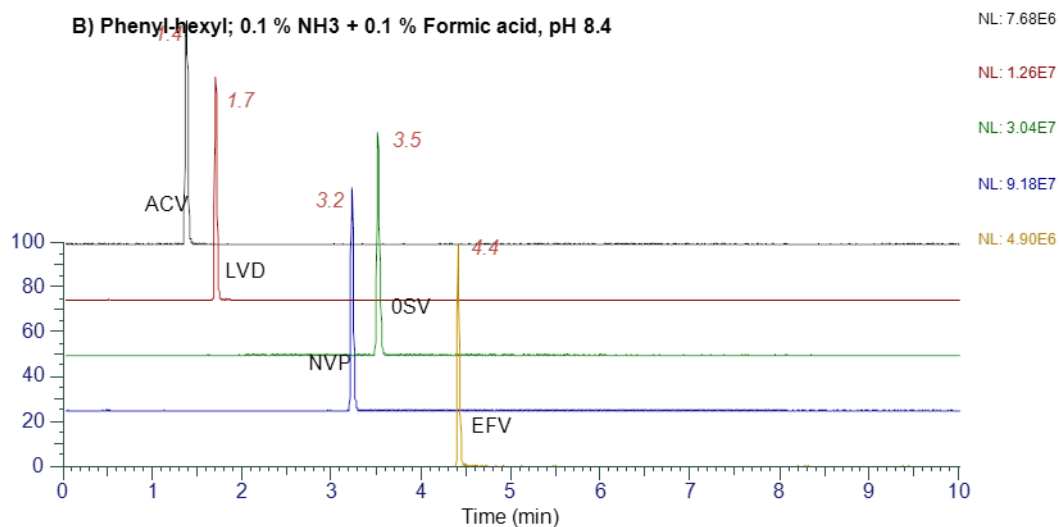
Figure 2.7. Separation of 5 ARVDs in (A) C18 and (B) phenyl-hexyl in 0.1 % NH$_3$ + 0.1 % FA (pH 8.4) mix eluent

Figure 2.7 A and B show that the ARVDs exhibited identical separation patterns in C18 and phenyl-hexyl columns when the 0.1 % NH$_3$ + 0.1 % FA mix was used as the eluent. Similarly, an identical separation pattern was observed when 10 mM AmFo (pH 8.4) was used as the eluent, as shown in Figure 2.8 A and B.
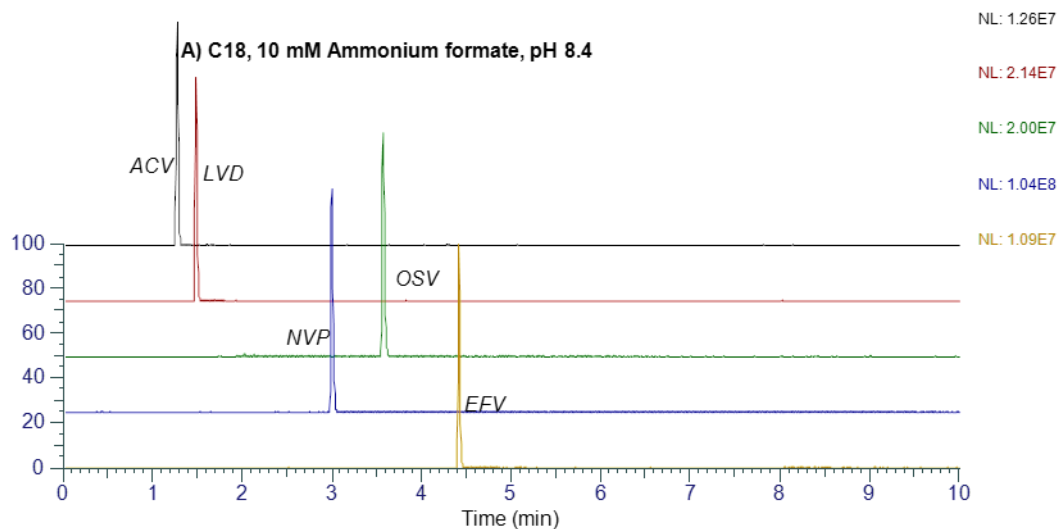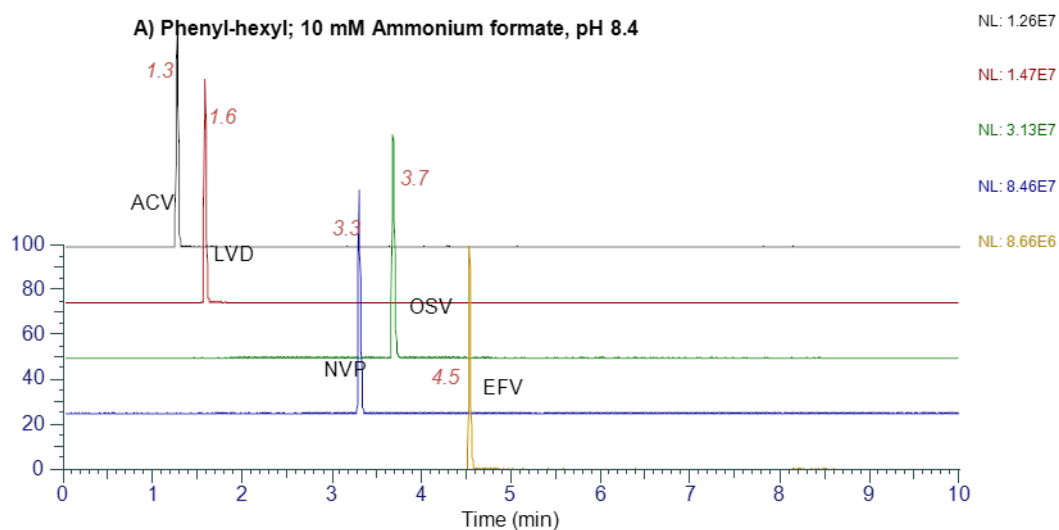
Figure 2.8. Separation of 5 ARVDs in (A) C18 and (B) phenyl-hexyl with 10 mM Ammonium formate (pH 8.4) as eluent
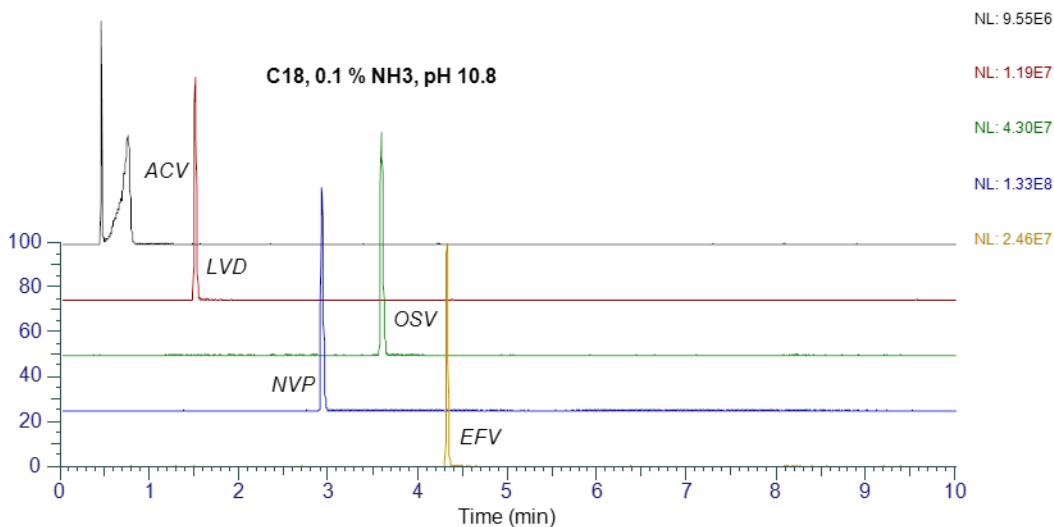
Figure 2.9: Separating the 5 ARVDs in the C18 stationary phase, using 0.1 % NH$_3$ (pH 10.8) as the eluent.

While the ammonia only, most alkaline mobile phase (0.1 % NH$_3$ pH 10.8) yielded one of the highest ESI signal responses amongst the test eluents (Figure 2.4), its selectivity towards ACV in the C18 stationary phase was not satisfactory, as shown in Figure 2.9. ACV was early-appearing, < 1 minute, and exhibited peak fronting tendencies.

Figure 2.10 summarises the observations made in Figure 2.5 to Figure 2.9. It illustrates the phenyl-hexyl column retention times normalized to C18 column retention times for all the test eluents. A retention time factor > 1 implied relatively longer phenyl-hexyl retention times.   Generally, relatively longer retention times were realized in the alkaline mobile phases, pH > 8.0 and the phenyl-hexyl columns for all analytes except for EFV in only three eluents.
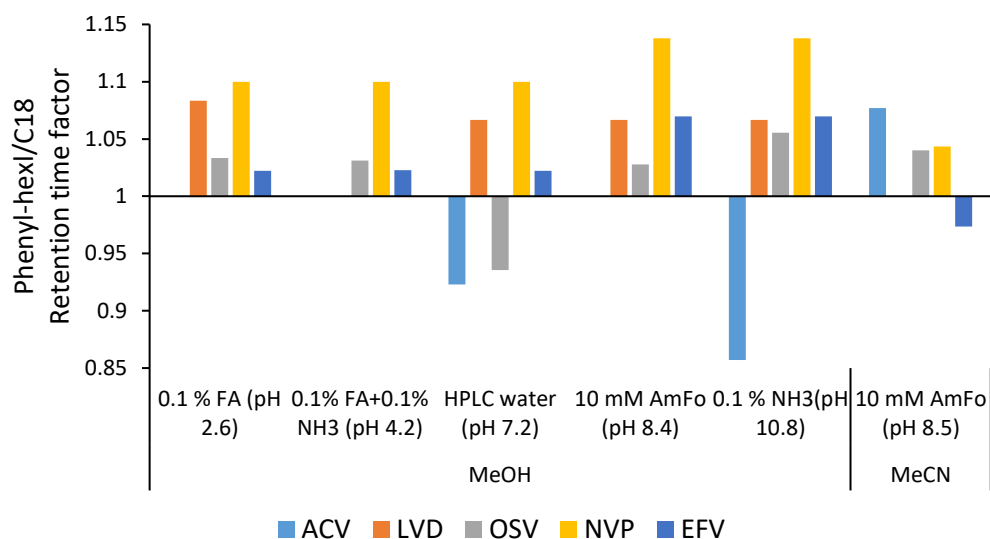
Figure 2.10. Phenyl-hexyl ARVD retention times normalized to C18 obtained retention time, retention time factor >1 indicate longer retention time in phenyl-hexyl column

The alkaline eluents achieved better resolution in the phenyl-hexyl columns than in the acidic eluents in the C18 stationary phase. The resolution of the problematic adjacent ACV-LVD and OSV-NVP was compared between the C18 and phenyl-hexyl columns using basic and acidic eluents and was presented in Figure 2.11.
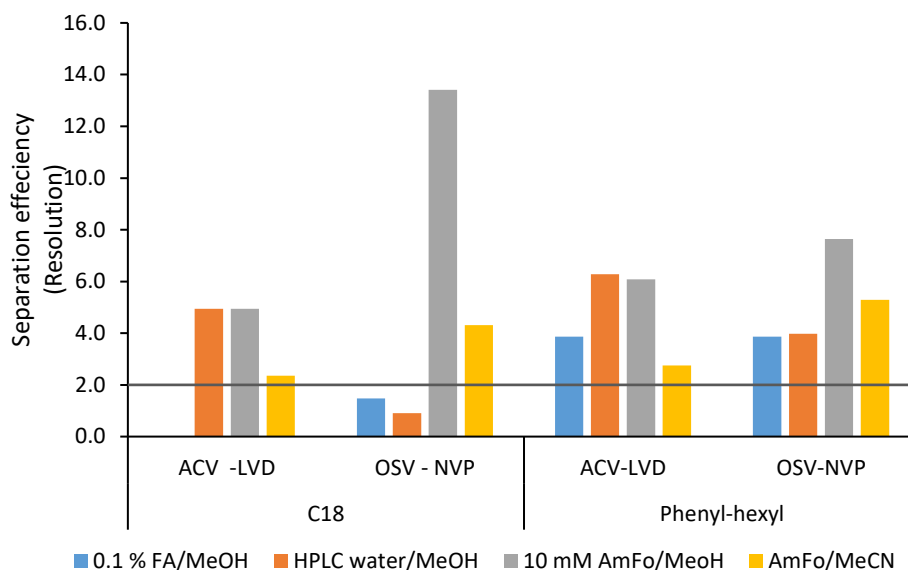
Figure 2.11. Resolution between adjacent ARVD compounds from different eluents in the C18 and phenyl-hexyl stationary phases.

Usually, a minimum resolution of 1.7-2.0 between two adjacent peaks is considered adequate (LCGC, 2016). Figure 2.11 shows that separating the 'problematic' compounds was satisfactory in the phenyl-hexyl column as the resolution obtained was greater than 2, as indicated by the target line at level 2. The resolution of the molecules in the C18 column was weaker, especially between OSV-NVP in the eluents with pH ≤ 7.0.

From the data gathered, two mobile phases, the 10 mM AmFo and the 0.1 % NH_3 + 0.1 % FA mixture, both having pH 8.4, were considered candidate mobile phases for subsequent analyses. They induced similar separation with satisfactory resolution (Figure 2.7 and Figure 2.8) and exhibited the second-highest ESI ion count signal (Figure 2.4). In (Dong and Boyes, 2018), while aqueous ammonia hydroxide was considered a sufficient alkaline modifier, ammonium formate yielded excellent peaks for basic drugs. Elsewhere, ammonium formate buffer was used as a high pH eluent in pharmaceutical studies, such as in (Berg et al., 2013), whereby buprenorphine and fentanyl (opioids) were analyzed in human blood and in

Amundsen et al., (2013), where fifteen basic pharmaceuticals were also analyzed in bodily fluids. For these reasons, the 10 mM AmFo additive was preferentially selected for all subsequent analysis

Acidic mobile phases are associated with peak tailing and low separation efficiency (Tan and Fanaras, 2019), consistent with the separation observed in Figure 2.6, where adjacent molecules, ACV-LVD and OSV-NVP, exhibited poor resolution and showed co-elution tendencies. When compounds co-elute, ion suppression is induced (Rainville et al., 2012). This co-elution likely contributed to the low ESI ion count signal response measured in the 0.1 % FA eluent, which was approximately three magnitudes lower than the alkaline-induced signal.

While low pH eluents are preferentially used in ARVD pharmaceutical analyses, as highlighted in Table 2.1, the present research has shown that higher signals may be obtained with alkaline mobile phases. A two-fold increase in response signal was measured when 25 pharmaceutical compounds were analyzed in a high-pH environment than when they were analyzed in eluents modified by an acidic additive (Mess et al., 2009). Similarly, an LC-MS/MS study observed a 1.2-9.6 fold increase in the peak area of 21 out of 24 test compounds in basic aqueous eluents (pH 10) than in a standard acidic environment (pH 3) (Rainville et al., 2012). Delatour and Ledercq (2005) obtained the most efficient separation of 11 drugs at pH 8.5.

Several mechanisms have been theorized to compensate for potential signal loss in the weakly basic compounds analyzed using neutral and alkaline eluents (since the basic compounds will be least ionized in this environment). One mechanism proposes that surface enrichment on the basic molecules with protons obtained from the electronically desorbed protons occurs in the surface layer of the nebulized droplets in the high potential regions in

the mass spectrometer. In contrast, proton transfer from the ammonium ions to the basic molecules may also occur (Delatour and Ledercq, 2005).

The weakest signal in the present study was observed in the weakly basic ACV and LVD. This weak signal was not directly attributed to their basicity or acidity since their weak signal relative to the acidic compounds was constant in both alkaline and acidic environments. The weak signal was likely compound-specific since the two molecules exhibited the least lipophilicity.

Concerning buffer concentration in the eluents, initially, conventional approaches employed higher buffer concentrations of up to 50 mM. Modern trends, however, recommend that concentration ranges between 5-20 mM (Dong and Boyes, 2018). The concentration of the AmFo buffer was not varied in the present study but was constantly maintained at 10 mM. In (Delatour and Ledercq, 2005), the ammonium formate and ammonium bicarbonate buffer varied between the 2-20 mM concentration range and did not impact the sensitivity in the analyses of 11 pharmaceuticals. Contrastingly, > 10 mM buffer concentrations were reported to increase ion suppression (Lupo and Kahler, 2017).

It is noteworthy to mention that, at times, the effect of buffers on ionization is not well understood as it tends to be compound-specific (Tan and Fanaras, 2019). For this reason, while the present experiment endeavoured to monitor compound-specific responses, the overall objective was to identify chromatographic conditions that would simultaneously enhance optimum signal response and separation of all five ARVD molecules. For this reason, the 10 mM concentration was selected as an appropriate level for the AmFo eluent buffer.

2.3.3 Signal-to-noise ratio

While an increase in the ion intensity signifies a higher detection capability (sensitivity) (Page et al., 2007), the signal-to-noise (S/N) ratio data is essential as it is related to the limits of detection that may be attained (FDA, 2018).
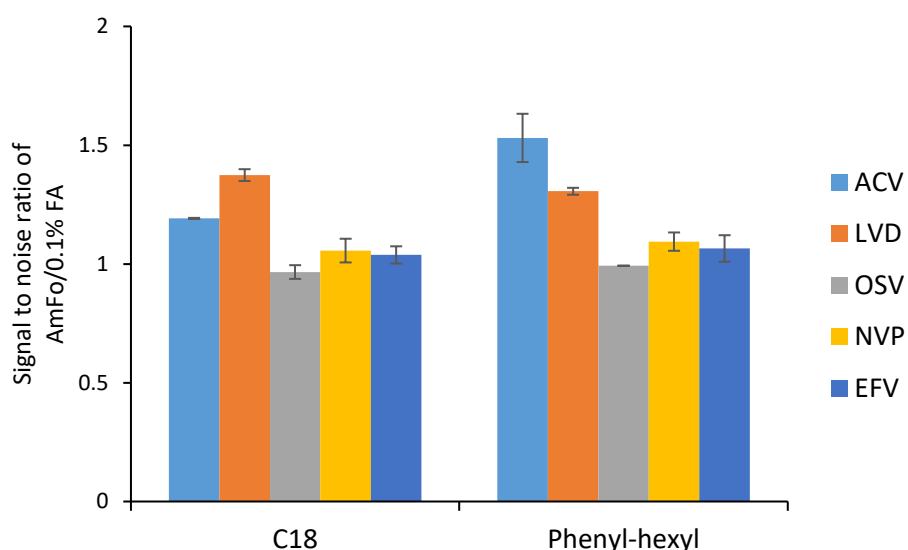
Figure 2.12. Signal-to-noise ratio across the C18 and phenyl hexyl stationary phases for AmFo (pH 8.4) normalized to 0.1 % FA mobile phases (n=4 ± SD)

The mean S/N ratio between the C18 and phenyl-hexyl stationary phases was 14.6 and 13.4, respectively, and was not statistically different (p=0.68). When S/N of 0.1 % FA normalized the S/N of AmFo, all values were > 1, indicating higher potential S/N from AmFo eluent, Figure 2.12. The AmFo yielded S/N ratios were higher and different (p=0.002) from the 0.1 % FA obtained S/N, with a mean of 14.8 to 13.0, respectively. The S/N value of the weakly basic ACV and LVD was highest, as illustrated in Figure 2.12, consistent with Tan and Fanaras (2019), who noted that due to the improved peak shape and symmetry, basic compounds tend to have higher S/N ratios.

2.3.4 Column efficiency

The column efficiency (N) may sometimes be evaluated by determining the number or height

of the theoretical plate (h) between two selected columns using a mobile phase.
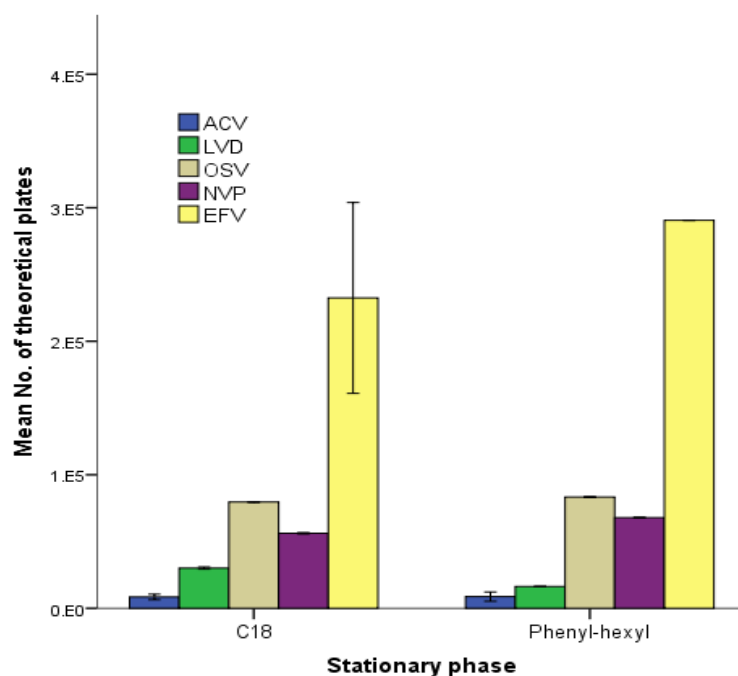
Figure 2.13. Number of theoretical plates (n=3 ±SD)

Usually, the higher the value of N, the more efficient a column is in the analyses of a

compound. Figure 2.13 showed that apart from LVD, the phenyl-hexyl column efficiency for

ACV, OSV, NVP, and EFV was between 3.5 to25.8 % higher than in the C18 column.

2.3.5 Stationary phase selection

Regarding the stationary phase, Figure 2.4 showed that the signal response difference

between the C18 and phenyl-hexyl column was less than 0.1 % across all the ARVDs and tested

eluents. On the other hand, the phenyl-hexyl column yielded better resolution, induced the

preferred late-appearing peaks and possessed higher column efficiency for most ARVDs. For

these reasons, the phenyl-hexyl was selected for subsequent analyses.

Several factors impacted the interaction between the ARVDs molecules and the surfaces of the stationary phases. In the C18 column, the unavailability of the alkyl chains for interaction likely contributed to the relatively early-appearing peaks relative to the phenyl-hexyl column. Often, when using highly aqueous mobile phases (> 90 % water), the water molecules aggregate around the C8 and C18 alkyl chains, blocking the groups, thus minimizing separation potential (Bocian and Krzemińska, 2019). In the present study, such high mobile phase aqueous levels occurred at the onset of the gradient flow when the aqueous fraction in the binary mobile phase was 100 % before gradually reducing. One remedy to this challenge was incorporating a phenyl group, into the bonded phases. The phenyl group provides complementary selectivity to a molecule's aromatic functional group, unlike the alkyl-only chain in a C18 column.

Another unique characteristic of ARVDs is their aromaticity (Jain et al., 2013). For this reason, another layer of phenyl-ARVD interactions involved π–π interactions between delocalized electrons in the molecules' aromatic centres and the stationary phase phenyl group. π–π interactions are direct attractive non-covalent interactions between aromatic moieties (Zhao et al., 2015). Hence it resulted in relatively longer retention times and enhanced the resolution of the phenyl-hexyl stationary phase. The C18 stationary phase has a higher carbon content (7 %) than the phenyl-hexyl (4.6 %) column (Table 2.5), implying it is more hydrophobic and was expected to induce stronger interaction with the solute in the eluent (Chromatography Today, 2022). However, this hydrophobic-only interaction was weaker than the two-prong interactions in the phenyl-hexyl stationary phase, even for highly hydrophobic compounds such as EFV. For these reasons, the phenyl-hexyl column was selected for subsequent analyses.

2.3.6 Organic modifiers

It is essential to mention that the already presented was generated while utilizing MeOH as mobile phase B. In this section, the selectivity of MeCN and MeOH is compared in terms of resolution and signal strength.
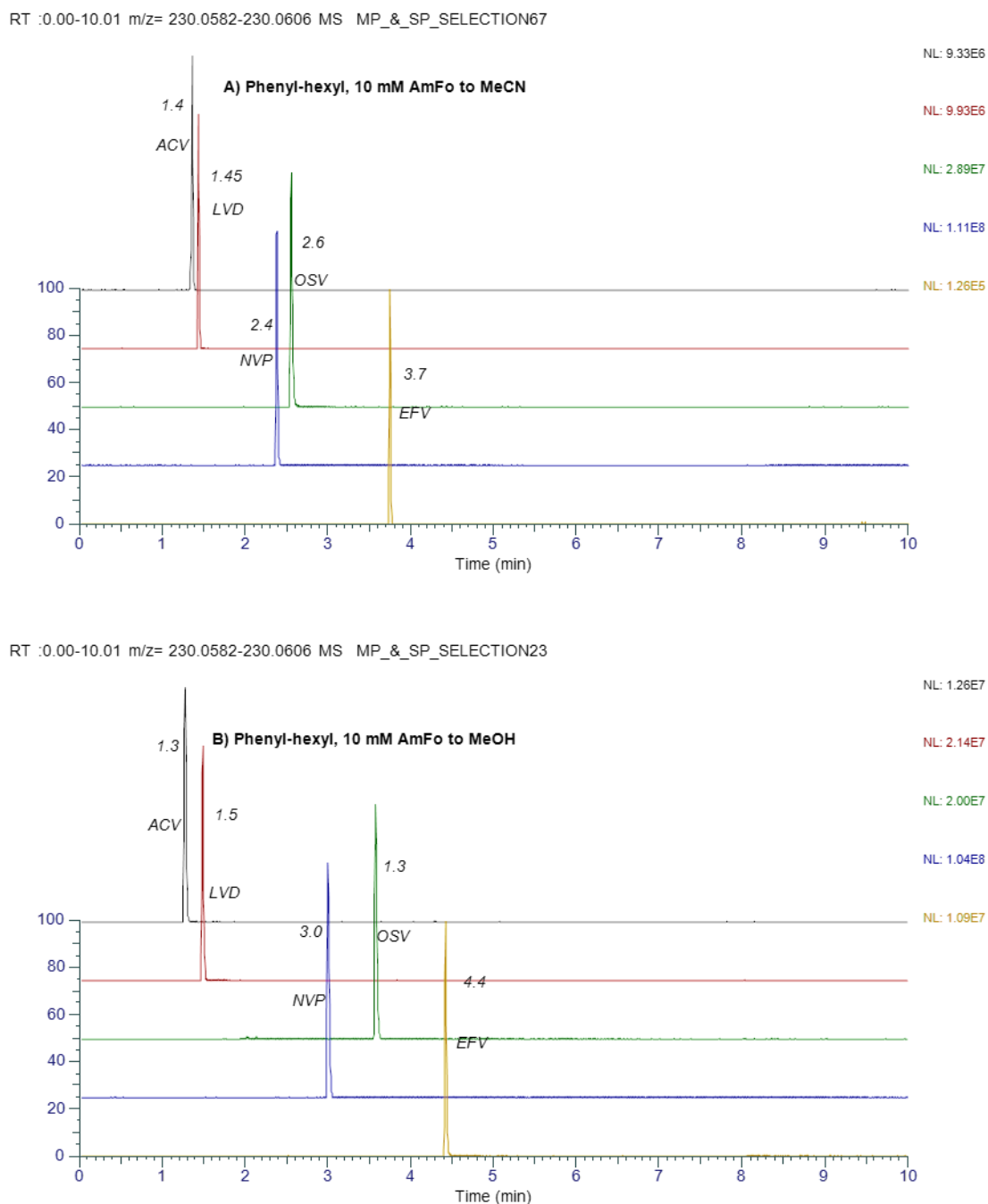
Figure 2.14. Separation of ARVDs in **(A)** MeCN **(B)** MeOH organic modifiers in the phenyl column.

Poor separation was noted between the ACV-LVD when MeCN was used as an organic modifier; Figure 2.14A contrasted with the better MeOH-induced separation, Figure 2.14 B. The early-appearing peaks in MeCN (an apolar solvent) were possibly due to the reduced hydrogen bonding interactions. MeCN is an aprotic solvent deficient in dissociable hydrogens (Advanced Material Technology, 2007).

Regarding the signal response, Figure 2.15 shows the MeOH signal normalized to the MeCN signal graph for each solute A > 1 signal implying a higher response in MeOH than MeCN. Generally, a narrow variation in signal response, ≤ 5 times, was exhibited between all ARVDs except EFV. EFV was 100 times less responsive in MeCN than in MeOH.
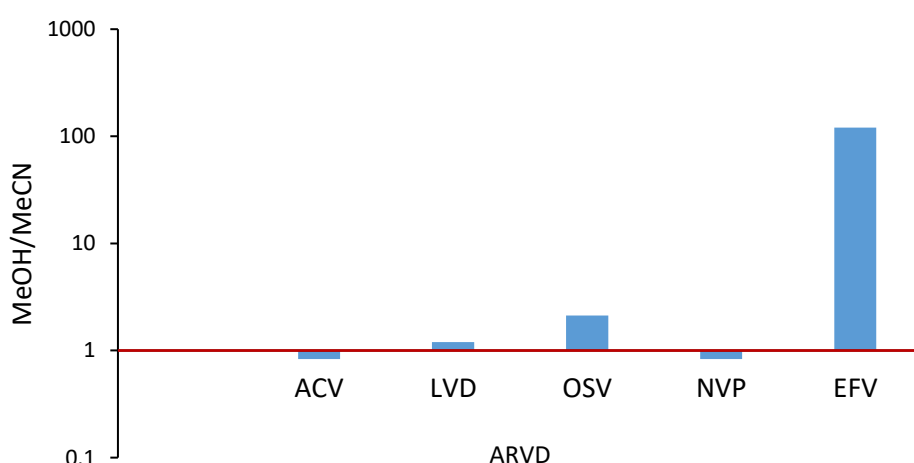
Figure 2.15. Signal response of ARVD molecules obtained in MeOH normalized with MeCN

Sometimes additives can be added to an organic modifier (e.g. in Abafe et al. 2018; Ferrari et al. 2019; and Mlunguza et al. 2020b). However, the drawback of such an approach is that the organic strength of the modifier may be compromised; moreover, it is another layer of complexity in sample preparation (Boyes and Dong, 2018). Nonetheless, MeCN has better separation efficiencies at low pHs than MeOH due to its low viscosity. At such low pH,

silanolphilic interactions are suppressed. However, extending to intermediate and higher pHs, MeOH provides better efficiencies as its deactivating effect on silanol groups are induced (McCalley, 1996 and McCalley, 2010a).

MeOH and MeCN present varying selectivity and are excellent tools for method development. The 100- times difference in signal response measured in EFV between MeOH and MeCN highlights the need to perform method development tests because most compounds behave uniquely. MeOH was therefore selected as the preferred organic modifier for subsequent analyses.

2.3.7 Adduct selection

The signal response generated by the protonated $[M+H]^+$, ammoniated $[M+NH_4]^+$ and sodiated $[M+Na]^+$ adducts were measured. The adduct that yielded the highest signal response was selected for identification and quantification purposes. All data presented in the sections before were obtained from the individual ARVD protonated ion. Adduct formation is influenced by the mobile phase in use and plays an essential role in identifying specific species in the mass spectrum (Kruve and Kaupmees, 2017).
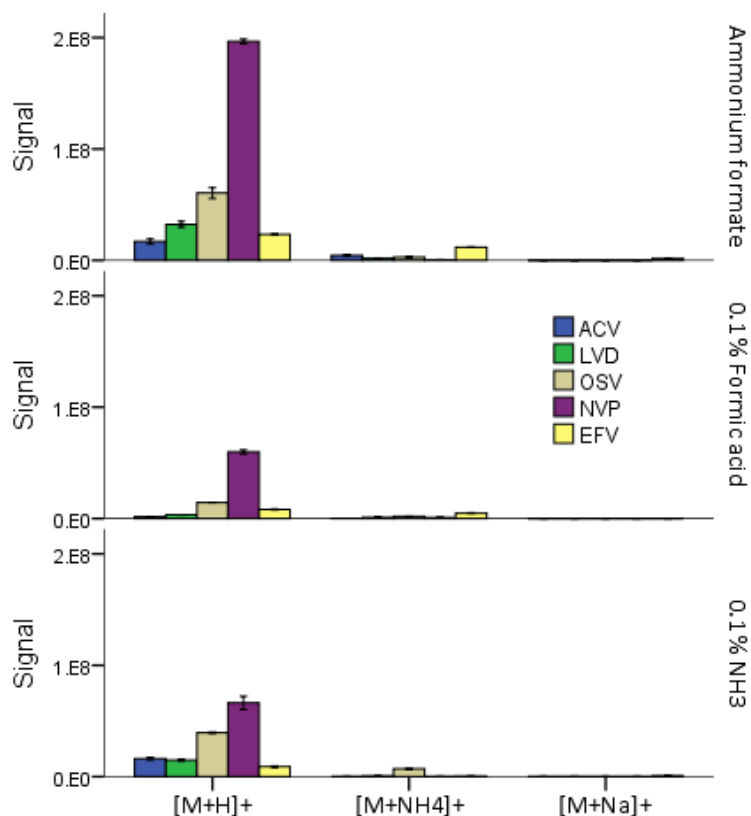
Figure 2.16: ESI signal ion count intensities from protonated, ammoniated and sodiated ion adducts obtained from separate eluents (n=3, ±SD)

Figure 2.16 shows that the protonated adduct yielded approximately seven times higher magnitude ion count response than the other two adducts' signal response in all three tested mobile phases. The dominance of the protonated ion was beneficial because multiple adducts generating comparable intensities may sometimes induce signal suppression (Kruve and Kaupmees, 2017). Therefore, the adduct was selected for subsequent identification and quantification purposes. While various factors impact the ESI ion count signal, adding trace amounts of aqueous ammonia to an eluent significantly increases the protonated ion signal via gas-phase proton transfer from the ammonium ion (Jin Yang et al., 2013). Therefore, the high protonated signal in the AmFo mobile phases was enhanced by 0.1 M aqueous ammonia solution pH adjustment. The ESI signal response of 11 protonated pharmaceutical analytes analyzed with NH$_4$OH amended additive at pH 8.2 was 2-6 times higher than in an identical

ammonia solution adjusted to a lower pH (pH 6.6). At the same time, the signal was 110 %

higher than in 0.1 % formic acid in the aqueous solution mobile phase (Jin Yang et al., 2013),

which is consistent with the observation in the present research.

2.3.8 Electrospray ionization mode

The analytical runs were tested in three ionization modes, positive, negative and switching

modes, to determine the most appropriate approach to generate the highest ESI signal

response and be adapted for subsequent analytical runs.
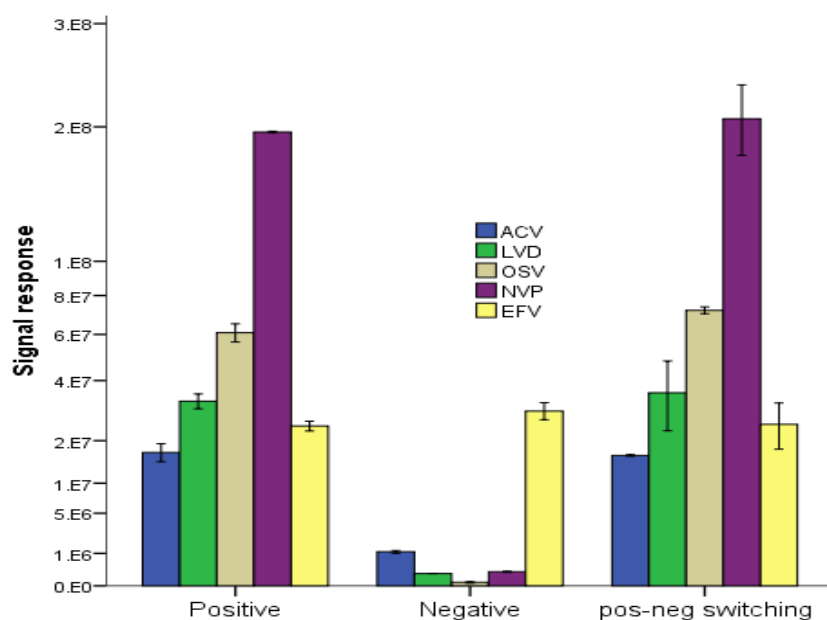
Figure 2.17. ESI ion count signal response generated at the positive, negative, switching mode
(n=3 ± SD).

Figure 2.17 shows that the negative mode generated the lowest signal response,

approximately 85 % times lower than the signal generated in the positive and switching mode.

The ion count from the positive-negative switching mode was 2 % higher than the positive

ionization mode signal. However, the variation in response in the switching ionization mode

was wider between individual molecules. A noteworthy observation was that, of all the ARVD

molecules, EFV exhibited constant and identical signal responses across all ionization modes,

including the negative mode. Henriksen et al. (2005) reported that acidic molecules might be preferentially analyzed in the negative ionization mode compared with basic molecules. In Table 2.1, Mosekiemang et al. (2019a), Barreiros et al. (2017), and Adeola et al. (2021) show that the molecule is frequently analyzed in negative ionization mode. Herein, all molecules were analyzed in the positive ionization mode. Usually, tuning the mass spectrometer to either positive or negative operating mode is guided by the proton affinity of the compound. Basic analytes are preferably analyzed in the positive mode as they can be protonated to form cations. Acidic molecules are deprotonated and detected in the anionic form using the negative mode (Henriksen et al., 2005; Steckel and Schlosser, 2019).

2.4 Conclusion

Data analyzed in the study showed that high-pH additives are sufficient to induce better selectivity, up to 5- times higher signal response and two times higher resolution in the analyses of both acidic and basic ARVDs. MeOH induced higher resolution and signal response at high pH than acidic eluents. Ammonium formate (10mM, pH 8.7), amended with aqueous ammonia, was selected as the aqueous mobile phase and methanol as the organic modifier. While there was minimal difference in the signal response between the C18 and phenyl-hexyl columns, the latter had superior resolution and produced desirable late-appearing peaks. Of all molecules, the efavirenz signal response was constant in both negative and ionization modes. However, its signal was 100- times lower when MeCN was used as an organic modifier. While positive-negative switching mode induced a comparable signal response to positive mode only, it was accompanied by wide variability.

Chapter 3

Uptake, Accumulation and Impact of Antiretroviral and Antiviral Pharmaceuticals Compounds in Lettuce (*Lactuca sativa*) grown in a Hydroponic Environment

This chapter is an edited version of the article:

Overview

This study evaluated the root uptake mechanism of the ARVDs compounds in a lettuce plant that was hydroponically grown in a nutrient solution containing the ARVD pharmaceutical mixture in the 1-100 µg L^{-1} concentration range. The measured bioaccumulation showed that efavirenz and lamivudine accumulated the highest and lowest at concentrations of 3463 ng g^{-1} and 691 ng $g^{-1,}$ respectively. The translocation factor between the root and leaf for nevirapine was greater than 1. The highest concentration of the pharmaceutical mixture had a physiological impact on the Lettuce. Potential toxicity was evidenced by a statistically significant 34 % (p = 0.04) mean reduction in root and leaf biomass in the 100 µg L^{-1} ARVD exposed Lettuce compared with the controls. This study showed that when exposed to plant roots, ARVDs can accumulate in plants and act as a sink for ARVD molecules in an agroecosystem. It further elucidates the plant-root interactions and the ensuing mechanistic uptake of ARVDs based in plants based on the molecule's physical-chemical interactions and the potentially toxic effects of ARVDs on plants.

3.1 Introduction

Uptake of pharmaceutical (APIs) molecules by plants has been measured in contaminated aquatic and terrestrial environments (Ahmed et al., 2015; Goldstein et al., 2014; Hurtado et

al., 2016; Stacia R et al., 2014; Ben Mordechay et al., 2018; Paz et al., 2016; Carter et al., 2018a; Kodešová et al., 2019).

Contamination of plants via uptake by ARVDs is a public health concern, primarily because of the toxicity of ARVDs. A Q-SAR modelling study revealed that ARVDs were highly potent. In a class of 50 therapeutic APIs, ARVDs were predicted to be among the top eight most hazardous drugs (Sanderson et al., 2004). Furthermore, concerns about long-term risk from the untargeted wide-scale release of ARVD into the environment is the potential development of antiviral resistance in microorganisms (Jain et al., 2013; Bártíková et al., 2016; Nannou et al., 2020).

In agroecosystems, besides the public health concern on contamination of food crops, is that APIs may also induce toxic effects on plants affecting their physiological and development processes (Christou et al., 2018; Hillis et al., 2011; Liu et al., 2013; Rede et al., 2019; Sun et al., 2018). A review of the impacts of APIs on plants revealed several toxic effects brought by antibiotics, anti-parasitic drugs, hormones, growth promoters and antifungals on plants but hardly provided any information on the physiological impact of ARVDs accumulated in plants (Bártíková et al., 2016). For example, the leaves exhibited burn-like features when the cucumber was exposed to a mixture of 17 pharmaceutical molecules at up to 1000 µg L-1 (Sun et al., 2018).

Plant-API uptake studies with an African perspective include Sibeko et al. (2019). They opportunistically detected non-steroidal anti-inflammatory drugs (NSAIDs) naproxen, ibuprofen, and diclofenac at concentrations of up to 12 ng g^{-1} in water hyacinth (*Eichhornia crassipes)* in river water in South Africa. Similarly, three antiretrovirals, emtricitabine, tenofovir disoproxil and efavirenz, accumulated at concentrations of 0.97 to 29.6 ng g^{-1} in

water hyacinth in wastewater treatment ponds (Mlunguza et al., 2020a). This latter study highlights the propensity of ARVD uptake in the natural aquatic environment. For these reasons, there is a need to elucidate the uptake mechanisms involved accurately. Such an implementation demands structured and systematic experiments, hence the present research. This study investigated the uptake of the four characteristically different ARVDs into Lettuce (Lactuca sativa). The advantage of hydroponic experiments is that they provide test conditions to rapidly screen and identify priority APIs that exhibit the highest uptake potential, which can inform in-depth plant–API fate studies. A drawback, however, is that hydroponic studies do not provide the complexity of a natural agroecosystem environment (Wu et al., 2015). Uptake processes can be either passive or active processes (Kumar and Gupta, 2016). This study focussed on active processes (solute specific), i.e. it solely concentrated on the molecule's characteristics rather than the existing environmental conditions.

3.2 Materials and methods

3.2.1 Preparation of standards and stock solutions

Preparation and storage of stock solutions and standards followed the European Commission (SANTE/11813/2017, 2018) guidelines. LVD and OSV stock solutions were prepared in 50 % (v/v) MeOH: HPLC water solution. NVP and EFV stock solutions were made in 100 % MeOH. The standard mix was prepared in a common vial at 1 mg L^{-1} and was diluted to the appropriate working concentration.

3.2.2 Liquid Chromatography – High-resolution mass spectrometry

Analyte separation was performed by liquid chromatography (Dionex Ultimate 3000, Thermo Scientific) on a PhenylHexyl (*Ace ultracore*) (2.5 μm × 100 mm) stationary phase. The column

temperature was isocratic at 50 °C. The analytical run time was 9.8 min, starting from a mobile phase composition of 100 % 10 mM ammonium formate adjusted to pH 8.4 before transitioning to 100 % MeOH. The equilibration time was 2 minutes and a flow rate of 500 µL min⁻¹. The mass spectrometric conditions were unchanged and are listed in Table 2.3.

3.2.3 Method validation and optimization for extraction of ARVDs from the plant matrix

The performance characteristics of the method of analyses were evaluated using extraction recoveries of the analytes from plant material, instrument and method linearity, method limit of detection and quantification (MLoD and MLoQ) and evaluation of matrix effects (ME).

3.2.3.1 Determination of extraction pH and recoveries

The ultrasonic-assisted extraction (UAE) approach adapted from (Wu et al., 2012) was employed to extract analytes from the plant matrix. Fresh Lettuce sourced from a local grocer was washed with high-purity water (HPW), chopped and freeze-dried. The freeze-dried sample was ground to powder. The recovery experiment was performed at two spiking levels, 10 ng g⁻¹ and 50 ng g⁻¹. A 0.2 mass of ground lettuce was placed in a 50 mL polypropylene centrifuge tube and spiked with the four ARVD external standard mix stock to attain the two desired spiking levels. Spiked samples were allowed to equilibrate for 24 hours. A 10 mL aliquot of the extraction solvent (MeOH: MeCN; 1:1, v/v) was added to the sample, and the tube was placed in an ultrasonic bath operated at 50 Hz for 15 min. The resulting supernatant was collected and centrifuged at 4000 rpm for 5 min. The sample residue was re-extracted, and the supernatants were combined before solvent reduction to ca 500 µL under a gentle stream of nitrogen gas. The reduced extract was diluted with 20 mL HPW water and then filtered through a 0.7 µm glass fibre filter (GF/F). The optimal extraction pH was obtained by

extracting a set of samples (n = 3) at four pH values, i.e. pH 2.4, 5.4 (native sample pH),7.4 and 9.4.

3.2.3.2 Solid-phase extraction/clean-up

Solid-phase extraction was implemented using a 60 mL HLB sorbent (Waters, UK). Before sample loading, the sorbent was conditioned sequentially with MeOH and HPLC water (2.5 mL aliquots). The 20 mL sample extract was loaded onto the cartridge at a rate of 2 mL min^{-1}. After loading, the sorbent was dried and washed with 1 mL of HPLC water. Two aliquots (2 x 2.5 mL) of the extraction solvent mix were used for sample elution. The 5 mL extract was evaporated to almost dryness and reconstituted to 1 mL with 30 % MeOH in water. Finally, the 1 mL sample was filtered using a 0.22 μm GFF filter and stored at 4° C in the dark awaiting analysis.

3.2.3.3 Linear range, method detection limits (MLoD andMLoQ) and matrix effect

The LC-HRMS was calibrated at the $0.1 - 100$ μg L^{-1} concentration range using matrix-matched (MM) standard solutions prepared according to EU (SANTE/11813/2017, 2018) guidelines. The stock solution (ARVD mix standard) in the MM made up 10 % of the total standard solution volume, and the remaining 90 % comprised the unspiked plant extract. The MLoD and MLoQ were calculated according to the ICH guidelines (ICH, 1995), based on the calibration curve of the MM working standards. Potential background contamination from the locally obtained lettuce was investigated by screening the extract for the four analytes of interest. Matrix effects (ME) were evaluated by comparing the slope of the calibration curve in the matrix with the slope of the calibration curve using solvent Equation (3.1)

$$\text{Matrix effect (\%)} = \left(\frac{\textit{Slope of calibration curve in matrix}}{\textit{slope of calibtration curve in solvent}} - 1 \right) \times 100 \quad \text{(3.1)}$$

3.2.4 Hydroponic experiments

The hydroponic system was housed in a greenhouse. The experimental approach was adapted from the OCSPPC 850.4800 Plant Uptake and Translocation Test guidelines (EPA, 2012). Young lettuce seedlings (10 days old) of the *Analora* genus were obtained from Defland Nurseries, UK. Before the actual exposure test, the plants were exposed to a dilute water fertilizer solution for seven days to nurture and acclimatize the roots to a water-only environment. The lettuce seedlings were exposed to a nutrient solution spiked with the ARVDs at 3 concentration levels (1, 10 and 100 µg L^{-1}) for 21 days. The set-up consisted of 6 replicates per exposure concentration. In total, there were 24 lettuce plant samples. The sample containers (glass) were covered with aluminium foil, and the top was sealed to allow only the roots to be in contact with the nutrient solution. The solution was automatically aerated for 10 minutes every hour. The experiment was run for 21 days, with the exposure solution renewed on days 7 and 14. Loss of water due to evaporation and evapotranspiration during the growing period did not exceed 20 % of the initial volume of the nutrient solution placed at the beginning of each experiment.

3.2.5 Measurement of accumulation and physiological effect of ARVDs on Lettuce

After test termination, the plant samples were washed immediately with HPW and dabbed dry. Lettuce samples were separated into roots and leaves and then weighed. The harvested samples were freeze-dried and analyzed according to the optimized method described in

section 3.2.3. Potential physiological effects on the plant were assessed by comparing the control biomass (root and leaves) with the biomass ARVD exposed samples.

The uptake of ARVDs in this study was characterized using four parameters: bioconcentration factor (BCF), root concentration factor (RCF), leaf concentration factor (LCF) and translocation factor (TF), Equations (3.2), (3.3), (3.4) and (3.5) respectively. TF quantifies the movement of the organic analyte from the root to above-ground tissues.

$$BCF(mL/g) = C_{plant}/C_{exposure\ solution} \tag{3.2}$$

$$RCF\ (mL/g) = C_{root}/C_{exposure\ solution}a \tag{3.3}$$

$$LCF\ (mL/g) = C_{leaf}/C_{exposure\ solution} \tag{3.4}$$

$$TF(mL/g) = C_{leaf}/C_{root} \tag{3.5}$$

Where C_{leaf}, C_{root}, C_{plant}, and $C_{exposure\ solution}$ is the API concentration in the leaf, root, plant and nutrient solution, respectively (Emhofer et al., 2018; Goldstein et al., 2014; Hurtado et al., 2016).

3.2.6 Data analyses

Data were analyzed using Ms Excel 2016 and IBM SPSS Statistic v 24 software. One-way analysis of variance (ANOVA) and Dunnett's T3 test was used to measure statistical differences between means at the 95 % confidence interval.

3.3 Results and discussion

3.3.1 Method optimization

Recoveries and influence of pH on sample recovery

The objective of this test was to select the optimal pH of extraction of the target analytes. Extraction efficiency was tested across four pHs ranging from acid pH 2 to alkali pH 9.4 and

across two spike concentration levels. The recovery of an analyte in extraction experiments usually is concentration-dependent. Therefore, selecting an analytically appropriate spike level range is necessary during optimisation experiments instead of a single spike level (Thompson et al., 1999). Since pharmaceuticals are typically detected at the nanogram level in the environment, the ten ng g^{-1} and 50 ng g^{-1} levels were selected as critical spike levels for the recovery test.
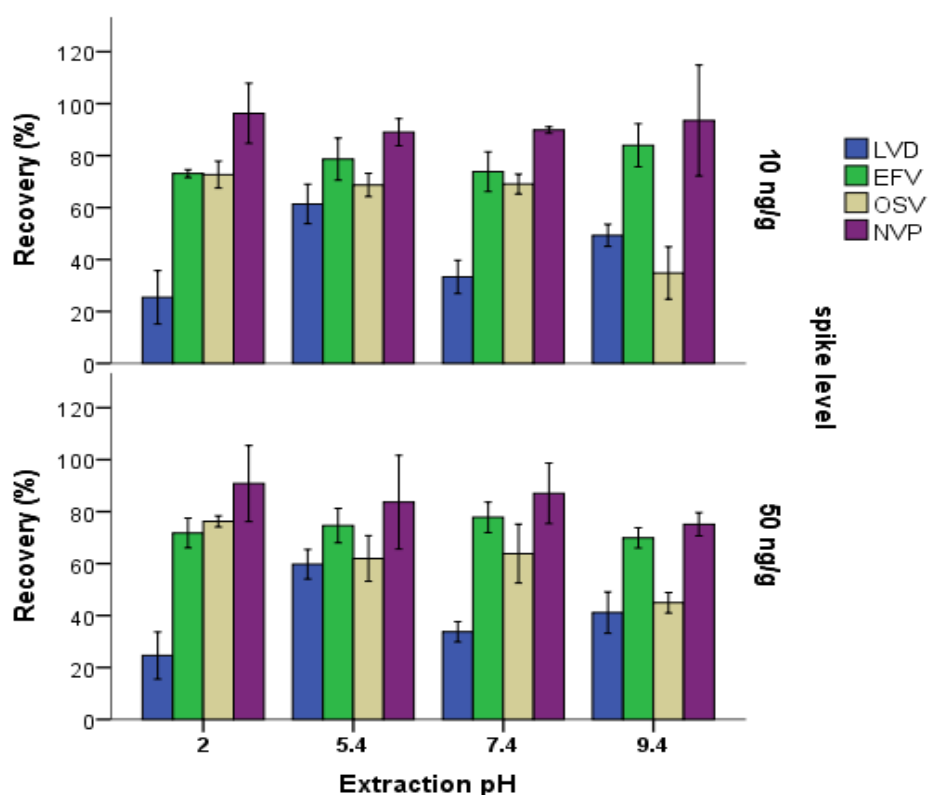
Figure 3.1 Extraction recoveries for the four analytes in the lettuce matrix at the 10 ng g^{-1} and 50 ng g^{-1} spike levels at the four extraction pH levels (n=3, ± SD)

The measured analyte extraction recoveries are shown in Figure 3.1. Cumulatively evaluated across the two spike levels. Cumulatively across the two spike levels, the mean ARVD recoveries did not vary significantly (p=0.55), 68 ±21.8 % (± SD) and 64 ± 19.2 % for the 10 ng g^{-1} and 50 ng g^{-1} levels, respectively. Individually, NVP exhibited the highest recoveries (mean 88.1 %). EFV and OSV exhibited the second and third-highest recoveries at 75.4 % and 61.5 %,

respectively. LVD yielded the lowest recoveries, an average of 41.7 %. Variation of least influenced NVP and EFV recoveries. OSV recoveries were relatively consistent across three (pHs 2-7.4) but minimally dropped in a high pH environment. In contrast, LVD recoveries varied widely, ultimately contributing to its low mean recoveries, which were approximately 40 % lower across the pH range.

Cumulatively, the highest ARVD extraction means recoveries were obtained at pH 5.4 (72.2 %). At pH 2.0, 7.4 and 9.4, mean analyte recoveries of 66.3 %, 66.0 % and 61.5 %, respectively, were obtained. While EFV and NVP at pH 5.4 had recoveries of > 70 %, LVD and OSV exhibited recoveries of < 65 % in the same environment. The EU SANTE/11813/2017 guidelines state that satisfactory extraction recoveries may vary between 70-120 %. Nonetheless, it clarifies that reproducible recoveries of 30-70 % are also acceptable. For this reason, pH 5.4 was selected as the optimal pH for subsequent extraction procedures. Noteworthy to mention is that pH 5.4 was also the native extraction pH, so extraction implies that subsequent buffer additions were unnecessary.

3.3.2 Linearity, MLoD and MLoQ

Whereas the relationship between the analyte signal and the analyte in solution is often linear, the relationship between the analyte signal and the analyte in the matrix is not routinely linear due to the influence of matrix components (Kruve et al., 2015). For this reason, linearity was assessed using an analyte in the matrix.

Table 3.1 shows that the analyte in matrix linearity was satisfactory at $r^2 > 0.990$.

Table 3.1. Summary data for linearity, MLoD, MLoQ and matrix effect

ARVD	Linearity		Detection limits		Matrix effect
	Pure solvent (MeOH) (r^2)	In matrix (r^2)	Method LOD (ng g^{-1})	Method LOQ (ng g^{-1})	(% ion suppression)
Lamivudine	0.994	0.998	1.66	5.53	32
Nevirapine	0.999	0.995	3.87	12.9	50
Oseltamivir	0.999	0.998	1.51	5.13	50
Efavirenz	0.994	0.990	5.61	18.7	46

Likewise, the detection limit is also matrix-dependent (Kruve et al., 2015b) accordingly, matrix-spiked samples were used to determine MLoD and MLoQ. The MLoD of the ARVD analytes varied from 1.51 to 5.61 ng g^{-1} and the MLoQ from 5.13 to 18.7 ng g^{-1}

3.3.3 Matrix effects (ME)

Ultrasonic extraction mechanically breaks down the sample matrix, allowing the target analytes to release (Tadić et al., 2019;Schantz, 2006). Its drawback, however, is its lack of selectivity, necessitating intensive clean-up processes (Ros et al., 2016). It was necessary to evaluate the effect of the matrix on the detection of analytes. As indicated in

Table 3.1, the matrix effect induced ion suppression in all the analytes. LVD experienced the lowest ion suppression at   32 %. NVP, OSV, and EFV, on the other hand, showed ion suppression ranging from 46–50 %. In the classification of ME, according to (Barreales-Suárez

et al., 2018), ME < 20 % is considered low, 20 - 40 % as medium, 40-60 % as high and ME as 60 % as very high. The measured ME varied in the medium to high-level region, indicating significant signal suppression. ME following the UAE-SPE method has been reported elsewhere. For example, ME of 26 -29 % were noted during the analyses of antibiotics in four vegetable matrices (Tadić et al., 2019), and ion suppression of 30 - 60 % was measured in the analyses of 7 antibiotics in lettuce (Albero et al., 2019). Overall, the data from this study is consistent with Furey et al., 2013) and Tadić et al. (2019), who suggest that signal enhancement or suppression due to the matrix is unpredictable. It presents itself unsystematically and indiscriminately and is, therefore, unique for each analysis.

3.3.4 Accumulation of ARVDs in the lettuce plant

The magnitude of accumulation of the ARVDs in the plants from each nutrient solution is shown in Figure 3.2.
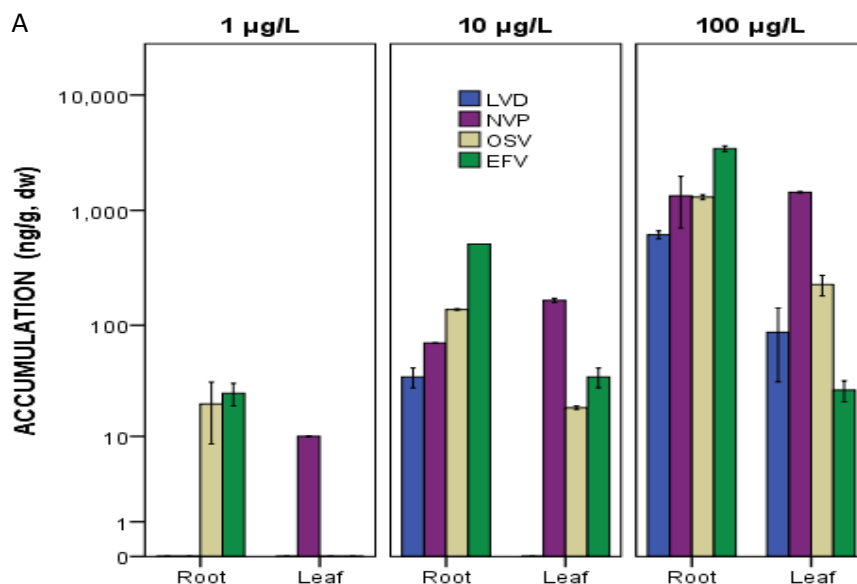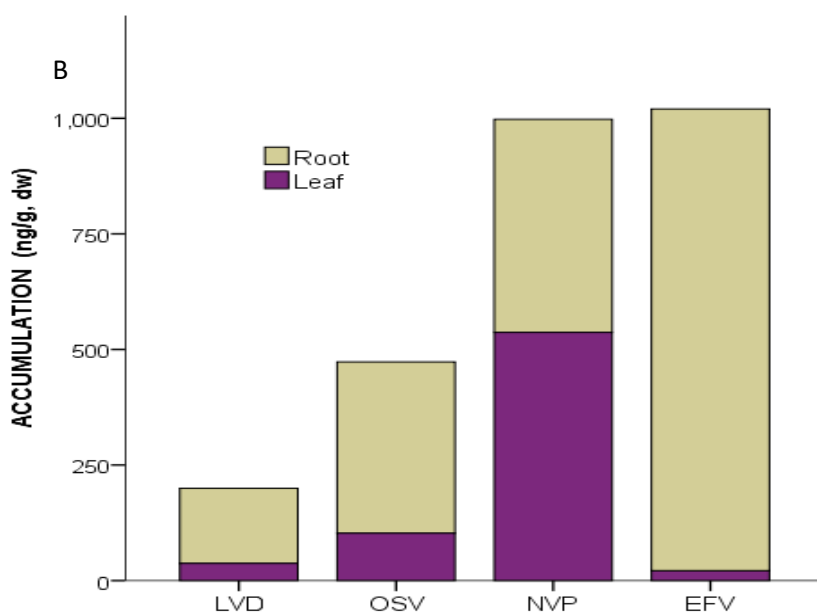
Figure 3.2. **(A)** Root and leaf accumulation concentrations (dry weight) across the three exposure levels in lettuce plants (n = 3, ± SD) **(B)** ARVD distribution between the root and leaf tissues averaged across the three exposure levels and a comparison of the magnitude of bioaccumulation between the individual ARVDs.

The four ARVDs studied had a molecular weight of < 400 Da; molecules of this size may penetrate the root via the epidermis into the bulk of the root (Miller et al., 2015). At the lowest exposure concentration (1 µg L^{-1}), the accumulation of LVD, OSV, and EFV in the leaf was below the MLoD and was not quantified. Similarly, in NVP and LVD, root concentrations for NVP and LVD were below the detection limit.

The overall plant accumulation of the ARVDs in the Lettuce varied from < MLoQ to 3463 ng g^{-1} and < MLoD to 1647 ng g^{-1} for the root and leaf, respectively, across the three exposure levels. EFV exhibited the highest total tissue biomass accumulation (3463 ng g^{-1}) measured in the 100 µg L^{-1} exposed sample. This accumulation was five times higher than the concentration of the lowest accumulated ARVD, LVD (691 ng g^{-1}) in the same treatment level.

NVP and OSV accumulations were 2625 ng g^{-1} and 1541 ng g^{-1}, respectively, in the 100 µg, L^{-1} exposed samples.

The extent of accumulation over the three exposure levels was such that the higher the concentration of the API in the nutrient solution, the higher the measured accumulation, which is consistent with Al-Farsi et al. (2017 and González García et al. (2018) reports. In separate hydroponic API exposure experiments, their research showed that the magnitude of accumulation is directly associated with the pharmaceutical concentration in the exposure solution. In the current study, the mean plant concentration factor (CF) rise between the 1 µg L^{-1} and 10 µg L^{-1} treatment was 17 ± 9.3 (± SD), while the CF between the 10 µg L^{-1} and 100 µg L^{-1} treatment was 12. ± 5.7 (± SD). Cumulatively, the mean increased CF in the plant matrix between the lowest (1 µg L^{-1}) and highest exposure solution treatment (100 µg L^{-1}) was 189 ± 87.5.

The RCF, BCF and TF values discussed herein are the means across the 10 µg L^{-1} and 100 µg L^{-1} exposure levels. Figure 3.2B illustrates that more than 80 % of the OSV and LVD API mass fractions accumulated in the roots, whereas EFV root accumulation was higher than 95 %. Accordingly, the RCFs were such that EFV > OSV > NVP > LVD (0.043 > 0.013 > 0.08 > 0.05 mL g^{-1}, respectively. BCF (mL g^{-1}) was evaluated to determine accumulation in the bulk of the plant. The mean BCF across the ten µg L^{-1} and 100 µg L^{-1} exposure region showed that EFV had the highest whole plant tissue accumulation. The ascending order with regards to BCF was EFV > NVP > OSV > LVD at (0.044 > 0.025 > 0.016 > 0.005 mL g^{-1}.

Regarding transport within the plant, NVP exhibited the highest TF values, with Figure 3.3 indicating that it was readily translocated to the leaves. Typically, a TF (L g^{-1}) > 1 suggests that

a molecule can indeed migrate from the roots and its largest fraction accumulate in the above

root tissues (Chuang et al., 2019).
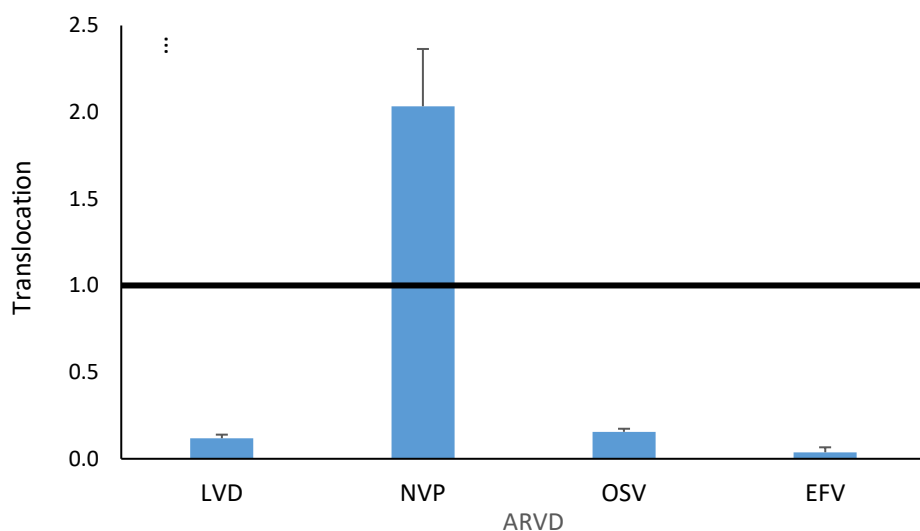
Figure 3.3. Translocation factors (TF) of the ARVDs compounds (n=3, ±SD)

Therefore, a TF > 2 implied that NVP was twice more likely to bioaccumulate in the leaves.

3.3.5 Relationship between Log D_{ow} and extent of uptake

As highlighted in section 1.2, there is little information on the plant uptake of ARVDs. For this

reason, the discussion in this study will refer to and relate to pharmaceutical compounds of

different therapeutic groups but with comparable physicochemical characteristics to the

ARVDs studied here.

An API's solubility, hydrophobicity, molecular weight and ionization tendencies may influence

its uptake potential (Al-Farsi et al., 2017; Chuang et al., 2019). Of all factors, the octanol-water

partitioning coefficient (log K_{ow}) is possibly the most extensively investigated API property

influencing uptake. For non-ionic compounds, log K_{ow} is linearly related to uptake (Collins et

al., 2006; Prosser et al., 2014a). However, log K_{ow} is adjusted to log Dow for ionizable

compounds to reflect the environmental pH. The present study was conducted at a constant nutrient solution pH of 6.5.

Characterization of the relationship between log D_{ow} and uptake of the APIs was achieved by plotting to log D_{ow} against log BCF, RCF, and TF, respectively, as shown in Figure 3.4.
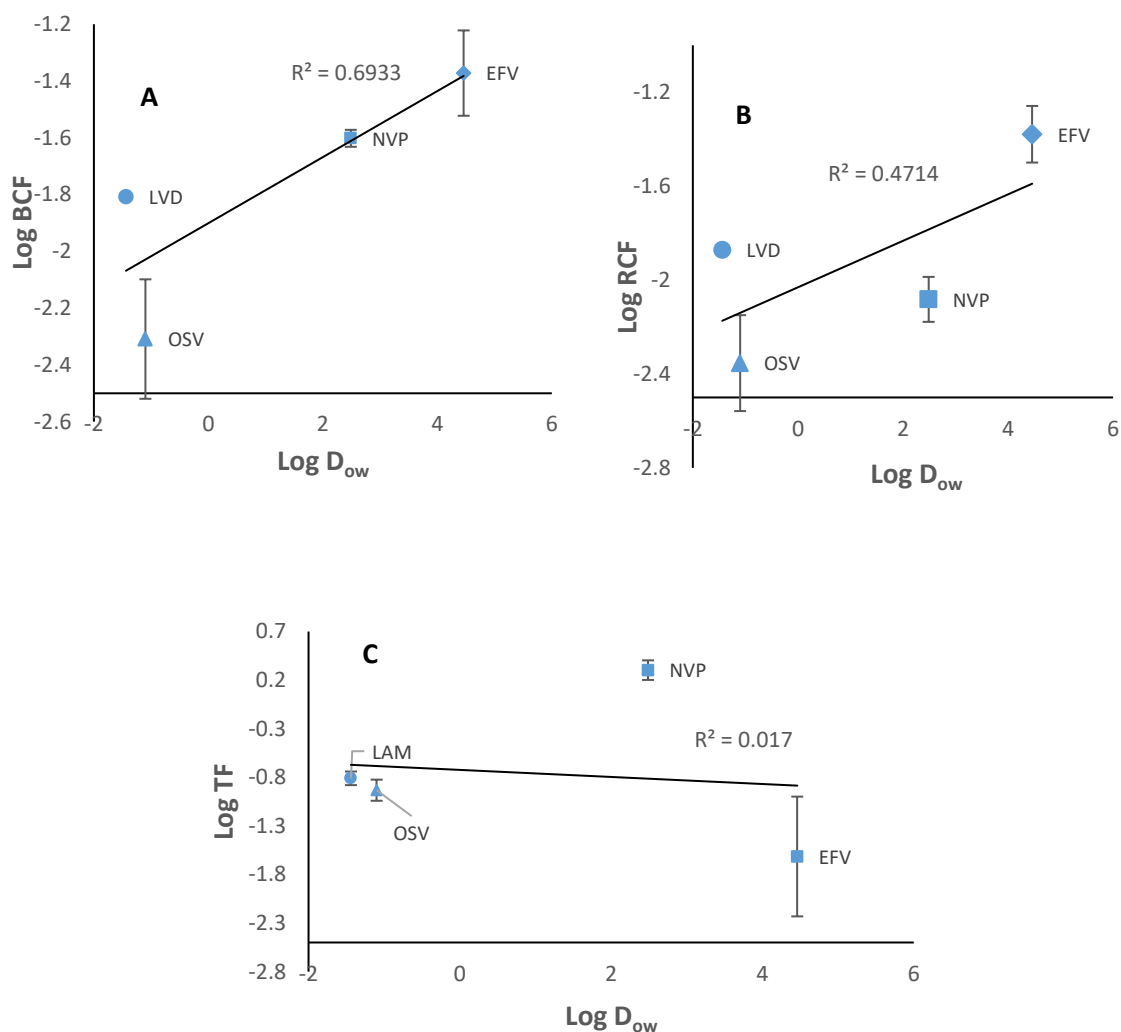
Figure 3.4. **A:** Linear relationship between Log Dow and BCF **(B)** Relationship between Log Dow and RCF, **(C)** Relationship between Log Dow and RCF

BCF exhibited an R^2 value of 0.69, as indicated in Figure 3.4 A. Linearity, in this case, was influenced mainly by the neutral and lipophilic NVP and EFV (Table 3.2)). The hydrophilic LVD and OSV (log Dow = -1.1 and -1.44, respectively)hardly contributed to the measured linearity.

Inspection revealed that if the log K_{ow} of OSV were unchanged, stronger linearity, $R^2 = 0.97$ value would have been realized. For this reason, log D_{ow} of hydrophilic ionizable molecules (in this study OSV and LVD) may not accurately describe uptake in plants.

The relationship between the RCF and log D_{ow} $R^2 =0.47$ is shown in Figure 3.4B. It was 30 % weaker than the relationship between log D_{ow} and BCF ($R^2=0.69$). Other factors besides hydrophobicity likely appeared responsible for the root uptake (or its lack thereof). For this reason, it was more logical to relate whole plant accumulation (BCF) with hydrophobicity rather than RCF. Similarly, (Chuang et al., 2019) reported a weak relationship ($R^2 = 0.293$) between the RCF and log D_{ow} in Lettuce exposed to 13 ionizable APIs via hydroponic growth. Again, Miller et al., (2015), in an extensive review of plant API uptake, concluded that there is hardly any statistically significant relationship between LCF and hydrophobicity. It may be plausible to extend this inference to RCF.

As shown in, Figure 3.4C, no relationship existed between log D_{ow} and TF, $R^2 = 0.017$. This is consistent with Chuang et al. (2019) and Li et al. (2019), who established no statistically significant relationship between hydrophobicity and TF for APIs with log D_{ow} from -3 to 4.

3.3.6 Speciation of ARVD compounds and influence on plant uptake

The cell walls of plant root hairs are negatively-charged. As a result, the uptake of anionic molecules is constrained by the electrostatic repulsion by the root hair cells (Trapp, 2000; Miller et al., 2015; Christou et al., 2019). The root cell wall is approximately 0.4 µm thick and composed of polysaccharides which naturally reduce the cell wall permeability to solutes. Physiologically the cell vacuole is larger than the cytoplasm, occupying up to 95 % of a plant cell's volume. It has a pH of 5.5 compared to pH of 7 of the cytoplasm. Nonetheless, it is the cytoplasm that is in contact with the root cell wall (Trapp, 2000; Goldstein et al., 2014), and

the transport of molecules is predominantly via the symplastic pathway (through the cell's cytoplasm) rather than the apoplastic pathway (Goldstein et al., 2014; Pan et al., 2014; Prosser et al., 2014b; Al-Farsi et al., 2017).

Table 3.2. ARVD speciation at test pH (pH 6.5)

ARVD	Log K_{ow}[a]	Log D_{ow} (pH 6.5)[a]	Neutral fraction (%)[a]	Ionic fraction (%)[a]
Lamivudine	-1.09	-1.10	99.3	0.7 cationic
Oseltamivir	1.2	-1.4	0.2	99.8 cationic
Nevirapine	2.5	2.5	100	0
Efavirenz	4.5	4.5	100	0

[a] Chemaxon https://chemaxon.com/

OSV was the only ARVD fully ionized at the pH of the growing medium (pH 6.5), being 99.8 % in the cationic form (Table 3.2). OSV was, therefore, electrostatically attracted to the negatively charged root hairs. In contrast, LVD, NVP, and EFV were predominantly neutral at the exposure pH. However, strong retention due to sorption could have impeded the permeation of the highly cationic OSV further into the roots. One may relate the characteristics of OSV to the antibiotic trimethoprim (TMP). At pH 5.8 (approximately one pH unit lower than this study pH), TMP was chiefly cationic (95%) and exhibited a log D_{ow} of -0.43. In Chuang et al., (2019), lettuce was exposed to 50 µg L^{-1} of TMP in a hydroponic-based experiment. The concentration of TMP in the leaf was < 25 % of the API's total accumulation, which is similar to the OSV leaf accumulation measured (< 20 %) in this study (Figure 3.2B). TMP also exhibited a TF value of 0.1, demonstrating its limited ability to be translocated to the above root tissues.

In contrast to OSV, NVP (log D_{ow} 2.5) was neutral and exhibited the highest TF of the four ARVDs, Figure 3.3. NVP lies in moderate hydrophobicity (1 < log Dow < 3). Organic molecules within this hydrophobic window region exhibit the highest predisposition to be transported above root tissues (Li et al., 2019a). Kumar and Gupta (2016), in Figure 3.5, illustrate the sigmoidal relationship that exists between the transpiration stream factor (the ratio of the amount of the contaminant in the xylem to exposure medium) and log K_{ow}, whose maxima lie in the range between log K_{ow} 2-2.5, a region consistent with NVP's log K_{ow}.
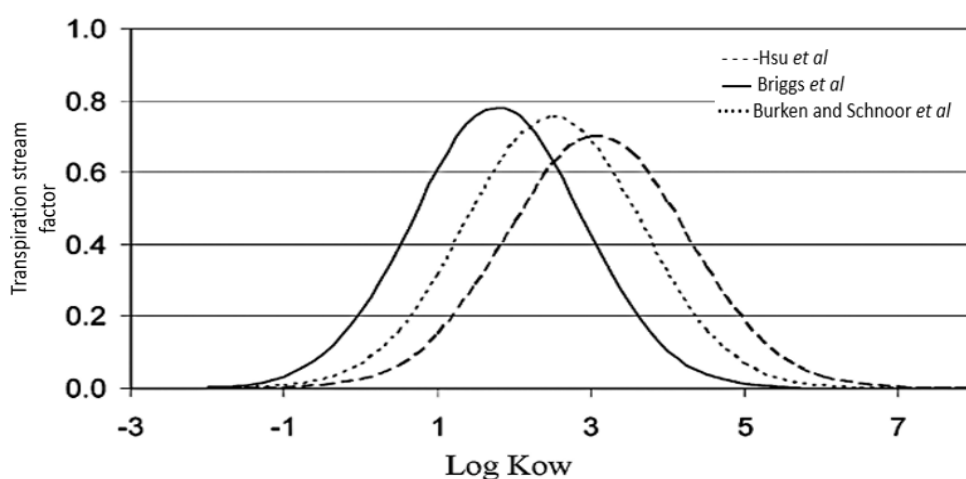
Figure 3.5. Sigmoidal relationship between transpiration stream concentration factor with hydrophobicity postulated by (Briggs et al. 1982; Burken and Schnoor, 1998; Hsu et al., 1990) (Abstracted from (Kumar and Gupta, 2016)

Carbamazepine (CBZ) has comparable characteristics to NVP (i.e., log D_{ow} 2.5 and neutral charge). Lettuce under hydroponic conditions exhibited the highest TF among 13 APIs in lettuce (Chuang et al., 2019). The concentration of CBZ was 82 % higher in leaves compared to roots in three varieties of Lettuce irrigated with CBZ-spiked treated wastewater (González García et al., 2018). This phenomenon thus provides the most definitive account in describing the measured NVP's high TF value.

EFV exhibited the highest whole-plant bioaccumulation in Lettuce compared to the other ARVDs (Figure 3.2 B). However, more than 95 % of its mass was measured in the roots, presenting the highest RCF value. Characteristically, EFV was unionized and neutral at the experimental pH. Organic compounds with log D_{ow} > 4.5 hardly experience significant translocation to above-ground tissues (Kumar and Gupta, 2016).

However, it will be expedient to perform root EFV sorption experiments better to comprehend EFV's high accumulation tendencies on the roots. Sorption tests will facilitate accurate estimation of EFV that was adsorbed onto the root surface and the actual fraction that permeated into the bulk of the roots. Uncertainties on the accurate accumulation of highly lipophilic molecules were reported by Boxall et al. (2006), and Miller et al. (2015) whereby, for example, reported a significant amount of APIs was detected on the exterior of root crops (peels) following rather than the core of the plant. In this study, an assumption was made that the bulk of the EFV permeated into the root. It then implies that the EFV did not migrate to the vascular tissues (i.e., the phloem and xylem). According to (Collins et al., 2006), neutral non-ionizable organic compounds with log K_{ow} (> 4) are primarily retained by the lipid cell components in the endodermis. They do not reach the vascular tissues for subsequent transport to the above root tissues. As EFV was in its neutral form and log D_{ow} = log K_{ow} = 4.3 (Table 1.2), it was not likely that it partitioned through the vascular tissue and was primarily retained at the endodermis. The interaction between EFV and the plant root in this research is analogous to the diclofenac (DCF) accumulation in lettuce (González García et al., 2018). DCF, an NSAID, has a log D_{ow} of 4.5, which is similar to EFV, but differs in terms of pK_a. (González García et al., 2018) measured 89 % of DCF on lettuce roots. Likewise, Zhang et al., (2012) reported higher root accumulation factors (0.40-1.36 mL g^{-1}) of DCF in the roots of the

macrophyte *Scirpus validus,* compared with the shoot accumulation (0.17–0.51 mL g^{-1}). These two studies affirm that the roots retain highly hydrophobic APIs (log Dow > 4).

LVD exhibited the lowest bioaccumulation in lettuce (Figure 3.2B). Characteristically, it presents with the lowest log D_{ow} value. As with OSV, minimal accumulation of LVD was attributed to its hydrophilic nature. Low lipophilicity implies minimal permeation into the lipophilic root cell membranes. LVD was primarily uncharged at the test pH. LVD uptake can be compared with caffeine, which is highly soluble in water and has a log K_{ow} value of -0.77. Accumulation of caffeine in cucumber leaves was lower than in the root (Goldstein et al., 2014). In contrast, Chuang et al. (2019) reported a TF value of > 1 for caffeine in Lettuce. These two conflicting degrees of uptake highlight the need for more in-depth investigations into the uptake of LVD and other similar hydrophilic molecules into vascular plant tissues.

3.3.7 Impact of ARVD on plant physiology

Accumulation of APIs in plants may induce toxicity (at high concentrations) or hormesis (at lower concentration levels) (Christou et al., 2018). Hormesis is a positive, non-distress effect experienced by a plant when exposed to small doses of xenobiotics, characterized by a non-linear dose-response relationship. Sometimes described by the unexpected increase in roots' length and the number or size of leaves (Agathokleous et al., 2018). Toxicity, on the other hand, presents as perturbations in plant growth, e.g. lowered germination rates, chlorosis, tissue deformation, and reduced length or mass of the root and shoot. Also, reduced reproduction rate and enzymatic activity (Liu et al., 2013; Bártíková et al., 2016; Christou et al., 2018; Sun et al., 2018). The current study focussed on the visible physiological effects on the measurable mass of the leaf and root.
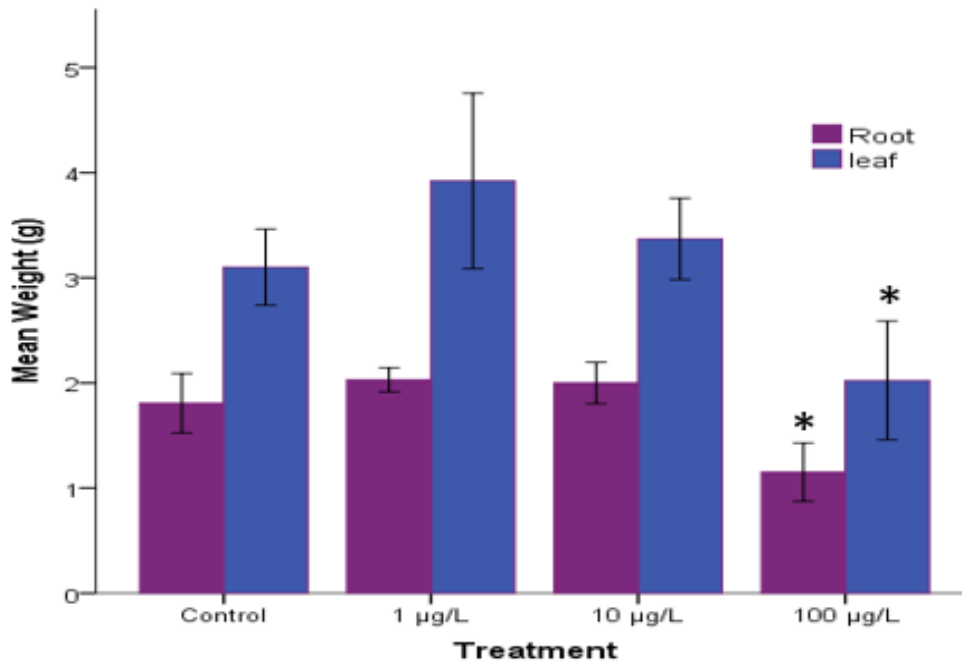
Figure 3.6. Variation of mean root and leaf biomass across the exposure concentration (0 – 100 µg L^{-1}) illustrates the potential impact of ARVD on lettuce biomass after a 21-day exposure period (n=6) (* denotes a significant difference with control)

Figure 3.6 shows the root and leaf mean wet weight (n=6) across the four concentration exposure levels (including the control). The control sample's mean biomass (root and leaf mass) differed (Dunnett's T3 test, p=0.039) from the 100 µg L^{-1} exposed sample. Likewise, the 1 and 10 µg L^{-1} treatment contrasted with the 100 µg L^{-1} treated sample (Dunnett's T3, p=0.012 and p=0.07, respectively). The mean root and leaf mass of the control was 1.8 ± 0.26 g (± SD) and 3.1 ± 0.34 g, respectively, while for the 100 µg L^{-1} exposed. Lettuce was 1.25 ± 0.32 g and 2.02 ± 0.53 g, respectively, representing a mean 34 % reduction in mass.

A 40 % decline in the root mass of ryegrass was measured when exposed to tetracycline applied at 1, 10 and 100 mg kg^{-1}. The significant difference in tissue mass between the control and ARVD-exposed samples was a likely indicator of the potential physiological effect of ARVDs. Root elongation of Lettuce was inhibited when exposed to a mixture of 10 antibiotics

at concentrations of 1, 10, 100, 1000 and 10000 µg L-1 Hillis et al. (2011). In the same study, shoot (leaf) inhibition was less impacted than the root. However, the physiological impacts of Wei et al. (2009) differ from this study in that the most significant biomass variation occurred in the shoots (leaves) rather than with the roots.

A possible hormetic influence was exerted on the 1 µg L^{-1} and 10 µg L^{-1} treated samples. An inspection of Figure 3.6 shows that the two sets of treated lettuce samples had relatively higher mean biomasses (though not significantly different, p=0.70 and p=0.96 respectively) of 18 % and 8 % higher, respectively, compared with the control. A comparable response was exhibited by *Phragmites australis* (common wetland plant) when exposed to a mixture of 3 antibiotics, ciprofloxacin, oxytetracycline and sulfamethazine in the 0.1 -1000 µg L^{-1} concentration range (Liu et al., 2013). Hormetic response (on root activity) was evident at the lower exposure level (0.1 - 10 µg L^{-1}) and not in the > 100 µg L^{-1} treatment range. Root activity in the 0.1 - 10 µg L^{-1} exposed plants displayed a negative inhibition rate. In contrast, toxicity was dominant in the 100 and 1000 µg L^{-1} exposed plants, depicting a positive inhibition of root activity at 18 % and 36 % compared to the control.

3.4 Conclusion

This study provides an optimized protocol for determining ARVDs in biological matrices. It also provides evidence of ARVD uptake in plants. Moreover, it shows that ARVDs' interaction with plant roots can be related to other APIs of similar physical-chemical characteristics. Uptake is primarily influenced by molecules' hydrophobicity of the ARVDs, however, along the confines of a sigmoidal relationship. At low and high concentration levels, a mixture of ARVDs induces both hormetic and toxic effects on plants.

Chapter 4
Screening for anti(retro)viral pharmaceuticals metabolites in lettuce using LC-HRMS
Overview

This section investigated the likelihood of in-plant biotransformation of accumulated ARVDs in lettuce. Analyses were executed under full-scan high mass resolution using the single-stage orbitrap mass spectrometry approach. Two metabolites, lamivudine sulfoxide and 12-hydroxyl-nevirapine glucuronide were detected in the root and leaf tissues. The metabolites were detected in the samples exposed to the most concentrated solution. A semi-quantitative examination showed that each metabolite was equally concentrated in the leaf and root tissue. This study contributes to understanding the fate of pharmaceutical compounds in the environment, particularly the natural biodegradation of pathways of antiretroviral pharmaceutical compounds in the environment.

4.1 Introduction

Enzymes catalyze the diverse chemical transformations in plants identically, like the mammalian liver (Miller et al., 2015). The cytochrome CYP 450 enzyme is often associated with the biotransformation of xenobiotics in plants (Chefetz et al., 2019). Biotransformation reduces an exogenous chemical biological half-life, accelerating its excretion from a plant. The process enhances its hydrophilicity by incorporating polar functional groups, such as hydroxyl and amino functional groups, within the molecule (Cole, 1994; MacHerius et al., 2012; Wu et al., 2016; Dudley et al., 2019; Sheludko et al., 2020; Wu et al., 2016). The extent and rate of detoxification are usually plant-specific (Chefetz et al., 2019; Coleman et al., 1997).

 A summary of in-plant API biotransformation-related studies (2017-2020) shown in Table 4.1 reveals little information on the biotransformation of several pharmaceuticals, including

ARVDs. Existing literature mainly highlights in-plant biotransformation of nonsteroidal anti-inflammatory drugs (NSAIDs) and antibiotics. For example, Klampf (2019) reported on the transformation of carbamazepine and diclofenac, which are persistent in the aquatic environment. Tian et al. (2019) showed the biotransformation of the antibiotics clarithromycin and sulfadiazine. Biotransformation products of ARVDs, e.g., acyclovir, penciclovir and oseltamivir, were detected in wastewaters, blood, urine, and saliva (Lindegårdh et al., 2007). This breakdown product shows their predisposition for transformation, suggesting the need to investigate their fate in plants.

Sometimes biotransformation products could be more toxic and occur at a higher concentration than the parent compound. For example, concentrations of 8 conjugates of triclosan metabolites resulting from phase II biotransformation of triclosan were five times higher than the parent molecule (MacHerius et al., 2012; Jia et al., 2017; Klampfl, 2019).. Similarly, metabolites of benzotriazole were 60 % higher in concentration than in the parent molecule in the *Arabidopsis* plant (LeFevre et al., 2015). Therefore, the significance of metabolite data is that it aids in estimating an actual xenobiotic concentration in plant tissue (Klampfl, 2019). The absence of this critical information may compromise risk assessment and misrepresent the threat posed to humans or the environment (Kosjek et al., 2007; Riemenschneider et al., 2017; Emhofer et al., 2018).

Liquid chromatography–high-resolution-mass spectrometry (Orbitrap-MS or time-of-flight-MS) is the instrument of choice in metabolite identification studies (Henry et al., 2012). The technique yields high-mass accuracies and high resolution even when operated infull-scan mode. Itmeans that within an analytical run, high-resolution mass spectrometry (HRMS) can screen for an unlimited number of candidatebiotransformation products. It can also confirm

candidate biotransformation products accurately without reference standards (Moschet et al., 2013; Saito-Shida et al., 2018).

This chapter reports on the in-plant biotransformation of accumulated ARVDs in lettuce, following evidence of accumulation reported in Chapter 3. Overall, the study's objective was to advance the knowledge of the fate of ARVDs, particularly the formation of metabolites, after accumulation in plants. Additionally, it aimed to show a stepwise approach to identifying metabolites under the single-stage mass (MS^1) spectrometry level.

Table 4.1. Studies on the in-plant biotransformation of pharmaceuticals

API class	Individual API	Plant tissue	Exposure Media/ concentration	Extraction/ clean-up	Detection	Author
Anticonvulsant	Lamotrigine	Fungus	Petri dish 10 -100 mgL^{-1}	Sonication/ Filtration	LC- HR-MS, (ion trap) MS^2	(Chefetz et al., 2019)
Anticonvulsant	Carbamazepine	Radish root	Flask culture 10-250 µM	Grinding/ &filtration	LC-UHR-QTOF-MS analysis.	(Sauvêtre et al., 2018)
Benzodiazepine	diazepam, lorazepam, oxazepam chlordiazepoxide clonazepam,	Radish, silver beet	Soil 0.5 mg kg^{-1}	Sonication/ SPE (HLB)	LC-MS/MS	(Carter et al., 2018b)
Anticonvulsant	Carbamazepine,	tomato	Hydroponics 50 µg L^{-1}	Sonication/ filtration	UPLC- QTOF-MS	(Riemenschneider et al., 2017)
X-ray agent	Iopromide	*Typha latifolia*	Hydroponics 20 µmol L^{-1}	Sonication/ SPE (HLB)	LC-MS/MS	(Cui et al., 2017)
Analgesic	Acetaminophen	cucumber roots,	Hydroponics 5 mg L^{-1}	SPE (HLB)	UPLC- QqQ-MS	(Sun et al., 2019)
NSAIDs	Diclofenac, Ketoprofen, mefenamic acid	Cress plant	Hydroponics 0.1 mg L^{-1}	Homogenize/ Filtration QuEChERS SPE (strata-x)	LC- QqQ-MS	(Emhofer et al., 2018)
Antibiotics	Sulfadiazine clarithromycin	Lettuce	Hydroponics 1 mg L^{-1}	Sonication/ SPE (HLB)	UPLC-QTOF-MS/MS	(Tian et al., 2019)

			& UPLC-QqQ-MS/MS		
Pesticide	Imidacloprid	Tomato fruit	Real field trial 2.5 L ha $^{-1}$	QuEChERS	UHPLC/Q-Orbitrap MS	(J. Li et al., 2019)
Benzodiazepine	Diazepam	Thaliana cells & cucumber, radish	Petri dish Hydroponics 1 µg L^{-1}1 mg L^{-1}	Sonication/ SPE (HLB)	UPLC-QqQ-MS/MS	(Dudley et al., 2019)
Antidepressants	Sertraline Clomipramine trazodone	Cress	Hydroponics 10 mg L^{-1}	Homogenization, centrifuge, filtration	LC-QTOF orbitrap MS	(Reichl et al., 2018)
Antibiotics	Fluoroquinolones Sulphonamides Lincosamides	Vegetables	Soil- real field	Sonication/ SPE (strata-x)	LC-MS/MS	(Tadić et al., 2019)

2

4.2 Materials and methods

4.2.1 Selection of candidate metabolites

Metabolites can be measured via the untargeted, quantitative targeted or suspect screening approach (Vaclavik et al., 2014; Wu et al., 2016; Chefetz et al., 2019; Dudley et al., 2019). The suspect screening approach was selected for this research. It first involved reviewing candidate ARVD metabolites that exist in the literature. Afterwards, these suspect metabolites were screened from the full-scan chromatogram data using their exact mass as *a priori* information (Moschet et al., 2013; Bletsou et al., 2015). Candidate metabolites listed in Table 4.2 were selected based on the human (mammalian) biotransformation of the parent molecules identified in the pharmaceutical database Drugbank (Drugbank, 2020; DrugBank, 2019). Non-targeted approaches provide more details since they involve global profiling of the biotransformation product (Zhang et al., 2016). However, the primary limitation of this targeted/suspect screening method relative to the non-targeted approach is the requirement to have a *priori* knowledge of the biotransformation product. The technique does not yield holistic information about the metabolite because it relies on biotransformation product-specific signals.

Table 4.2. Candidate metabolites selected for investigations

Parent ARVD	Suspect metabolite	Chemical formula
Efavirenz	8-Hydroxy efavirenz (8-OH-EFV)	$C_{14}H_9ClF_3NO_3$
	8-hydroxy efavirenz glucuronide (8-EFV-Gluc)	$C_{20}H_{17}ClF_3NO_9$
Nevirapine	2/3/8/ 12- hydroxy nevirapine (2/3/4/12- OH-NVP) (isomers)	$C_{15}H_{14}N_4O_2$
	4-carboxynevirapine (4-carb-NVP)	$C_{15}H_{12}N_4O_3$
	8/12- Hydroxy nevirapine glucuronide (isomers)	$C_{21}H_{22}N_4O_8$
Lamivudine	Lamivudine sulfoxide (LVD sulfoxide)	$C_8H_{11}N_3O_4S$
Oseltamivir	Oseltamivir carboxylate (OSV carboxylate)	$C_{16}H_{28}N_2O_4$

4.2.2 Exposure to ARVDs, analyte extraction and metabolite identification

The lettuce plant was exposed to ARVDs as described in Section 3.2.4. Analytes were extracted, separated and analyzed according to the protocols described in Section 3.2.5. The metabolites were screened on the generated total ion chromatograms (TIC).

4.3 Data analyses

All treatments and chromatographic runs were performed in triplicate (n = 3). Chromatograms were visually inspected, and graph and mean calculations were constructed using IBM SPSS Statistic 24 and MS Excel 2016. The Estimation Program Interface program, v 4.11 (EPI Suite, US Environmental Protection Agency, 2000-2017), was used to predict the parent and metabolite molecules' physical and chemical properties.

4.3.1 Metabolite identification

Before the screening, the exact mass and simplified molecular-input line-entry system (SMILES) notation of the candidate metabolites were obtained from ACD/ChemSketch (2018 freeware) program. Screening involved exact mass mining from the full-scan high-resolution, total ion chromatogram (TIC) previously obtained from the analysis of ARVD accumulation in the lettuce leaves and roots in Chapter 3. The screening was carried out at an accuracy of 5 ppm. The extracted ion chromatogram (EIC) was visually inspected for symmetry and scanned for the suspect metabolite. The double bond equivalence (DBE) value was calculated using Equation (4.1) from (Bletsou et al., 2015). Metabolite fragments (product/daughter ions) were deduced based on the simple heterolytic (inductive) cleavage mechanism.

$$\text{Double bond equivalence} = C - \left(\frac{H}{2}\right) + \left(\frac{N}{2}\right) + 1 \qquad (4.1)$$

Mass accuracy tests on the measured masses were performed using Equation (4.2).

(Where C is the number of carbon atoms, H is the number of hydrogen and halogen molecule, and N is the number of nitrogen atoms)

$$\text{Accuracy (ppm)} = \left(\frac{\text{Measured accurate mass} - \text{Exact calculated mass}}{\text{Exact calculated mass}}\right) \times 10^6 \qquad (4.2)$$

4.4 Results and discussion

4.4.1 Identification of suspect metabolites

Only two of the seven suspected metabolites were identified, 12-hydroxy nevirapine glucuronide ($C_{21}H_{22}N_4O_8$) and lamivudine sulfoxide ($C_8H_{11}N_3O_4S$). Detection was confirmed following the accurate measurement of their $[M+H]^+$, $[M+NH_4]^+$ and $[M+Na]^+$ adducts for the 12-hydroxy nevirapine glucuronide and $[M+H]^+$ for lamivudine sulfoxide with satisfactory

accuracy (Table 4.3). Due to the unavailability of pharmaceutical metabolite primary standards, the accurate mass measurement of the molecular and daughter fragments ion exact masses remains one of the tools for mining metabolites. This approach is widely employed in untargeted and suspect screening analyses. For example, the approach was used to identify metabolites of imidacloprid (a pesticide), lamotrigine, clarithromycin and carbamazepine (Calza et al., 2012; Chefetz et al., 2019; J. Li et al., 2019).

Table 4.3. Detected ARVD metabolites, metabolite fragments and mass accuracy of target ions (ppm) from the 100 µg L^{-1} exposed lettuce

Metabolite	Fragment	Exact mass	Mean accurate measured (n=3)	mean accuracy (limit ± 5 ppm)	DBE values Manual/Auto
Lamivudine sulfoxide	[M+H]$^+$	246.05430	246.05424	-0.23	5.0/4.5
12-hydroxy-nevirapine - glucuronide	[M+H]$^+$	459.15104	459.15135	0.67	13.0/12.5
	[M+Na]$^+$	481.13298	481.13172	-2.62	
	[M+NH$_4$]$^+$	476.17758	476.17637	-2.55	
	C$_{15}$H$_{13}$N$_4$O$^+$	265.10837	265.10715	-4.63	
	C$_{20}$H$_{21}$N$_4$O$_6$$^+$	413.14556	413.14165	-9.46	
	C$_{21}$H$_{21}$N$_4$O$_7$$^+$	441.14047	441.13690	-8.08	

The majority of mass spectrometers system have robust elemental calculators that help minimize uncertainties in structure elucidation exercises (De Vijlder et al., 2018). The elemental composition calculator function of the mass spectrometer (Xcalibur 4.2, Qualbrowser feature) was used to verify the chemical formula of the identified metabolites, providing a perfect match to the DrugBank retrieved chemical (DrugBank, 2022). The in-built

calculator was further used to automatically compute the DBE values of the two metabolites. The software obtained DBE values were compared them to the externally calculated values. The system-generated DBE values for 12-hydroxy-nevirapine glucuronide and lamivudine sulfoxide were 12.5 and 4.5, respectively, while the manually-calculated values were 13 and 5, respectively (Table 4.3). The 0.5 difference in the DBE values arose from the extra H atom in the software-generated value $[M+H]^{+}$, while the manually calculated value was derived from the monoisotopic mass, [M]. The identical DBE values indicated that the literature retrieved and experimental metabolites were identical.

4.4.2 Extraction of analytes

Simultaneous analyses of parent molecules and their metabolites are challenging, partly due to variations in physicochemical characteristics and the lower concentration levels of metabolites (Tina et al.,2016; Emhofer et al., 2018; Klampfl, 2019). The EPI Suite program, Table 4.4, predicted the parent and metabolite physicochemical characteristics. The molecules were characterized by aqueous solubilities and octanol-water partitioning coefficients, which demanded selective pre-treatment and detection approaches. HLB SPE cartridges were selected for sample extraction and clean-up, as reported in section 3.2.3.2. Studies in Table 4.1 indicate the preferential utilization of the HLB in pharmaceutical metabolite extraction. HLB sorbent typically retains molecules of varying polarity (Ibáñez et al., 2012; Picó and Barceló, 2015). Although there might be a reduction in the retention of a highly hydrophilic molecule when using SPE (Emhofer et al., 2018), it compensates by minimizing the interference of the matrix during identification.

Table 4.4: Predicted physicochemical characteristics of identified metabolites using EPI suite.

Molecule	Water solubility (mg L^{-1})	Log K$_{ow}$
Nevirapine	42.36	3.89
12-hydroxy Nevirapine Glucuronide	4.703	1.57
Lamivudine	9366	-2.62
Lamivudine sulfoxide	1E^6	-4.76

4.4.3 Impact of matrix on separation and identification of metabolites

The matrix in the plant extract presented a challenge in identifying the suspect metabolites on the raw TICs, as evidenced by the complex TIC in Figure 4.1A. Therefore, mining the suspect metabolites necessitated the acquisition of corresponding EICs, as described in Section 4.3.1. Figure 4.1 B and D are the EICs of the parent molecules (lamivudine and nevirapine, respectively). Figure 4.1C is the protonated EIC of the lamivudine sulfoxide, and Figure 4.1E is the ammonium adduct ([M+NH$_4$]$^+$) of 12-hydroxide nevirapine glucuronide. Metabolite identification was characterized by a low ion population, markedly for lamivudine sulfoxide (Figure 4.1C), which affected its symmetry. Unsymmetrical peaks lead to mass inaccuracies which contribute to poor precision in individual and replicate determinations. (Webb et al., 2004).

Notably, the identified metabolites (Figure 4.1C and E) are characterized by shorter retention times than their respective parent ions(Figure 4.1 B and D). Metabolites are more hydrophilic than their parent molecules, an example being sulfate conjugates (secondary metabolites) which are more water-soluble than the non-sulfated parent molecule (Hirschmann et al., 2014).
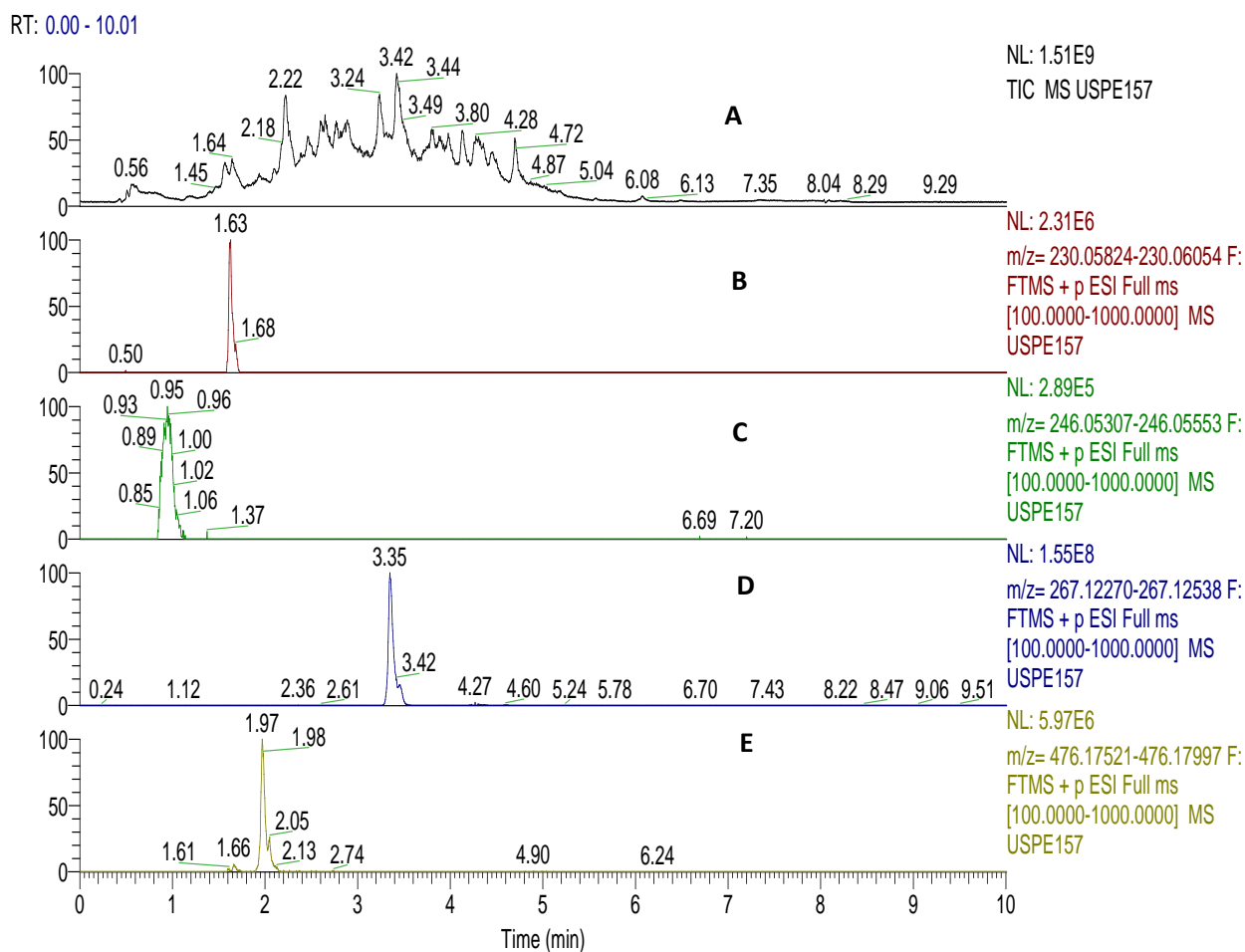
Figure 4.1 TIC and EICs of the root extract exposed to the 100 µg L^{-1} exposure solution (**A**, TIC of the Root extract; **B**, Lamivide EIC; **C**, EIC of lamivudine sulfoxide; **D**, EIC of Nevirapine; **E**, EIC of 12-Hydroxyl nevirapine glucuronide).

4.4.4 Concentration and distribution of metabolites

The occurrence of metabolites in the lettuce samples depended on the concentration of the ARVDs in the exposure solution (Figure 4.2). Considering that the metabolites were neither detected in the exposure solution nor the control samples, it implies that the biotransformation of the ARVDs was in-plant. The metabolites were hardly detected in the 1 and 10 µg L^{-1} but were present in the 100 µg L^{-1} exposed samples. A study identified 16

metabolites associated with ketoprofen, naproxen, mefenamic acid, and diclofenac in the cress plant grown hydroponically in 100 μg L^{-1} solution (Emhofer et al., 2017). These sub mg L^{-1} exposure levels (including the present study) are ideal for metabolite-related studies as they mimic natural environmental conditions. At a lower exposure concentration level of 1 and 10 μg L^{-1}, the metabolite of lamotrigine (an anticonvulsant) was not identified in the exposed white-rot fungus, which necessitated increasing the exposure solution concentration to 100 mg L^{-1} to induce the occurrence of associated metabolites (Chefetz et al., 2019). Triclosan and triclocarban metabolites occurred in carrot cell tissues after exposure to 1 mg L^{-1} solution (MacHerius et al., 2012). In the latter two studies, exposure concentrations were 1000 and 10 times higher than those used in the study. Such high xenobiotic exposure levels are a primary drawback of plant API biotransformation studies. Whereas elevated xenobiotic concentration levels may promptly induce the occurrence and detection of associated metabolites, they may not represent an actual environmental scenario (Klampfl, 2019). A semi-quantitative analysis based on ion count shown in Figure 4.2 indicated that the concentration of 12-hydroxyl nevirapine glucuronide was approximately 15 times higher than lamivudine sulfoxide. The concentrations in the roots and leaves for each metabolite were relatively comparable. The advantage of whole-plant experiments like the present study is that they help identify metabolite distribution in the host tissue, unlike cell-based experiments (Klampfl, 2019).
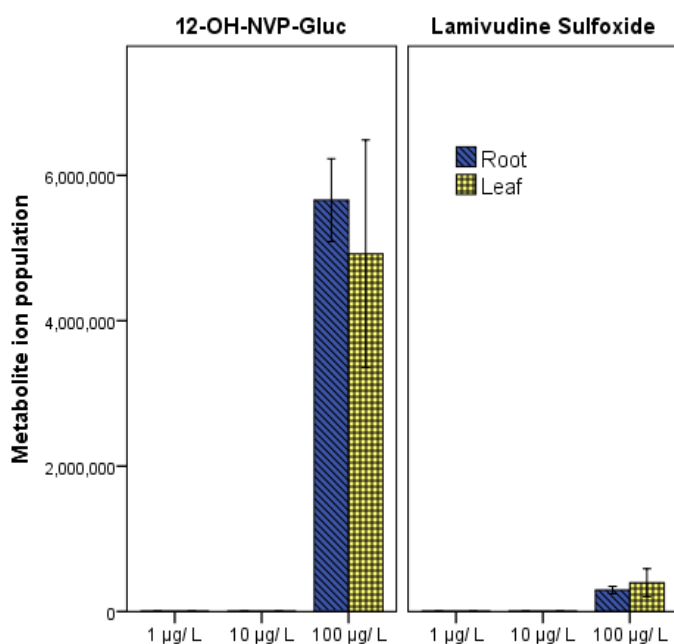
Figure 4.2. The relative concentration of metabolites in the leaf and root tissues of lettuce across the exposure range.

Compared with their parent molecules, the metabolites were an order of magnitude lower in ion count (the ion population of parent molecules was shown in the EICs in (Figure 4.1). According to Moschet et al. (2013), ion count remains the only way to quantify or compare the concentration of target organic pesticide metabolites in the absence of primary standards.

4.4.5 Identification of metabolite product (daughter) ions

The US-FDA criterion for identifying metabolites using exact mass requires that, in addition to the detection and identification of the main precursor (molecular) ion, one structurally significant fragment (product/daughter) has to be positively identified, too (FDA, 2015). Therefore, the most plausible fragmentation pathways that yielded were explored to aid in

identifying associated fragment ions. Since this study was undertaken under the low energy single-stage mass spectrometry level (MS[1]), minimal fragmentation was experienced. Hence, fewer product ions were expected. This study approach contrasted with higher energy Collision-Induced Dissociation (CID) strategies, which employ > MS[1]-based studies, i.e., MS[2] and MS[3], that result in intensive fragmentation of target analytes (Olsen et al., 2007).

Figure 4.3 A and B hypothesized the fragmentation pathways for lamivudine sulfoxide and 12-hydroxy nevirapine glucuronide. They followed the inductive cleavage of the carbon-heteroatom bonds accompanied by a charge migration to the alpha-carbon and a neutral loss. This fragmentation pattern is analogous to ESI-charged molecules proposed by De Vijlder et al. (2018). The suspect nevirapine metabolite structurally consisted of 4 isomers; the 12-hydroxy-substituted structure was selected since its product ion was observed in the generated mass spectrum. The non-discrimination between stereoisomers probably remains one limitation of mass spectrometry (Kind and Fiehn, 2006). Some plant-induced pharmaceutical biotransformation studies have been undertaken using LC-HR-MS at the MS[1] level. Related studies (though not targeting metabolites) that have utilized the single-stage - orbitrap HRMS approach include quantification of allergens in caseinate wines (Monaci et al., 2011) and screening for veterinary and mycotoxins in food commodities (De Dominicis et al., 2012). The parent molecule was the target compound of interest in these studies, and the product ion was not investigated.
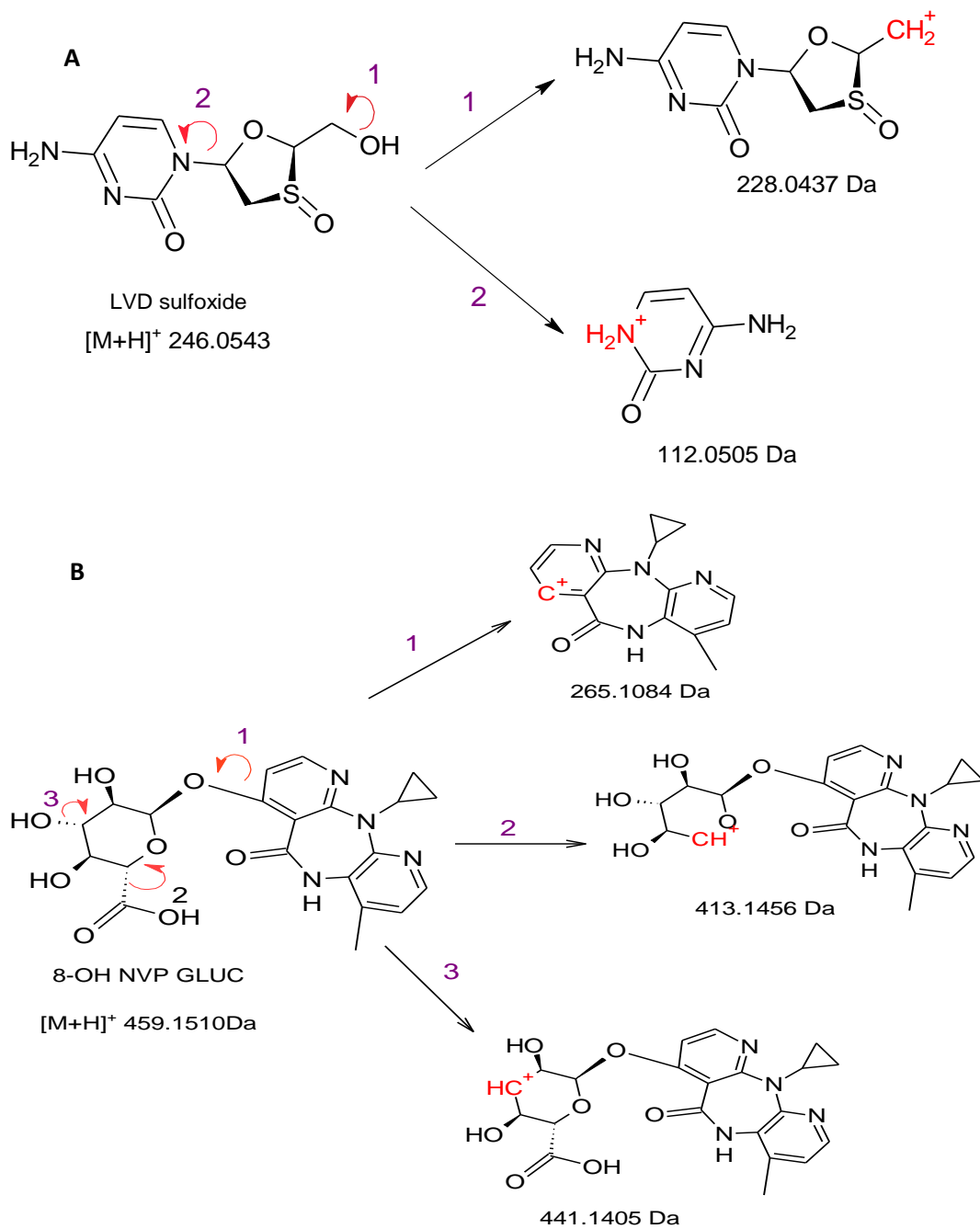
Figure 4.3. Proposed fragmentation pathway of **(A)** lamivudine sulfoxide and **(B)** 12-hydroxy nevirapine glucuronide.

97

4.4.6 Mass spectrum and mass accuracy of metabolites and product ions

Inspection of the mass spectrum of the 12-hydroxy nevirapine glucuronide metabolite (*Figure 4.4* B revealed a greater relative abundance of the $[M+Na]^+$ and $[M+NH_4]^+$ adducts than its $[M+H]^+$ ion. The mass spectrum contained other non-defined intense ions originating from the complex matrix, an occurrence uncommon with ESI-generated mass spectra. Despite the low ion intensity, both the precursor and product ions were accurately measured as they exhibited satisfactory accuracy, as indicated in Table 4.3.

Unlike 12-hydroxy-glucuronide, only the main molecular ion, $[M+H]^+$of lamivudine sulfoxide (Figure 4.4 A), was measured. None of the proposed fragments ions in Figure 4.3 were identified. In Table 4.3, lamivudine sulfoxide was the most hydrophilic analyte in this study (log K_{ow}, -4.76). Its retention in the SPE sorbent during extraction and LC- column during analysis was weaker. Nonetheless, given the sensitivity of the Orbitrap ion-trap technology, which allows sufficient ion accumulation, detecting low-concentration target ions, such as the metabolite, is achieved (Reichl et al., 2018). Lamivudine sulfoxide EIC, Figure 4.4A, indicates an ion population (count) of $2.89 \times 10^{5,}$ which is lower than the tuned automatic gain control count (AGC) of 1×10^6. Lower ion population counts, lower than the tuned AGC target, are characterized by reduced mass accuracy (Kalli et al., 2008).
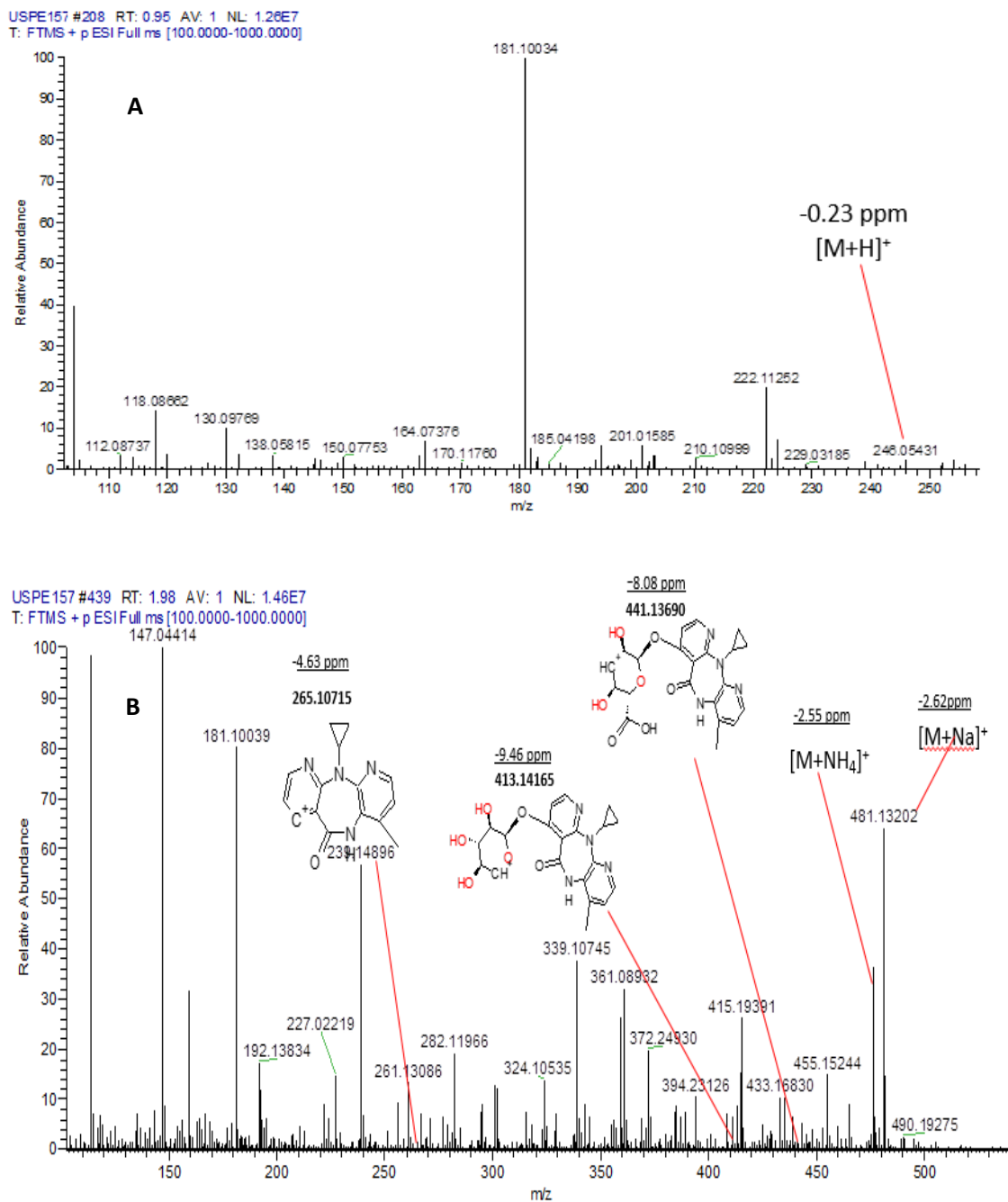
Figure 4.4. Mass spectrum for (A) lamivudine sulfoxide (B) 12- hydroxy nevirapine glucuronide

The mass accuracy (mass measurement error) and their respective product ions were ascertained arithmetically using Equation (4.1). According to Table 4.3, the accuracy of the measured $[M+H]^+$, $[M+Na]^+$ and $[M+NH_4]^+$ of the metabolites molecular ions was within the ±5 ppm limit. The product ions, however, had an accuracy of > ±5 ppm. Theoretically, a

fragment's mass should fall within the small narrow accuracy window (±5 ppm) to be deemed 'accurately' identified. However, the uncertainty of mass accuracy increases in a complex matrix (Henry et al., 2012), as experienced in the plant matrix of the present study. Under such conditions, it has been suggested that an accuracy of up to ± 10 ppm is acceptable to avoid reporting false negatives (De Dominicis et al., 2012). For example, the carbamazepine metabolites in the hairy root of horseradish vegetables lay within ±10 ppm (Sauvêtre et al., 2018). Similarly, one triclosan metabolite transformed by carrot was unequivocally identified at an accuracy of 6 ppm (MacHerius et al., 2012).

As the metabolite masses were ca 400 Da, mass accuracy was annotated using eight significant figures (five decimal places), which addresses inconsistencies that may arise due to rounding errors before the final presentation of four decimal figures (Brenton and Godfrey, 2010). Accuracy measurement was obtained through replication (n=3), which helped inform the accuracy and precision of each analyte. A guide to assign confidence levels in HR-MS-based studies during the identification of small molecules, consisting of five confidence levels, levels 1-5, was developed by Schymanski et al. (2014). Level 1 confidence level represents an ideal situation, i.e., the highest level of confidence requires the proposed structure to be confirmed via a reference standard with MS, MS/MS and retention time matching. In this study, the exact mass (*m/z)* and the molecular formula were unambiguously assigned to the biotransformation products, so confidence level 4 was achieved.

4.5 Conclusion

This study found that in-plant biotransformation of accumulated ARVD compounds is possible. Since metabolites were detected in root and leaf tissues, either in-plant pharmaceutical transformation likely occurs below, and above ground plant tissues or the

transformation, products are transported from one compartment. The single-stage mass spectrometric level, using a high-resolution mass spectrometer, can identify in-plant biotransformation products. Nonetheless, without metabolite standards, non-targeted approaches with > MS^2 ability are ideal for analysing in-plant biotransformation products.

Chapter 5
Impact of wastewater matrix on uptake of antiviral pharmaceuticals in plants in an aquatic environment

Overview

This study investigated the impact of dissolved organic matter and particulate wastewater components on the bioavailability of antiviral and antiretroviral (ARVDs) pharmaceuticals to plants through controlled batch experiments. The influence of sorption on the uptake of ARVDs by lettuce (*Lactuca sativa*) was assessed by comparing the accumulation resulting from hydroponic irrigation with fresh water and synthetic wastewater (which simulated actual wastewater). The exposure solutions were spiked with the ARVD mixture at 100 μg L^{-1} for each molecule. In the sorption experiment, 4-75 % of the ARVDs remained in the wastewater matrix. The uptake of ARVDs in the wastewater-irrigated lettuce was 37-97 % lower than in the freshwater medium. This study was developed to understand the fate of ARVD molecules in a simple two-phase system, i.e., an ARVD-wastewater-plant environment (given that the molecules first reside in the wastewater). Before transitioning to a complex three-phase agroecosystem, i.e. ARVD-wastewater-terrestrial (soil)-plant system.

5.1 Introduction

In aquatic environments, the uptake of contaminants is impacted by the transport of the solute, either close to or removed from the root zone. The mobility of these organic contaminants is considerably influenced by the magnitude of retention to the wastewater-borne components, namely dissolved organic matter (DOM) and suspended particulate matter (SPM) (Graber and Gerstl, 2011;Hajj-Mohamad et al., 2017). For this reason, an in-depth understanding of the nature, transport and fate of pharmaceuticals in the aquatic

environment is vital for accurately estimating environmental exposure and risk assessments in aquatic biota (Pan et al., 2009; Fountouli and Chrysikopoulos, 2018a).

Accumulation of APIs in plants in contaminated water bodies has been reported. For example, three NSAIDs, naproxen, ibuprofen and diclofenac, were detected in water-based hyacinth reed at concentrations of up to 12 ng g^{-1} (Sibeko et al., 2019). Likewise, three ARVDs, emtricitabine, tenofovir disoproxil and efavirenz, were detected in water hyacinth harvested from a freshwater reservoir and wastewater treatment ponds at a concentration between 0.98 -17.2 µg kg^{-1} (Mlunguza et al., 2020a). Curiously, water hyacinth has been cited as potential animal feed (Survival Gardner, 2015), indicating that its consumption is a pathway fo food chain contamination.

This study aimed to develop a quantitative understanding of the impact of wastewater-borne constituents on the uptake of ARVD molecules by plants. The perceived impact could only be assessed after determining the distribution pattern of the ARVD in a wastewater environment. Accordingly, sorption experiments were undertaken herein before the plant uptake experiments. The ARVDs molecules' association with wastewater constituents, specifically DOC and SPM, was measured. The binding potential was then compared with the magnitude of accumulation in lettuce irrigated with ARVD-spiked synthetic wastewater (SW). Sorption experiments further enabled the generation of critical distribution coefficient data (K_d) on the interaction of ARVDs with wastewater constituents.

5.2 Materials and methods

In addition to the protocols followed, the rationale for selecting various experimental approaches is described in this section.

5.2.1 Preparation of synthetic wastewater

Synthetic wastewater was prepared according to the procedure and list of ingredients provided by (Boeije et al., 1999a) and Lees. (2018), Table 5.1. It was composed of sources of carbohydrates, proteins and minerals. Lyophilized sewage sludge was added to provide primary SPM material. The ingredients were appropriately weighed and placed in a 2 L conical flask covered with aluminium foil. 1 L of HPW was added to the flask, and the mixture was stirred for 24 hours. The mixture was collected in an amber glass bottle and stored in a freezer at -20 °C before use. The SW was prepared at 10 times the standard concentration and was diluted appropriately before any experiment. The pH was adjusted to 7.5 using 10 mM phosphate buffer

Table 5.1. Synthetic wastewater constituents

	Component	Medium	Chemical formula	Concentration (mg L^{-1})
1	Carbohydrate	Sodium acetate	$C_2H_3NaO_2$	330
2	Proteins	Meat extract	-	150
3	Carbohydrate	Lactose monohydrate	$C_{12}H_{22}O_{11} \cdot H_2O$	330
4	Carbohydrate	Potato starch	$(C_6H_{10}O_5)n$	330
5	Carbohydrate	Glycerol	$C_3H_8O_3$	200
6	Carbohydrates	Peptone	-	280
7	Nitrates	Ammonium chloride	NH_4Cl	110
8	Nitrates	Urea	CH_4N_2O	750
9	Nitrates	Uric acid	$C_5H_4N_4O_3$	90
10	Phosphates	Potassium phosphate monobasic	KH_2PO_4	200
11	Sulphates	Magnesium sulfate heptahydrate	$MgSO_4 \cdot 7H_2O$	250
12	Sewage simulation	Genapol® C-100	-	30
13	Sewage simulation	Kieselguhr, pure white	O_2Si	10
14	Sewage simulation	Dextrin	$(C_6H_{10}O_5)x$	330

15	Sewage simulation	Genapol® X-080	HO(CH$_2$CH$_2$O)n(CH$_2$)mH	30
16	Sewage simulation	Lyophilized activated sludge		2000.0
17	Minerals and trace metals	Calcium chloride dihydrate	CaCl$_2$·2H$_2$O	50.0
18	Minerals and trace metals	Sodium bicarbonate	NaHCO$_3$	250.0
19	Minerals and trace metals	Iron(III) sulphate hydrate	Fe$_2$O$_{12}$S$_3$·5H$_2$O	100.0
20	Minerals and trace metals	Cobalt(II) chloride hexahydrate	CoCl$_2$·6H$_2$O	0.5
21	Minerals and trace metals	Chromium(III) nitrate nonahydrate	Cr(NO$_3$)·9H$_2$O	6.8
22	Minerals and trace metals	Copper(II) chloride dihydrate	CuCl$_2$·2H$_2$O	4.8
23	Minerals and trace metals	Ethylenediaminetetraacetic acid (EDTA)	C$_{10}$H$_{16}$N$_2$O$_8$	2.2
24	Minerals and trace metals	Potassium molybdate	K$_2$MoO$_4$	0.2
25	Minerals and trace metals	Manganese(II) sulphate monohydrate	MnSO$_4$·H$_2$O	1.0
26	Minerals and trace metals	Nickel(II) sulphate hexahydrate	NiSO$_4$·6H$_2$O	3.0
27	Minerals and trace metals	Zinc chloride anhydrous	ZnCl$_2$	1.8

5.2.1.1 Characterization of synthetic wastewater

The DOC and SPM component characterized the SW. DOC represented the total dissolved organic matter content in the SW and was indirectly estimated from the SW's chemical oxygen demand (COD) values. COD (COD$_{cr}$) was determined by titration using the potassium dichromate standard method according to APHA method 5220 (Standard Methods, 2018).

Equation (5.1) was used to estimate the DOC level. The Equation was derived from a relationship between laboratory-measured DOC and COD levels of wastewater influent collected from over 600 wastewater (sewer) collection points in the UK (Research, 2019).

$$DOC = (0.1406 \times COD) - 25.92 \qquad (5.1)$$

Suspended particulate matter (SPM) was determined using APHA method 2540 (Standard Methods, 2018), whereby the component was gravimetrically measured after filtration of the SW through a 0.7 μm (GF/F) followed by drying at 105 °C.

5.2.2 Sorption experiments

The sorption tendencies of the ARVDs were measured in two environments, both buffered at pH 7.5, (1) in an SW environment consisting of both the SPM and DOC fractions and (2) in a DOC-only component. Measurements were indirectly evaluated by quantifying the amount of ARVD molecule that remained in the solution after the sorption experiment.

The sorption experiments were designed such that the ARVD distribution in the SW was evaluated at three concentrations: i.e. standard-strength (1×), 2-times (2×) and 3-times (3×). The strongest SW concentration was selected to simulate sorption in a worst-case environmental scenario (Bagnis et al., 2018a). The DOC-only fraction was obtained by filtering the SW through 0.7 μm GF/Fs to separate the SPM component. During sorption experiments, sodium azide (0.2 g L^{-1}) was added to the diluted fraction to inhibit microbial growth.

Accurate and uniform dilutions of SW were achieved by drawing aliquots from the SW stock under constant stirring. The SW aliquot and ARVD stock mixture spike were transferred into a volumetric flask. Using high-purity water (HPW, 18.2 MΩ cm resistivity), the mixture was made to the mark to obtain the ARVDs at the desired concentration (100 μg L^{-1}). This mixture

was divided into three replicates and transferred into identical glass centrifuge tubes. The tubes were wrapped with aluminium foil and reciprocally shaken for 12 hours. The solution was centrifuged for 10 minutes at 1900 g and filtered through a 0.7 μm GF/F. A 1 mL aliquot of the filtered solution was stored at 4 °C until analysis. The filtered samples were directly injected into the LC-HRMS, and matrix-matched calibrations were used to quantify the ARVDs in the filtrate.

5.2.2.1 Determination of K_d values

The experimental solid-water distribution coefficients, $K_{d\ exp}$ values (L kg^{-1}), defined the distribution of the molecules between the aqueous phase and SW suspended solid sorbent and were estimated using Equation (5.2)

$$k_{d(exp)} = C_{sorbed} \ / \ C_{soluble} \tag{5.2}$$

Where $C_{soluble}$ was the concentration of ARVD in the filtrate and C sorbed concentration in the SPM. C sorbed was obtained from the difference between C soluble and the initial amount of the spike (100 μg L^{-1}).

A modelled distribution coefficient value, $K_{d\ mod}$, was also ascertained using Equation (5.3). $K_{d\ mod}$ considered the influence of pH on the ionic pharmaceutical molecules, i.e. the pH-dependent octanol-water distribution constant (Log D_{ow}) as formulated by Lin et al. (2010).

$$Log\ k_{d\ (mod)} = 0.74 \ \times \log D_{ow} + 0.15 \tag{5.3}$$

5.2.3 Plant exposure experiments

Two sets of lettuce roots were hydroponically exposed to fresh water and SW, and both spiked with the 5 ARVD mixture at 100 μg L^{-1}. The SW was at the ×2 concentration level, midway between the standard concentration and the worst-case scenario. The exposure

solution was replenished every two days with fresh water to compensate for evapotranspiration losses. Transpiration losses were determined by weighing the mass of the remaining solution before replenishment with fresh water. Accumulation of ARVDs was assessed as a function of time through the sacrificial sampling of triplicate samples during harvesting days, i.e. days 1, 3, 6, 9 and 15. In addition, a control set of lettuce plant samples whose irrigation water was unspiked was included in the experiment. Microbial abundance in the SW was expected to be significantly lower than in actual treated wastewater. As it is a biocide, sodium azide was not added to the irrigating SW. Lettuce samples were prepared as described earlier in Section 3.2.5.

Root concentration factors (RCFs), translocation factors (TFs) and bioconcentration factors were determined according to Equations (3.2), (3.3), (3.4) and (3.5).

ARVD mass balance in the system was estimated using Equation (5.4).

$$M_{total=} M_{plant} + M_{solution} + M_{unaccounted} \qquad (5.4)$$

Where, M_{total}, M_{plant}, $M_{solution}$ and $M_{unaccounted}$, are the total amount of the ARVDs in the system, accumulated in the plant, remaining in solution and the mass not accounted for, respectively.

5.2.3.1 Selection of SW and exposure concentrations

Although the exposure concentration was approximately 100 times higher than routinely measured environmental concentrations (Nason et al., 2019), quantitative measurements were enabled. Since its components and characteristics are known, synthetic wastewater was used rather than treated wastewater. Additionally, it aided in interpreting and comparing the data obtained from the sorption experiments. Actual wastewater composition is highly

variable both within and between wastewater treatment works, particularly in Low and Low Middle-Income Countries (LLMIC) (Tchobanoglous et al., 2003). Given this inherent variability, the use of 'natural' versus synthetic wastewater is an ongoing debate with benefits and drawbacks associated with each approach, encapsulated by (O'Flaherty and Gray, 2013) for example. Since these experiments aimed to generate untreated surrogate wastewater to assess the partitioning behaviour of ARVDs, a consistent, reproducible and stable starting matrix was needed for testing. As such, a synthetic wastewater (SW) formulation was used, as informed by previous studies (Boeije et al., 1999a; Bagnis et al., 2018b).

5.2.4 Data analyses

Data analyses were performed using MS Excel 2016 and IBM SPSS 24 statistics software. The significance tests were performed by ANOVA, student's t-tests and Dunnett's 3T-test, where $p < 0.05$ was considered significant.

5.3 Results and Discussion

5.3.1 Quality of synthetic wastewater

SW characteristics may be varied to suit experimental objectives. In this study, for example, the SPM component was introduced by adding lyophilized sludge from actual primary settled sludge. Figure 5.1 shows that the DOC and SPM levels in the SW varied between 5-60 mg L^{-1} and 239-560 mg L^{-1}, respectively. The concentration of SPM in 3× SW was approximately 2.5 times the amount measured at standard SW concentration.
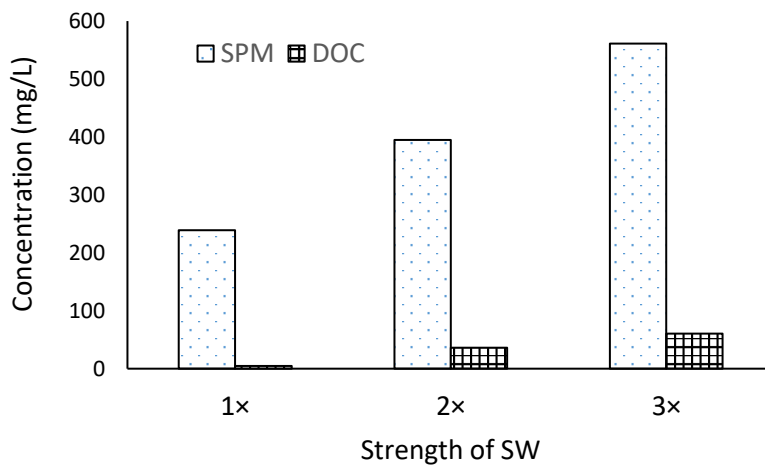
Figure 5.1. DOC and SPM concentrations in the synthetic wastewater

The SPM levels lay within the maximum allowable limits of total suspended solids discharges into sewers by the National Environmental Management Authority (NEMA) of Kenya, capped at 2000 mg L^{-1} (Authority, 2006). It also lay close to the 296 mg L^{-1} mean value of suspended solids measured in influents and effluents obtained from 26 wastewater treatment plants in the UK (Gardner et al., 2013). SPM values in wastewater are highly variable and largely depend on the influent sources. DOC levels in surface waters are equally varying. For example, Mecha et al. (2016) reported DOC levels of 20 mg L^{-1} in municipal wastewater effluents. SW prepared with similar ingredients to this study but without sewage sludge had DOC levels of 7.44 mg L^{-1} (Hossain et al., 2019) and 4.24-15 mg L^{-1} (Kim et al., 2002). Overall, SW prepared for the present study simulated natural wastewater as it contained both proteinaceous and humic qualities and the SPM component.

5.3.2 ARVD molecules binding to wastewater components
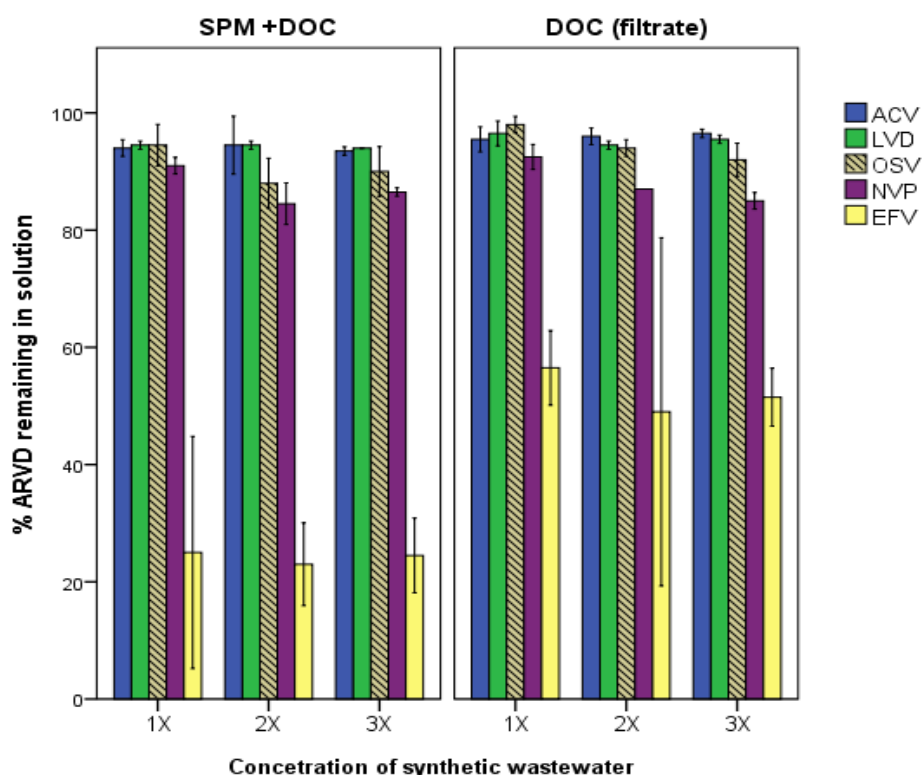
Figure 5.2. ARVD concentrations in the two SW test environments across the three SW concentrations (n=3, ± 1 SD)

The mean ARVD concentration remaining in the filtrate across 1×, 2×, and 3× SW strength levels were 84 ± 23.4 (SD), 80 ± 24.9 (SD) and 81 ± 23.4 µg L^{-1}, respectively, as shown in Figure 5.2. (The % amount in this experiment may also be taken as µg L^{-1} concentration as the initial spike level for each molecule was 100 µg L^{-1}). Theoretically, the amount of the ARVD remaining in the dissolved phase in the 2× and 3× concentrations was expected to be distinctly lower than in the 1× SW fraction. Curiously, the cumulative mean concentration of ARVD compounds in the dissolved phase at the three SW concentration levels in the two SW test environments was not different (Dunnett's T3 test, p = 0.89). Figure 5.2 shows that 4-10 % of

ACV, LVD and OSV were sorbed to the SW components, and 13 % of NVP was also bound to the SW components. The pharmaceutical EFV exhibited the highest magnitude of SPM sorption at 75 %, approximately six times higher binding than the NVP's. A lower cumulative mean for all 5 ARVDs remaining in solution was measured in the SPM + DOC treatment compared with the DOC-only treatment (78 and 85 %, respectively). However, there was no significant difference in sorption between the two fractions (independent sample t-test, $p=0.24$). The DOC component sorbed twice as much EFV (> 50 %) than SPM (25 %). This study's indirect measurement of sorption from the amount of solute remaining in the solution was analogous to the procedure in the batch experiment reported (Lucas et al., 2018). An ideal approach, however, would have been to directly extract and analyze the amount of the ARVDs in the filtered SPM, e.g. (Carballa et al., 2008; Azuma et al., 2017; Wilkinson et al., 2017 Aminot et al., 2018). Nevertheless, the approach described has been successfully applied in sorption experiments, e.g. Bagnis et al. (2018). An assumption made in this study was that the concentration variance of ARVDs in the filtrate was entirely due to binding to the SW constituents, and losses from biological biodegradation were non-existent.

Emphasis on the investigations into the distribution of ARVDs between the DOC and SPM fraction was informed by previous studies, which indicated that effluent-derived DOM, sewage sludge and biosolids directly impact the behaviour of organic compounds. Since the SPM is 36-75 % organic, these matrices preferentially interact with the organic micropollutants impacting their fate (Shon et al., 2006; Miller et al., 2015; Fu et al., 2016).
As illustrated in Figure 5.2, the binding of ARVDs was not consistent with SW concentration, which was unexpected. However, these behaviours bore similarities to results from an adsorption study, whereby a plant-based adsorbent nanofiber (extracted from the roots of

*Mondia white*i, herbaceous climber) was used to remove select ARVDs and associated pharmaceuticals from aqueous (wastewater) samples (Kebede et al., 2020). Here, the nanofiber's dosage (mass) efficiency was tested in the mass range of 10 to 60 mg. Results showed that maximum removal of the pharmaceuticals was measured at the 10 mg dosage level, and a further increase of the adsorbent mass, up to 60 mg, did not induce any further increase in the removal efficiency (keeping all other factors constant). A further increase in the mass of the adsorbent above the 10 mg mass level led to a decreased removal efficiency. This outcome has been attributed to aggregation or overlapping of the active sites of the particulates in suspension, which ultimately limited the organic pollutants' ability to reach the active sites (Crini and Badot, 2008).

In the classification of sorption potential, molecules with log K_{ow} values ranging between -7.1-2.7 lie below the adsorption threshold (Rogers, 1996; Azuma et al., 2017). Applying the classification to this study (see ARVDs log K_{ow} values in Table 5.3) implied that all the test ARVDs (except EFV) exhibited negligible binding affinities. NVP (log K_{ow} 2.5) is unique because it lies on the boundary of hydrophobicity and hydrophilicity. Another measure for sorption potential suggests that if < 4.7 % of a molecule is sorbed to the SPM, its sorption is negligible, and the concentration of the pharmaceutical molecule in the dissolved phase is therefore not adversely affected (Baker and Kasprzyk-Hordern, 2011). Again, this approach implies that ACV, LVD and OSV exhibited marginal binding potential since these three molecules had 4-10 % of their masses sorbed to the SW components. In a previous study, compounds with comparable low octanol-water coefficients, iopromide (log D_{ow} -0.44) and venlafaxine (log D_{ow} -0.69) had significantly lower fractions of their masses (≤ 1 %) sorbed onto fungal biomass in a sorption test (Lucas et al., 2018). Their hydrophilicity drove significantly low sorption tendencies (Lucas et al., 2018). The sorption of ACV to biomass was negligible due to its low

log K_{ow} value (Xu et al., 2017). More than 99 % of ACV in wastewater was primarily transported in the filtrates (Peng et al., 2014), where ranges matched values obtained in this study. Likewise, OSV had a low affinity for sediment, and its adsorption to activated sludge was negligible (Ghosh et al., 2010; Prasse et al., 2010). A comparable amount of NVP and carbamazepine (CBZ) (75% and 83 %, respectively) remained in the solution in experiments utilizing SW sorbent. NVP and CBZ are neutral at the test pH, have log K_{ow} 2.5 and possess a butterfly-like structural conformation (Ayala et al., 2007; He et al., 2019). CBZ is a moderately hydrophobic molecule (Teo et al., 2016) and, together with NVP, exhibits a similar mid-hydrophobic character.

The SPM component in the SW in the present study was derived from sewage sludge. Due to the high carbon content of such matrix, up to 75% carbon (Shon et al., 2006), its interaction with EFV was enhanced. EFV's sorption magnitude was also elevated due to its lipophilicity and neutrality in the test environment, pH 7.5. As noted in this study, the distribution of EFV towards SPM indicates a   likelihood of inaccurate (under-estimation) reporting of the actual concentration of organic micropollutants in aquatic environments, particularly in turbid surface and waste water environments. In most studies, only the micro contaminant in the dissolved phase (filtrate) is measured, and compounds in the suspended particulate fraction are ignored (Maskaoui and Zhou, 2010; Baker and Kasprzyk-Hordern, 2011). DOC usually comprises permeates and retentates (colloids) (Nie et al., 2014). These are characterized as high surface area sorbents with a high affinity for organic contaminants, thus imparting the greatest impact on the distribution and fate of pharmaceuticals in aquatic environments (Lead and Wilkinson, 2006; Yan et al., 2015). The organic content of colloids is 2-4 times higher than for the SPM fraction, indicating its higher capacity to act as a sink for oestrogens (Nie et al., 2014), an observation consistent with this study. The data presented here also correlates

with several field studies. For example, the distribution of 9 pharmaceuticals in a river estuary heavily loaded with untreated sewage discharges was such that the pharmaceutical molecules were least concentrated in the SPM and sediment, with concentrations 2-5 times higher in the filtrate. Also, the contribution of SPM to sorption was significant for hydrophobic compounds only (Yang et al., 2011).

5.3.3 Solid-water distribution coefficient (K_d) values

The mean concentration of each ARVD across the test SW environment was used to estimate the solid-water partitioning coefficient, as shown in Table 5.2. $K_{d\ mod}$ factored in pH related to the log D_{ow} component (Lin et al., 2010). K_d usually accounts for the overall sorption, i.e. both adsorption and absorption on the solids exposed to organic molecules in the liquid phase (Lucas et al., 2018).

Table 5.2. The mean concentration of ARVDs in the dissolved phase and the corresponding experimental ($K_{d\ exp}$) and predicted ($K_{d\ mod}$) solid-water distribution coefficients.

ARVD	ACV	LVD	OSV	NVP	EFV
Concentration in the filtrate ($\mu g\ L^{-1}$)	94.16	94.33	90.55	87.28	38.25
Log $K_{d\ exp}$ ($L\ kg^{-1}$)	-1.2	-1.22	-0.98	-0.83	0.20
Log Kd mod ($L\ kg^{-1}$)	-0.61	-0.65	-0.31	1.99	3.4

Table 5.2 indicates a variation between the experimental and modelled derived K_d values. As expected, the partitioning values increased with an increase in lipophilicity. Across all molecules, the experimental partitioning values were lower than the predicted values.

For related molecules, using a similar experimental approach found, log $K_{d\ exp}$ and log $K_{d\ mod}$ for NVP to be 2.9 L kg^{-1} and 2.0 L kg^{-1}, respectively. The predicted distribution (log $K_{d\ mod}$)

values in these two experiments were not expected to differ since the pH (log D_{ow}) factor in the two experiments was not different. Log $K_{d\ exp}$ for NVP in these two studies contrasted 0.83 L kg^{-1} in the present study and 2.0 L kg^{-1} in Bagnis et al. (2018a).

There is limited sorption data on the distribution of ARVDs within wastewater sorbents; therefore, comparing the obtained wastewater sorbent K_d values for reported ARVDs data was somewhat restricted. Overall, except for EFV, the negative log Kd values for ACV, LVD, OSV and NVP, as indicated in Table 1.2, showed that these four ARVD molecules were preferentially distributed to the liquid phase than the SW sorbent.

5.3.4 ARVD accumulation in lettuce plants from plant exposure experiments

Accumulation of ARVDs in the freshwater-irrigated lettuce was higher than in the SW-irrigated plants Figure 5.3 and Figure 5.4. Across the two irrigation regimes, accumulation increased with increased exposure time. Figure 5.3 shows that within the first 24 hours of exposure, the lettuce plants accumulated a quantifiable amount of ARVD, > 1000 ng g^{-1} of NVP and EFV.
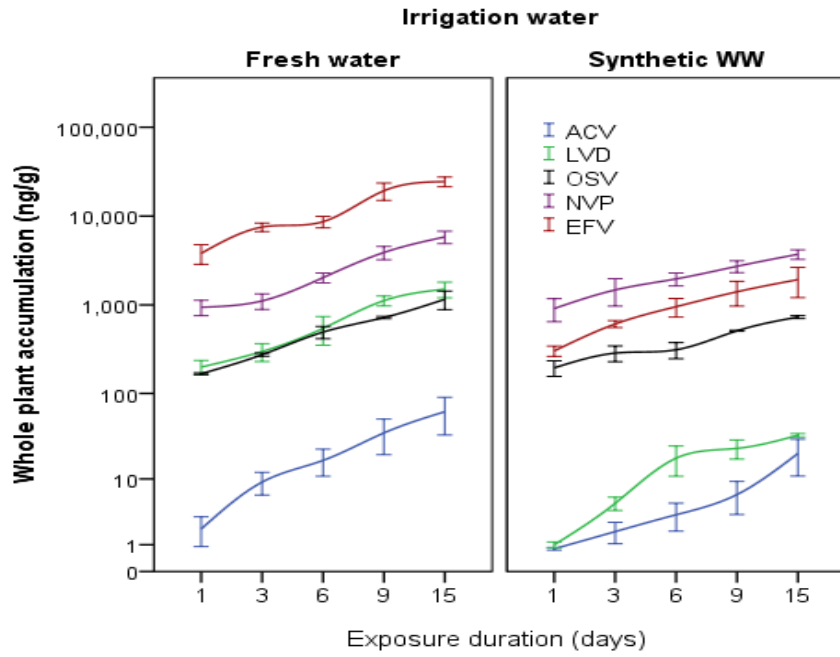
Figure 5.3. Whole-plant dry weight (d.w.) accumulation of ARVD pharmaceuticals in lettuce plants.
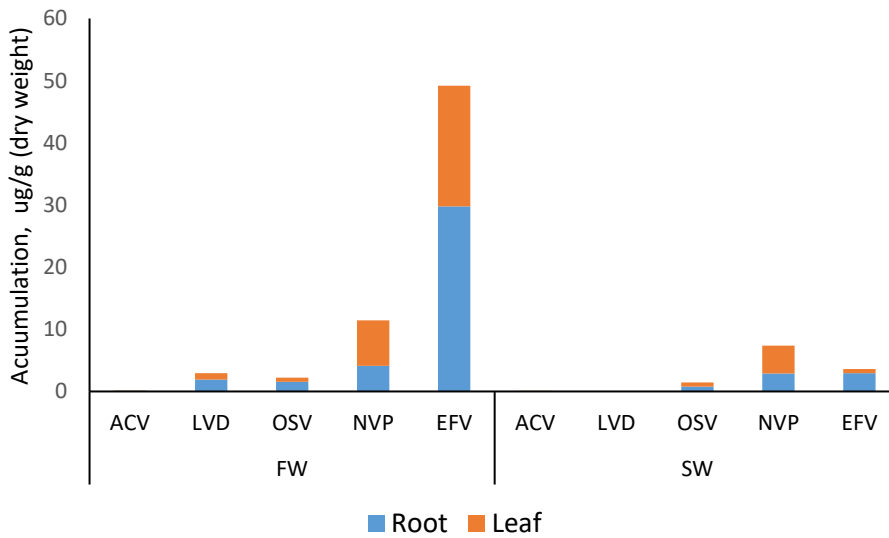
Figure 5.4. Distribution of accumulated ARVDs in roots and leaf across the freshwater and synthetic wastewater regiment

Table 5.3. ARVD speciation at exposure pH in the fresh and SW irrigation water

ARVD	Log K_{ow}[a]	Freshwater		Synthetic wastewater	
		Log D_{ow} at pH 6.2		Log D_{ow} at pH 7.2	
Acyclovir	-1.03	-1.03	Neutral	-1.03	Neutral
Lamivudine	-1.09	-1.1	98.7 % neutral [a]	-1.09	Neutral
			1.3 % cationic [a]		
Oseltamivir	1.2	-1.6	100 % cationic [a]	-0.86	99.1 % cationic [a]
Nevirapine	2.5	2.5	Neutral	2.5	Neutral
Efavirenz	4.5	4.5	Neutral	4.5	Neutral

[a] Log K_{ow} and speciation data from ChemAxon
https://chemaxon.com/products/chemicalize

An identical accumulation pattern as the one reported in Section 3.3.4 was observed.

In the freshwater-irrigated lettuce, as shown in Figure 5.4, EFV exhibited the highest accumulation at 49.1 µg g^{-1} (day 15). The bulk of the EFV was measured at the root (29.7 µg g^{-1}) and thus exhibited the highest root concentration factor (RCF) values. The accumulation of NVP in the lettuce was 11.6 µg g^{-1}, approximately 75 % less than EFV. NVP was predominantly localized in the leaves, exhibiting the highest translocation factor (TFs) of 1.77, approximately two times more concentrated in the leaves than in the roots. OSV and LVD exhibited an interesting analogous accumulation pattern in the freshwater solution (Figure 5.3). From test commencement to test termination, accumulating to 2.1 µg g^{-1} and 3.0 µg g^{-1}, respectively. As with OSV and LVD, ACV accumulation levels were correspondingly lower. It exhibited the least accumulation at levels below quantification limits.

For OSV and LVD, their log D_{ow} values were in the same range at -1.6 and -1.1, respectively, and the two molecules ionized to cationic species at pHs beyond their pKa (Table 5.3). As a result, the cationic species would have been preferentially attracted to the negatively-charged root surface sites explaining the uniform uptake pattern shown in Figure 5.3.

However, as these two ARVDs are hydrophilic, their uptake was limited when contrasted with EFV and NVP. The cationic OSV was accumulated mainly in the roots. The inability of ACV to transform into a cationic form at the exposure pHs could also have contributed to its lower accumulation compared to OSV and LVD.

Accumulation measured in the SW irrigated lettuce was significantly lower than for the freshwater irrigated lettuce (Figure 5.4). While EFV uptake was most significant in the freshwater irrigation regime, NVP exhibited the highest accumulation in SW irrigated lettuce, two times higher than EFV accumulation, i.e.,7.4 µg g^{-1}, compared with EFV at 3.8 µg g^{-1}. The reduction in accumulation for EFV and NVP compared with the freshwater irrigated lettuce was 97.8 % and 47.0 %, respectively. LVD, ACV and OSV recorded a significant decline in accumulation, 98 %, 68 % and 37 %, respectively. As in freshwater irrigated regimes, NVP exhibited > 1 TF in the SW irrigation (Figure 5.4). While the reduced accumulation of EFV and NVP in the lettuce can chiefly be attributed to the binding of the ARVD molecules to the SW matrix, as discussed in Section 5.3.2, the decline in uptake of LVD, ACV and OSV may partially be attributed to sorption and possibly other abiotic factors. Since it was one constituent of SW, it probably induced some transformation tendencies in the pharmaceutical molecules. For example, manganese oxide (an inorganic metal) and an ingredient of the SW) transformed the parent molecule of oxytetracycline and sulfamethazine (antibiotics) into a different molecule (Rubert IV and Pedersen, 2006; Gao et al., 2012).

Wastewaters usually contain higher levels of nitrogen and phosphorus, which are vital for plant growth (Ofori et al., 2021). As at test termination in this study, the SW matrix was yet to induce any physical observable growth benefits to the SW-exposed lettuce (in terms of biomass). According to Figure 5.5, the growth rate across the exposure solutions was not

significantly different at test termination (p=0.7). Likewise, no physical observable phytotoxic

effect was noticeable in any plants.
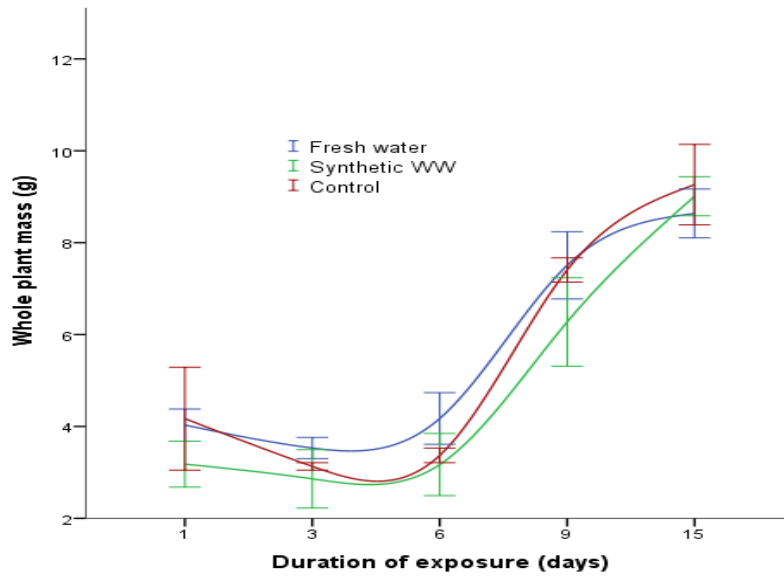
Figure 5.5. Growth curves of lettuce irrigated in freshwater, SW and control (unspiked freshwater)

5.3.5 Mass Balance

The distribution of the mass of each ARVD in the hydroponic system is shown in Figure 5.6.

The proportion of the   ARVD that accumulated in the plant ranged from 0.2-59 % and 0.1-16

% in the FW and SW solutions, respectively.
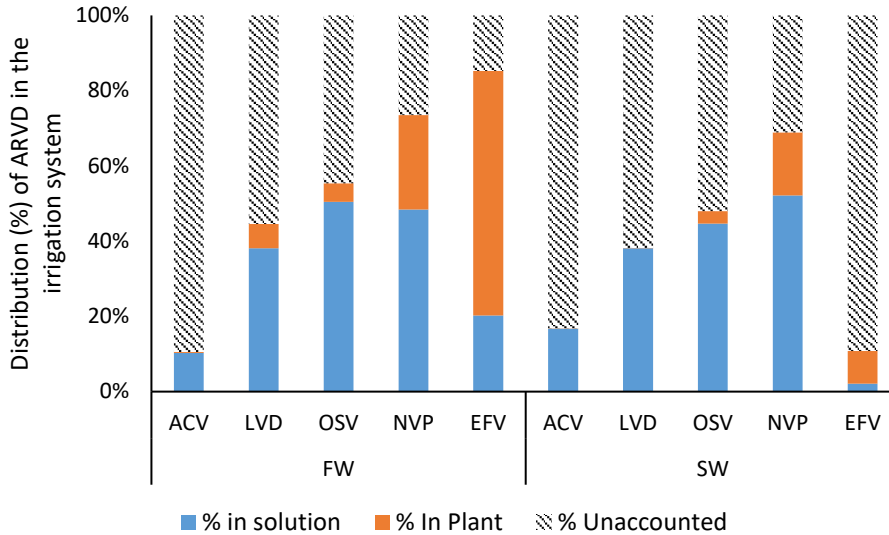
Figure 5.6. Mass balance (%) of individual ARVDs in the irrigation system

More than 75 % and 50 % of NVP and OSV were measured in the two irrigation regimes. The fraction of the unaccounted portion increased with increasing hydrophilicity of the molecule. More than 65 % of ACV was not accounted for in the FW and SW solutions. The 90 % EFV not accounted for in the SW regime was lost to the SW constituent, as demonstrated during the sorption experiments in section 5.3.2. Considering that ACV exhibited the least plant accumulation tendencies and was least retained by the SW matrix, as was measured during the sorption experiments, it was expected to persist in the irrigation water at appreciable levels.

On the contrary, less than 30 % of this molecule was measured in the FW and SW solutions. ACV and EFV exhibited a rapid loss in the exposure solution compared with other molecules, as depicted in Figure 5.7. While EFV loss was due to binding to the roots in the freshwater and wastewater sorbents in the SW, the loss of ACV, which accounts for its low concentration, was unclear.
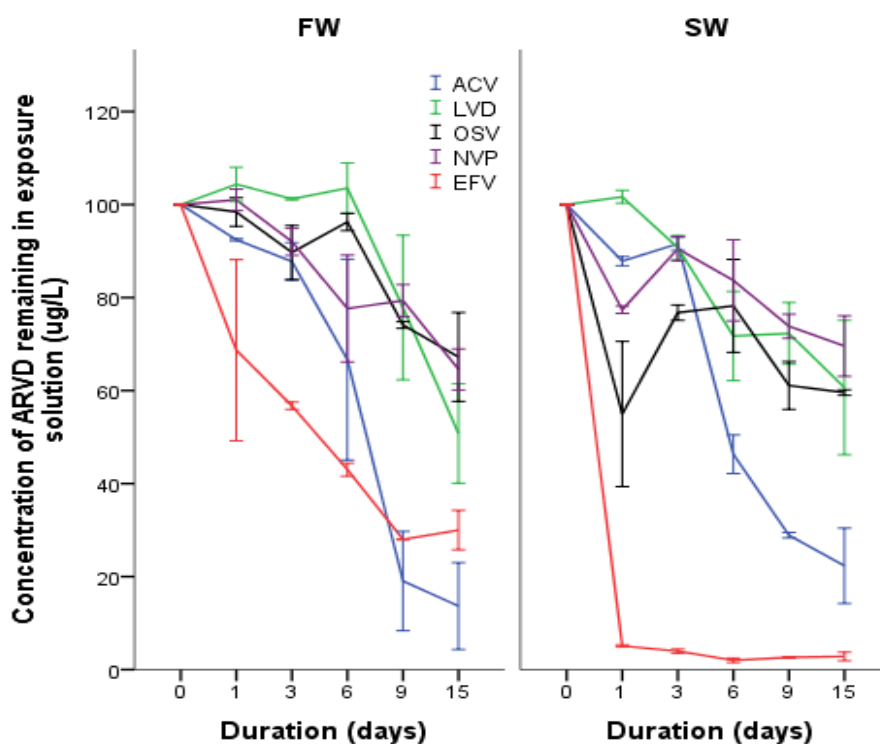
Figure 5.7. The concentration of the ARVD that remained in the solution during the exposure period (initial concentration was 100 μg L^{-1}).

At the experimental exposure pH (pH 6.2 – 7.2), ACV was 100 % unionized. Therefore, other processes, e.g. biotransformation, microbial action or photolytic degradation, remain the most probable reason for its loss. In-plant transformation and biotransformation in the exposure solutions are sometimes responsible for the loss of the parent molecule. (Huber et al., 2016)(Nason et al., 2019). ACV was less stable in solution than in solid-state form, with 11 % photolytic loss measured over time (Sinha et al., 2007).

5.4 Conclusion

In this study, molecule lipophilicity was the main driver ofbinding potential since ≥ 75 % mass of EFV (log K$_{ow}$ 4.5) in suspension was retained by the wastewater constituents. Concurrently, the wastewater constituents retained less than 15 % mass of mid-hydrophobic to hydrophilic

ARVDs (2.5 ≤ log Kow ≤ -1.0). The concentration of the hydrophilic ARVDs, ACV and LVD that remained in solution was approximately 30-70 %, yet these molecules least accumulated in the exposed plants. It was noted that their dissipation rate was higher than the lipophilic molecules, implying that in actual environments, such hydrophilic pharmaceuticals' parent molecules would have the least impact on exposed receptors. Accumulation of ARVDs in the SW-exposed lettuce was up to 5 times lower than for freshwater-spiked lettuce. It implies that the accumulation of characteristically similar molecules in turbid waters would experience comparable low accumulation levels. An increase in turbidity levels was revealed to not necessarily imply a positive correlation with an increase in the binding potential to the pharmaceutical molecules. The sorption experiment showed that the dissolved organic and the suspended component retained 50 % and 25 % of the lipophilic molecule, respectively. Approximately 75 % of lipophilic EFV was retained in the SW components. Therefore, for accurate risk assessments in actual aquatic environment compartments, it is also crucial to directly measure microcontaminants that have partitioned to the suspended particulate and settled sediments.

Chapter 6
Sorption/desorption of anti(retro)virals pharmaceuticals in soils

Overview

Sorption/desorption trends of five anti(retro)virals (acyclovir, lamivudine, oseltamivir, nevirapine and efavirenz) intwo types of soil were undertaken using OECD 106 methods. Variations in sorption tendencies were evaluated using synthetic wastewater (as a proxy for actual wastewater) relative to the routinely used $CaCl_2$ solution (representing freshwater). Soil characterization showed that the two test soils differed mainly in organic matter. The soil with high organic content (approximately 10 times higher) exhibited high adsorptive characteristics. The sorption potential tendency across the two soils was such that efavirenz>oseltamivir >nevirapine >acyclovir >lamivudine. Due to potential biodegradation, the sorption tendencies for lamivudine and acyclovir were less obviously correlated to the soil properties.

6.1 Introduction

Various interdependent processes, including volatilization, sorption-desorption, chemical and biological degradation and leaching, are responsible for the fate of pharmaceuticals in the terrestrial environment (Müller et al., 2007). Sorption/desorption processes, in particular, are important in controlling the input, transport and transformation of these molecules in the terrestrial environments, significantly influencing the fate of pharmaceutical residues in agroecosystems (Martínez-Hernández et al., 2014; Fountouli and Chrysikopoulos, 2018a). Even before irrigation, the wastewater matrix properties (e.g. ion content, dissolved organic matter concentration, pH and electrolyte composition) control the fate of a compound either by increasing its mobility or sequestering it to wastewater sorbents (Müller et al., 2007;

Martínez-Hernández et al., 2014). It is important to mention that accurate estimation of pharmaceutical soil-water distribution affinities is vital in assessing the molecule's fate in agroecosystems. Soil-water distribution coefficients (K_d) can be experimentally determined or indirectly estimated from octanol-water partitioning coefficients (K_{ow}). They can also be derived from computational modelling using free energy calculations (Wegst-Uhrich et al., 2014). Presently, there is insufficient information regarding the sorption of pharmaceuticals in soils. Even for frequently measured pharmaceuticals, sorption tendencies data is available for only 6 % of the estimated 1912 pharmaceuticals in the British market on an estimated 100 types of soils (Li et al., 2020).

Therefore, this study's objective was to evaluate the sorption/desorption tendencies of the five anti(retro)virals molecules in two soils using synthetic wastewater (which simulated actual wastewater) $CaCl_2$ solution (representing freshwater). The sorption experiment intended to simulate the transfer of the pharmaceuticals from an irrigation agent while desorption infiltration into the soils by actual wastewater or rainwater).

6.2 Materials and method

6.2.1 Origin of soils

The sorptive potential of the ARVDs was tested on two types of soils. One soil was obtained from Lufa Speyer, Germany, from land previously not irrigated or treated with wastewater nor amended with fertilizer or biosolids in the previous five years. The second soil was obtained from the University of Plymouth (UoP) greenhouse gardens. Some agricultural activities had previously been carried out on this site, including occasional fertilizer application. However, wastewater had never been applied to the soil, only rainwater.

6.2.2 Soil characterization

6.2.2.1 Determination of soil organic matter

SOM was estimated using the Loss-on-Ignition method (LOI). The organic matter (% OC) in this method was estimated based on a change in mass after high-temperature oxidation of the organic component of the soil. Initially, the soils were sifted through a 1 mm sieve and oven-dried at 105°C for 1 hour. Afterwards, the dried soil samples were placed in pre-weighed crucibles, and a muffle furnace operated at 450 ^{0}C for 4 hours.

6.2.2.2 Estimation of particle size

Soil particle size was estimated using the particle size analyzer. Soil samples were air-dried and sifted through a 1 mm sieve. A small subsample of approximately 0.5 g was placed in a 12 mL digestion vial. Three mL of 3 % H_2O_2 solution was added to the soil, and the mixture was left to stand for 12 hours. The samples were then placed in a water bath and heated to 90 °C for 2 hours. After cooling, the samples were marked up to volume with ultrapure water and analyzed using particle size estimator, Malvern MS2000 laser diffraction equipped with autosampler. Five replicate samples were identically prepared. Soil texture characterization was obtained from an algorithm available at Land Information system UK (LandIS, 2021).

6.2.2.3 Soil pH

pH measurements were obtained from triplicate samples taken using a calibrated pH meter. The soil pH was measured in a solution of 10 mM $CaCl_2$ solution at a soil-solution ratio of 1:5, whereby 2 g of soil was placed in a tube of 50 mL, and the $CaCl_2$ solution was added. The mixture was shaken for 10 minutes and allowed to stand for 1 minute. The overall soil charge was estimated by comparing the pH obtained from $CaCl_2$ and the pH measured using reverse osmosis (RO)- soil solution following soil pH protocols (Rowell , 1994).

6.2.2.4 Dissolved organic carbon (DOC) and total nitrogen (TN)

Soil DOC and TN were extracted from soil using a soil: HPW ratio of 1:10. The soil-water mixture was placed in a glass centrifuge tube, shaken in a mechanical shaker for 2 hours, then centrifuged for 15 minutes at 4000 rpm. The supernatant was filtered through a 0.7 µm GFF, and an appropriately diluted aliquot was transferred to a clean-ashed glass vial. The samples were acidified using 20 µL of concentrated HCl and preserved at 4 ^{0}C until analyses. Analyses were performed using a Shimadzu TOC-V analyzer equipped with a TN analyzer that allowed for simultaneous measurement of DOC and TN. The DOC standard was prepared using potassium hydrogen phthalate, TN using sodium nitrate, and the calibration plot was used to quantify the measured DOC and TN.

6.2.2.5 ARVD loss from 10 mM CaCl$_2$ solution to soil.

6.2.2.6 Adsorption

The sorption tendencies of the ARVDs to the soils were measured according to the OECD 106 adsorption-desorption batch equilibrium method (OECD, 2000). The initial aqueous ARVD concentration range was selected based on the molecule's solubility, the SOM and the instrument's known detection limits.

Two grams of the test soils were placed in a glass centrifuge tube containing 9.5 mL of 10 mM CaCl$_2$. This mixture was shaken for 12 hours in a reciprocal shaker operated at 150 rpm. A 1:5 (w/v) ratio was used experiment. After the shaking, a 0.5 mL aliquot of the ARVD standard stock was added to the mixture to reach a final volume of 10 mL and the desired aqueous phase concentration. Equilibration time was established by sacrificially sampling the tubes at 0, 3, 6, 9, 12 and 24 hours. The tubes were covered with aluminium foil to minimize direct exposure to light during agitation. Control tubes (spiked with ARVDs but without soil) were

included to monitor potential losses from the shaking process. After shaking, the samples were immediately centrifuged, filtered and stored in a freezer at -20 ^{0}C until analysis. The solution's pH and DOC concentration were determined for each sample.

The concentration of ARVDs that remained in the filtrate was used to determine the soil-water distribution coefficient, K_d. The organic carbon normalized coefficient, log K_{oc}, according to Equations (6.1) and (6.2), respectively.

$$K_d = \frac{m_{s(eq)}}{m_{aq\ (eq)}} \cdot \frac{v_o}{m_{soil}}$$

(6.1)

Where K_d is the soil distribution coefficient (mL g^{-1}), $m_{s\ (eq)}$ mass of ARVD sorbed to the soil at equilibrium (g), $m_{aq\ (eq)}$ is the mass of ARVDs in the aqueous phase at equilibrium (g), v_o is the initial volume of the aqueous phase (mL), m_{soil} mass of soil (g).

The organic carbon-normalized adsorption coefficient K_{oc} compares soils with different organic content levels.

$$K_{oc} = K_d \cdot \frac{100}{\%\ OC}$$

(6.2)

K_{oc} is the organic normalized adsorption coefficient (mL g^{-1} OC^{-1}), and % OC is the organic carbon content in the soil.

The K_{oc} for non-hydrophobic molecules was predicted using Equation (6.3)   (Sabljic et al., 1994).

$$log \, K_{OC} = 0.52 * log_{Kow} + 1.02 \tag{6.3}$$

6.2.2.7 Desorption

For desorption, an equal volume of the supernatant removed after centrifugation during adsorption was replaced in the tube. The soil plug in the tube was resuspended by vigorous shaking for 15 seconds. The tubes were then returned to the orbital shaker, agitated and sacrificially sampled at hours 3, 6, 12 and 24. Similarly, the centrifuged aqueous fraction was filtered using a 0.7 µm GFF and stored at -20 ^{0}C until analyses. Different solutions from the individual soils were used to prepare matrix-matched standards for quantification.

Desorption was estimated using Equation (6.4), which indicated the amount of molecules removed from the soil as a percentage of the initially adsorbed molecule mass.

$$D = \frac{m_{des \, aq}}{m_{ads \, s}}.100 \tag{6.4}$$

Where D is the % molecule desorbed, $m_{ad \, s}$ is the mass ARVD adsorbed to the soil at equilibrium (µg) and m des aq is the mass of ARVD desorbed from the soil at equilibrium.

The apparent desorption coefficient, K_{des} was determined using Equation (6.5), which is the ratio between the molecule's mass in the soil and the mass concentration of the desorbed compound in the aqueous solution when desorption is attained.

$$K_{des} = \frac{m_{ads \, s}}{m_{des \, aq}}.\frac{v_T}{m_{soil}} \tag{6.5}$$

Where K_{des} is the desorption coefficient (mL g^{-1}), V_t the volume of aqueous phase (mL), m_s mass of the soil (g)

6.2.3 Adsorption isotherms

Adsorption isotherms were evaluated in the 50 – 1000 µg L^{-1} and 5 - 200 µg L^{-1} ARVD concentration ranges for UoP and Lufa soil, respectively, generally spanning the recommended two orders of magnitude concentration range following the OECD method 106 (OECD, 2000). The 1:5 soil: solution ratio was maintained. The pharmaceuticals in the aqueous phase were introduced as a mixture in a single centrifuge tube to minimize the number of samples. After overnight soil-solution agitation, an aliquot of the mixed standard was added to yield the desired aqueous concentration. The mixture was afterwards equilibrated for 12 hours. The mass of the molecule remaining in the aqueous phase was measured using LC-HR-MS. The adsorption capacity of the soils was estimated by plotting a graph of the mass adsorbed onto the soil against the concentration in the aqueous phase at equilibrium using the Freundlich and Langmuir isotherms shown in Equations (6.6) and (6.7), respectively.

$$Log \; q_e = Log \; K_F + 1/n \; log \; (C_e) \qquad (6.6)$$

Where q_e (µg g^{-1}) represents the amount of molecule adsorbed at the soil surface at equilibrium, C_e is the concentration in the aqueous phase at equilibrium (µg L^{-1}), n the Freundlich constant, which describes the degree of surface heterogeneity, defining the distribution of the adsorbed molecules on the adsorbent surface.

K_F is the Freundlich exponent (µg g^{-1}), indicating the adsorption capacity of the adsorbent (soil) towards the adsorbate (ARVD molecule).

Langmuir's adsorption model was demonstrated using Equation (6.7).

$$\frac{C_e}{q_e} = \frac{1}{K_L q_{max}} + \frac{C_e}{q_{max}} \qquad (6.7)$$

Where C_e (µg L^{-1}) and q_e (µg g^{-1}) are the concentration of the molecules in the aqueous phase and the amount of the adsorbed molecules in the soil at equilibrium, respectively; q_{max} is the maximum adsorption capacity of the soil (µg g^{-1}), and K_L is the Langmuir constant (L µg^{-1}).

6.2.4 Transfer of ARVDs from CaCl$_2$ and synthetic wastewater to soils

Identical ARVD concentrations were introduced to the CaCl$_2$ and SW aqueous matrices, and the magnitude of the transfer of the ARVDs to the soils was compared.

6.3 Results and Discussion

6.3.1 Soil characteristics

Table 6.1. Soil texture composition, organic matter and pH

Origin	Composition (%)				pH (CaCl$_2$)	Soil type	Abbreviation
	Sand	Silt	Clay	OC			
Lufa Speyer	67	31	2	0.6	5.7	Sandy Loamy	SL
University of Plymouth (UoP)	55	44	1	9.50	7.3	Sandy Loamy	OSL

Table 6.1 shows that the SOM of the UoP soil was approximately 15 times higher (9.5 %) than the Lufa-Speyer obtained soils (0.6%). Nonetheless, the two soils were categorized as sandy-loamy based on sand, silt, and clay content. The sandy-loamy soil type represents one type that has been amended with wastewater or biosolids in an agroecosystem (Karnjanapiboonwong et al., 2010). A 1.5 unit pH difference was measured between the two soils. In the remainder of the study, to differentiate the two soils, Lufa soil was abbreviated as SL and UoP soil as OSL, where O- indicated its higher organic content.

Table 6.2. Variation of soil pH measured in RO water and 0.01 M CaCl$_2$ solution (n=5, ± SD)

	RO water	10 mM CaCl$_2$	Overall charge
SL soil	6.4±0.06	5.6±0.12	negative
OSL soil	7.4±0.03	7.0±0.06	negative

Table 6.2 shows that soil pH measured in RO water was 0.8 and 0.4 pH units higher in the SL and OSL soils, respectively, indicating that both soils were negatively charged. Soils with a net negative charge are approximately 0.5 pH units higher in water than in CaCl$_2$ solution due to the displacement of the H$^+$ from the soil (Lees, 2018).

6.3.1.1 Soil DOC and Total Nitrogen concentration

Table 6.3 shows that synthetic wastewater (SW) and CaCl$_2$ OSL soil extracts contained approximately three times higher DOC concentrations than their associated SL extracts. The SW and CaCl$_2$ TN extract from the OSL soil were 8 and 2 times higher than their associated SL extract. Overall, SW extracts in both soils contained higher levels of DOC and TN.

Table 6.3. Freshwater (CaCl$_2$) and Synthetic wastewater (SW) extracted DOC and Total nitrogen concentration levels for SL and OSL soils (n=6,±SD)

	Freshwater (CaCl$_2$)		Synthetic wastewater	
	DOC (mg L^{-1})	TN (mg N L^{-1})	DOC (mg L^{-1})	TN (mg N L^{-1})
OSL	866 ± 30.2	170 ± 80.0	1018 ± 20.3	390 ± 37.4
SL	309 ± 40.3	23 ± 9.8	378 ± 45.0	221 ± 25.0

6.3.2 Adsorption experiment

The pH variation in the two soil suspensions was monitored during the adsorption experiment. The overall pH difference between the two soils was < 1.5 pH units, varying from 6.3 to 7.0 (Figure 6.1).
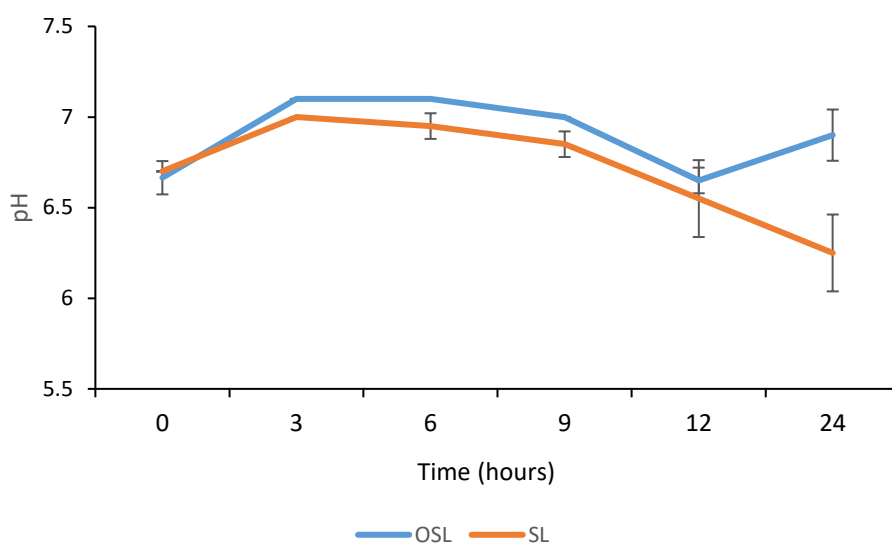
Figure 6.1. Variation of soil pH in suspension during the 24-hour agitation period (n=3, ± SD)

While measuring adsorption in SL soils, a uniform initial concentration of 150 µg L^{-1} for all the molecules was selected, Table 6.4. The concentrations were considered appropriate since the SL soils contained relatively lower SOM and DOC levels than the OSL soils. The initial ARVD concentration in the aqueous phase for the OSL soil varied from 200 -500 µg L^{-1}. Consideration for the initial aqueous concentration also reflected the molecules' theoretical lipophilicities.

Table 6.4. Anti(retro)viral molecule solubilities, lipophilicities and initial concentration in the aqueous phase (CaCl$_2$) for the adsorption experiment

	Solubility (µg L^{-1})[a]	Log K$_{ow}$[a]	Initial concentration in the aqueous phase (µg L^{-1})	
			SL soils	OSL
ACV	9.0 ×10^6	-1.0	150	200
LVD	13.8 ×10^6	-1.0	150	200
OSV	8.1×10^3	1.0	150	400
NVP	1.9×10^6	2.5	150	400
EFV	9.3[b]	4.3	150	500

[a] ChemAxon, https://chemaxon.com/products/chemicalize
[b] US EPA, 2012

An important requirement in adsorption-desorption experiments is that the concentration of the test molecule should not exceed its solubility in the aqueous phase (OECD, 2000), hence the significance of Table 6.4. According to Table 6.4, all the ARVDs were within their aqueous solubility limits, except for EFV. EFV exhibits low solubility, estimated to be 9.3 µg L^{-1} (US EPA, 2012) or is sometimes considered insoluble in water (ChemAxon, 2021). EFV was introduced at 1.5 and 5 times higher than its actual aqueous solubility in the SL and OSL soil matrix.

Nonetheless, it was demonstrated that the apparent aqueous solubility of such hydrophobic compounds increases in the presence of particulate matter and colloids (Delgado-Moreno et al., 2010). An alternative approach would have been to reduce the OSL soil's mass to minimize the molecule's loss from the aqueous phase.

As much as the initial EFV concentration was not optimal, it was a mechanistic trial. A higher initial concentration was necessary to permit detection in the aqueous phase after sorption. The detection limits for the ARVD in the two soils were estimated from the constructed matrix-matched calibrations using the ICH approach (ICH, 1995) (the approach was described

in section 3.2.3). They varied from 0.8 to 1.5 µg L^{-1} and 0.7 to 2.4 µg L^{-1} in SL and OSL, respectively, Table 6.5.

Table 6.5. LC-HRMS method detection limits (µg L^{-1}) for ARVDs in SL and OSL soil matrix in aqueous $CaCl_2$

	Detection limits (µg L^{-1})	
	SL soil	**OSL soil**
ACV	0.8	0.7
LVD	0.8	1.1
OSV	1.2	1.0
NVP	0.7	0.5
EFV	1.5	2.4

Rapid sorption was measured on the filtrate collected within the first 3 hours, as illustrated in Figure 6.2 and Figure 6.3, which reflected the availability of active soil sorption sites. After the initial 3 hours, the loss of ARVDs to the solid phase was insignificant, possibly due to repulsive forces between the ARVD molecules, slowing adsorption (Kumar et al., 2008). However, fully occupied and hence unavailable active sites remained the most probable reason for the slowed loss to the solid sorbent. Eventually, an aqueous equilibrium concentration was attained within 24 hours of agitation. Equilibration times vary across experiments. For example, Lees (2018) extended the equilibration process to 120 hours. OECD guidelines, however, infer that acceptable equilibrium can be attained within 24 hours for most molecules (OECD, 2000).
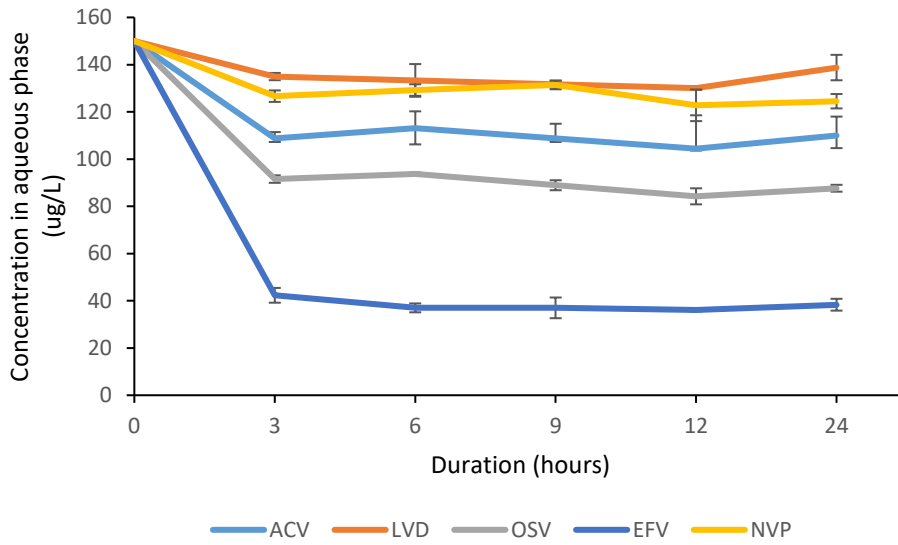
Figure 6.2. Equilibrium concentration of the ARVDs in the aqueous phase in the SL soils over 24 hrs of agitation (n=3, ± SD)
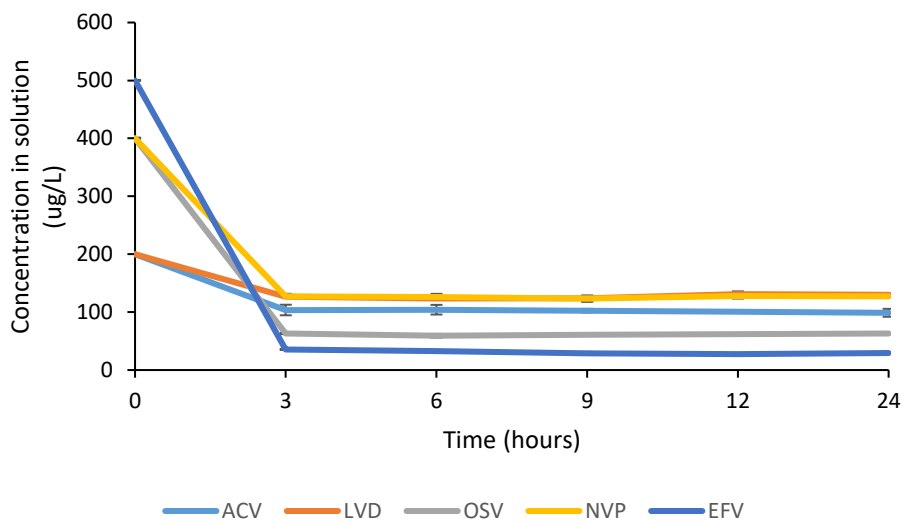
Figure 6.3. Equilibrium concentration of ARVDs in the aqueous phase of OSL soils over 24 hrs of shaking (n=3, ± SD)

.

Concerning initial aqueous concentrations, sorption experiments should be performed at environmentally relevant pharmaceutical residue concentrations (Wegst-Uhrich et al., 2014). The initial aqueous phase concentrations in the two soils in the present study varied between 5-1000 µg L^{-1}. While the initial concentrations were consistent with OECD guidelines and previous studies on the lower end, < 10 µg L^{-1}, they were higher than routinely measured environmental and pharmaceutical concentrations, especially in the higher end, > 100 µg L^{-1}. ARVDs have been spatially measured at exceptionally high concentrations in surface water and wastewater, particularly in Africa. For example, efavirenz was measured in surface and wastewater at concentration ranges from 12 to 228 µg L^{-1} in South Africa, Zambia and Kenya (Madikizela et al., 2020;Ngumba et al., 2020 ; Adeola and Forbes, 2022). As adapted in the present research, previous studies have employed higher than environment-measured initial aqueous concentrations in pharmaceutical sorption experiments. For example, the interaction of acyclovir and fluconazole with quartz sand was performed at an initial concentration of 3-10 mg L^{-1}, a concentration 1000-times higher than in the present study (Fountouli and Chrysikopoulos, 2018b). Also, the sorption of carbamazepine and lamotrigine in soils was measured at initial concentrations > 5 mg L^{-1} (Paz et al., 2016b). Furthermore, in measuring the sorption kinetics of efavirenz to graphene wool, initial aqueous concentrations were prepared in the range of 1-20 mg L^{-1}, considerably above the solubility of EFV (Adeola et al., 2021).

The ARVDs were introduced into the soils as a mixture rather than separate individual molecules in the present study. Whereas pharmaceutical mixtures can impact individual sorption tendencies, such as competing for existing active sites (Kočárek et al., 2016), the present experiment approach replicates an actual environmental scenario.

When the adsorbate and adsorbent are at equilibrium, a defined solute distribution is developed between the solid and fluid phases, and no further net adsorption is realized (Doran, 2013). Table 6.6 shows the amount of the ARVD partitioned from the aqueous phase to the soils at equilibrium.

Table 6.6. Measured ARVD soil sorption equilibrium properties in OSL and SL soils (n=3, ± SD)

Soil	ARVD	Loss from the aqueous phase to soil (%)	K_d (mL g^{-1})	log K_{oc} (mL g^{-1} OC^{-1}) (experimental)	Log K_{oc} (predicted)
SL	ACV	43.5±5.6	1.6±0.7	2.5±0.2	-0.6
	LVD	33.1±0.07	0.60±0.006	2.0±0.0	-0.6
	OSV	55.8±0.06	3.4±0.01	2.8±0.001	-1.1
	NVP	36.5±1.6	0.91±0.2	2.2±0.07	2.0
	EFV	80.9±1.2	15±1.2	3.4±0.03	3.4
OSL	ACV	82.3±2.1	39±8.1	2.6±0.09	-0.6
	LVD	55.2±3.5	11.6±0.0	2.1±0.0	-0.6
	OSV	58.4±2.5	24 ±0.82	2.4±0.01	-1.0
	NVP	42.9±3.0	13 ±0.59	2.1±0.01	2.0
	EFV	99.6±0.2	285 ±2.0	3.5±0.0	3.48

In the SL soils, the filtrate concentrations were such that EFV > OSV > ACV > NVP > LVD at 81, 56, 44, 37 and 33 %, respectively. Significantly higher sorption, 16-90 % (based on loss from the aqueous phase), was measured in the OSL than in SL soils. In the OSL soils, the extent of ARVD transfer from the aqueous phase in descending order was EFV > ACV > OSV > LVD > NVP

i.e., 99, 82, 58, 55 and 42 % respectively. Accordingly, the K_d values in the OSL soil were greater than in the SL soils, varying from 11-285 and 0.16-14 mL g^{-1}, respectively.

The experimental and predicted log K_{oc} properties for neutral NVP and EFV were nearly identical ($\pm$ 0.2) but differed for OSV, LVD and ACV. The log K_{oc} variation in the three molecules from predicted values highlights the inadequacy of using mathematical models to determine log K_{oc} values of ionizable molecules and, therefore, the significance of actual sorption experiments (Wegst-Uhrich et al., 2014; Lucas et al., 2018). The predicted and experimental measured log K_{oc} similarity between the neutral NVP and hydrophobic EFV gave confidence in the selected experimental conditions and initial pharmaceutical concentrations employed.

Scrutiny of the loss from suspension to soil data (Table 6.6) shows that the hydrophilic ACV and LVD exhibited unexpectedly high losses relative to OSV and NVP. Based on ACV's and LVD's octanol-water characteristics (Table 6.4), the two highly hydrophilic molecules were expected to exhibit minimal losses compared with NVP and OSV since they are not cationic. For this reason, the assumption that all ARVD loss from suspension to soils was primarily from sorption was likely, not valid for ACV and LVD. It was possible that other unspecified processes (e.g. degradation or complexation in solution) contributed to their uncharacteristically high losses relative to less polar and cationic molecules. For example, in the OSL soil, it is theoretically not feasible for ACV (82 % loss) to have a naturally high sorption tendency, K_d 39.2 mL g^{-1}, than with OSV's (58 % loss) K_d 24 mL g^{-1} in the same soil environment. The possibly noted non-sorption losses from ACV and LVD were highest in the OSL soil. Notably, no significant losses (> 8 %) were measured in the ARVD stability test; therefore, the suspected non-sorption losses were potentially soil matrix specific.

OSV, NVP, and EFV K_d values were 6-20 times higher in the OSL soil than in the SL soil (ignoring ACV and LVD due to their uncertainties). OSV exhibited a 22 % difference, the most considerable difference in sorption between SL and OSL soils, 22 %, while EFV and NVP values were 19 and 6 %, respectively.

Normalizing the K_d values by the soil OM content generated identical log K_{oc} values across the two soils for all the molecules (Table 6.6). The generation of identical log K_{oc} from soil organic matter values indicates that sorption is primarily governed by soil organic matter OM content (Paz et al., 2016b).

6.3.3 Desorption

Desorption data provides essential information regarding the mobility of pharmaceuticals in soils. It also indicates how strong a molecule is bound to soil particles (Petruzzelli and Pedron, 2020) and depicts whether there is a risk in the soil compartment either from irreversible or reversible-sorbed pharmaceuticals (Mohan and Karthikeyan, 1997). Table 6.7 shows that within the 24 hours equilibration time, desorption was more pronounced in the SL than in the OSL soil, 20-96 % and 1-62 %, respectively. Accordingly, the measured K_{des} values SL soil were 2.5 to 17 times lower than in the OSL soils.

Table 6.7. ARVD soil desorption equilibrium properties in OSL and SL soils (n=3, ± SD)

Soil	ARVD	ARVD concentration in the aqueous phase	% desorption	K_{des} (mL g^{-1})
SL	ACV	18.5±1.8	41.9±9.2	7.2±2.6
	LVD	21.2±1.4	95.9±11.0	0.4±0.4
	OSV	31.8±0.5	48.5±3.2	5.3±0.7
	NVP	12.9±0.0	48.9±12.0	5.5±2.5
	EFV	23.1±0.5	20.2±0.3	19.6±0.4
OSL	ACV	18.9±0.07	19.1±0.36	21±0.5
	LVD	47.9±0.0	62.6±1.14	2.9±0.15
	OSV	57.3±1.3	16.8±0.24	24.6±004
	NVP	70.9±0.6	25.6±0.7	14.5±0.6
	EFV	7.1±0.01	1.5±0.02	326.4±3.3

In both soils, LVD exhibited the highest desorption at 95 and 62 % in SL and OSL, respectively and the lowest K_{des} value at 0.4 and 2.9 mL g^{-1}. OSV and NVP in the SL soil exhibited reversibility tendencies as approximately 50 % of their mass was desorbed from the soil, i.e. 48.9 and 48.5 % in NVP and OSV, respectively. EFV exhibited the least desorption in the OSL soil, with < 2 % of its initially adsorbed mass partitioned back to the aqueous phase. The K_{des} and K_d for NVP and OSV in the OSL soils were identical.

Recalling the sorption uncertainties of ACV and LVD described in Section 6.3.2, it is likely that the same unpredictability was transferred to desorption since the experimental process was continuous. The individual adsorption and desorption tendencies of these molecules will be discussed in Section 6.3.5.

6.3.4 Adsorption isotherms

Determination of sorption via adsorption isotherms is ideal for estimating concentration-dependent soil-water distribution properties (Wegst-Uhrich et al., 2014). Table 6.8 showed that the Freundlich model adequately reflected the sorption behaviour of the ARVD molecules in the OSL soils as indicated by higher correlation coefficient R^2 values, 0.9392--0.9995, compared with the Langmuir model, which exhibited lower R^2 values, 0.0365-0.608. Isotherm data on SL soil was not presented due to concentration in the aqueous phase being lower than the MLoQ at two concentration levels; estimating isotherms from three data points would be unreliable.

Table 6.8. Sorption isotherm data for ARVD in OSL soil

		Freundlich			Langmuir		
	ARVD	K_F ($\mu g^{-1-1/n} L^{1/n} g$)	n	R^2	K_L (L μg^{-1})	M (g g^{-1})	R^2
	ACV	0.3678	0.7	0.9641	0.11	30.2	0.608
OSL	LVD	0.3328	0.56	0.9682	0.18	111.1	0.1219
	OSV	0.2018	0.97	0.9983	0.02	57.6	0.1475
	NVP	0.2018	0.91	0.9392	-4.7	94.1	0.0365
	EFV	0.670	0.44	0.9995	0.42	1.8	0.7942

Figure 6.4 and Figure 6.5 illustrate the linearization of the Freundlich and Langmuir models, respectively.
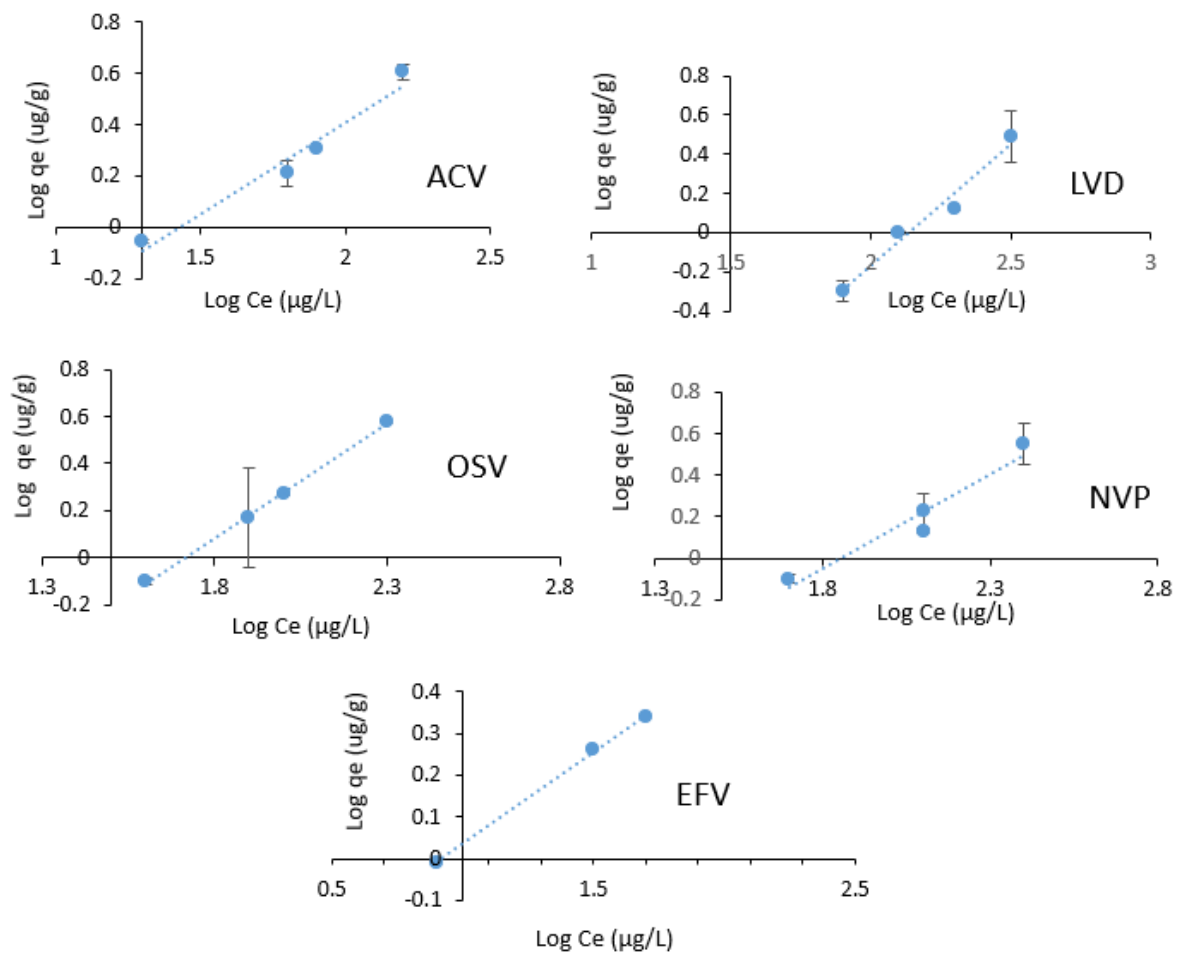
Figure 6.4. Linearized Freundlich isotherms for ARVDs in OSL soils (n=3, SD)
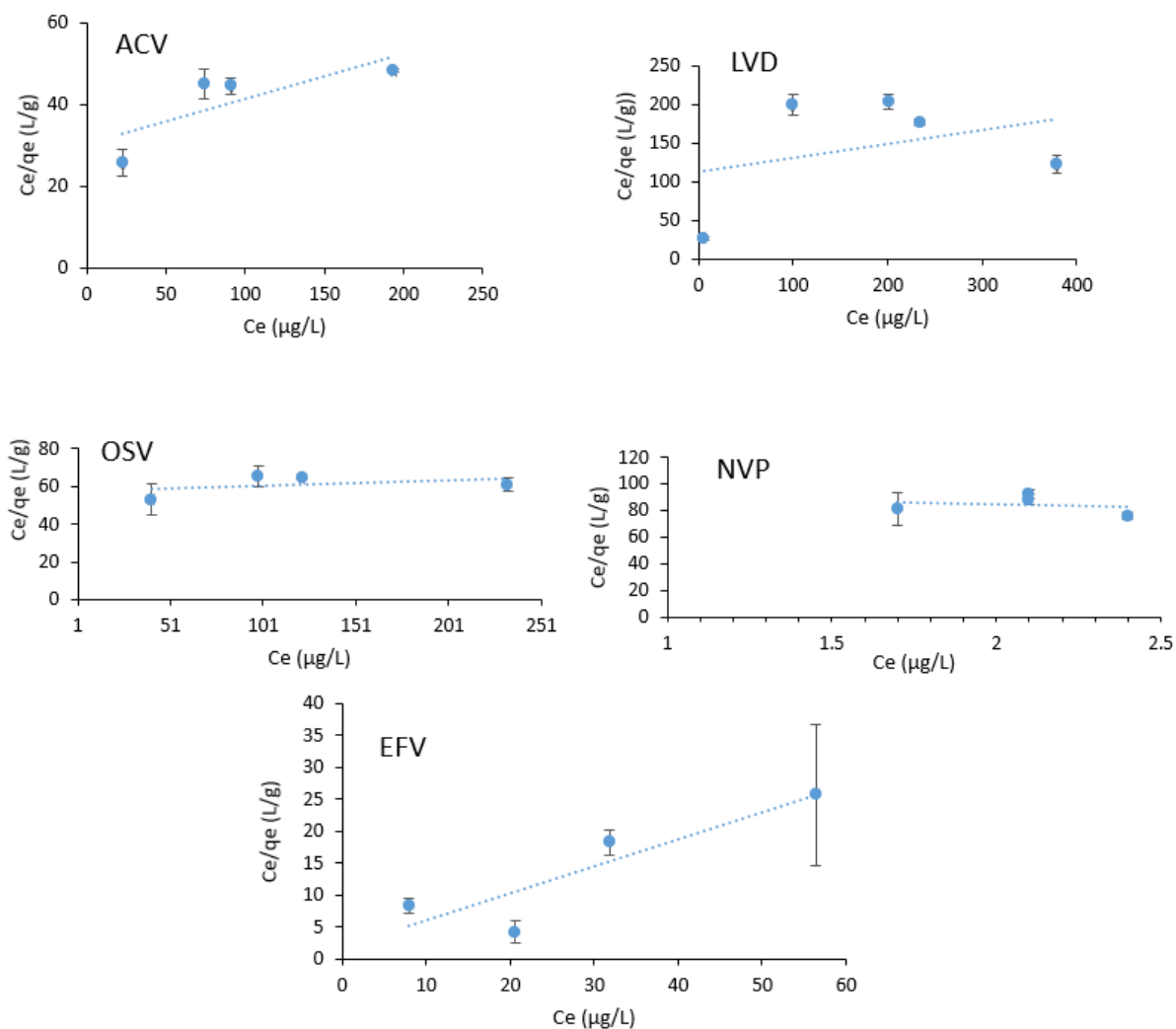
Figure 6.5. Linearized Langmuir isotherms for ARVDs in the OSL soils (n=3, ± SD)

Table 6.8 showed that the Freundlich isotherm, n, for all ARVDs was < 1, indicating an unfavourable and thus non-linear adsorption for most of the ARVDs molecules in the OSL soils. An exception was NVP and OSV, whose n was close to 1, i.e. 0.91 and 0.97, respectively, implying some degree of favourable sorption. In (Lees, 2018), the NVP Freundlich isotherm was almost linear in loam soil, i.e..n= 0.94, which was analogous to the estimated n value for NVP in the present study, i.e. n=0.91. It is not uncommon for pharmaceutical molecules isotherms to be non-linear. For example, CBZ isotherms in soils irrigated with treated wastewater exhibited non-linear characteristics, with n varying from 0.64-0.91 (Drillia et al.,

2005). In highly organic soils, n for CBZ was 1.49, which diminished to 1.05 after homogenizing the highly organic soils with characteristically less organic content (Drillia et al., 2005). The observation implied that elevated soil organic levels in the OSL soils favoured non-linearization.

Concerning the Langmuir isotherm, the maximum adsorption capacity of the soil, M, inversely varied with the magnitude of sorption of the individual ARVDs, which was expected. As shown in Table 6.8, the estimated M for EFV, OSV, NVP and LVD was 1.8, 57.6, 94.1 and 111.1 $\mu g\ g^{-1}$, respectively. An exception is ACV, notably due to its uncharacteristic sorption tendency previously discussed in section 6.3.2.

6.3.5 Molecule-specific adsorption-desorption characteristics

This section discusses the results of the theory behind the sorption tendencies measured in Sections 6.3.2 and 6.3.3.

6.3.5.1 Acyclovir

Acyclovir loss from the aqueous phase in the OSL matrix to the soils was two times higher than losses measured in the SL soils, at 83 and 42 %, respectively, with K_d values of 39 and 1.6 mL g^{-1}, respectively, (Table 6.6). The lipophilicity of ACV at the experimental pH was constant and at -1.0. Characteristically comparable antiviral molecules ganciclovir (log D_{ow} -1.6) and valganciclovir (log Dow -0.69) did not significantly sorb to sediment, so the soil was ruled out as a significant sink for the ARVDs. The two ARVDs in the study were degraded and considered non-persistent in sediments (Straub, 2017). In like manner, ACV was expected to weakly partition to the soil and simultaneously degrade, as was noted with ganciclovir and valganciclovir. The larger K_d value in OSL soil implies that the soil's organic component and

DOC levels either enhanced its sorption or another soil property was the genesis of non-sorption loss from the aqueous phase.

In Fountouli and Chrysikopoulos, (2018a), under dynamic and static experimental conditions, the K_d values for ACV obtained in quartz soils (a low OC soil matrix with a sand composition comparable to SL soils in the present study) varied between 50 – 200 mL g^{-1}. The values were up to 120 times higher than the 1.6 mL g^{-1} obtained from the SL soils in the present study, an indicator of the varying sorptive capacity of soils with relatable characteristics.

Degradation studies revealed ACV's short half-life, 5.3 hours and demonstrated that it rapidly biotransformed in sewage sludge (Fountouli and Chrysikopoulos, 2018a). Again, ACV exhibited a low affinity for soils, was weakly adsorbed to the sandy matrix and thus expected to be mobile in environmental systems with a possibility of migration to subsurface water resources (Fountouli and Chrysikopoulos, 2018a). ACVs' low affinity to the soils and short half-life susceptibility to biotransformation earlier highlighted in Fountouli and Chrysikopoulos, (2018a) is consistent with the present study's supposition. ACV sorption, especially in OSL soil, could not be higher relative to cationic OSV, and thus the measured loss from the aqueous phase to soils could not be attributed to sorption alone.

Sorption of ACV to the soils would have probably been enhanced if the matrix pH was < 4.5, which is unlikely in the environment. At this pH, the three amine groups in ACV would have acquired positive charges and electrostatically interacted with the negatively charged soils.

6.3.5.2 Lamivudine

Little information is available concerning the sorption mechanism of LVD to environmental matrices. In the OSL soils, the loss of LVD from the aqueous phase (55 %) was comparable to OSV's loss (58 %). Based on the molecule characteristics, LVD was expected to exhibit

significantly lower losses and, therefore, lower sorption potential to the soils. Nonetheless, the hydrophilicity of LVD corresponded to its partitioning potential, exhibiting the lowest soil-water partitioning coefficients in both SL and OSL soil, 0.6 and 11 mL g^{-1}, respectively. It, therefore, implied that LVD is least sorbed to the soil organic matter and the soil DOC. LVD is only unstable in acidic, pH < 4.5 or alkaline, pH > 12.5 environments, which is unlikely in the natural terrestrial environment. It is stable in neutral conditions (Bedse et al., 2009) (ChemAxon, 2021).

An adsorptive water-compatible molecularly imprinted polymer (MIP) material was developed to extract selected antiviral pharmaceuticals from human tissue. Data from the experiment indicated LVD's low adsorptive potential compared with ACV, which exhibits similar hydrophilicity. LVD exhibited a lower interaction potential with the MIP, shown by its lower distribution coefficient relative to ACV, i.e., 51.4 mL g^{-1} to 60.4 mL g^{-1}, respectively (Pourfarzib et al., 2015). LVD's lower K_d value was due to its weaker hydrogen-bonding interaction with the MIP sorbent (Pourfarzib et al., 2015). Accordingly, its weak hydrogen bonding potential likely contributed to its low soil-water K_d values in the present study.

6.3.5.3 Oseltamivir

OSV partitions to soils by diverse mechanisms. OSV was predicted to be 99.9 % cationic in the SL soil (pH 6.0) and 98.9 in the OSL soil (pH 7.2). In addition to hydrophobic interaction, stronger electrostatic attraction interactions were involved (Wang et al., 2015). This multi-faceted adsorption approach is the probable basis for why a hydrophilic molecule such as OSV (log DoW -1.1) partitioned relatively strongly (55-58 %) to the soils compared with the neutral and mid- hydrophobic NVP (36-42 %), which solely relies on the hydrophobic interactions.

OSV cationic charge diminishes at pH > 7, so other non-electrostatic interactions, i.e., van-der-Waals and H-bonding, complement the reduced main electrostatic forces (Wang et al., 2015). At pH > 7, as was the case for the OSL soil, the primary electrostatic adsorption would have reduced due to a lower NH_3^+: NH_2 molar ratio as the OSV loses its charge to < 50 % due to deprotonation (Wang et al., 2015). The van-der-Waals and H-bonding – complementing the hydrophobic interaction was the likely reason for the continued strong adsorption in the OSL soil, despite the slight increase in pH in the OSL soil, up to pH 7.2.

OSV exhibited moderate affinity towards an eco-friendly granular bioplastic material formulated to remove OSV from effluent. Approximately 50 % of the OSV was dissipated to the bioplastic (Accinelli et al., 2010a). However, in terms of K_d, the calculated K_d value, 47.1 mL g^{-1} (Accinelli et al., 2010a), was two times higher than the values obtained in the OSL soils in the present study (23.9 mL g^{-1}). As earlier mentioned in (Accinelli et al., 2010a), 50 % of ACV was lost from the aqueous phase to the granular bioplastic. The measured loss was comparable to the losses from the aqueous phase measured in the present study, i.e. 58 and 55 % loss in the OSL and SL suspension, respectively. The 50 % loss in was classified as moderate loss. Employing a similar classification, it was concluded that OSV equivalently exhibited moderate affinity towards the soils in the present study. Contrary to the present study, however, in Accinelli et al. (2010), the loss of OSV to the solid phase did not fit the Freundlich isotherm.

The likelihood of increased mobility of OSV due to reduced adsorption strength is high in sandy and silty soils. A nine-month monitoring study of surface waters revealed that OSV and its metabolite oseltamivir carboxylate (OSC) had lower adsorption rates on the sandy and silty sediment and were, therefore preferentially transported downstream (Azuma et al.,

2017). The measured K_d values in the sandy and silty sediments varied from 0.8 - 1.0 mL g^{-1}, implying that OSV was preferentially partitioned in the aqueous phase. The K_d values reported are consistent with those obtained in the present study's SL soils (i.e. 3.4 mL g^{-1}), which have comparable sand composition and lower OC content.

The extent of sorption for oseltamivir carboxylate (OSC), the primary OSV metabolite, was measured in sediment with the following properties, sand levels 91-94 %, % OM 2.6-2.9 % and soil pH 6.9 – 7.6. The initial OSC concentration was in the range of 20 -100 µg L^{-1}. 65-70 % of the OSC remained in the solution implying a 30-35 % sorption to the sediment (Saccà et al., 2009). The dissipation percentage was lower than the extent of the present study, 55 -58 %. The disparity was due to a lower sand proportion of 55-67 % and a higher % OM range, 0.6-9.5%, in the soils of the present study. There was minimal variation in soil pH 6.9-7.6 and 6.0-7.0 between these two studies. Therefore variation in adsorptive strength between these two studies was due to the elevated hydrophobic interaction between the molecule and soil in the present study. Also, increased H-bonding and van-der-Waal forces are experienced in the present study since fewer active sites were present in the sandy soils of Saccà et al. (2009). However, the main difference was because OSC was a metabolite and, therefore, slightly more hydrophilic than the parent compound OSV. The metabolite increased hydrophilicity contributed to its minimal sorption with the soil DOC and organic matter. Direct extraction of the OSC from the sediment in Saccà et al. (2009) using organic solvent found that only 4-7 % of the OSC partitioned to the soil was permanently bound to the residues, an indication that OSC was less likely to persist in soils, and exhibits high desorption tendencies.

6.3.5.4 Nevirapine

Nevirapine was neutral and unionized at the experimental pH and therefore experienced minimal hydrophobic interactions and hardly any electrostatic interactions with the soils. Theoretically, it was expected that NVP would exhibit stronger partitioning to the solids compared with LVD and ACV. In the SL soils, 36 % of NVP sorbed to the soils, giving a K_d of 0.9 mL g^{-1}. The coefficient did not vary widely from the 0.6 and 1.6 mL g-1 obtained from LVD and ACV, respectively. In the OSL soil, NVP exhibited a K_d of 13.2 mL g^{-1}. CBZ, which has similar characteristics to NVP, just as in the SL soils of the present study, exhibited negligible sorption, 0.4 – 1.3 mL g^{-1} in sediment composed of 92 % sand content (Martínez-Hernández et al., 2014) sand levels 50 % higher than in SL soils s in the present study.

Generally, the measured low sorption tendencies towards soil can be attributed to NVP's neutrality and the absence of charge interaction with the soil. In the OSL soil, K_d was 13 times higher, demonstrating increased hydrophobic interactions with increased soil OM and DOC content.

Lees, (2018) reported that NVP exhibited K_d and log K_{oc} values of 1.4 mL g^{-1} and 1.9 mL g^{-1}OC^{-1}, respectively, in an SL identical soil. The reported values were consistent with the sorption coefficient measured in the present study, i.e. 0.9 mL g^{-1} and 2.2 mL g^{-1}OC^{-1}, respectively. In NVP, the electron pairs on the nitrogen atom in the aromatic pyridine structure may facilitate the formation of a covalent bond with electrophiles in the sorbent (the soils) (Adeola et al., 2021). This is the most probable interaction mechanism of NVP with soil sorbent. NVP's low adsorption coefficient relative to the ionizable OSV and neutral ACV implies enhanced mobility. The relatively higher desorption capacity also implies that NVP is neither degraded

nor lost in the system but is somewhat mobile rather than partitioned to the bulk of the soil and OM component (Schoeman et al., 2017).

6.3.5.5 Efavirenz

Table 6.6 showed that EFV exhibited the highest K_d and log K_{oc} values across the two soils and amongst the five ARVDs. Table 6.7, on the other hand, showed EFV exhibited the lowest desorption values, demonstrating its limited mobility tendencies. Its loss to soils was 19 % higher in the OSL soils (99 %) compared with the SL soils, 80 %. The distribution of EFV in wastewater treatment plants indicates that it preferentially partitions to solids. For example, 21-70 % of EFV was bound to solids; hence it was the primary method of removal from the WWTPs (Schoeman et al., 2017). Its low water solubility accelerates its preferential distribution to solids (Mlunguza et al., 2020). The highly electronegative fluorine in the EFV molecule suggests the possibility of solid electrostatic attractions with electron-rich negatively charged soils; combined with hydrophobic interaction; the mechanisms account for its high adsorptive tendencies in the soils.

In addition to hydrophobic bonding, NVP and EFV may also experience pi- and H- bonding (Adeola et al., 2021). Soil pH least impacts the sorption mechanism of these two molecules. The molecules were neutral across the environmental pH range. EFV becomes anionic only at pH >11, which is highly unlikely in an actual environment (Adeola et al., 2021). Contrastingly NVP may convert to a cation at < pH 4.5, which is an extremely low pH for a natural ecosystem.

Occasionally, other factors dissimilar from bonding mechanisms may influence adsorption. For example, NVP, despite being less hydrophobic, was strongly retained by organic graphene wool, a carbon-based adsorbent specifically designed for water purification systems. The sorbent demonstrated a higher adsorptive capacity K_d 2.54 L g^{-1} for NVP, approximately two

times higher than for EFV (1.48 L g^{-1}). In this case, the size of active sites on the adsorbent preferentially favoured adsorption of NVP rather than EFV (Adeola et al., 2021).

The impact of clay on sorption in this study was ignored. Table 6.1 shows that the clay content in the two soils was < 2 %, indicating that clay presented the most negligible impact on the measured adsorption.

6.3.6 Classification of mobility of ARVDs

K_d and log K_{oc} are critical parameters in assessing a contaminant's mobility in water relative to soils (Chen et al., 2016). The classification was based on FAO's template on the mobility of pesticides in soils based on log K_{oc} (FAO, 2000). The premise, according to FAO, is that the higher the log K_{oc}, the lower the mobility of the species. In this approach, log K_{oc} 2-3, 3-4, 4-5, and > 5 molecules are classified as moderately mobile, slightly mobile, hardly mobile and immobile, respectively. The mean log K_{oc} between SL and OSL soil exhibited by ACV, LVD, OSV and NVP was 2.55, 2.05, 2.6 and 2.15. Accordingly, the four molecules were classified as moderately mobile. EFV, log K_{oc} 3.45 was categorized as slightly mobile. None of the ARVD exceeded log K_{oc} > 4.0. According to FAO, any molecules exceeding this threshold are of concern. While such a molecule does not leach to the ground, it may impact terrestrial organisms, calling for further toxicity tests.

6.3.7 Transfer of ARVD from synthetic wastewater to soils

6.3.7.1 Adsorption

This section discusses the measured difference in magnitude of the transferred molecules between freshwater (0.01 M CaCl$_2$) and the soil's synthetic aqueous wastewater phases.

A 1.5 pH difference was measured across the suspension of the SL-CaCl$_2$, OSL-CaCl$_2$, SL-SW and OSL-SW (6.7-7.5), Figure 6.6. The OSL-SW suspension had a relatively stable pH, probably

due to the phosphate buffer present in the SW matrix. While pH may be stable in controlled experiments, natural wastewater characteristics vary widely depending on the influent sources and treatment technologies (Von Sperling, 2015). Accordingly, irrigation with SW significantly either initiates an increase, decrease or sometimes does not institute significant pH changes in soils (Christou et al., 2017b).
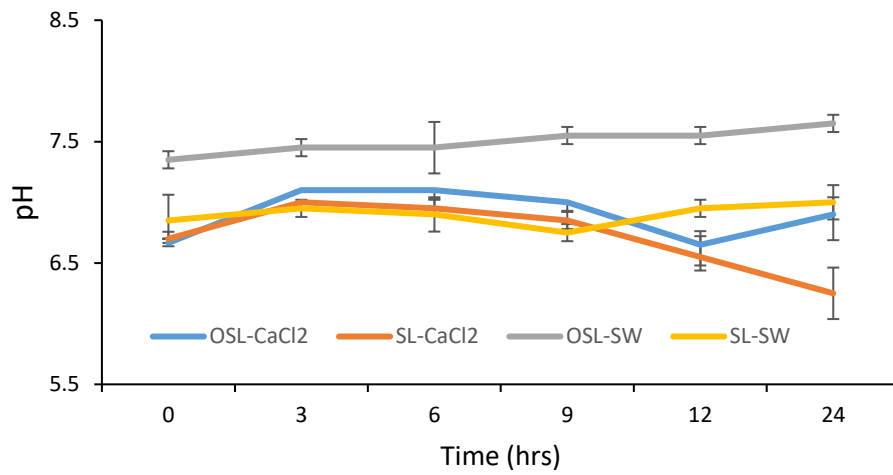
Figure 6.6. pH levels measured in the SL-CaCl$_2$, OSL-CaCl$_2$, SL-SW and OSL-SW suspension during the adsorption experiment.

Table 6.9 shows the difference in the amount of ARVD partitioned from the aqueous phase to the soils between the CaCl$_2$ and SW matrices. The ensuing soil-water coefficient values are also presented

Table 6.9. Table loss of ARVD between SW and CaCl$_2$ to soils (n=3, ± SD)

Soil	ARVD	Irrigation matrix	% Loss from the aqueous phase	K$_d$ (mL g^{-1})
SL	ACV	CaCl$_2$	23.2±4.5	1.5±0.4
		SW	14.1±1.5	0.8±0.1
	LVD	CaCl$_2$	28.0±2.1	2.0±0.2
		SW	18.2±1.4	1.1±0.1
	OSV	CaCl$_2$	34.0±0.3	2.6±0.0
		SW	58.2±2.8	7.0±0.8
	NVP	CaCl$_2$	30.9±3.3	2.0±0.3
		SW	29.3±1.0	2.1±0.1
	EFV	CaCl$_2$	80.1±1.5	20.3±2.0
		SW	90.2±2.6	48.2±14.3
OSL	ACV	CaCl$_2$	32.3±0.6	2.4±0.1
		SW	23.3±1.9	1.5±0.2
	LVD	CaCl$_2$	33.3±0.1	2.5±0.0
		SW	23.7±1.2	1.6±0.1
	OSV	CaCl$_2$	58.4±2.5	19.1±1.5
		SW	74.8±1.1	34.8±1.8
	NVP	CaCl$_2$	42.9±3.0	12.6±0.9
		SW	37.4±1.6	11.0±0.4
	EFV	CaCl$_2$	94.0±1.7	212.7±60.4
		SW	97.6±6.3	518.0±4.1
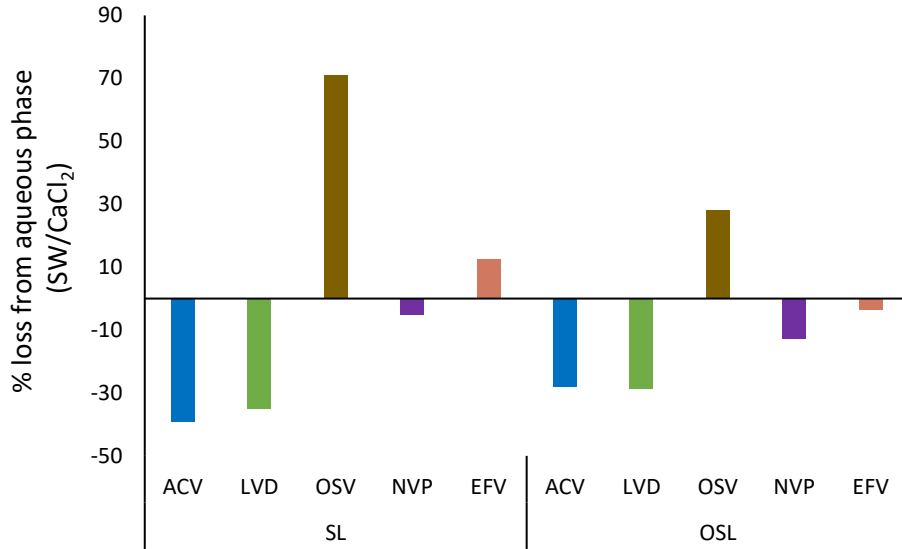
Figure 6.7. Graph comparing ARVD losses from SW relative (normalized) to losses from CaCl$_2$, values > 1 indicated higher losses from SW than from CaCl$_2$

Figure 6.7 was constructed to visualize better data presented in Table 6.9 by normalizing the loss from SW relative to partitioning from CaCl$_2$. Values > 1 signified higher losses from SW to the soils than from the freshwater for the same molecule. In the SL soil, OSV and EFV exhibited higher transfer magnitude from SW suspension than CaCl$_2$. Relative OSV partitioning was highest, 70 % higher than associated CaCl$_2$ losses. The neutral and hydrophobic EFV loss from SW relative to CaCl$_2$ was lower, being < 10 % lower than from CaCl$_2$. While Table 6.9 shows EFV exhibited the highest loss from SW (90 and 97 %, respectively), the discussion here is based relative on each molecule's associated loss in the CaCl$_2$ matrix, and hence the consideration that OSV in the SW exhibited the highest partitioning from SW than from in CaCl$_2$ solution.

Overall, the mean K_d for SW was higher than from CaCl$_2$, 7.1 and 4.1 mL g^{-1}, respectively. The SW matrix wastewater's impact on the ARVD-soil interaction mechanisms is a direct contribution of the DOC inherent in the SW, as revealed in the data presented in Table 6.3.

The consistent transfer of OSV from suspension to both soils is unique to OSV only. OSV was cationic in both solutions. It is likely that The SW solution's chemistry, especially the presence of inorganic ions, greatly impacts the transfer of cationic organic molecules to the soils. Sorption of cationic species, caffeine and atenolol, onto natural sandy loam from synthesized reclaimed water was higher than for anionic (sulphamethoxazole) and neutral (carbamazepine) (Martínez-Hernández et al., 2014). The observation was consistent with the transfer pattern in the present study. Accordingly, a molecule's type and degree of ionization strongly influence its transfer from wastewater-type related matrix to soils.

Peña et al. (2020) reported that irrigation with wastewater increased the sorption potential of hydrophobic pesticides, log Kow > 4.6 to the soils is consistent with observations in the present study. Figure 7 showed that EFV similarly exhibited a higher tendency of transfer from SW to the soils than from freshwater, especially in the SL soil. At the same time, adsorption of low and mid-polarity pesticides was least impacted by the wastewater irrigation matrix (Peña et al., 2020), which explains the absence of a clear adsorption pattern by the mid-polar NVP and less polar ACV and LVD as shown in Figure 6.7.

6.3.7.2 Desorption potential of SW and CaCl$_2$

Herein the desorption potential of SW and CaCl$_2$ was compared on soils initially infiltrated with SW laden with the ARVD molecules. Table 6.10 showed that the magnitude of desorption realized by the two solvents in the SL soil was directly proportional to the log K_{ow} of the molecule, i.e., ACV>LVD>OSV>NVP>EFV.

Table 6.10. SW and CaCl$_2$ matrix-induced desorption statistics on soils (n=3, ±SD)

Soil	ARVD	Desorbing matrix	% Desorption	K$_{des}$ (mL g^{-1})
SL	ACV	CaCl$_2$	73±1.4	1.8±0.1
		SW	82±0.8	1.3±0.5
	LVD	CaCl$_2$	61.9±2.4	3±0.04
		SW	58.7±2.1	3.5±0.6
	OSV	CaCl$_2$	64.1±0.4	2.7±0.05
		SW	36.2±0.9	8.7±0.9
	NVP	CaCl$_2$	21±0.2	18.8±0.09
		SW	16.3±1.0	25.5±0.4
	EFV	CaCl$_2$	8.8±0.3	52±1.1
		SW	16.5±0.4	25.2±0.6
OSL	ACV	CaCl$_2$	65.8±1.1	2.6±0.2
		SW	98.7±0.8	0.07±0.003
	LVD	CaCl$_2$	113.3±1.1	-0.5±0.04
		SW	133.3±2.3	-1.2±0.04
	OSV	CaCl$_2$	18.5±0.6	21.8±0.8
		SW	9.4±0.2	47.7±0.7
	NVP	CaCl$_2$	30.7±1.8	11.2±0.5
		SW	32.6±0.4	10.3±0.3
	EFV	CaCl$_2$	0.51±0.03	105.2±1.1
		SW	0.93±0.12	54.7±0.3

.
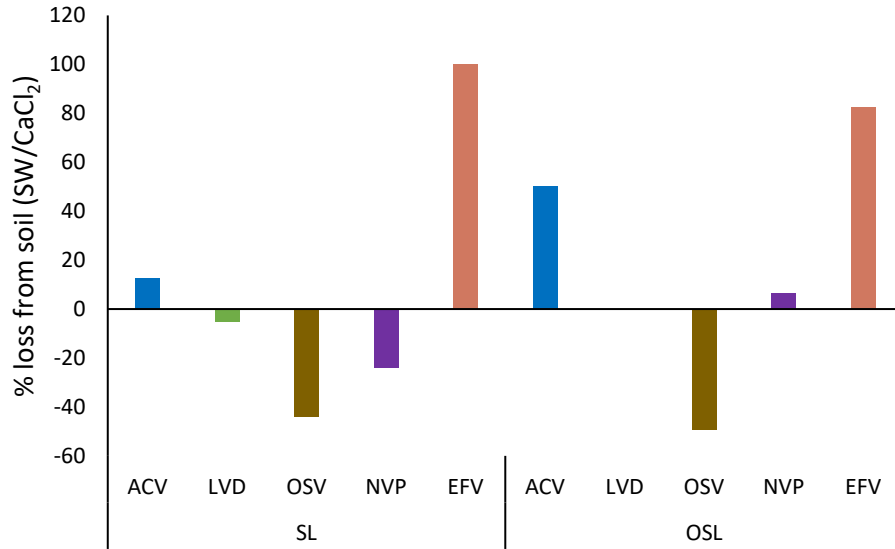
Figure 6.8. Graph comparing SW's relative (normalized) desorption potential to $CaCl_2$ on individual molecules. Values > 1 indicated higher desorption potential from SW.

Figure 6.8 shows that EFV exhibited the highest desorption potential between the SW and CaCl2 solutions. In the SL and OSL soil, EFV desorption by the SW was approximately two times and 1.5 times higher than the $CaCl_2$-induced desorption. The SW-DOC interaction was likely stronger than the existing EFV-SOM complex. Therefore, the EFV-DOC complex was transported outside the bulk of the soil, typically between hydrophobic compounds and wastewater DOC (Peña et al., 2020). Notably, the extent of desorption was inversely proportional to the amount of SOM. The cationic OSV was least impacted by infiltration of SW; it was approximately half less likely to be desorbed from the soils by the SW solution than the $CaCl_2$ (freshwater) solution. NVP exhibited the least variability in desorption tendencies from the action of the two solution matrices.

6.3.7.3 Conclusion

Soil organic matter directly impacted sorption in the two soils as normalization of K_d values with SOM resulted in identical log K_{oc} for each molecule across the two soils. At the same time,

molecule hydrophobicity or ionization influenced sorption significantly. EFV was the most hydrophobic and correspondingly exhibited the highest soil-water distribution coefficients. OSV, which was fully cationic, exhibited the second-highest sorption tendencies. OSV exhibited reversibility tendencies over the 24-hour equilibration period as approximately 50 % of its initially sorbed mass was transferred to solution in the desorption experiments. The neutral and mid-polar nevirapine exhibited low sorption tendencies relative to EFV and OSV. The uncharacteristically high losses of ACV and LVD relative to OSV implied that processes besides sorption were influential. The two compounds experienced higher degradation tendencies than the EFV, OSV and NVP. OSV exhibited the highest magnitude transferred from SW aqueous phase to soils relative to transfer from the $CaCl_2$ solution. On the other hand, EFV exhibited the highest desorption losses from soils when desorbed by SW relative to $CaCl_2$ solution.

Chapter 7
Impact of wastewater irrigation on uptake of ARVDs in lettuce

Overview

This chapter presents and discusses data from the uptake and accumulation experiments performed in the soil matrix. The rationale for selecting experimental protocols and procedures is described. In the study, ARVD molecules were introduced into the soils via irrigation using spiked synthetic wastewater and spiked freshwater. OSV, NVP and EFV were detected and quantified in the soil and the plant matrices. However, the hydrophilic ACV and LVD were not detected in either matrix. The mean ARVD accumulation in the lettuce grown in sandy soils was eight times higher (323 ng g^{-1}) than in lettuce grown in organic-rich soils (39 ng g^{-1}). At the same time, the mean accumulation in lettuce was six times higher (320 ng g^{-1}) in the synthetic wastewater-irrigated soils than in thefreshwater-irrigated lettuce (52 ng g^{-1}).

7.1 Introduction

Due to the complex nature of wastewater, its reuse can induce varying influences on the fate of the existing or newly introduced organic contaminants in soils (Peña et al., 2020). In soil-plant systems, the amount of organic contaminant that accumulates in the plant will depend on several factors. Such factors include the extent of its sorption/desorption, its physical-chemical characteristics and its predisposition for degradation or transformation (Thiele-Bruhn et al., 2004; Pan and Chu, 2016; Y. Li et al., 2019b). Since an exogenous chemical is transported mainly by the soil's pore water, this portion of the chemical is more readily bioavailable for uptake into the plant roots (Miller et al., 2015).

While ARVDs residue occurrence data in surface waters and wastewater is available, (Adeola and Forbes, 2022; K'oreje et al., 2018b; Madikizela et al., 2020; Mlunguza et al., 2020a;

Ngumba et al., 2020 and Adeola and Forbes, 2022). However, information on the interaction between ARVDs and the soil, particularly in agroecosystems, is unavailable. Studies in Table 7.1 show that commonly investigated pharmaceuticals in soils are antibiotics, NSAIDs and stimulants.

The present study incorporates soil and is an upscale of the wastewater-only-based hydroponic experiment described in Chapter 5. Therefore, the objective of this study was to investigate the impact of SW (simulating actual wastewater) irrigation on the uptake of five ARVDs in two soils in a controlled soil-plant system. This environment simulated the complexities of actual agroecosystems. The resultant ARVD accumulation in soil and lettuce was measured. Bioconcentration factors were calculated based on ARVD concentration in the bulk of soil and the pore-water. The potential risk to humankind from consuming contaminated lettuce was evaluated.

Table 7.1. Pharmaceutical-soil-plant system interaction studies

Class	Pharmaceutical	Plant	Spike/ exposure amount	Irrigation agent/ Study environment	Concentration in soil (ng g^{-1})	Concentration in plants ng g^{-1}	study
Antibiotics	Tetracycline Amoxicillin	Lettuce Carrot	0.1 – 15 mg L^{-1}	Soil irrigated with freshwater FW in Greenhouse study	-	4.4-45.2	(Azanu et al., 2016)
Stimulant, antibiotic, anticonvulsant Lipid lowering agent	Bezafibrate, Caffeine, Carbamazepine , Clofibric acid, Ibuprofen, Ketoprofen, lamotrigine	Cucumber Tomatoes	0.02 -2.44 µg L^{-1}	Soil irrigated with FW-spiked TWW-spiked TWW- unspiked Field study	> LOQ – 50	> LOQ– 450	(Goldstein et al., 2014)
Antibiotics, anti-epileptics, hormones	15 pharma	Radish	µg g^{-1}	Soil irrigated with FW Greenhouse study	-	14.1-14080	(Y. Li et al., 2019b)
Antibiotics	Lincomycin, oxytetracycline sulfamethoxaz ole	Lettuce	1 mg L^{-1}	Soil irrigated with FW in a Greenhouse study	-	>LOQ to 66	(Sallach et al., 2018)
Antibiotics NSAIDs	Diclofenac Sulfamethoxaz ole	Tomatoes	-	Soil irrigated with Field TWW	0.06-0.98	11.63	(Christou et al., 2017b)

	Trimethoprim			(unspiked) in the field			
Sulphonamides, oestrogens, stimulants, biocides		Lettuce	4- 40 µg g^{-1}	Spiked soil irrigated with FW (rainwater) Greenhouse study	0.3-167	LOQ -1630	(Hurtado et al., 2016)
12 trace organic contaminants		alfafa	-	Soil irrigated with TWW (unspiked) in the field	> LOQ -329	<1-49	(Sharma et al., 2020)
Antidepressants Stimulants	Atenolol, caffeine, CBZ, naproxen, gemfibrozil	Cabbage, barley, zucchini, beans		Soils irrigated with Field unspiked TWW in the field	48-96	34-125	(Picó et al., 2019)
Antibiotics, painkillers	Ciprofloxacin, sulfamethoxazole, diclofenac, metoprolol, clarithromycin	leek	10 µg L^{-1}	Soil irrigated with spiked and unspiked TWW in the field	1-30	1-660	(Manasfi et al., 2021)
Antibiotic	enrofloxacin	Soybean, bean and corn	10 µg L^{-1}	Soil irrigated with spiked FW in the greenhouse	-	1.68- 51.0	(Marques et al., 2021)

7.2 Material and methods

7.2.1 Lettuce irrigation

Five-week-old lettuce seedlings (romaine variety) were transplanted from a seedbed into porous cylindrical plastic containers (10 cm diameter X 10 cm height). The pots contained 400 g of either OSL or SL soils (soil characteristics in section 6.3.1). The transplanted seedlings were watered with stored rainwater (FW) for seven days to acclimate to the new soil environment. Afterwards, one set of the lettuce seedlings was irrigated with spiked synthetic wastewater (SW) (characterized in Section 5.2.1) and FW, containing a mixture of the ARVDs, all at 50 μg L^{-1}. The control was irrigated with unspiked SW and FW. Each potted plant was irrigated every three days with 50 mL of the irrigation matrix. The irrigation matrix was delivered to the base of the plant to avoid any deposition on the leaves. Triplicate lettuce plants, soil samples and pore water were sacrificially harvested and collected every three days, days 1, 3, 6, 9, 12, 16 and 20, for analyses. A control setup was irrigated with the unspiked FW and SW separately at the same frequency as the ARVD-exposed plants. Fertilizer was not added during the entire irrigation period.

7.2.2 Data collection

The pH of the freshly prepared SW from the stock was routinely measured before each irrigation exercise. The soil's average moisture content (% MC) was obtained using a soil moisture meter. The mean soil MC was an average of the measurements taken immediately after irrigation and during harvesting. The concentration of the ARVDs in the leachates (irrigation water that permeated the soils and exited the pot) was collected and measured. Afterwards, the soil's pore-water (PW) component was obtained by centrifugation of a subsample of the soil. A portion of the pore-water samples was filtered through a 0.42 μm

GFF and analyzed for ARVDs. All the samples were stored at 4 °C until analyses. The plug of soil that remained in the tube during pore-water extraction was frozen at -20 °C, freeze-dried and had ARVDs extracted from it. The remaining soil subsample (not centrifuged) was air-dried and stored in aluminium foil for soil pH and soil organic matter (SOM) measurements. These parameters were measured using the methods previously described in Section 6.2.2.1. ARVD residues in the plant and soil samples were extracted according to the protocols described in Section 3.2.5

Usually, the pharmaceutical distribution in soil-water-plant systems is characterized by the bioconcentration factor (BCF), which is a ratio of the molecule concentration in the plant to the concentration of the molecule in the soil or the pore-water (Hurtado et al., 2016). Accordingly, the soil and pore-water BCFs were estimated from the measured whole-plant accumulation in lettuce, the measured ARVD concentration in the soil and the pore-water fraction, as shown in Equations (7.1) and (7.2).

$$BCF_{soil} = \frac{C_{whole\ plant}}{C_{soil}} \tag{7.1}$$

$$BCF_{pore-water} = \frac{C_{whole\ plant}}{C_{pw\ (pore-water)}} \tag{7.2}$$

Where $C_{whole\ plant}$ is the concentration of the ARVDs in the plant (ng g^{-1}, dry weight), $C_{pore-water}$ is the ARVD concentration in the pore-water (ng mL^{-1}), and C_{soil} is the ARVD concentration in the bulk of the soil (ng g^{-1}).

7.2.3 Estimation of health risk

Potential health risks that could have arisen from the consumption of contaminated lettuce was estimated by comparing the daily dietary intake (DDI) of each chemical per kilogram

bodyweight (μg kg^{-1} d^{-1}), estimated according to Equation (7.3) from (Legind and Trapp, 2009).

$$DDI = \frac{C \times consumption}{body\ weight\ (bw)} \qquad (7.3)$$

Where C is the concentration of the ARVD in plant tissue (μg g^{-1}, wet weight), consumption is the average daily consumption of lettuce (g d^{-1}) and body weight- is the standard average body weight of an adult (taken as 70 kg).

7.2.4 Experimental conditions

7.2.4.1 Experimental design

The two common approaches to introducing pharmaceuticals in soils are listed in studies shown in Table 7.1, i.e., directly introducing the molecule to the soil before irrigation or via the irrigation agent. Since the purpose of the present study was to mimic introduction via irrigation, application via spiked FW/SW matrix to the surface of the soil approach was selected. The present study's experimental approach was employed in Goldstein et al. (2014), Azanu et al. (2016) and Paz et al. (2016), whereby continuous irrigation with either pharmaceutical spiked freshwater (FW) or spiked treated/reclaimed wastewater (TWW) was undertaken. The alternative approach, of introducing of the contaminant directly into the soil and then irrigating using unspiked FW or TWW, was reported by Williams et al. (2015b), Hurtado et al. (2016) and Li et al., (2019b). The advantage of the latter approach is that it is more feasible to perform mass balances in the system as the target molecule remains constant. The present study's approach nevertheless reflects the dynamism of agroecosystems whereby there is continuous addition and removal of the molecule via irrigation. A comparison between overhead and soil-surface irrigation revealed higher

detection of pharmaceuticals on the leaves in the overhead-irrigated vegetables (Bhalsod et al., 2018), emphasizing the need to apply an irrigation matrix closest to the soil surface.

7.2.4.2 Exposure concentration

Broad exposure concentrations, ng L^{-1} to mg L^{-1}, have been employed in controlled soil-plant pharmaceutical uptake studies, as observed in studies listed in Table 7.1. However, there is a debate on the ideal exposure concentrations or range for uptake and accumulation studies. For example, Sun et al. (2018) suggested that environmentally relevant concentrations for pharmaceutical experiments should be confined within the 0.5-50 µg L^{-1} levels. (Nason et al., 2019) were of the contrary opinion, recommending concentrations ≤ 1 µg L^{-1} as ideal and concluded that concentrations in the 100 µg L^{-1} were inappropriate since they are 100 times above regularly measured environmental residue concentrations. Interestingly, concentrations > 1 mg L^{-1} have been used before in plant exposure experiments (Sallach et al., 2018). This study used an exposure concentration of 50 µg L^{-1} for all the ARVDs in the irrigation media. This concentration is within the routinely measured ARVD environmental concentration range (20 to 167,100 ng L^{-1}) measured in surface waters and WWTPs in Africa (Fekadu et al., 2019; Adeola and Forbes, 2022).

7.2.4.3 Irrigation agent

This study used two irrigation matrices: freshwater, FW (unchlorinated stored rainwater), and synthetic wastewater (SW) in place of actual treated wastewater (TWW). Justification for the use of SW was comprehensively provided in Section 5.2.3.1. Table 7.1 shows that actual TWW is preferentially used in soil-plant experiments as an irrigation matrix. So far, information on experiments that have utilized SW as a surrogate for plant irrigation is not readily available. Nonetheless, SW has been used in experiments that measured the impact of wastewater

irrigation on soil hydraulic properties (Erfani Agah et al., 2017) and in column experiments to measure the impact on the mobility of pharmaceuticals in soil (Borgman and Chefetz, 2013). Again SW has been used in pharmaceutical sorption experiments (Bagnis et al., 2018a; Lees, 2018). In this study, SW was purposefully selected due to the impracticability of continuously obtaining TWW with the same characteristics for continuous experiments over three years. Storage challenges were foreseeable since TWW is usually malodorous, biologically and chemically active; therefore, storage for an extended duration in shared laboratories would not have been ideal. This study's SW was prepared following a defined process with ingredients comprising inorganic, organic, and particulate material (Table 5.1). It was ideal for experiments as it was easily replicable (Boeije et al., 1999b; Tchobanoglous et al., 2003; O'Flaherty and Gray, 2013).

7.3 Results

7.3.1 Soil and irrigation water matrix pH

The mean pore-water and soil pH obtained from the cumulative individual measurements over the 21-day experiment duration is shown in Table 7.2.

Table 7.2 Mean soil and pore-water pH measured over the 21-day exposure duration (n=14, ± SD)

	Irrigation matrix	Pore-water pH	Irrigated soil pH
SL	SW	6.3 ±0.6	5.7±0.1
	FW	6.9 ± 0.7	5.6±0.09
OSL	SW	6.7 ± 0.4	5.8±0.1
	FW	6.9 ± 0.5	6.0±0.1

The pH of the SW used for irrigation was not stabilized with phosphate buffer (as it was during the adsorption experiments), and it, therefore, was slightly acidic (pH 6.3). The FW from the stored rainwater reservoir was similarly pH 6.8, on average 0.5 pH unit higher than the SW pH. Table 7.2 shows that the mean FW and SW pore-water pH across the soils during the entire irrigation period was 6.8 ±0.5 and 6.3 ±0.8, respectively. Generally, the pore-water pH was approximately one pH unit higher than the corresponding soil pH. The acidic SW irrigation matrix-induced pH reduction in the soils was particularly evident in the OSL soil. Its initial unamended pH was 7.0; it was altered to pH 5.7 post-SW irrigation.

7.3.2 Soil moisture content

The soil moisture content in the system was also monitored during the irrigation period and is shown in Table 7.3.

Table 7.3. Soil moisture content (% MC) measured during exposure experiment (n=3 ± SD)(SL- sandy soils, OSL- sandy soil swith higher organic content)

	Moisture content (%)			
	SW		FW	
Time (day)	SL	OSL	SL	OSL
1	21.4± 0	50.0±0.0	32.4±0.0	50.0±0.0
3	30.4 ±7.1	50.0±0.0	27.6± 9.8	49.2±1.0
6	19.6 ±1.6	45.2±4.5	22.2±10.1	37.2±0.3
9	18.2 ±1.0	37.3±3.7	29.5 ±9.1	34.1±0.7
13	26.2± 0.2	41.4± 9.0	30.7±8.1	35.2±0.2
16	37.7 ±2.4	29.1±1.0	28.6 ±5.1	33.2±2.5
20	22.1 ±1.1	24.9 ±1.4	15.4±8.2	28.7±12.4

Table 7.3 shows a wide MC variation between the SL and OSL soils. The SL soil MC varied from 15 to 32 %, while the OSL MC varied from 28 to 50 %. The maximum measured OSL MC was up to 1.5 times higher than the highest level measured in the SL soil.

Usually, in uptake experiments, it is recommended that irrigation volumes should not exceed field water maximum water holding capacity (MWHC) to minimize the leaching of the target contaminants (Hurtado et al., 2016). At the same time, adequate moisture content is necessary for the organic contaminant uptake in the soils to be realized since the transpiration stream is the main driving force of the uptake of solutes from the root to above-ground tissues (Dodgen et al., 2013).

The SL's soil MWHC was approximately 35 % (according to the vendor). Though not provided, the estimated MWHC of the OSL soil was presumably at least two times higher, as noted in the measured MC, since it contained less sand and a higher % organic matter capacity than the SL soil. For this reason, the irrigation volume was selected not to exceed the MWHC of the soils, 50 mL, which was ca 16 % by mass of soils.

7.3.3 Soil organic matter (SOM)

The mean post-irrigation SOM between the FW and SW irrigated OSL soils was not different (p=0.7), i.e., 9.3 % and 9.7 %, respectively (

Table 7.4). Likewise, the SOM in the SL soil did not differ between the two irrigation regimes, i.e., FW 0.73 % and SW 0.75 %.

Table 7.4. SW and FW post-irrigation soil organic matter in the SL and OSL soils (n=3, SD)

Time (day)	Soil organic matter (%)			
	OSL		SL	
	SW	FW	SW	FW
Initial-unirrigated soil	9.5	9.5	0.62	0.62
1	8.5 (0.7)	9.1 (0.5)	0.64 (0.01)	0.50 (0.19)
3	8.2 (0.3)	8.5 (0.0)	0.54 (0.0)	0.64 (0.01)
6	9.8 (0.05)	7.6 (0.08)	0.68 (0.21)	0.60 (0.04)
9	8.5 (0.0)	9.3 (2.4)	0.56 (0.07)	0.53 (0.05)
13	10.1 (0.0)	11.8 (0.4)	0.81 (0.0)	1.29 (0.68)
16	9.2 (0.01)	9.5 (0.5)	0.88 (0.009)	0.91 (0.13)
20	9.2 (0.01)	12.0 (0.0)	1.0 (0.4)	0.77 (0.13)

The amount of SOM in the soils varied during irrigation. For example, in the OSL-SW compartment, between days 1 and 3, an approximately 1.1 % decline in SOM was measured from the initial 9.5 %. From day 9, a 1.5 % increase was measured, and another drop was again noted at test termination. Contrastingly, in the SL-SW compartment, there was a

continual increase from 0.6 to 1.0 % between days 13 to day 20. An increase of SOM in the FW compartment was not expected as the FW matrix contained neither DOC nor any organic suspended particulate matter.

Notwithstanding, both the increase and decrease of SOM were measured in the compartment during the irrigation period. The SOM increase measured in the FW irrigated compartment suggests a possible contribution from organic root debris. As the plant grew, more root tissue was introduced into the system. Possibly not all root matter was eliminated during the sifting process prior to OM measurement.

A collection of studies that analyzed data from TWW irrigation in actual soils revealed an average 5.9 % increase in SOM in the soils. For soils irrigated with TWW for 2-47 years, the measured SOM increase was independent of the irrigation duration (Emde et al., 2021). As in the present study, where SOM increase was prominent in the SL SW irrigated soil, in Emde et al. (2021), increased SOM was observed in fine and medium-textured soils characteristically similar to SL soils.

The intermittent variation of SOM in the SW-irrigated soils this study highlights the dynamic nature of SOM in soils. For example, (Jueschke et al., 2008) showed that while irrigation with treated wastewater increases the SOM content in the topsoil, continuous irrigation with the same media may simultaneously reduce SOM residing in the subsoil. Sometimes also, while the quantity of SOM may be unchanged, its quality may be altered. For example, irrigation with TWW increases the charge of the carboxylic groups in SOM (Dalkmann et al., 2014b).

7.3.4 ARVD concentration in pore-water and soil

The concentration of the ARVD in the pore water and the soil was measured after each harvest for 21 days. Figure 7.1 and Figure 7.2 show the concentration of ARVD measured in the soil-derived pore-water and the soils, respectively.
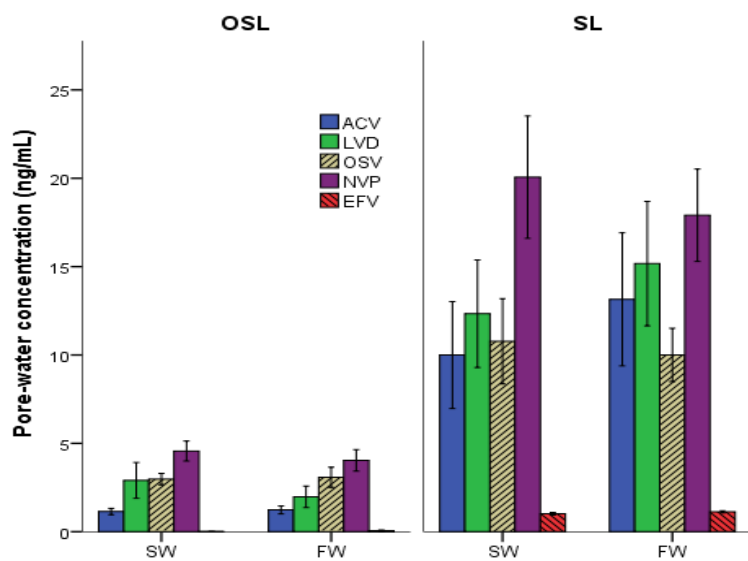
Figure 7.1. The mean concentration of ARVD in the OSL and SL-derived soil pore-water over the 20 day exposure duration (n=14, ± 1SE)
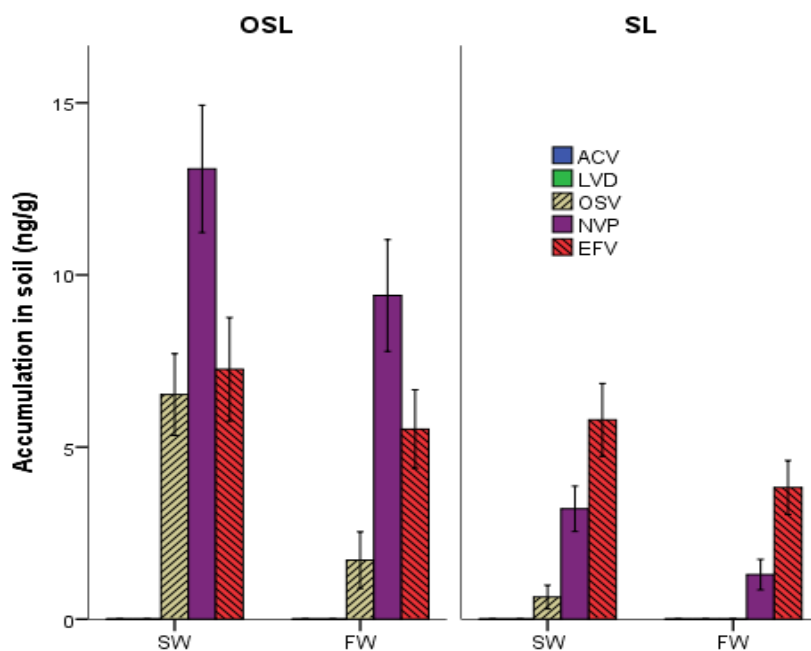
Figure 7.2. The concentration of ARVD in soil (n=14, ±SE)

The accumulation pattern in the pore-water and soil was not identical. Generally, while higher ARVD concentrations were measured in the SL than in OSL soil-derived pore-water samples (mean 11.1 ng mL^{-1} and 2.3 ng mL^{-1} respectively, Figure 7.1), higher accumulation in soils was measured in the OSL soils than in the SL soils (overall mean of 4.3 ng g^{-1} and 1.4 ng g^{-1} respectively, Figure 7.2).

Focusing on the soil-derived pore-water concentrations, Figure 7.1 showed that NVP exhibited the highest concentration in the SL-extracted pore-water, a mean of 18.9 ng mL^{-1}. The ACV, LVD, OSV, and EFV concentrations were approximately 0.5 to 10 times lower, i.e., 11.5, 13.7, 10.3 and 1.6, 11.1 ng mL^{-1}, respectively. The mean SL soil-pore water concentration was approximately five times higher than OSL-extracted pore-water concentrations, whose individual concentrations varied between < LOD - 4.4 ng mL^{-1}. EFV concentration in the OSL-derived pore-water was below the detection limit (method validation data presented in

APPENDIX 2). Similarly, in the OSL soil, NVP exhibited the highest pore-water concentration. Noticeably, while OSV concentration in the OSL-obtained pore-water was the second highest in concentration, on the contrary, in the SL soils, LVD and ACV concentrations were higher. The pore-water concentration between FW and SW irrigated fractions in the individual soil compartments was not statistically different (p=0.71 and p=0.84 in SL and OSL, respectively). Overall, ARVD accumulation in the pore-water and soil increased with continual irrigation (APPENDIX 3 and APPENDIX 4).

Figure 7.2 shows the accumulation of ARVDs in the soils. Noticeably, ACV and LVD were not detected in either of the soils. At the same time, the concentration of OSV in the FW SL compartment was below the detection limit. The mean ARVD accumulation in OSL soils was 5.9 ng g^{-1}, two times greater than the mean accumulation in the SL soils, i.e., 2.6 ng g^{-1}. In both soils, ARVD residues accumulated two times higher in the SW irrigated soil compartments than in the FW irrigated soils. In the OSL soils, NVP exhibited the highest accumulation at 11.2 ng g^{-1}. EFV and OSV accumulated approximately two and three times lower, i.e., 6.3 ng g^{-1} and 4.1 ng g^{-1} across the two irrigation regimes. While NVP concentration was highest in the OSL soils, the concentration of EFV was two times greater in the SL soils, i.e., 4.8 to2.4 ng g^{-1}.

7.3.5 Leachates

Since the experimental setup simulated an actual agricultural setting, it was not a closed system, and the ARVDs were measured in the irrigation water (leachates) drained through the soils. Figure 7.3 shows that all ARVDs were detected in the leachates at varying concentrations. The combined mean concentration of all ARVDs permeated through SL soils

was 12.8 µg L^{-1}, approximately four times higher than the leachates recovered from the OSL

soils, 2.9 ng L^{-1}.
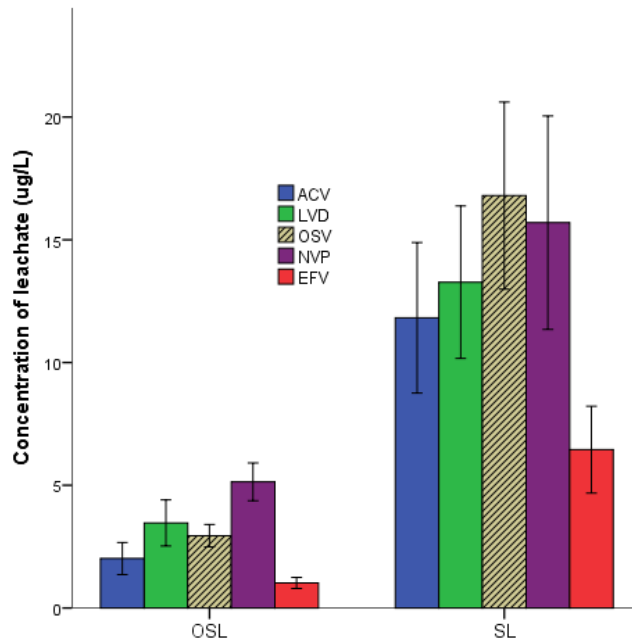
Figure 7.3. The concentration of leachates obtained from SL and OSL soils (n=14, ± SE)

It should be noted that the concentration in the leachates was not absolute. Leachates were

obtained by chance; therefore, it was impossible to gravimetrically determine the exact mass

of ARVD lost from the system via leaching. Nonetheless, the measured concentrations

indicated the potential adsorption capacities of the two soils. Sealing the porous bases of the

pots would otherwise have caused flooding and shifted the system to hydroponics, which was

not the study's intent.

7.3.6 Accumulation in plants

The accumulation and distribution of the ARVDs in the lettuce tissues across the two soils and

the two irrigation regimes are shown in Figure 7.4. The lowest accumulation was measured

in the OSL soils, a mean of 39.9 ng g^{-1}, which was eight times lower than the accumulation measured in SL soil-grown lettuce (323.3 ng g^{-1}). Accumulation in the FW compartments was six times lower, 52 ng g^{-1}, than the SW fraction, 310 ng g^{-1}. The bulk of accumulation in the SW irrigated soils, > 95 %, was measured in the SL soils.
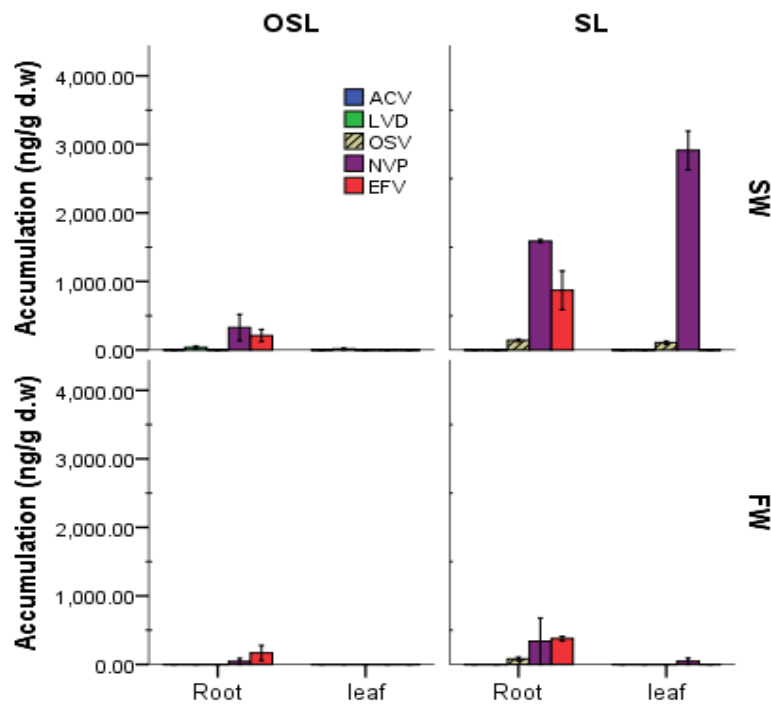
Figure 7.4. Accumulation of ARVDs in the irrigated lettuce in the four soil irrigation compartments (n=3, ± SD)

Summation of individual accumulation across the system shows that OSV exhibited the lowest accumulation in both leaf and root at 139 and 106 ng g^{-1}, respectively. EFV was the second highest in concentration, 872 ng g^{-1}. However, its accumulation was localized in the roots only.

NVP exhibited the highest root and leaf accumulation, approximately 3 to 5 times higher than OSV and EFV, respectively, i.e., 2912 ng g^{-1} and 1588 ng g^{-1} in the leaf and root. ACV and LVD were not detected in any lettuce from the four compartments.

7.3.7 Bioconcentration potential

The accumulation potential of contaminants from soil to plants is suitably described using contaminant concentration in the pore-water or soil, i.e., BCF $_\text{pore water}$ or BCF $_\text{soil,}$ respectively (Li et al., 2019a). The present study only estimated BCFs from the SW compartment and derived this from whole-plant accumulation, Table 7.5.

Table 7.5. SL and OSL-SW irrigated pore-water and soil whole plant bioconcentration factors (n=3, ±SD)

Soil	ARVD	BCF $_\text{soil}$ (g g^{-1})	BCF $_\text{pore water}$ (mL g^{-1})
	NVP	1406 (135)	225 (21.7)
SL	EFV	153 (70.3)	62.3 (28.6)
	OSV	382 (99.2)	22.8 (5.9)
	NVP	21.9 (4.1)	62.7 (11.8)
OSL	EFV	38.3(12.6)	394 (98.7)
	OSV	-	-

All BCFs were > 1, indicating a higher concentration of the ARVD in the plant tissue than in the soil or pore-water. The BCF $_\text{soil}$ varied from 21.9 - 1406 g g^{-1} and BCF $_\text{pore water}$ from 62 – 393 mL g^{-1}. While higher BCF $_\text{pore water}$ was measured in the SL soils relative to OSL soils, lower BCF $_\text{soil}$ values were measured in the OSL soils with respect to BCF $_\text{pore water}$.

7.4 Discussion

There is insufficient information on the mechanistic uptake of ARVD pharmaceuticals in both hydroponic and soil-plant systems. For this reason, molecule-specific discussion in this study was often based on pharmaceutical molecules from other therapeutic classes which exhibit corresponding physical-chemical characteristics to ARVDs.

7.4.1 ARVD speciation in soil and pore-water environment

The molecules' speciation characteristics in this pot-plant (soil) study in Table 7.6 matched the speciation data presented while describing the ARVD uptake mechanisms in hydroponics-based experiments in Table 3.2 and Table 5.3. For this reason, less uptake mechanisms were discussed in this present section. The discussion herein focussed on ARVD interactions with the soil and wastewater properties and their potential impact on uptake. Also, many references will be made to the adsorption/desorption experiments discussed in Chapter 6.

Table 7.6. ARVD molecule speciation at experimental pH[a]

ARVD	Log K_{ow}[a]	Pore-water environment			Soil environment		
		Log D_{ow} at pH 6.7		Solubility (mg mL^{-1})	Log D_{ow} at pH 5.7		Solubility (mg mL^{-1})
Acyclovir	-1.03	-1.03	Neutral	9.09	-1.03	Neutral	9.11
Lamivudine	-1.09	-1.1	Neutral	13.8	-1.09	Neutral	13.8
Oseltamivir	1.2	-1.2	99.9 % cationic [a]	294	-1.7	99.9 % cationic [a]	312
Nevirapine	2.5	2.5	Neutral	0.19	2.5	Neutral	0.19
Efavirenz	4.5	4.5	Neutral	0.0005	4.5	Neutral	0.0005

[a] ChemAxon Chemicalize

7.4.2 ARVD concentration in soil-derived pore-water

Since the soils contrasted mainly in the amount of SOM and DOC concentration (as was measured in Chapter 6), these two components likely influenced the occurrence of the ARVDs in the porewater. In Carter et al., (2016), the pore-water concentration of three pharmaceuticals, carbamazepine (CBZ), diclofenac, fluoxetine and orlistat (a lipase inhibitor) introduced at a varying nominal concentration (26-44 µg kg^{-1}) in five soils (including sandy

soils, similar to the present study) differed widely over a 21 day observation period. The variation was attributed to individual soil characteristics rather than the initial spike levels. Accordingly, the highest pore-water concentration was obtained from silty and sandy soil, consistent with measurements from the sandy SL soils in the present study. Although Carter et al. (2016) study differed in design from the present study, i.e., the components of their study were contained in enclosed non-perforated containers, it still provided an informative background on the potential distribution of pharmaceuticals in the pore-water fraction in soil-plant systems.

The concentration of NVP in the present study was highest in the sandy soils and lower in the SOM-laden OSL soil. In the present study, the sandy soils contained 10 times less SOM content, which explains why a larger ARVD portion is partitioned to the SL-derived pore-water due to weak NVP-soil interaction. The sorption/desorption experiments in Chapter 6 revealed weak NVP-DOC interactions comparable to polar ACV and LVD. Hence the NVP molecule was readily available for detection in the aqueous pore water fraction.

Regarding OSV, the molecule was cationic at the present study pH (Table 7.6) and thus bound to the negatively charged sites of the soil as reported in Sections 6.3.2 and 6.3.3 (adsorption/desorption experiments), the weaker electrostatic than hydrophobic interactions favored partitioning of the OSV to the pore-water. An identical sorption pattern was observed in characteristically cationic fluoxetine (an antidepressant), whereby a considerable decrease in its concentration was measured in the pore water with increase in SOM (Carter et al., 2016). As OSV in the present study, the concentration of fluoxetine in pore-water was higher than the more hydrophobic diclofenac (Carter et al., 2016), whose equivalent in the present study is EFV. Not forgetting OSV-DOC interactions, in Figure 6.8, OSV was least transferred (desorbed) from soils by the SW. Therefore, the relatively weaker OSV-DOC

interactions favoured its detection hence the higher measured levels compared to EFV. The concentration of EFV was low in the SL soil and below the detection limit in the OSL soil. EFV, the most lipophilic molecule, expectedly experienced the strongest interaction with the SOM.Hence it exhibited the weakest tendency to partition into the pore-water in the OSL-derived pore-water.

Recalling Section 6.3.7.2, desorption experiments using SW as an infiltration agent, the highest loss from soils was exhibited by EFV more than any other ARVD (Figure 6.8). Therefore, possibly due stronger EFV-DOC complex, EFV was not available for detection or was simultaneously lost as leachates. According to Peña et al., (2020), strong molecule-DOC complexes are not uncommon for hydrophobic compounds aqueous environment

7.4.3 ARVD accumulation in soils

Only OSV, NVP, and EFV were detected and quantified in the soils. Contrary to the pore-water's accumulation pattern, a two times higher accumulation of ARVD was measured in the OSL soils than in the sandy SL soils (Figure 7.2). Regarding the irrigating media, accumulation in the SW was two times higher than in the FW irrigated compartment.

Table 7.4 revealed an increase in SOM in the SW irrigated compartments (although intermittently) from the SW's inherent DOC and particulate matter. The present study was comparablewith Borgman and Chefetz (2013), who reported that irrigation with wastewater enhanced retardation (slow migration solutes relative to the mobile carrier) of

181

pharmaceutical molecules in terrestrial environments, i.e., consequently increasing their accumulation in soils. The study, a soil column leaching experiment, best described the observed ARVD accumulation data measured in the present study. The mobility and hence the retardation factors (coefficient expressing how slow a contaminant is transported relative to water, (EPA, 2021) of eight characteristically different pharmaceuticals were undertaken in 5 % compost-amended and unamended sandy soils. Two infiltration agents employed in the experiment were 0.01 M $CaCl_2$ (freshwater) and DOC- amended $CaCl_2$ ($CaCl_2$-DOC) (pH 6.2) solutions. Foremost, independent of the irrigation matrix, Higher retardation factors were measured in the compost-amended soils (0.99-5.48) than in the unamended soil (0.93-3.67) (Borgman and Chefetz, 2013). This observation is consistent with the higher accumulation of the three ARVDs in the SOM-rich OSL soils in the present study, whereby irrespective of the irrigation agent, the concentration of the ARVDs in the OSL soil was higher in the SL soils, as shown in Figure 7.2. The observation demonstrated the significance of SOM in limiting the mobility of pharmaceutical molecules in the soils.

In Borgman and Chefetz, 2013), the highest variability in retardation factors was measured in the cationic lamotrigine and hydrophobic diclofenac, whose equivalent in the present study is OSV and EFV, respectively. The retardation factor for hydrophobic diclofenac was two times greater (5.23) in the $CaCl_2$-DOC than in the pure $CaCl_2$ (2.32). The enhanced retardation in $CaCl_2$-DOC demonstrated the significance of the wastewater DOC component in sequestering the hydrophobic molecule to the bulk of the soil. The observation is consistent with the measured accumulation in the present study, whereby the concentration of EFV was 1.5 times higher (6.3 ng g^{-1}) than OSV (4.1 ng g^{-1}) in the SW irrigated OSL soil, as reported in the adsorption experiments in Section 6.3.7.1, where $CaCl_2$ was compared side by side with SW, the SW yielded K_d for EFV was approximately two times larger than the $CaCl_2$ derived one

(Table 6.9), i.e., 518 mL g^{-1} and 212 mL g^{-1}, respectively. It was the same with OSV (34.8 mL g^{-1} and 19.1 mL g^{-1}, respectively).

In the present study, ACV and LVD did not accumulate in either of the soils, nor was their accumulation enhanced with SW irrigation. Relatedly, other compounds such as ketoprofen, ibuprofen, bezafibrate, naproxen, and sulfamethoxazole, which were either anionic or exhibited log K_{ow} < 1.7, presented the lowest retardation factors (enhanced mobility) (0.93-2.29) when introduced to the soils with either pure $CaCl_2$ or the $CaCl_2$-DOC in both compost amended and unamended soils (Borgman and Chefetz, 2013), indicating that these molecules potentially pose the least risk in soils.

In the 0.01 M $CaCl_2$-only permeated soils (comparable to FW in the present study), cationic lamotrigine exhibited a retardation factor of 5.48 in the compost-amended soils, which was approximately 1.5 times higher than in the non-amended sandy soil (3.67), demonstrating that SOM independently enhances retardation even in the absence of DOC in the irrigating agent. Contrastingly, using $CaCl_2$-DOC for infiltration in the compost-amended soils lowered the retardation of OSV by approximately 15 % to 4.93 from the previous 5.48 measured when $CaCl_2$-only solution was used as the mobile agent in the composted soils. This observation by Borgman and Chefetz, (2013) suggested a possible competition for the cationic lamotrigine between the irrigation agent DOC and the compost-laden organic matter in the soil. The observation adequately describes the lower accumulation of OSV relative to EFV measured in the present study. Some of the OSV presumably were retained with the DOC in the SW and were not available for detection. At the same time, some OSV presumably leached with the SW; accordingly, from Figure 7.3, there is a higher concentration of OSV than EFV in the OSL-derived leachates (Borgman and Chefetz, 2013). Consistently, SW desorption experiments data in Table 6.10 revealed higher levels of hydrophobic EFV than cationic OSV were desorbed

from both OSL and SL soils. However, it is noteworthy to mention that the SW in the present study contained a higher nominal concentration of inorganic ions, absent in the (Borgman and Chefetz, 2013) DOC-laden $CaCl_2$ eluent (present study's SW equivalent), highlighting the significance of monitoring wastewater quality during irrigation as it can impact the accumulation of an individual pharmaceutical in several ways.

Sandy soils present a worst-case agroecosystem contamination situation in that their diminished SOM content reduces the soil's adsorptive capacity and results in molecules not bonded to soil and pore water constituents and hence are likely to be more bioavailable (Karnjanapiboonwong et al., 2010). This occurrence is consistent with the present study as Figure 7.2 shows that accumulation was lowest in the SL soils. OSV was not detected in the FW-SL irrigated compartment, possibly due to the absence of charged sites to facilitate electrostatic interactions. The bulk of the OSV in the SL-FW compartment was dissipated as leachate, as shown in Figure 7.3 and was highest in concentration among the five SL-derived leachates.

Noticeably, the hydrophobic EFV concentration was also higher than NVP and OSV in the SL-FW soil irrigated compartment. The likely reason for this accumulation pattern was that, since SOM was limited in the SL soil, the interaction mechanism with the soil shifted and became molecule-specific; that is, the interaction depended on the physical-characteristic of the molecule. Therefore, since EFV was more hydrophobic, it would have a stronger tendency to sorb than the less hydrophobic OSV and NVP.

A higher concentration of NVP in the OSL soils in the present study can be related to the concentration of CBZ measured in soils in Dalkmann et al. (2014a). The neutrality of NVP signified weaker sequestration to the bulk of the OSL soils than OSV and EFV; hence, the

molecule was bioavailable for extraction. Like CBZ, its sorption is non-specific, not related to the charged carboxylic groups deposited in the soils and therefore highly reversible and kinetically controlled (Dalkmann et al., 2014b). In the OSL soils, the concentration of NVP is higher than for EFV, yet EFV is more hydrophobic. The recalcitrance of NVP also likely contributed to its significant concentration and ease of extraction from the OSL soil.

7.4.4 Accumulation in plants

The magnitude of accumulation of the ARVDs in lettuce varied across the different soil irrigation regimes, Figure 7.4. Usually, variation in plant uptake trends is more pronounced in soil-plant systems than in hydroponics, and these differences are attributed to several factors such as differential water consumption and inherent plant growth-rate difference (Goldstein et al., 2014; Hsu et al., 1990 .
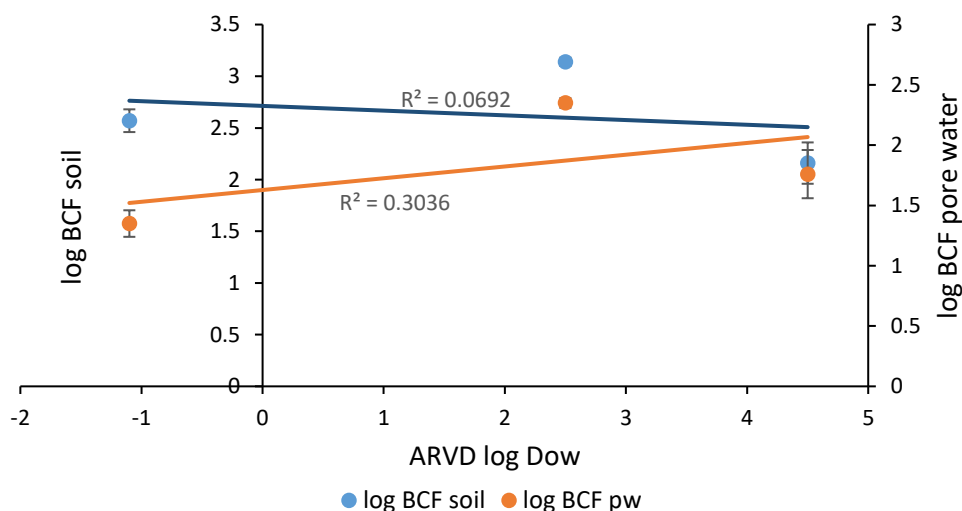

Figure 7.5. Relationship between pore-water and soil bioconcentration factors

The relationship between soil and pore-water BCF and the accumulated ARVD molecule log D_{ow} is shown in Figure 7.5. A stronger relationship was obtained from the pore-water BCF (R^2=0.31) than the soil concentration (R^2=0.08). These data (though limited, i.e., three data

points) are consistent with suppositions from (Hung et al., 2009 and Li et al., 2019a) that in soil-plant systems, the contaminant concentration in the soil does not reflect its actual bioavailability. The pore-water concentration forms a realistic basis for evaluating the uptake potential of pharmaceutical soil-plant systems. The wide intra-molecule BCF variation shown in Table 7.5 indicates the complex influence of matrix in soil and pore-water environments in pharmaceutical uptake in different soil-plant systems.

Goldstein et al. (2014) undertook a comparable greenhouse-based study, monitoring the accumulation of nine non-ARVD pharmaceuticals in cucumber leaves in different soils over four months. The measured accumulation varied in the three separately irrigated soils with spiked freshwater (SFW) or spiked treated wastewater (STWW) at an exposure concentration of 0.74 to 2.4 μg L^{-1}. The lowest plant accumulation was measured in alluvial soils, soils containing 2 to 5 times higher organic content (1.78 %) than the sandy and aeolian soils, 0.39 and 0.73 % OM, respectively. Most notably, and analogous to the present study, the highest soil accumulation was measured in the STWW irrigated sandy soils, not the SFW sandy soil or alluvial soils. The highest accumulation was exhibited by the non-ionic carbamazepine and sparingly cationic lamotrigine (at environmental pH 7.8), approximately 420 and 70 ng g^{-1}, respectively, an accumulation which was 60 % higher than in the associated SFW irrigated cucumber. The present study indicated that actual wastewater may enhance the accumulation of certain pharmaceuticals in plants in agroecosystems. Figure 7.4 in the present study is consistent with Goldstein et al., (2014) as it revealed higher pharmaceutical accumulation in plants in the SL–SW irrigated compartment, which received similar treatment to the STWW. Besides CBZ, other pharmaceuticals (Goldstein et al., (2014) exhibited lower accumulation (below 15 ng g^{-1}) in the cucumber even when irrigated with SFW. As mentioned in this study, CBZ and NVP share similar characteristics. Lamotrigine in Goldstein et al., (2014)

was partially cationic, just like OSV of the present study; however, it was more lipophilic (log D_{ow} 1.9). In the study, the accumulation of CBZ was approximately one order of magnitude higher than the other pharmaceuticals. In the present study, the accumulation of NVP was up to four times higher relative to the OSV and EFV.

Likewise, in Goldstein et al., (2014), pharmaceutical accumulation in soil was highest in alluvial soils (soils with the highest SOM content) and irrigated with STWW. The non-ionic CBZ exhibited the highest soil accumulation (15 ng g^{-1}). NVP likewise exhibited the highest accumulation in the OSL soils, as discussed and shown in Figure 7.2. In Goldstein et al., 2014), lamotrigine and caffeine exhibited 1.5 and 2 times lower accumulation, i.e., 10 and 4 ng $g^{-1,}$ respectively.

As with LVD and ACV in the present study, the accumulation of the ionic, acidic, and highly hydrophilic molecules varied from below the detection limit to 0.5 ng g^{-1} (Goldstein et al., 2014). Accumulation of CBZ and lamotrigine in the plants in the STWW irrigated sandy soils was 2 to 3 times higher than in the associated SFW irrigated soils. The present study's variation was broader, more than 10-times higher than the FW irrigated lettuce (Figure 7.4).

The present study data is consistent with Boxall et al. (2006), where soils with low organic matter were identified to present a worst-case scenario regarding the maximum bioavailability of pharmaceuticals to plants. Sallach et al., (2018) demonstrated the impact of increased sand content in soils, where the reduction of clay and silt content, substituted with sand in pot plant experiments, induced an eight-time increase in the concentration of sulfamethoxazole in lettuce from 3.3 ng g^{-1} in pure loam soil to 25 ng g^{-1} in the newly amended sandy soil. However, the sand in the soils was inversely proportional to the accumulation of cationic lincomycin (Sallach et al., 2018). This observation best explains why OSV, which was

99 % cationic in the present study (Table 7.6), least accumulated in the sandy SL soils (Figure 7.2) and lettuce (Figure 7.4), possibly because there were insufficient charged sites in the sandy soils which weakened the electrostatic interactions responsible for soil OSV accumulation.

Regarding the translocation mechanism, NVP exhibited a > 1 translocation factor, as noted by the higher leaf than root concentration in the SL-SW irrigated regime (Figure 7.4). However, with the accumulation of EFV, uncertainties still exist regarding the accurate measurement of the accumulation of highly hydrophobic molecules with log K_{ow} > 4 (Miller et al., 2015). The exterior surface of the root is organic (Trapp, 2000) hence the strong exterior surface interaction with hydrophobic organic contaminants. Likely, the thorough rinsing and washing of the roots undertaken before sample preparation is not adequate to fully desorb all the EFV molecules adsorbed on the root's exterior. Recalling Table 6.7 data, EFV exhibited the least desorption tendencies among the 5 ARVDs. Only 1.5 % of its adsorbed mass was desorbed compared with 16-64 % by mass of the other ARVDs, suggesting that further assessment is needed to determine the accurate uptake and accumulation potential of EFV devoid of its binding tendencies on the roots surfaces.

7.4.5 Degradation of ARVDs

ACV and LVD, which were hydrophilic and neutral (Table 7.6), were not detected in the soils or the plant matrix but only in the pore-water. Pharmaceutical degradation occurs in the soil environment, which may limit plant uptake and soil accumulation (Sallach et al., 2018).

For ACV, a possible reason that limited its accumulation and, therefore, its non-detection was the pH of the test environment (5.7 - 6.7 pH range). ACV-based stress studies showed that ACV is rapidly degraded in an acidic environment, and approximately 50 % of its parent

molecule was lost in 0.1 N HCl solution (Sinha et al., 2007). Although 0.1 N HCl is a strongly acidic environment compared with the pH range used in this study and hardly occurs in the natural environment, it shows ACV's predisposition for dissipation in a low pH environment. This loss possibly commenced in the irrigation matrix, implying that the molecule's loss had begun before its deposition onto the soils.   Nonetheless, the hydrophilicity and high desorption levels remain the most probable reason for their non-accumulation in the OSL and SL soils.

The rate of indirect photodegradation of ACV, and LVD, is enhanced in the presence of chromophoric nitrate in DOM in the aquatic environment (Zhou et al., 2015). The pot plants were under direct sunlight in the greenhouse, though not in a hydroponic setting. Photodegradation of ACV and LVD was likely since the pots were directly exposed to the Sun. Accelerated degradation of ACV was measured in agricultural soils with > 15 mg L^{-1} nitrate level (An et al., 2016). In Chapter 6, during the adsorption-desorption experiments, the loss of ACV was two times higher in the OSL soils (82 %) than in the SL soils (43%), indicating the higher capacity of the OSL soils to induce losses. Recalling that the OSL soil had been obtained from grounds that had previously been amended with fertilizer, the existing nitrate residues in the soil contributed to the rapid non-sorption dissipation of this molecule.   The total nitrogen (TN) data in Table 6.3 indicated nitrates' presence in the soils. The TN levels in the OSL soils were 2 to 7 times higher than in the SL soils in both FW and SW irrigated soils, varying from 23 to 390 mg L^{-1}. Accordingly, the higher levels of TN in OSL soils account for the higher dissipation of ACV in the OSL soils compared to the SL soils.

For LVD over 90 % of LVD was removed in WWTP in South Africa (Abafe et al., 2018). Since LVD has a poor sorption tendency, degradation processes such as photodegradation or biotic

processes were responsible. Also, if extended to a terrestrial environment, LVD's relatively short half-life in wastewaters (< 5 days, (Aminot et al., 2018) indicates very low persistence in environmental matrices and low bioavailability in soils, as observed in the present study.

Data on the degradation of OSV in soils is not readily available. Nonetheless, available information highlights its persistence in the aquatic environment, which, if extrapolated to terrestrial environments, may aid in understanding its possible dissipation pathways. Oseltamivir exhibited a half-life of 53 days in surface waters (Accinelli et al., 2010b) and was correspondingly considered a persistent molecule in water bodies and non-biodegradable in normal WWTPs (Fick et al., 2007; Södertröm et al., 2009). The active moiety of OSV was not degraded substantially by UV light radiation (Fick et al., 2007). In Accinelli et al., (2007), a small amount of OSV was lost when an aliquot of non-sterilized sediment was introduced in an initially sterilized sediment environment that contained spiked OSV, thus suggesting that losses of OSV via microbial pathways are possible in soil.

In the present study, EFV and NVP were the most persistent ARVDs tested in effluents and surface waters (Adeola and Forbes, 2022). Assuming their recalcitrance could be extended to the terrestrial environment, their resistance to degradation contributed to their relatively high soil accumulation, as shown in Figure 7.2. A distinct characteristic of EFV and NVP that accounts for their stability during wastewater treatment is that, rather than diminishing during the chlorination of treated wastewater, their persistence is enhanced. The enhancement is due to the de-conjugation of their hydroxylated metabolites and the reduction in the binding ability of the two compounds (Adeola and Forbes, 2022). Overall, this accounts for why EFV and NVP molecules were detected in the soils at appreciable levels than OSV, LVD and ACV. In literature, however, there are no studies on the recalcitrance of the

two molecules (EFV and NVP) associated with their hydrophobicity, pKa or solubility (Adeola and Forbes, 2022).

7.4.6 Risk to human health

The potential risk to human health from lettuce consumption was estimated using Equation (7.3). Nevirapine was selected as a pharmaceutical of concern as it exhibited the highest TF values and primarily accumulated in the leaf. The recommended maximum daily dose (MDD) for NVP for an individual ≥ 16 years old is 400 mg day^{-1} (Foissac et al., 2013). Therefore for an individual weighing 70 kg, the maximum acceptable daily intake for NVP is 5714 µg Kg^{-1} d^{-1}. The concentration of the NVP in the leaf was 2.9 µg g^{-1} d.w. The calculated DDI from consumption of the contaminated lettuce was 2.9 µg Kg^{-1} d^{-1} which is 2000 times lower than the maximum daily acceptable nevirapine intake. Health risk from consumption was, therefore, insignificant. Perceived risk from consumption was low , given that a factor of 10^1 to 10^3 margin is recommended between the DDI and the MDD for safe consumption (Prosser and Sibley, 2015).

7.4.7 Occurrence of ARVD metabolites in the soil environment

Screening for metabolites in soil was performed as previously described in Chapter 3. While parent molecules have been detected in wastewater and surface water environments, data on their associated metabolites' occurrencelimited (Mosekiemang et al., 2019b ;Olabode, 2021). There is no available report on ARVD metabolites in the terrestrial environment. Nonetheless, nevirapine and efavirenz metabolites, i.e. 12-hydroxy-Nevirapine and 8,14-dihydroxy-Efavirenz, were detected in wastewater samples (Mosekiemang et al., 2019b).

The ARVD metabolites identified in Chapter 3 were screened for soil, pore water, and plants. Table 7 shows that no known metabolite was detected in any of the matrices.

Table 7.7. Screening for metabolites in the soil-plant system

Parent API	Metabolite	$[M+H]^+$	Plant	Soil	Pore-water
Efavirenz	8-hydroxy-Efavirenz	332.02958	×	×	×
	8-Efavirenz-Glucoronide	508.06167	×	×	×
Lamivudine	Lamivudine Sulfoxide	246.05430	×	×	×
Nevirapine	12-hydroxy-nevirapine	283.11895	×	×	×
	4-carboxy-Nevirapine	297.09822	×	×	×
	12-hydroxy-Nevirapine Glucuronide	459.15104	×	×	×
Oseltamivir	Oseltamivir carboxylate	285.18088	×	×	×

× No metabolite detected

7.5 Conclusion

The study reveals that ARVD pharmaceuticals (log K_{ow} >1) accumulate in leafy plants grown in contaminated soils. HydrophilicARVDs (log < 1) were not detected in the plant tissues. The measured accumulation was at five-times higher in the synthetic wastewater-irrigated soils with higher in sand and low organic matter content. Binding the ARVDs to the soil and wastewater constituents strongly influenced the mass of pharmaceuticals available for uptake. Uptake depended on the bioavaiability of ARVDs in the soil pore water (log BCF $_{pore-water}$ (R^2=0.37) than in the in the soil (log BCF $_{soil}$ R^2=0.08). The health risks from consuming contaminated lettuce were minimal, up to 10^3 below the maximum recommended daily dose of nevirapine.

Chapter 8 CONCLUSIONS

The overall aim of this research was to assess the fate of anti(retro)virals (ARVDs) in agroecosystems, i.e. in the wastewater-soil-plant-receptor (man) interface. This objective was achieved by evaluating the processes and variables influencing their mobility and accumulation in wastewater, soil and plant matrices. Figure *8.1* summarises the main findings across the seven chapters of this study.

Chapter 1, a literature survey, highlighted the existing knowledge gaps and areas that warrant further research. First, it was shown that while ARVDs occur in aquatic environments (wastewater and surface water used for irrigation)   at relatively high concentrations (nanogram to microgram levels), understanding their fate in agroecosystems is limited. The areas of interest studied in this research include chromatographic analysis methods, uptake potential in soil and aquatic environments, and their sorption/desorption characteristics in soil and wastewater environment. Five ARVDs, i.e., acyclovir, lamivudine, oseltamivir, nevirapine and efavirenz, which have varied physical-chemical characteristics, were selected as test molecules.

In Chapter 2, optimization of the chromatographic conditions found that alkaline mobile phases (7.0 < pH < 9.0) and hexyl-phenyl stationary phase were ideal for analysis. The combination of these two phases yielded two times higher signal response and resolution than conventional acidic (pH ≤ 7.0) and octadecyl stationary (C18) phases.

Figure 8.1. Schematic summary of the chapter conclusions
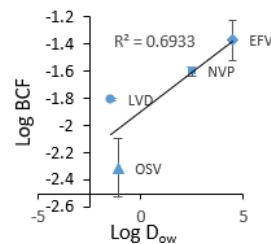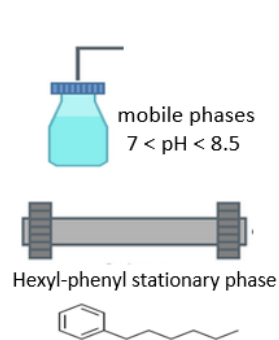
A hydroponic (aquatic-only) mechanistic plant exposure experiment was undertaken in Chapter 3 to identify priority ARVD molecules and find out compound-specific characteristics of the ARVDs that influence accumulation in leafy plants (lettuce) and possible phytotoxic effect on the plant from accumulation. Efavirenz and nevirapine, log K_{ow} 4.3 and 2.5, respectively, exhibited five times higher accumulation than the hydrophilic acyclovir and lamivudine, log K_{ow} < 1.0 ARVDs. It implied that bioconcentration depends on molecule lipophilicity; however, within a sigmoidal window. The lettuce exposed to the highest concentration (100 ug L^{-1}) exhibited significantly lower (30 %) leaf and root biomass than the control, indicating a possible phytotoxic effect.

Chapter 4 described a stepwise protocol used in the suspect screening approach, a technique used to identify in-plant biotransformation of exogenous chemicals accumulated in plant products using high-resolution mass spectrometry at the single-stage level. Two biotransformation products, lamivudine sulfoxide and nevirapine glucuronide were detected in the plant matrix, highlighting the plant's overall ability to biotransform accumulated exogenous chemicals. Since these two molecules were not detected in the exposure solution, it implied that the biotransformation was primarily plant induced. However, the biotransformation products were measured at level 4 confidence. The low-end confidence level does not necessarily negate the presence of the metabolite molecules. For enhanced confidence levels, levels 1-3, analysis using > MS^2 mass spectrometry approaches is necessary.

The lipophilic EFV was retained three times higher in the dissolved organic matter constituent than in the suspended particulate, as shown in Chapter 5. Contrastingly, approximately 15 % of the hydrophilic molecules (log K_{ow} < 2.5) were bound to the wastewater constituents.

Overall, the extent of retention to the wastewater constituents was EFV>NVP>OSV>LVD>ACV. In the sorption trials in Chapter 5, the ARVD molecules' retention did not increase with the increased mass of the wastewater constituents. There was no difference in the retention of the ARVDs between the nominal, two-times and three-times synthetic wastewater concentrations. The environmental implication of this observation is that it is likely that the concentration of organic contaminants in turbid surface waters could be no less than in less turbid waters. The suspended matter bounds 25 % of the lipophilic efavirenz. For this reason, accurate estimation of aquatic pollution by organic molecules demands concentration data of the target analyte in the suspended particulate matter. The ARVDs accumulated five times less in lettuce exposed to ARVDs in the wastewater, implying that, in a contaminated aquatic agroecosystem, while the wastewater is a source of contamination, its constituents bind to the solutes, minimizing their bioavailability for accumulation.

Five times less accumulation of the ARVDs into the lettuce was measured in the hydroponic (wastewater-irrigated) experiment in Chapter 5. Contrastingly, in the pot soil experiments in Chapter 7, accumulation in lettuce irrigated with wastewater was six times higher than in the freshwater-irrigated lettuce. The contrasting accumulation patterns reveal the deficiency of hydroponic experiments in mimicking real-life pollution scenarios in agroecosystems. Hydroponics should be limited to identifying priority contaminants, not the intricate nature of accumulation in terrestrial environments. In chapter 6, when the soil water partitioning coefficients (K_d) were normalized with the organic matter content, it resulted in identical log K_{oc} for the individual molecules across the two soils. The similar log K_{oc} indicated that soil organic matter is a primary sink for organic molecules in soils. Consequently, the accumulation of the ARVDs in the organic-rich soils (OSL) was two times higher (5.6 ng g^{-1}) than in the sand soils (SL) (2.6 ng g^{-1}). The lipophilic efavirenz and cationic oseltamivir

accumulated twice and thrice lower, respectively (6.3 and 4.1 ng g^{-1}) than the mid-polar nevirapine in the soils. The significant binding of oseltamivir to the soils shows that not only classical lipophilic contaminants accumulate in soils but also cationic molecules in equal measure and may impact earth-living organisms. The hydrophilic lamivudine and acyclovir (log K_{ow} < 1) neither accumulated in the soils nor the lettuce in the soil experiments. For this reason, characteristically similar compounds pose the least risk to exposed receptors.

Nevirapine was identified as the priority pollutant as it is the only ARVD that exhibited > 1 translocation factor, i.e., its accumulation in the leaves was higher than in the roots. Nonetheless, its accumulation was 2000 times lower than the recommended daily dietary intake (DDI). Consuming such lettuce may pose lower health risks. Overall, wastewater reuse regulatory authorities should be concerned with molecules characteristically similar to efavirenz, oseltamivir and nevirapine. The former two because they tend to accumulate in soils, and the latter because of its propensity to accumulate in plants.

Recommendations

The main limitation of the present research is the absence of pharmaceutical accumulation of data from actual agroecosystems irrigated with contaminated wastewater. Accumulation data from real-fied samples facilitate accurate estimation of health risks than values obtained from laboratory-controlled experiments. For this reason, undertaking actual fieldwork in urban agroecosystems irrigated with contaminated surface waters is a priority for future work. Similarly, toxicity endpoints of the ARVDs of pharmaceutical molecules are unavailable. The significance of the endpoints is that they are also necessary for estimating the hazard and risk quotients of ARVD molecules to facilitate health and ecological risk assessments. Appropriate experiments ought to be undertaken to generate toxicity data.

ARVD biotransformation products were detected in the plant tissues at level 4 confidence limits using single-stage mass spectrometry. However, a higher measurement confidence level is needed to verify the biotransformation products' presence. For this reason, mining for the ARVD metabolites should be undertaken using >MS^2 mass spectrometric approaches.

The accurate estimation of the accumulated lipophilic molecules (log K_{ow} > 4.0), especially in plant roots, is still uncertain due to their tendency to adhere to organic surfaces. Appropriate sorption and uptake experiments should be designed to distinguish between the two processes

The hydrophilic ARVDs, neither accumulated in the lettuce nor the soil. To understand their ecological risk, it is essential to investigate their degradation tendencies in soil and aquatic environments.

Appendices

APPENDIX 1. Pharmacology of selected antiviral and antiretroviral molecules

Molecule	Action	Dose (mg/day)	% Excretion	Side effects	Reference
Lamivudine	Anti HIV [a] Anti HBV [a]	10-300 [b]	71±16 [b]	Nausea fatigue diarrhea and cough [b]	[a] (Wang et al., 2019), (Singh et al., 2019) [b] (DrugBank, 2019c), (Strauch et al., 2011)
Nevirapine	Anti HIV [c]	100 - 400 [c]	10 [c]	Fatigue, fever insomnia, vertigo, and vomiting and weight loss [d]	[c] (DrugBank, 2019a) [d] (Notter et al., 2019), (Devarbhavi and Raj, 2019), (Ahmadi et al., 2019)
Efavirenz	Anti HIV [e]	30 - 600 [f]	< 1 [e]	Impaired concentration, insomnia, nausea [g]	[e] (Duarte et al., 2017) [f] (Atwine et al., 2018) [g] (Yee and Preuss, 2022)
Oseltamivir	Anti-influenza [h]	30-150 [i]	< 5 [i]	Mild gastrointestinal upset [m]	[h] (DrugBank, 2022a), [i] (Davies, 2010) [m] (Doucette and Aoki, 2005)
Acyclovir	Antiviral [j]	800- 40000 [k]	90-92 [l]	nausea or vomiting diarrhoea skin being sensitive to sunlight [j]	[j] (DrugBank, 2022b), [k] (EMC, 2022) [l] (King, 1988)

APPENDIX 2 .Soil extraction recoveries and detection limit

	Extraction recovery in soils (%)		Method detection limits		
	SL	OSL	Pore-water (ng mL^{-1}) (OSL)	SL soil (ng g^{-1})	OSL (ng g^{-1})
ACV	67	65	0.7	1.4	1.9
LVD	68	64	0.88	1.2	1.3
OSV	77	68	0.89	0.9	1.2
NVP	84	73	0.6	0.6	0.9
EFV	65	60	1.5	2.1	3.9

APPENDIX 3. Concentration of ARVD in soil-pore water across the irrigation duration (n=3, ±1 SD)
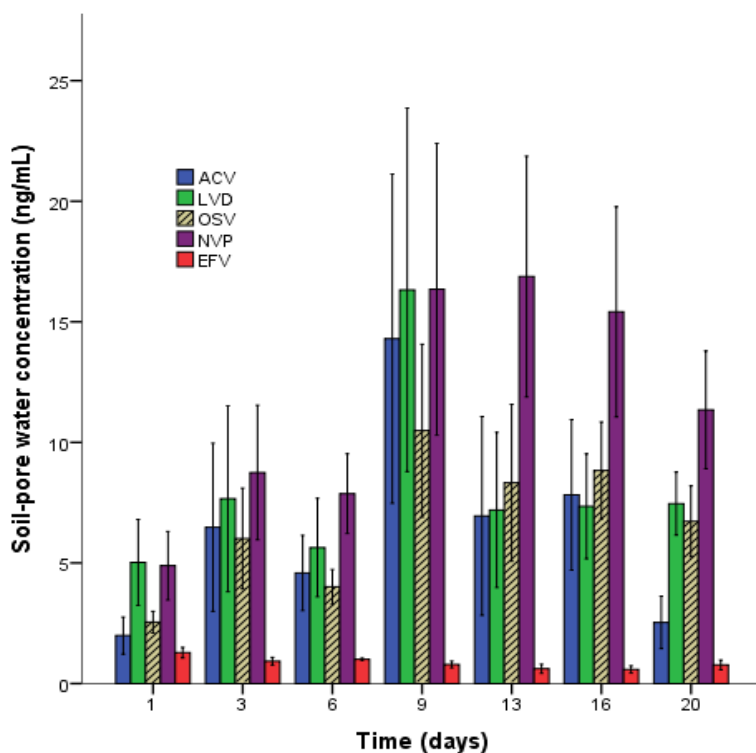
APPENDIX 4. The concentration of ARVD in soil water across the irrigation duration (n=3, ±1 SD)
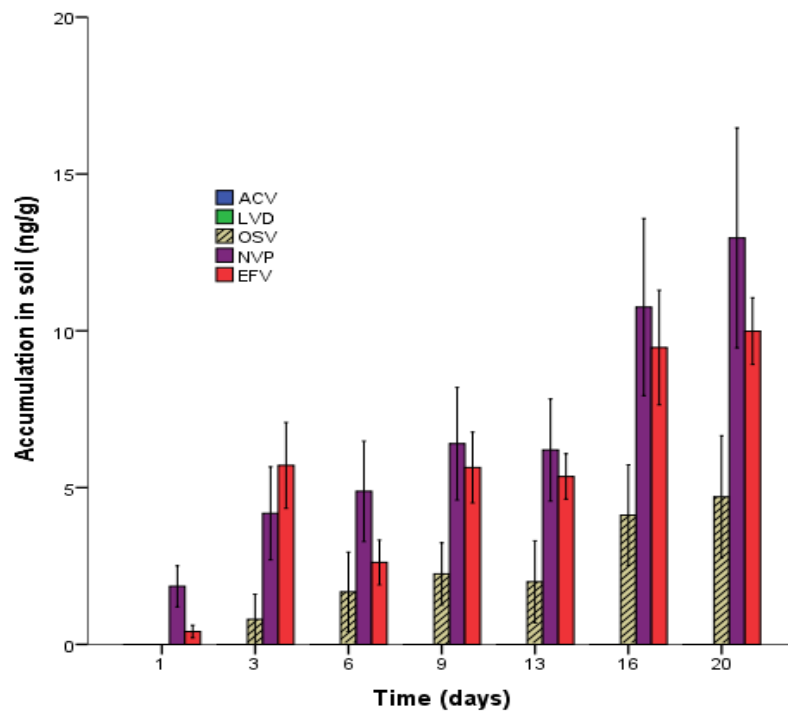
Reference

Abafe, O.A., Späth, J., Fick, J., Jansson, S., Buckley, C., Stark, A., Pietruschka, B., Martincigh, B.S., 2018. LC-MS/MS determination of antiretroviral drugs in influents and effluents from wastewater treatment plants in KwaZulu-Natal, South Africa. Chemosphere 200, 660–670. https://doi.org/10.1016/j.chemosphere.2018.02.105

Accinelli, C., Caracciolo, A.B., Grenni, P., 2007. Degradation of the antiviral drug oseltamivir carboxylate in surface water samples. Int J Environ Anal Chem 87, 579–587. https://doi.org/10.1080/03067310601151894

Accinelli, C., Saccà, M.L., Batisson, I., Fick, J., Mencarelli, M., Grabic, R., 2010a. Removal of oseltamivir (Tamiflu) and other selected pharmaceuticals from wastewater using a granular bioplastic formulation entrapping propagules of Phanerochaete chrysosporium. Chemosphere 81, 436–443. https://doi.org/10.1016/j.chemosphere.2010.06.074

Accinelli, C., Saccà, M.L., Fick, J., Mencarelli, M., Lindberg, R., Olsen, B., 2010b. Dissipation and removal of oseltamivir (Tamiflu) in different aquatic environments. Chemosphere 79, 891–897. https://doi.org/10.1016/J.CHEMOSPHERE.2010.02.022

Adeola, A.O., de Lange, J., Forbes, P.B.C., 2021. Adsorption of antiretroviral drugs, efavirenz and nevirapine from aqueous solution by graphene wool: Kinetic, equilibrium, thermodynamic and computational studies. Applied Surface Science Advances 6. https://doi.org/10.1016/j.apsadv.2021.100157

Adeola, A.O., Forbes, P.B.C., 2022. Antiretroviral Drugs in African Surface Waters: Prevalence, Analysis, and Potential Remediation. Environ Toxicol Chem 41, 247–262. https://doi.org/10.1002/etc.5127

Advanced Material Technology, 2007. HALO PHENY-HEXYL 1–7.

Agathokleous, E., Kitao, M., Calabrese, E.J., 2018. Human and veterinary antibiotics induce hormesis in plants: Scientific and regulatory issues and an environmental perspective. Environ Int 120, 489–495. https://doi.org/10.1016/j.envint.2018.08.035

Ahmadi, E., Eyvani, M.R., Riahifar, V., Momeneh, H., Karami, C., 2019. Amperometric determination of nevirapine by GCE modified with c-MWCNTs and synthesized 11-mercaptoundecanoyl hydrazinecarbothioamide coated silver nanoparticles. Microchemical Journal 146, 1218–1226. https://doi.org/10.1016/j.microc.2019.02.054

Ahmed, M.B.M., Rajapaksha, A.U., Lim, J.E., Vu, N.T., Kim, I.S., Kang, H.M., Lee, S.S., Ok, Y.S., 2015. Distribution and accumulative pattern of tetracyclines and sulfonamides in edible vegetables of cucumber, tomato, and lettuce. J Agric Food Chem 63, 398–405. https://doi.org/10.1021/jf5034637

Albero, B., Tadeo, J.L., Del Mar Delgado, M., Miguel, E., Pérez, R.A., 2019. Analysis of multiclass antibiotics in lettuce by liquid chromatography-tandem mass spectrometry

to monitor their plant uptake. Molecules 24. https://doi.org/10.3390/molecules24224066

Al-Farsi, R.S., Ahmed, M., Al-Busaidi, A., Choudri, B.S., 2017. Translocation of pharmaceuticals and personal care products (PPCPs) into plant tissues: A review. Emerg Contam 3, 132–137. https://doi.org/10.1016/j.emcon.2018.02.001

Aminot, Y., Fuster, L., Pardon, P., Le Menach, K., Budzinski, H., 2018. Suspended solids moderate the degradation and sorption of waste water-derived pharmaceuticals in estuarine waters. Science of the Total Environment 612, 39–48. https://doi.org/10.1016/j.scitotenv.2017.08.162

Amundsen, I., Øiestad, Å.M.L., Ekeberg, D., Kristoffersen, L., 2013. Quantitative determination of fifteen basic pharmaceuticals in ante- and post-mortem whole blood by high pH mobile phase reversed phase ultra high performance liquid chromatography-tandem mass spectrometry. J Chromatogr B Analyt Technol Biomed Life Sci 927, 112–123. https://doi.org/10.1016/j.jchromb.2012.12.039

An, J., Li, G., An, T., Nie, X., 2016. Indirect photochemical transformations of acyclovir and penciclovir in aquatic environments increase ecological risk. Environ Toxicol Chem 35, 584–592. https://doi.org/10.1002/etc.3238

Arye, G., Dror, I., Berkowitz, B., 2011. Fate and transport of carbamazepine in soil aquifer treatment (SAT) infiltration basin soils. Chemosphere 82, 244–252. https://doi.org/10.1016/J.CHEMOSPHERE.2010.09.062

Atwine, D., Bonnet, M., Taburet, A.M., 2018. Pharmacokinetics of efavirenz in patients on antituberculosis treatment in high human immunodeficiency virus and tuberculosis burden countries: A systematic review. Br J Clin Pharmacol 84, 1641–1658. https://doi.org/10.1111/bcp.13600

aus der Beek, T., Weber, F.A., Bergmann, A., Hickmann, S., Ebert, I., Hein, A., Küster, A., 2016. Pharmaceuticals in the environment-Global occurrences and perspectives. Environ Toxicol Chem 35, 823–835. https://doi.org/10.1002/etc.3339

Authority, N.E.M., 2006. WATER QUALITY REGULATIONS APPLICATION FORM FOR EFFLUENT DISCHARGE LICENCE WATER QUALITY LICENSING GUIDANCE PACK a) Guidelines to Filling in Application Form for Effluent Discharge Licence b) Fourth Schedule Monitoring Guide for Discharge into the Enviro, Gazette.

Ayala, A.P., Siesler, H.W., Wardell, S.M.S.V., Boechat, N., Dabbene, V., Cuffini, S.L., 2007. Vibrational spectra and quantum mechanical calculations of antiretroviral drugs: Nevirapine. J Mol Struct 828, 201–210. https://doi.org/10.1016/j.molstruc.2006.05.055

Azanu, D., Mortey, C., Darko, G., Weisser, J.J., Styrishave, B., Abaidoo, R.C., 2016. Uptake of antibiotics from irrigation water by plants. Chemosphere 157. https://doi.org/10.1016/j.chemosphere.2016.05.035

Azuma, T., Ishida, M., Hisamatsu, K., Yunoki, A., Otomo, K., Kunitou, M., Shimizu, M., Hosomaru, K., Mikata, S., Mino, Y., 2017. Fate of new three anti-influenza drugs and one prodrug in the water environment. Chemosphere 169, 550–557. https://doi.org/10.1016/j.chemosphere.2016.11.102

Bagheri, M., Al-jabery, K., Wunsch, D.C., Burken, J.G., 2019. A deeper look at plant uptake of environmental contaminants using intelligent approaches. Science of the Total Environment 651, 561–569. https://doi.org/10.1016/j.scitotenv.2018.09.048

Bagnis, S., Fitzsimons, M., Snape, J., Tappin, A., Comber, S., 2018a. Sorption of active pharmaceutical ingredients in untreated wastewater effluent and effect of dilution in freshwater: Implications for an "impact zone" environmental risk assessment approach. Science of the Total Environment 624, 333–341. https://doi.org/10.1016/j.scitotenv.2017.12.092

Bagnis, S., Fitzsimons, M.F., Snape, J., Tappin, A., Comber, S., 2018b. Processes of distribution of pharmaceuticals in surface freshwaters : implications for risk assessment. Environ Chem Lett. https://doi.org/10.1007/s10311-018-0742-7

Baker, D.R., Kasprzyk-Hordern, B., 2011. Multi-residue determination of the sorption of illicit drugs and pharmaceuticals to wastewater suspended particulate matter using pressurised liquid extraction, solid phase extraction and liquid chromatography coupled with tandem mass spectrometry. J Chromatogr A 1218, 7901–7913. https://doi.org/10.1016/j.chroma.2011.08.092

Barreales-Suárez, S., Callejón-Mochón, M., Azoulay, S., Bello-López, M.Á., Fernández-Torres, R., 2018. Liquid chromatography quadrupole time-of-flight mass spectrometry determination of six pharmaceuticals in vegetal biota. Uptake study in Lavandula dentata. Science of the Total Environment 622–623, 655–663. https://doi.org/10.1016/j.scitotenv.2017.11.244

Barreiros, L., Cunha-Reis, C., Silva, E.M.P., Carvalho, J.R.B., das Neves, J., Sarmento, B., Segundo, M.A., 2017. Development and validation of a liquid chromatography-MS/MS method for simultaneous quantification of tenofovir and efavirenz in biological tissues and fluids. J Pharm Biomed Anal 136, 120–125. https://doi.org/10.1016/j.jpba.2016.12.028

Bártíková, H., Podlipná, R., Skálová, L., 2016. Veterinary drugs in the environment and their toxicity to plants. Chemosphere 144, 2290–2301. https://doi.org/10.1016/J.CHEMOSPHERE.2015.10.137

Bartrons, M., Peñuelas, J., 2017a. Pharmaceuticals and Personal-Care Products in Plants. https://doi.org/10.1016/j.tplants.2016.12.010

Bartrons, M., Peñuelas, J., 2017b. Pharmaceuticals and Personal-Care Products in Plants. Trends Plant Sci 22, 194–203. https://doi.org/10.1016/j.tplants.2016.12.010

BBC, 2022. Europe's drought the worst in 500 years - report - BBC News [WWW Document]. URL https://www.bbc.co.uk/news/world-europe-62648912 (accessed 9.5.22).

Bedse, G., Kumar, V., Singh, S., 2009. Study of forced decomposition behavior of lamivudine using LC, LC-MS/TOF and MSn. J Pharm Biomed Anal 49, 55–63. https://doi.org/10.1016/j.jpba.2008.10.002

Ben Mordechay, E., Tarchitzky, J., Chen, Y., Shenker, M., Chefetz, B., 2018. Composted biosolids and treated wastewater as sources of pharmaceuticals and personal care products for plant uptake: A case study with carbamazepine. Environmental Pollution 232, 164–172. https://doi.org/10.1016/j.envpol.2017.09.029

Berg, T., Jørgenrud, B., Strand, D.H., 2013. Determination of buprenorphine, fentanyl and LSD in whole blood by UPLC-MS-MS. J Anal Toxicol 37, 159–165. https://doi.org/10.1093/jat/bkt005

Bhalsod, G.D., Chuang, Y.H., Jeon, S., Gui, W., Li, H., Ryser, E.T., Guber, A.K., Zhang, W., 2018. Uptake and Accumulation of Pharmaceuticals in Overhead- and Surface-Irrigated Greenhouse Lettuce. J Agric Food Chem 66, 822–830. https://doi.org/10.1021/acs.jafc.7b04355

Bletsou, A.A., Jeon, J., Hollender, J., Archontaki, E., Thomaidis, N.S., 2015. Targeted and non-targeted liquid chromatography-mass spectrometric workflows for identification of transformation products of emerging pollutants in the aquatic environment. TrAC - Trends in Analytical Chemistry 66, 32–44. https://doi.org/10.1016/j.trac.2014.11.009

Bocian, S., Krzemińska, K., 2019. The separations using pure water as a mobile phase in liquid chromatography using polar-embedded stationary phases. Green Chem Lett Rev 12, 69–78. https://doi.org/10.1080/17518253.2019.1576775

Boeije, G., Corstanje, R., Rottiers, A., Schowanek, D., 1999a. Adaptation of the CAS test system and synthetic sewage for biological nutrient removal. Part I: Development of a new synthetic sewage. Chemosphere 38, 699–709. https://doi.org/10.1016/S0045-6535(98)00311-7

Boeije, G., Corstanje, R., Rottiers, A., Schowanek, D., 1999b. ADAPTATION OF THE CAS TEST SYSTEM AND SYNTHETIC SEWAGE FOR BIOLOGICAL NUTRIENT REMOVAL PartPart II: Design and validation of test units. Science (1979) 38, 711–727.

Borgman, O., Chefetz, B., 2013. Combined effects of biosolids application and irrigation with reclaimed wastewater on transport of pharmaceutical compounds in arable soils. Water Res 47, 3431–3443. https://doi.org/10.1016/j.watres.2013.03.045

Boxall, A.B.A., Johnson, P., Smith, E.J., Sinclair, C.J., Edward Stutt, A., Levy, L.S., 2006. Uptake of Veterinary Medicines from Soils into Plants. https://doi.org/10.1021/JF053041T

Boyes, B.E., Dong, M.W., 2018. Modern Trends and Best Practices in Mobile-Phase Selection in Reversed-Phase Chromatography [WWW Document]. LCGC North America. URL

https://www.chromatographyonline.com/view/modern-trends-and-best-practices-mobile-phase-selection-reversed-phase-chromatography-0 (accessed 11.18.21).

Briggs, G.G., Bromilow, R.H., Evans, A.A., 1982. Relationships between lipophilicity and root uptake and translocation of non-ionised chemicals by barley. Pestic Sci 13, 495–504. https://doi.org/10.1002/ps.2780130506

Burken, J.G., Schnoor, J.L., 1998. Predictive relationships for uptake of organic contaminants by hybrid poplar trees. Environ Sci Technol 32, 3379–3385. https://doi.org/10.1021/es9706817

Calza, P., Medana, C., Padovano, E., Giancotti, V., Baiocchi, C., 2012. Identification of the unknown transformation products derived from clarithromycin and carbamazepine using liquid chromatography/high-resolution mass spectrometry. Rapid Communications in Mass Spectrometry 26, 1687–1704. https://doi.org/10.1002/rcm.6279

Carter, L.J., Chefetz, B., Abdeen, Z., Boxall, A.B.A., 2019. Emerging investigator series: Towards a framework for establishing the impacts of pharmaceuticals in wastewater irrigation systems on agro-ecosystems and human health. Environ Sci Process Impacts 21, 605–622. https://doi.org/10.1039/c9em00020h

Carter, L.J., Ryan, J.J., Boxall, A.B.A., 2016. Effects of soil properties on the uptake of pharmaceuticals into earthworms. Environmental Pollution 213, 922–931. https://doi.org/10.1016/j.envpol.2016.03.044

Carter, L.J., Williams, M., Martin, S., Kamaludeen, S.P.B., Kookana, R.S., 2018a. Sorption, plant uptake and metabolism of benzodiazepines. Science of the Total Environment 628–629, 18–25. https://doi.org/10.1016/j.scitotenv.2018.01.337

Carter, L.J., Williams, M., Martin, S., Kamaludeen, S.P.B., Kookana, R.S., 2018b. Sorption, plant uptake and metabolism of benzodiazepines. Science of the Total Environment 628–629, 18–25. https://doi.org/10.1016/j.scitotenv.2018.01.337

Celiz, M.D., Tso, J., Aga, D.S., 2009. Pharmaceutical metabolites in the environment: analytical challenges and ecological risks. Environ Toxicol Chem 28, 2473–2484. https://doi.org/10.1897/09-173.1

Chefetz, B., Marom, R., Salton, O., Oliferovsky, M., Mordehay, V., Ben-Ari, J., Hadar, Y., 2019. Transformation of lamotrigine by white-rot fungus Pleurotus ostreatus. Environmental Pollution 250, 546–553. https://doi.org/10.1016/j.envpol.2019.04.057

Chefetz, B., Mualem, T., Ben-Ari, J., 2008. Sorption and mobility of pharmaceutical compounds in soil irrigated with reclaimed wastewater. Chemosphere. https://doi.org/10.1016/j.chemosphere.2008.06.070

ChemAxon, 2021. Chemicalize - Instant Cheminformatics Solutions [WWW Document]. URL https://chemicalize.com/app/calculation/efavirenz (accessed 3.13.22).

Christou, A., Agüera, A., Bayona, J.M., Cytryn, E., Fotopoulos, V., Lambropoulou, D., Manaia, C.M., Michael, C., Revitt, M., Schröder, P., Fatta-Kassinos, D., 2017a. The potential implications of reclaimed wastewater reuse for irrigation on the agricultural environment: The knowns and unknowns of the fate of antibiotics and antibiotic resistant bacteria and resistance genes – A review. Water Res 123, 448–467. https://doi.org/10.1016/j.watres.2017.07.004

Christou, A., Karaolia, P., Hapeshi, E., Michael, C., Fatta-Kassinos, D., 2017b. Long-term wastewater irrigation of vegetables in real agricultural systems: Concentration of pharmaceuticals in soil, uptake and bioaccumulation in tomato fruits and human health risk assessment. Water Res 109, 24–34. https://doi.org/10.1016/j.watres.2016.11.033

Christou, A., Kyriacou, M.C., Georgiadou, E.C., Papamarkou, R., Hapeshi, E., Karaolia, P., Michael, C., Fotopoulos, V., Fatta-Kassinos, D., 2019a. Uptake and bioaccumulation of three widely prescribed pharmaceutically active compounds in tomato fruits and mediated effects on fruit quality attributes. Science of The Total Environment 647, 1169–1178. https://doi.org/10.1016/j.scitotenv.2018.08.053

Christou, A., Michael, C., Fatta-Kassinos, D., Fotopoulos, V., 2018. Can the pharmaceutically active compounds released in agroecosystems be considered as emerging plant stressors? Environ Int 114, 360–364. https://doi.org/10.1016/j.envint.2018.03.003

Christou, A., Papadavid, G., Dalias, P., Fotopoulos, V., 2019b. Ranking of crop plants according to their potential to uptake and accumulate contaminants of emerging concern 170, 422–432. https://doi.org/10.1016/j.envres.2018.12.048

Christou, A., Papadavid, G., Dalias, P., Fotopoulos, V., Michael, C., Bayona, J.M., Piña, B., Fatta-Kassinos, D., 2019c. Ranking of crop plants according to their potential to uptake and accumulate contaminants of emerging concern. Environ Res 170, 422–432. https://doi.org/10.1016/j.envres.2018.12.048

Chromatography Today, 2022. Does Carbon Load Affect the Retention Times from Your Columns? Chromatography Today [WWW Document]. Labmate online. URL https://www.chromatographytoday.com/news/columns-lc/37/breaking-news/does-carbon-load-affect-the-retention-times-from-your-columns/46748 (accessed 5.12.22).

Chuang, Y.H., Liu, C.H., Sallach, J.B., Hammerschmidt, R., Zhang, W., Boyd, S.A., Li, H., 2019. Mechanistic study on uptake and transport of pharmaceuticals in lettuce from water. Environ Int 131, 104976. https://doi.org/10.1016/j.envint.2019.104976

Cogger, C.G., Bary, A.I., Kennedy, A.C., Fortuna, A.-M., 2013. Long-Term Crop and Soil Response to Biosolids Applications in Dryland Wheat. Journal of Environment Quality 42, 1872. https://doi.org/10.2134/jeq2013.05.0109

COLE, D., 1994. DETOXIFICATION AND ACTIVATION OF AGROCHEMICALS IN PLANTS. Pestic Sci 42, 209–222. https://doi.org/10.1002/ps.2780420309

Coleman, J.O.D., Blake-Kalff, M.M.A., Davies, T.G.E., 1997. Detoxification of xenobiotics by plants: Chemical modification and vacuolar compartmentation. Trends Plant Sci 2, 144–151. https://doi.org/10.1016/S1360-1385(97)01019-4

Collins, C., Fryer, M., Grosso, A., 2006. Plant uptake of non-ionic organic chemicals. Environ Sci Technol 40, 45–52. https://doi.org/10.1021/es0508166

Crini, G., Badot, P.M., 2008. Application of chitosan, a natural aminopolysaccharide, for dye removal from aqueous solutions by adsorption processes using batch studies: A review of recent literature. Progress in Polymer Science (Oxford) 33, 399–447. https://doi.org/10.1016/j.progpolymsci.2007.11.001

Cui, H., de Angelis, M.H., Schröder, P., 2017. Iopromide exposure in Typha latifolia L.: Evaluation of uptake, translocation and different transformation mechanisms in planta. Water Res 122, 290–298. https://doi.org/10.1016/j.watres.2017.06.004

Dalkmann, P., Siebe, C., Amelung, W., Schloter, M., Siemens, J., 2014a. Does long-term irrigation with untreated wastewater accelerate the dissipation of pharmaceuticals in soil? Environ Sci Technol 48, 4963–4970. https://doi.org/10.1021/es501180x

Dalkmann, P., Willaschek, E., Schiedung, H., Bornemann, L., Siebe, C., Siemens, J., 2014b. Long-term Wastewater Irrigation Reduces Sulfamethoxazole Sorption, but Not Ciprofloxacin Binding, in Mexican Soils. J Environ Qual 43, 964–970. https://doi.org/10.2134/JEQ2013.11.0473

Davies, B.E., 2010. Pharmacokinetics of oseltamivir: an oral antiviral for the treatment and prophylaxis of influenza in diverse populations. J Antimicrob Chemother 65 Suppl 2. https://doi.org/10.1093/JAC/DKQ015

De Dominicis, E., Commissati, I., Suman, M., 2012. Targeted screening of pesticides, veterinary drugs and mycotoxins in bakery ingredients and food commodities by liquid chromatography-high-resolution single-stage Orbitrap mass spectrometry. Journal of Mass Spectrometry 47, 1232–1241. https://doi.org/10.1002/jms.3074

De Vijlder, T., Valkenborg, D., Lemière, F., Romijn, E.P., Laukens, K., Cuyckens, F., 2018. A tutorial in small molecule identification via electrospray ionization-mass spectrometry: The practical art of structural elucidation. Mass Spectrom Rev 37, 607–629. https://doi.org/10.1002/mas.21551

Delatour, C., Ledercq, L., 2005. Positive electrospray liquid chromatography/mass spectrometry using high-pH gradients: A way to combine selectivity and sensitivity for a large variety of drugs [3]. Rapid Communications in Mass Spectrometry 19, 1359–1362. https://doi.org/10.1002/rcm.1923

Delgado-Moreno, L., Wu, L., Gan, J., 2010. Effect of dissolved organic carbon on sorption of pyrethroids to sediments. Environ Sci Technol 44, 8473–8478. https://doi.org/10.1021/es102277h

Devarbhavi, H., Raj, S., 2019. Drug-induced liver injury with skin reactions: Drugs and host risk factors, clinical phenotypes and prognosis. Liver International 39, 802–811. https://doi.org/10.1111/liv.14004

Ding, Q., Wu, H.L., Xu, Y., Guo, L.J., Liu, K., Gao, H.M., Yang, H., 2011. Impact of low molecular weight organic acids and dissolved organic matter on sorption and mobility of isoproturon in two soils. J Hazard Mater 190, 823–832. https://doi.org/10.1016/J.JHAZMAT.2011.04.003

Dodgen, L.K., Li, J., Parker, D., Gan, J.J., 2013. Uptake and accumulation of four PPCP/EDCs in two leafy vegetables. Environmental Pollution 182, 150–156. https://doi.org/10.1016/j.envpol.2013.06.038

Dong, M.W., 2006. Modern HPLC for Practicing Scientists. Wiley, Hoboken, New Jersey.

Dong, M.W., Boyes, B.E., 2018. Modern trends and best practices in mobile-phase selection in reversed-phase chromatography. LC-GC North Am 36, 752–767.

Doran, P.M., 2013. Unit Operations, in: Bioprocess Engineering Principles. Elsevier, pp. 445–595. https://doi.org/10.1016/B978-0-12-220851-5.00011-3

Doucette, K.E., Aoki, F.Y., 2005. Oseltamivir: a clinical and pharmacological perspective. http://dx.doi.org/10.1517/14656566.2.10.1671 2, 1671–1683. https://doi.org/10.1517/14656566.2.10.1671

Drillia, P., Stamatelatou, K., Lyberatos, G., 2005. Fate and mobility of pharmaceuticals in solid matrices. Chemosphere 60, 1034–1044. https://doi.org/10.1016/j.chemosphere.2005.01.032

DrugBank, 2022a. Oseltamivir: Uses, Interactions, Mechanism of Action | DrugBank Online [WWW Document]. URL https://go.drugbank.com/drugs/DB00198 (accessed 6.19.22).

DrugBank, 2022b. Acyclovir: Uses, Interactions, Mechanism of Action | DrugBank Online [WWW Document]. DrugBank. URL https://go.drugbank.com/drugs/DB00787 (accessed 6.19.22).

Drugbank, 2020. Efavirenz [WWW Document]. URL https://www.drugbank.ca/drugs/DB00625 (accessed 5.10.20).

DrugBank, 2019a. Nevirapine [WWW Document]. URL https://www.drugbank.ca/drugs/DB00238

DrugBank, 2019b. Lamivudine [WWW Document]. URL https://www.drugbank.ca/drugs/DB00709

DrugBank, 2019c. Lamivudine [WWW Document].

Duarte, H., Cruz, J.P., Aniceto, N., Ribeiro, A.C., Fernandes, A., Paixão, P., Antunes, F., Morais, J., 2017. Population Approach to Efavirenz Therapy. J Pharm Sci 106, 3161–3166. https://doi.org/10.1016/j.xphs.2017.06.004

Duarte, R.M.B.O., Duarte, A.C., 2020. Multidimensional analytical techniques in environmental research: Evolution of concepts. Multidimensional Analytical Techniques in Environmental Research 1–26. https://doi.org/10.1016/B978-0-12-818896-5.00001-6

Dudley, S., Sun, C., McGinnis, M., Trumble, J., Gan, J., 2019. Formation of biologically active benzodiazepine metabolites in Arabidopsis thaliana cell cultures and vegetable plants under hydroponic conditions. Science of the Total Environment 662, 622–630. https://doi.org/10.1016/j.scitotenv.2019.01.259

Duthaler, U., Berger, B., Erb, S., Battegay, M., Letang, E., Gaugler, S., Krähenbühl, S., Haschke, M., 2017. Automated high throughput analysis of antiretroviral drugs in dried blood spots. Journal of Mass Spectrometry 52, 534–542. https://doi.org/10.1002/jms.3952

EMC, 2022. Aciclovir Tablets BP 800mg - Summary of Product Characteristics (SmPC) - (emc) [WWW Document]. URL https://www.medicines.org.uk/emc/product/5696/smpc#gref (accessed 6.19.22).

Emde, D., Hannam, K.D., Most, I., Nelson, L.M., Jones, M.D., 2021. Soil organic carbon in irrigated agricultural systems: A meta-analysis. Glob Chang Biol 27, 3898–3910. https://doi.org/10.1111/gcb.15680

Emhofer, L., Himmelsbach, M., Buchberger, W., Klampfl, C.W., 2018a. Insights into the uptake, metabolization, and translocation of four non-steroidal anti-inflammatory drugs in cress (Lepidium sativum) by HPLC-MS2. Electrophoresis 39, 1294–1300. https://doi.org/10.1002/elps.201700438

Emhofer, L., Himmelsbach, M., Buchberger, W., Klampfl, C.W., 2018b. Insights into the uptake, metabolization, and translocation of four non-steroidal anti-inflammatory drugs in cress (Lepidium sativum) by HPLC-MS2. Electrophoresis 39, 1294–1300. https://doi.org/10.1002/elps.201700438

Emhofer, L., Himmelsbach, M., Buchberger, W., Klampfl, C.W., 2017. High-performance liquid chromatography – mass spectrometry analysis of the parent drugs and their metabolites in extracts from cress (Lepidium sativum) grown hydroponically in water containing four non-steroidal anti-inflammatory drugs. J Chromatogr A 1491, 137–144. https://doi.org/10.1016/j.chroma.2017.02.057

EPA, 2021. EPA On-line Tools for Site Assessment Calculation | Ecosystems Research | US EPA [WWW Document]. URL https://www3.epa.gov/ceampubl/learn2model/part-two/onsite/ard_onsite.html (accessed 8.2.22).

EPA, 2012. Plant Uptake and Translocation Test -OCSPP 850:4800, Ecological effects test guidelines.

Erb, R., Oberacher, H., 2014. Comparison of mobile-phase systems commonly applied in liquid chromatography-mass spectrometry of nucleic acids. Electrophoresis 35, 1226–1235. https://doi.org/10.1002/elps.201300269

Erfani Agah, A., Meire, P., De Deckere, E., 2017. Influence of synthetic wastewater on the transport and transformation in irrigated soils. Desalination Water Treat 72, 136–145. https://doi.org/10.5004/dwt.2017.20635

Espada, A., Rivera-Sagredo, A., 2003. Ammonium hydrogencarbonate, an excellent buffer for the analysis of basic drugs by liquid chromatography-mass spectrometry at high pH. J Chromatogr A 987, 211–220. https://doi.org/10.1016/S0021-9673(02)01819-8

FAO, 2012. Coping with water scarcity. An action framework for agriculture and food security. FAO Water Reports 38 |Policy Support and Governance| Food and Agriculture Organization of the United Nations [WWW Document]. URL https://www.fao.org/policy-support/tools-and-publications/resources-details/en/c/1395516/ (accessed 9.5.22).

FAO, 2000. Assessing soil contamination A reference manual [WWW Document]. URL https://www.fao.org/3/X2570E/X2570E06.htm (accessed 3.18.22).

FDA, 2018. Bioanalytical method validation- Guidance for Industry.

FDA, F. and V.M.P., 2015. Acceptance Criteria for Confirmation of Identity of Chemical Residues using Exact Mass Data f 0–16.

Fekadu, S., Alemayehu, E., Dewil, R., Van der Bruggen, B., 2019. Pharmaceuticals in freshwater aquatic environments: A comparison of the African and European challenge. Science of the Total Environment 654, 324–337. https://doi.org/10.1016/j.scitotenv.2018.11.072

Ferrari, D., Bagaglio, S., Raso, M., Galli, L., Premaschi, S., Messina, E., Morsica, G., Locatelli, M., Uberti-Foppa, C., Hasson, H., 2019. A liquid chromatography-tandem mass spectrometry method for simultaneous determination of simeprevir, daclatasvir, sofosbuvir, and GS-331007 applied to a retrospective clinical pharmacological study. J Chromatogr B Analyt Technol Biomed Life Sci 1120, 1–7. https://doi.org/10.1016/j.jchromb.2019.04.048

Fick, J., Lindberg, R.H., Tysklind, M., Haemig, P.D., Waldenström, J., Wallensten, A., Olsen, B., 2007. Antiviral oseltamivir is not removed or degraded in normal sewage water treatment: Implications for development of resistance by influenza A virus. PLoS One 2. https://doi.org/10.1371/journal.pone.0000986

Foissac, F., Bouazza, N., Frange, P., Blanche, S., Faye, A., Lachassinne, E., Dollfus, C., Hirt, D., Benaboud, S., Treluyer, J.M., Urien, S., 2013. Evaluation of nevirapine dosing recommendations in HIV-infected children. Br J Clin Pharmacol 76, 137–144. https://doi.org/10.1111/bcp.12069

Fountouli, T. V., Chrysikopoulos, C. V., 2018a. Adsorption and Thermodynamics of Pharmaceuticals, Acyclovir and Fluconazole, onto Quartz Sand under Static and Dynamic Conditions. Environ Eng Sci. https://doi.org/10.1089/ees.2017.0499

Fountouli, T. V., Chrysikopoulos, C. V., 2018b. Adsorption and Thermodynamics of Pharmaceuticals, Acyclovir and Fluconazole, onto Quartz Sand under Static and Dynamic Conditions. Environ Eng Sci 35, 909–917. https://doi.org/10.1089/ees.2017.0499

Fu, Q., Malchi, T., Carter, L.J., Li, H., Gan, J., Chefetz, B., 2019. Pharmaceutical an Personal Care Proucts: From Wastewater Treatment into Agro-Foo Systems. Environ Sci Technol 53, 14083–14090. https://doi.org/10.1021/acs.est.9b06206

Fu, Q., Wu, X., Ye, Q., Ernst, F., Gan, J., 2016. Biosolids inhibit bioavailability and plant uptake of triclosan and triclocarban. Water Res 102, 117–124. https://doi.org/10.1016/j.watres.2016.06.026

Furey, A., Moriarty, M., Bane, V., Kinsella, B., Lehane, M., 2013. Ion suppression; A critical review on causes, evaluation, prevention and applications. Talanta 115, 104–122. https://doi.org/10.1016/j.talanta.2013.03.048

Galani, A., Alygizakis, N., Aalizadeh, R., Kastritis, E., Dimopoulos, M.-A., Thomaidis, N.S., 2021. Patterns of pharmaceuticals use during the first wave of COVID-19 pandemic in Athens, Greece as revealed by wastewater-based epidemiology. Science of The Total Environment 798, 149014. https://doi.org/10.1016/j.scitotenv.2021.149014

Gallicano, K., Kashuba, A.D.M., 2000. Antiretroviral-drug concentrations in semen [2] (multiple letters). Antimicrob Agents Chemother 44, 1117–1118. https://doi.org/10.1128/AAC.44.4.1117-1118.2000

Gao, S., Zhang, Z.P., Karnes, H.T., 2005. Sensitivity enhancement in liquid chromatography/atmospheric pressure ionization mass spectrometry using derivatization and mobile phase additives. J Chromatogr B Analyt Technol Biomed Life Sci. https://doi.org/10.1016/j.jchromb.2005.04.021

Gardner, M., Jones, V., Comber, S., Scrimshaw, M.D., Coello-Garcia, T., Cartmell, E., Lester, J., Ellor, B., 2013. Performance of UK wastewater treatment works with respect to trace contaminants. Science of the Total Environment 456–457, 359–369. https://doi.org/10.1016/j.scitotenv.2013.03.088

Geissen, V., Mol, H., Klumpp, E., Umlauf, G., Nadal, M., van der Ploeg, M., van de Zee, S.E.A.T.M., Ritsema, C.J., 2015. Emerging pollutants in the environment: A challenge for water resource management. International Soil and Water Conservation Research 3, 57–65. https://doi.org/10.1016/j.iswcr.2015.03.002

Ghosh, G.C., Nakada, N., Yamashita, N., Tanaka, H., 2010. Occurrence and fate of oseltamivir carboxylate (Tamiflu) and amantadine in sewage treatment plants. Chemosphere 81, 13–17. https://doi.org/10.1016/J.CHEMOSPHERE.2010.07.023

Goldstein, M., Shenker, M., Chefetz, B., 2014. Insights into the uptake processes of wastewater-borne pharmaceuticals by vegetables. Environ Sci Technol 48, 5593–5600. https://doi.org/10.1021/es5008615

Gong, W., Jiang, M., Zhang, T., Zhang, W., Liang, G., Li, B., Hu, B., Han, P., 2020. Uptake and dissipation of metalaxyl-M, fludioxonil, cyantraniliprole and thiamethoxam in greenhouse chrysanthemum. Environmental Pollution 257, 113499. https://doi.org/10.1016/J.ENVPOL.2019.113499

González García, M., Fernández-López, C., Pedrero-Salcedo, F., Alarcón, J.J., 2018. Absorption of carbamazepine and diclofenac in hydroponically cultivated lettuces and human health risk assessment. Agric Water Manag 206, 42–47. https://doi.org/10.1016/j.agwat.2018.04.018

Graber, E.R., Gerstl, Z., 2011. Organic micro-contamination, sorption, transport, accumulation, and root uptake in the soil-plant continuum as a result of irrigation with treated wastewater. Isr J Plant Sci 59, 105–114. https://doi.org/10.1560/IJPS.59.2-4.105

Guo, J., Sinclair, C.J., Selby, K., Boxall, A.B.A., 2016. Toxicological and ecotoxicological risk-based prioritization of pharmaceuticals in the natural environment. Environ Toxicol Chem 35, 1550–1559. https://doi.org/10.1002/ETC.3319

Gworek, B., Kijeńska, M., Wrzosek, J., Graniewska, M., 2021. Pharmaceuticals in the Soil and Plant Environment: a Review. Water Air Soil Pollut 232. https://doi.org/10.1007/s11270-020-04954-8

Haham, H., Oren, A., Chefetz, B., 2012. Insight into the role of dissolved organic matter in sorption of sulfapyridine by semiarid soils. Environ Sci Technol 46, 11870–11877. https://doi.org/10.1021/ES303189F/ASSET/IMAGES/MEDIUM/ES-2012-03189F_0009.GIF

Hajj-Mohamad, M., Darwano, H., Duy, S.V., Sauvé, S., Prévost, M., Arp, H.P.H., Dorner, S., 2017. The distribution dynamics and desorption behaviour of mobile pharmaceuticals and caffeine to combined sewer sediments. Water Res 108, 57–67. https://doi.org/10.1016/j.watres.2016.10.053

He, K., Yonetani, T., Asada, Y., Echigo, S., Itoh, S., 2019. Simultaneous determination of carbamazepine-N-glucuronide and carbamazepine phase I metabolites in the wastewater by liquid chromatography-tandem mass spectrometry. Microchemical Journal 145, 1191–1198. https://doi.org/10.1016/j.microc.2018.12.014

Heinisch, S., Rocca, J.L., 2004. Effect of mobile phase composition, pH and buffer type on the retention of ionizable compounds in reversed-phase liquid chromatography: Application to method development. J Chromatogr A 1048, 183–193. https://doi.org/10.1016/j.chroma.2004.07.022

Henriksen, T., Juhler, R.K., Svensmark, B., Cech, N.B., 2005. The relative influences of acidity and polarity on responsiveness of small organic molecules to analysis with negative ion electrospray ionization mass spectrometry (ESI-MS). J Am Soc Mass Spectrom 16, 446–455. https://doi.org/10.1016/j.jasms.2004.11.021

Henry, H., Sobhi, H.R., Scheibner, O., Bromirski, M., Nimkar, S.B., Rochat, B., 2012. Comparison between a high-resolution single-stage Orbitrap and a triple quadrupole mass spectrometer for quantitative analyses of drugs. Rapid Communications in Mass Spectrometry 26, 499–509. https://doi.org/10.1002/rcm.6121

Hillis, D.G., Fletcher, J., Solomon, K.R., Sibley, P.K., 2011. Effects of ten antibiotics on seed germination and root elongation in three plant species. Arch Environ Contam Toxicol 60, 220–232. https://doi.org/10.1007/s00244-010-9624-0

Hirschmann, F., Krause, F., Papenbrock, J., 2014. The multi-protein family of sulfotransferases in plants: Composition, occurrence, substrate specificity, and functions. Front Plant Sci 5, 1–13. https://doi.org/10.3389/fpls.2014.00556

Hossain, S.M., Park, M.J., Park, H.J., Tijing, L., Kim, J.H., Shon, H.K., 2019. Preparation and characterization of TiO2 generated from synthetic wastewater using TiCl4 based coagulation/flocculation aided with Ca(OH)2. J Environ Manage 250, 109521. https://doi.org/10.1016/j.jenvman.2019.109521

Hsu, F.C., Marxmiller, R.L., Yang, A.Y.S., 1990. Study of root uptake and xylem translocation of cinmethylin and related compounds in detopped soybean roots using a pressure chamber technique. Plant Physiol 93, 1573–1578. https://doi.org/10.1104/pp.93.4.1573

Huber, C., Preis, M., Harvey, P.J., Grosse, S., Letzel, T., Schröder, P., 2016. Emerging pollutants and plants - Metabolic activation of diclofenac by peroxidases. Chemosphere 146, 435–441. https://doi.org/10.1016/j.chemosphere.2015.12.059

Hung, H.W., Daniel Sheng, G., Lin, T.F., Su, Y., Chiou, C.T., 2009. The organic contamination level based on the total soil mass is not a proper index of the soil contamination intensity. Environmental Pollution 157, 2928–2932. https://doi.org/10.1016/j.envpol.2009.07.007

Hurtado, C., Cañameras, N., Domínguez, C., Price, G.W., Comas, J., Bayona, J.M., 2017. Effect of soil biochar concentration on the mitigation of emerging organic contaminant uptake in lettuce. J Hazard Mater 323, 386–393. https://doi.org/10.1016/j.jhazmat.2016.04.046

Hurtado, C., Domínguez, C., Pérez-Babace, L., Cañameras, N., Comas, J., Bayona, J.M., 2016. Estimate of uptake and translocation of emerging organic contaminants from irrigation water concentration in lettuce grown under controlled conditions. J Hazard Mater 305, 139–148. https://doi.org/10.1016/J.JHAZMAT.2015.11.039

ICH, 1995. Validation of Analytical Procedures: Text and Methodology, in: ICH Steering Comittee. p. 278.

Ilias, A., Panoras, A., Angelakis, A., 2014. Wastewater Recycling in Greece: The Case of Thessaloniki. Sustainability 6, 2876–2892. https://doi.org/10.3390/su6052876

Jain, S., Kumar, P., Vyas, R.K., Pandit, P., Dalai, A.K., 2013. Occurrence and removal of antiviral drugs in environment: A review. Water Air Soil Pollut 224. https://doi.org/10.1007/s11270-012-1410-3

Jaramillo, F., Restrepo, I., 2017. Wastewater reuse in agriculture: A review about its limitations and benefits. Sustainability (Switzerland) 9. https://doi.org/10.3390/su9101734

Jia, W., Chu, X., Chang, J., Wang, P.G., Chen, Y., Zhang, F., 2017. High-throughput untargeted screening of veterinary drug residues and metabolites in tilapia using high resolution orbitrap mass spectrometry. Anal Chim Acta 957, 29–39. https://doi.org/10.1016/j.aca.2016.12.038

Jin Yang, X., Qu, Y., Yuan, Q., Wan, P., Du, Z., Chen, D., Wong, C., 2013. Effect of ammonium on liquid- and gas-phase protonation and deprotonation in electrospray ionization mass spectrometry. Analyst 138, 659–665. https://doi.org/10.1039/c2an36022e

Jueschke, E., Marschner, B., Tarchitzky, J., Chen, Y., 2008. Effects of treated wastewater irrigation on the dissolved and soil organic carbon in Israeli soils. Water Science and Technology 57, 727–733. https://doi.org/10.2166/WST.2008.173

Kalli, A., Smith, G.T., Sweredoski, M., Hess, S., 2008. Evaluation and Optimization of Mass Spectrometric Settings during Data-Dependent Acquisition Mode: Focus on LTQOrbitrap Mass Analyzers. J Proteome Res. 12, 3071–3086. https://doi.org/10.1021/pr3011588

Kamel, A.M., Brown, P.R., Munson, B., 1999. Effects of mobile-phase additives, solution pH, ionization constant, and analyte concentration on the sensitivities and electrospray ionization mass spectra of nucleoside antiviral agents. Anal Chem 71, 5481–5492. https://doi.org/10.1021/ac9906429

Karnjanapiboonwong, A., Morse, A.N., Maul, J.D., Anderson, T.A., 2010. Sorption of estrogens, triclosan, and caffeine in a sandy loam and a silt loam soil. J Soils Sediments 10, 1300–1307. https://doi.org/10.1007/s11368-010-0223-5

Kasprzyk-Hordern, B., Dinsdale, R.M., Guwy, A.J., 2008. The occurrence of pharmaceuticals, personal care products, endocrine disruptors and illicit drugs in surface water in South Wales, UK. Water Res 42, 3498–3518. https://doi.org/10.1016/j.watres.2008.04.026

Kebede, T.G., Seroto, M.B., Chokwe, R.C., Dube, S., Nindi, M.M., 2020. Adsorption of antiretroviral (ARVs) and related drugs from environmental wastewaters using nanofibers. J Environ Chem Eng 8, 104049. https://doi.org/10.1016/j.jece.2020.104049

Keerthanan, S., Jayasinghe, C., Biswas, J.K., Vithanage, M., 2021. Pharmaceutical and Personal Care Products (PPCPs) in the environment: Plant uptake, translocation, bioaccumulation, and human health risks. Crit Rev Environ Sci Technol 51, 1221–1258. https://doi.org/10.1080/10643389.2020.1753634

Kim, S.H., Ngo, H.H., Chaudhary, D., Kim, J.C., Vigneswaran, S., Moon, H., 2002. Characterization procedure for adsorption of DOC (Dissolved Organic Carbon) from synthetic wastewater. Korean Journal of Chemical Engineering 19, 888–894. https://doi.org/10.1007/BF02706985

Kind, T., Fiehn, O., 2006. Metabolomic database annotations via query of elemental compositions: Mass accuracy is insufficient even at less than 1 ppm. BMC Bioinformatics 7, 1–10. https://doi.org/10.1186/1471-2105-7-234

King, D.H., 1988. History, pharmacokinetics, and pharmacology of acyclovir. J Am Acad Dermatol 18, 176–179. https://doi.org/10.1016/S0190-9622(88)70022-5

Klampfl, C.W., 2019. Metabolization of pharmaceuticals by plants after uptake from water and soil: A review. TrAC - Trends in Analytical Chemistry 111, 13–26. https://doi.org/10.1016/j.trac.2018.11.042

Kodešová, R., Grabic, R., Kočárek, M., Klement, A., Golovko, O., Fér, M., Nikodem, A., Jakšík, O., 2015. Pharmaceuticals' sorptions relative to properties of thirteen different soils. Science of the Total Environment 511, 435–443. https://doi.org/10.1016/j.scitotenv.2014.12.088

Kodešová, R., Klement, A., Golovko, O., Fér, M., Nikodem, A., Kočárek, M., Grabic, R., 2019. Root uptake of atenolol, sulfamethoxazole and carbamazepine, and their transformation in three soils and four plants. Environmental Science and Pollution Research 26, 9876–9891. https://doi.org/10.1007/s11356-019-04333-9

K'oreje, K.O., Kandie, F.J., Vergeynst, L., Abira, M.A., Van Langenhove, H., Okoth, M., Demeestere, K., 2018a. Occurrence, fate and removal of pharmaceuticals, personal care products and pesticides in wastewater stabilization ponds and receiving rivers in the Nzoia Basin, Kenya. Science of the Total Environment 637–638, 336–348. https://doi.org/10.1016/j.scitotenv.2018.04.331

K'oreje, K.O., Kandie, F.J., Vergeynst, L., Abira, M.A., Van Langenhove, H., Okoth, M., Demeestere, K., 2018b. Occurrence, fate and removal of pharmaceuticals, personal care products and pesticides in wastewater stabilization ponds and receiving rivers in the Nzoia Basin, Kenya. Science of the Total Environment 637–638, 336–348. https://doi.org/10.1016/j.scitotenv.2018.04.331

Kosjek, T., Heath, E., Kompare, B., 2007. Removal of pharmaceutical residues in a pilot wastewater treatment plant. Anal Bioanal Chem 387, 1379–1387. https://doi.org/10.1007/s00216-006-0969-1

Kruve, A., Kaupmees, K., 2017. Adduct Formation in ESI/MS by Mobile Phase Additives. J Am Soc Mass Spectrom 28, 887–894. https://doi.org/10.1007/s13361-017-1626-y

Kruve, A., Rebane, R., Kipper, K., Oldekop, M.L., Evard, H., Herodes, K., Ravio, P., Leito, I., 2015. Tutorial review on validation of liquid chromatography-mass spectrometry methods: Part II. Anal Chim Acta 870, 8–28. https://doi.org/10.1016/j.aca.2015.02.016

Kuchař, L., Asfaw, B., Rybová, J., Ledvinová, J., 2016. Tandem Mass Spectrometry of Sphingolipids: Applications for Diagnosis of Sphingolipidoses. Adv Clin Chem 77, 177–219. https://doi.org/10.1016/BS.ACC.2016.06.004

Kumar, A., Prasad, B., Mishra, I.M., 2008. Adsorptive removal of acrylonitrile by commercial grade activated carbon: Kinetics, equilibrium and thermodynamics. J Hazard Mater 152, 589–600. https://doi.org/10.1016/j.jhazmat.2007.07.048

Kumar, K., Gupta, S.C., 2016. A framework to predict uptake of trace organic compounds by plants. J Environ Qual 45, 555–564. https://doi.org/10.2134/jeq2015.06.0261

Kuppusamy, S., Kakarla, D., Venkateswarlu, K., Megharaj, M., Yoon, Y.E., Lee, Y.B., 2018. Veterinary antibiotics (VAs) contamination as a global agro-ecological issue: A critical view. Agric Ecosyst Environ 257, 47–59. https://doi.org/10.1016/j.agee.2018.01.026

Kurwadkar, S.T., Adams, C.D., Meyer, M.T., Kolpin, D.W., 2011. Comparative mobility of sulfonamides and bromide tracer in three soils. J Environ Manage 92, 1874–1881. https://doi.org/10.1016/J.JENVMAN.2011.03.018

LandIS, 2021. LandIS - Land Information System - Tools and utilities [WWW Document]. URL http://www.landis.org.uk/services/tools.cfm (accessed 3.6.22).

LCGC, 2016. Chromatography and Sample Preparation Terminology Guide Supplement [WWW Document]. LCGC Europe. URL https://www.chromatographyonline.com/view/magnetic-nanoparticles-solid-phase-extraction (accessed 5.9.22).

Lead, J.R., Wilkinson, K.J., 2006. Aquatic Colloids and Nanoparticles: Current Knowledge and Future Trends. Environ. Chem 3, 159–171. https://doi.org/10.1071/EN06025

Leen, C., Bulteel, N., 2019. Current Antiretroviral Therapies and Future Trends in Management of Human Immunodeficiency Virus-1 Infection 41, 5–11. https://doi.org/10.14744/etd.2019.19210

Lees, K.E., 2018. The sorption fate of active pharmaceutical ingredients in soils receiving high wastwater inputs and implications for risk assessments. University of Plymouth.

LeFevre, G.H., Müller, C.E., Li, R.J., Luthy, R.G., Sattely, E.S., 2015. Rapid Phytotransformation of Benzotriazole Generates Synthetic Tryptophan and Auxin Analogs in Arabidopsis. Environ Sci Technol 49, 10959–10968. https://doi.org/10.1021/acs.est.5b02749

Legind, C.N., Trapp, S., 2009. Modeling the exposure of children and adults via diet to chemicals in the environment with crop-specific models. Environmental Pollution 157, 778–785. https://doi.org/10.1016/j.envpol.2008.11.021

Li, J., Carter, L.J., Boxall, A.B.A., 2020. Evaluation and development of models for estimating the sorption behaviour of pharmaceuticals in soils. J Hazard Mater 392, 122469. https://doi.org/10.1016/j.jhazmat.2020.122469

Li, J., Jiang, Y., Li, D., 2019. Determination of imidacloprid and its relevant metabolites in tomato using modified QuEChERS combined with ultrahigh-pressure liquid chromatography/Orbitrap tandem mass spectrometry. J Sci Food Agric 99, 5211–5218. https://doi.org/10.1002/jsfa.9769

Li, S., Tian, M., Row, K.H., 2010. Effect of mobile phase additives on the resolution of four bioactive compounds by RP-HPLC. Int J Mol Sci 11, 2229–2240. https://doi.org/10.3390/ijms11052229

Li, Y., Sallach, J.B., Zhang, W., Boyd, S.A., Li, H., 2019a. Insight into the distribution of pharmaceuticals in soil-water-plant systems. Water Res 152, 38–46. https://doi.org/10.1016/j.watres.2018.12.039

Li, Y., Sallach, J.B., Zhang, W., Boyd, S.A., Li, H., 2019b. Insight into the distribution of pharmaceuticals in soil-water-plant systems. Water Res 152, 38–46. https://doi.org/10.1016/j.watres.2018.12.039

Lin, A.Y.C., Lin, C.A., Tung, H.H., Chary, N.S., 2010. Potential for biodegradation and sorption of acetaminophen, caffeine, propranolol and acebutolol in lab-scale aqueous environments. J Hazard Mater 183, 242–250. https://doi.org/10.1016/j.jhazmat.2010.07.017

Lindegårdh, N., Hanpithakpong, W., Wattanagoon, Y., Singhasivanon, P., White, N.J., Day, N.P.J., 2007. Development and validation of a liquid chromatographic–tandem mass spectrometric method for determination of oseltamivir and its metabolite oseltamivir carboxylate in plasma, saliva and urine. Journal of Chromatography B 859, 74–83. https://doi.org/10.1016/J.JCHROMB.2007.09.018

Liu, L., Liu, Y.H., Liu, C.X., Wang, Z., Dong, J., Zhu, G.F., Huang, X., 2013. Potential effect and accumulation of veterinary antibiotics in Phragmites australis under hydroponic conditions. Ecol Eng 53, 138–143. https://doi.org/10.1016/j.ecoleng.2012.12.033

Lucas, D., Castellet-Rovira, F., Villagrasa, M., Badia-Fabregat, M., Barceló, D., Vicent, T., Caminal, G., Sarrà, M., Rodríguez-Mozaz, S., 2018. The role of sorption processes in the removal of pharmaceuticals by fungal treatment of wastewater. Science of the Total Environment 610–611, 1147–1153. https://doi.org/10.1016/j.scitotenv.2017.08.118

Lupo, S., Kahler, T., 2017. New Advice on an Old Topic: Buffers in Reversed-Phase HPLC. LCGC Europe 30, 362–371.

MacHerius, A., Eggen, T., Lorenz, W., Moeder, M., Ondruschka, J., Reemtsma, T., 2012. Metabolization of the bacteriostatic agent triclosan in edible plants and its consequences for plant uptake assessment. Environ Sci Technol 46, 10797–10804. https://doi.org/10.1021/es3028378

Madikizela, L.M., Ncube, S., Chimuka, L., 2020. Analysis, occurrence and removal of pharmaceuticals in African water resources: A current status. J Environ Manage 253, 109741. https://doi.org/10.1016/j.jenvman.2019.109741

Madikizela, L.M., Tavengwa, N.T., Chimuka, L., 2017. Status of pharmaceuticals in African water bodies: Occurrence, removal and analytical methods. J Environ Manage 193, 211–220. https://doi.org/10.1016/J.JENVMAN.2017.02.022

Manasfi, R., Brienza, M., Ait-Mouheb, N., Montemurro, N., Perez, S., Chiron, S., 2021. Impact of long-term irrigation with municipal reclaimed wastewater on the uptake and degradation of organic contaminants in lettuce and leek. Science of the Total Environment 765. https://doi.org/10.1016/j.scitotenv.2020.142742

Maoz, A., Chefetz, B., 2010. Sorption of the pharmaceuticals carbamazepine and naproxen to dissolved organic matter: Role of structural fractions. Water Res 44, 981–989. https://doi.org/10.1016/j.watres.2009.10.019

Marques, R.Z., Wistuba, N., Brito, J.C.M., Bernardoni, V., Rocha, D.C., Gomes, M.P., 2021. Crop irrigation (soybean, bean, and corn) with enrofloxacin-contaminated water leads to yield reductions and antibiotic accumulation. Ecotoxicol Environ Saf 216. https://doi.org/10.1016/j.ecoenv.2021.112193

Martínez-Hernández, V., Meffe, R., Herrera, S., Arranz, E., de Bustamante, I., 2014. Sorption/desorption of non-hydrophobic and ionisable pharmaceutical and personal care products from reclaimed water onto/from a natural sediment. Science of the Total Environment 472, 273–281. https://doi.org/10.1016/j.scitotenv.2013.11.036

Maskaoui, K., Zhou, J., 2010. Colloids as a sink for certain pharmaceuticals in the aquatic environment. Environ Sci Pollut Res 17, 898–907.

McCalley, D.V., 1996. Effect of organic solvent modifier and nature of solute on the performance of bonded silica reversed-phase columns for the analysis of strongly basic compounds by high-performance liquid chromatography. J Chromatogr A 738, 169–179. https://doi.org/10.1016/0021-9673(96)00136-7

McCalley, D. V., 2010a. The challenges of the analysis of basic compounds by high performance liquid chromatography: Some possible approaches for improved separations. J Chromatogr A 1217, 858–880. https://doi.org/10.1016/j.chroma.2009.11.068

McCalley, D. V., 2010b. The challenges of the analysis of basic compounds by high performance liquid chromatography: Some possible approaches for improved separations. J Chromatogr A. https://doi.org/10.1016/j.chroma.2009.11.068

McKone, T.E., Maddalena, R.L., 2007. Plant uptake of organic pollutants from soil: Bioconcentration estimates based on models and experiments. Environ Toxicol Chem 26, 2494–2504. https://doi.org/10.1897/06-269.1

Mecha, A.C., Onyango, M.S., Ochieng, A., Fourie, C.J.S., Momba, M.N.B., 2016. Synergistic effect of UV–vis and solar photocatalytic ozonation on the degradation of phenol in municipal wastewater: A comparative study. J Catal 341, 116–125. https://doi.org/10.1016/j.jcat.2016.06.015

Michael-Kordatou, I., Michael, C., Duan, X., He, X., Dionysiou, D.D., Mills, M.A., Fatta-Kassinos, D., 2015. Dissolved effluent organic matter: Characteristics and potential implications in wastewater treatment and reuse applications. Water Res 77, 213–248. https://doi.org/10.1016/j.watres.2015.03.011

Miller, E.L., Nason, S.L., Karthikeyan, K.G., Pedersen, J.A., 2015. Root Uptake of Pharmaceuticals and Personal Care Product Ingredients. https://doi.org/10.1021/acs.est.5b01546

Mira, Petrović; Susana, Gonzalez; Damià, B., 2003. Analysis and removal of emerging contaminants in wastewater and drinking water. Trac-Trends in Analytical Chemistry 22, 685–696.

Mlunguza, N.Y., Ncube, S., Mahlambi, P.N., Chimuka, L., Madikizela, L.M., 2020a. Determination of selected antiretroviral drugs in wastewater, surface water and aquatic plants using hollow fibre liquid phase microextraction and liquid chromatography - tandem mass spectrometry. J Hazard Mater 382, 121067. https://doi.org/10.1016/j.jhazmat.2019.121067

Mlunguza, N.Y., Ncube, S., Mahlambi, P.N., Chimuka, L., Madikizela, L.M., 2020b. Determination of selected antiretroviral drugs in wastewater, surface water and aquatic plants using hollow fibre liquid phase microextraction and liquid chromatography - tandem mass spectrometry. J Hazard Mater 382, 121067. https://doi.org/10.1016/j.jhazmat.2019.121067

Mohan, S.V., Karthikeyan, J., 1997. Removal of lignin and tannin colour from aqueous solution by adsorption onto activated charcoal. Environmental Pollution 97, 183–187. https://doi.org/10.1016/S0269-7491(97)00025-0

Monaci, L., Losito, I., Palmisano, F., Godula, M., Visconti, A., 2011. Towards the quantification of residual milk allergens in caseinate-fined white wines using HPLC coupled with single-stage Orbitrap mass spectrometry. Food Addit Contam Part A Chem Anal Control Expo Risk Assess 28, 1304–1314. https://doi.org/10.1080/19440049.2011.593191

Moreno-Jiménez, E., Beesley, L., Lepp, N.W., Dickinson, N.M., Hartley, W., Clemente, R., 2011. Field sampling of soil pore water to evaluate trace element mobility and

associated environmental risk. Environmental Pollution 159, 3078–3085. https://doi.org/10.1016/j.envpol.2011.04.004

Moschet, C., Piazzoli, A., Singer, H., Hollender, J., 2013. Alleviating the reference standard dilemma using a systematic exact mass suspect screening approach with liquid chromatography-high resolution mass spectrometry. Anal Chem 85, 10312–10320. https://doi.org/10.1021/ac4021598

Mosekiemang, T.T., Stander, M.A., de Villiers, A., 2019a. Simultaneous quantification of commonly prescribed antiretroviral drugs and their selected metabolites in aqueous environmental samples by direct injection and solid phase extraction liquid chromatography - tandem mass spectrometry. Chemosphere 220, 983–992. https://doi.org/10.1016/j.chemosphere.2018.12.205

Mosekiemang, T.T., Stander, M.A., de Villiers, A., 2019b. Simultaneous quantification of commonly prescribed antiretroviral drugs and their selected metabolites in aqueous environmental samples by direct injection and solid phase extraction liquid chromatography - tandem mass spectrometry. Chemosphere 220, 983–992. https://doi.org/10.1016/J.CHEMOSPHERE.2018.12.205

Mu, P., Xu, N., Chai, T., Jia, Q., Yin, Z., Yang, S., Qian, Y., Qiu, J., 2016. Simultaneous determination of 14 antiviral drugs and relevant metabolites in chicken muscle by UPLC-MS/MS after QuEChERS preparation. J Chromatogr B Analyt Technol Biomed Life Sci 1023–1024, 17–23. https://doi.org/10.1016/j.jchromb.2016.04.036

Müller, K., Magesan, G.N., Bolan, N.S., 2007. A critical review of the influence of effluent irrigation on the fate of pesticides in soil. Agric Ecosyst Environ 120, 93–116. https://doi.org/10.1016/j.agee.2006.08.016

Nakagawa, F., May, M., Phillips, A., 2013. Life expectancy living with HIV: Recent estimates and future implications. Curr Opin Infect Dis 26, 17–25. https://doi.org/10.1097/QCO.0b013e32835ba6b1

Nason, S.L., Miller, E.L., Karthikeyan, K.G., Pedersen, J.A., 2019. Effects of Binary Mixtures and Transpiration on Accumulation of Pharmaceuticals by Spinach. Environ Sci Technol 53, 4850–4859. https://doi.org/10.1021/acs.est.8b05515

Neuman, J., 2017. Soil Organic Matter Maintenance in No-Till and Crop Rotation Management Systems. Reference Module in Earth Systems and Environmental Sciences. https://doi.org/10.1016/B978-0-12-409548-9.10653-0

Ngumba, E., Gachanja, A., Nyirenda, J., Maldonado, J., Tuhkanen, T., 2020. Occurrence of antibiotics and antiretroviral drugs in source-separated urine, groundwater, surface water and wastewater in the peri-urban area of chunga in lusaka, Zambia. Water SA 46, 278–284. https://doi.org/10.17159/wsa/2020.v46.i2.8243

Nie, M., Yang, Y., Liu, M., Yan, C., Shi, H., Dong, W., Zhou, J.L., 2014. Environmental estrogens in a drinking water reservoir area in Shanghai: Occurrence, colloidal

contribution and risk assessment. Science of the Total Environment 487, 785–791. https://doi.org/10.1016/j.scitotenv.2013.12.010

Notter, J., Bregenzer, A., Vernazza, P., Kahlert, C.R., 2019. Nevirapine in HIV maintenance therapy - can "old drugs" survive in current HIV management? Swiss Med Wkly 149, w20053. https://doi.org/10.4414/smw.2019.20053

OECD, 2000. Adsorption - Desorption Using a Batch Equilibrium Method. OECD guidline for the testing of chemicals.

O'Flaherty, E., Gray, N.F., 2013. A comparative analysis of the characteristics of a range of real and synthetic wastewaters. Environmental Science and Pollution Research 20, 8813–8830. https://doi.org/10.1007/s11356-013-1863-y

Ofori, S., Puškáčová, A., Růžičková, I., Wanner, J., 2021. Treated wastewater reuse for irrigation: Pros and cons. Science of the Total Environment 760. https://doi.org/10.1016/j.scitotenv.2020.144026

Olabode, G.S., 2021. Spectroscopic and Chromatographic Analysis of Nevirapine , Lamivudine and Zidovudine Anti-Retroviral Compounds in Wastewater Samples from Selected Wastewater Treatment Plants , Cape Town Gbolahan Sunday Olabode. Cape Peninsula University of Technology.

Olsen, J. V, Macek, B., Lange, O., Makarov, A., Horning, S., 2007. Higher-energy C-trap dissociation for peptide modification analysis. Nat Methods 4, 709–712. https://doi.org/10.1038/nmeth1060

Oron, G., Adel, M., Agmon, V., Friedler, E., Halperin, R., Leshem, E., Weinberg, D., 2014. Greywater use in Israel and worldwide: Standards and prospects. Water Res 58, 92–101. https://doi.org/10.1016/j.watres.2014.03.032

Page, J.S., Kelly, R.T., Tang, K., Smith, R.D., 2007. Ionization and Transmission Efficiency in an Electrospray Ionization-Mass Spectrometry Interface. J Am Soc Mass Spectrom 18, 1582–1590. https://doi.org/10.1016/j.jasms.2007.05.018

Paltiel, O., Fedorova, G., Tadmor, G., Kleinstern, G., Maor, Y., Chefetz, B., 2016. Human Exposure to Wastewater-Derived Pharmaceuticals in Fresh Produce: A Randomized Controlled Trial Focusing on Carbamazepine. Environ Sci Technol 50, 4476–4482. https://doi.org/10.1021/acs.est.5b06256

Pan, B., Ning, P., Xing, B., 2009. Part V - Sorption of pharmaceuticals and personal care products. Environmental Science and Pollution Research 16, 106–116. https://doi.org/10.1007/s11356-008-0052-x

Pan, M., Chu, L.M., 2017. Fate of antibiotics in soil and their uptake by edible crops. Science of the Total Environment 599–600, 500–512. https://doi.org/10.1016/j.scitotenv.2017.04.214

Pan, M., Chu, L.M., 2016. Adsorption and degradation of five selected antibiotics in agricultural soil. Science of The Total Environment 545–546, 48–56. https://doi.org/10.1016/J.SCITOTENV.2015.12.040

Pan, M., Wong, C.K.C., Chu, L.M., 2014. Distribution of antibiotics in wastewater-irrigated soils and their accumulation in vegetable crops in the Pearl River Delta, Southern China. J Agric Food Chem 62. https://doi.org/10.1021/jf503850v

Pápai, Z., Pap, T.L., 2002. Analysis of peak asymmetry in chromatography. J Chromatogr A 953, 31–38. https://doi.org/10.1016/S0021-9673(02)00121-8

Patel, S.H., Ismaiel, O.A., Mylott, W.R., Yuan, M., Hauser, K.F., McRae, M.P., 2019. Simultaneous determination of intracellular concentrations of tenofovir, emtricitabine, and dolutegravir in human brain microvascular endothelial cells using liquid chromatography-tandem mass spectrometry (LC-MS/MS). Anal Chim Acta 1056, 79–87. https://doi.org/10.1016/j.aca.2019.01.015

Paz, A., Tadmor, G., Malchi, T., Blotevogel, J., Borch, T., Polubesova, T., Chefetz, B., 2016a. Fate of carbamazepine, its metabolites, and lamotrigine in soils irrigated with reclaimed wastewater: Sorption, leaching and plant uptake. Chemosphere 160, 22–29. https://doi.org/10.1016/j.chemosphere.2016.06.048

Paz, A., Tadmor, G., Malchi, T., Blotevogel, J., Borch, T., Polubesova, T., Chefetz, B., 2016b. Fate of carbamazepine, its metabolites, and lamotrigine in soils irrigated with reclaimed wastewater: Sorption, leaching and plant uptake. Chemosphere 160, 22–29. https://doi.org/10.1016/j.chemosphere.2016.06.048

Peña, A., Delgado-Moreno, L., Rodríguez-Liébana, J.A., 2020. A review of the impact of wastewater on the fate of pesticides in soils: Effect of some soil and solution properties. Science of the Total Environment 718, 134468. https://doi.org/10.1016/j.scitotenv.2019.134468

Penchala, S.D., Fawcett, S., Else, L., Egan, D., Amara, A., Elliot, E., Challenger, E., Back, D., Boffito, M., Khoo, S., 2016. The development and application of a novel LC-MS/MS method for the measurement of Dolutegravir, Elvitegravir and Cobicistat in human plasma. J Chromatogr B Analyt Technol Biomed Life Sci 1027, 174–180. https://doi.org/10.1016/j.jchromb.2016.05.040

Peng, X., Wang, C., Zhang, K., Wang, Z., Huang, Q., Yu, Y., Ou, W., 2014. Profile and behavior of antiviral drugs in aquatic environments of the Pearl River Delta, China. Science of The Total Environment 466–467, 755–761. https://doi.org/10.1016/J.SCITOTENV.2013.07.062

Petruzzelli, G., Pedron, F., 2020. Adsorption, desorption and bioavailability of tungstate in mediterranean soils. Soil Syst 4, 1–16. https://doi.org/10.3390/soilsystems4030053

Picó, Y., Alvarez-Ruiz, R., Alfarhan, A.H., El-Sheikh, M.A., Alobaid, S.M., Barceló, D., 2019. Uptake and accumulation of emerging contaminants in soil and plant treated with

wastewater under real-world environmental conditions in the Al Hayer area (Saudi Arabia). Science of the Total Environment 652, 562–572. https://doi.org/10.1016/j.scitotenv.2018.10.224

Pourfarzib, M., Dinarvand, R., Akbari-Adergani, B., Mehramizi, A., Rastegar, H., Shekarchi, M., 2015. Water-compatible molecularly imprinted polymer as a sorbent for the selective extraction and purification of adefovir from human serum and urine. J Sep Sci 38, 1755–1762. https://doi.org/10.1002/jssc.201401492

Prasse, C., Schlüsener, M.P., Schulz, R., Ternes, T.A., 2010. Antiviral Drugs in Wastewater and Surface Waters: A New Pharmaceutical Class of Environmental Relevance? Environ Sci Technol 44, 1728–1735. https://doi.org/10.1021/es903216p

Prosser, R.S., Lissemore, L., Topp, E., Sibley, P.K., 2014a. Bioaccumulation of triclosan and triclocarban in plants grown in soils amended with municipal dewatered biosolids. Environ Toxicol Chem 33, 975–984. https://doi.org/10.1002/etc.2505

Prosser, R.S., Trapp, S., Sibley, P.K., 2014b. Modeling Uptake of Selected Pharmaceuticals and Personal Care Products into Food Crops from Biosolids-Amended Soil. Environ Sci Technol 48, 11397–11404. https://doi.org/10.1021/es503067v

Pullagurala, V.L.R., Rawat, S., Adisa, I.O., Hernandez-Viezcas, J.A., Peralta-Videa, J.R., Gardea-Torresdey, J.L., 2018. Plant uptake and translocation of contaminants of emerging concern in soil. Science of the Total Environment 636, 1585–1596. https://doi.org/10.1016/j.scitotenv.2018.04.375

Qin, Q., Chen, X., Zhuang, J., 2015. The fate and impact of pharmaceuticals and personal care products in agricultural soils irrigated with reclaimed water. Crit Rev Environ Sci Technol 45, 1379–1408. https://doi.org/10.1080/10643389.2014.955628

Rainville, P.D., Smith, N.W., Cowan, D., Plumb, R.S., 2012. Comprehensive investigation of the influence of acidic, basic, and organic mobile phase compositions on bioanalytical assay sensitivity in positive ESI mode LC/MS/MS. J Pharm Biomed Anal 59, 138–150. https://doi.org/10.1016/j.jpba.2011.10.021

Rede, D., Santos, L.H.M.L.M., Ramos, S., Oliva-Teles, F., Antão, C., Sousa, S.R., Delerue-Matos, C., 2019. Individual and mixture toxicity evaluation of three pharmaceuticals to the germination and growth of Lactuca sativa seeds. Science of the Total Environment 673, 102–109. https://doi.org/10.1016/j.scitotenv.2019.03.432

Reichl, B., Himmelsbach, M., Emhofer, L., Klampfl, C.W., Buchberger, W., 2018. Uptake and metabolism of the antidepressants sertraline, clomipramine, and trazodone in a garden cress (Lepidium sativum) model. Electrophoresis 39, 1301–1308. https://doi.org/10.1002/elps.201700482

Research, U. water I., 2019. Water Research Reports Publications [WWW Document]. URL https://ukwir.org/eng/water-research-reports-publications (accessed 7.29.21).

Riemenschneider, C., Seiwert, B., Moeder, M., Schwarz, D., Reemtsma, T., 2017. Extensive Transformation of the Pharmaceutical Carbamazepine Following Uptake into Intact Tomato Plants. Environ Sci Technol 51, 6100–6109. https://doi.org/10.1021/acs.est.6b06485

Rimayi, C., Odusanya, D., Weiss, J.M., de Boer, J., Chimuka, L., 2018. Contaminants of emerging concern in the Hartbeespoort Dam catchment and the uMngeni River estuary 2016 pollution incident, South Africa. Science of The Total Environment 627, 1008–1017. https://doi.org/10.1016/J.SCITOTENV.2018.01.263

Rodriguez-Eugenio, N., McLaughlin, M., Pencock, D., 2018. Soil Pollution: a hidden reality, FAO. https://doi.org/10.5124/jkma.1998.41.10.1032

Rogers, H.R., 1996. Sources, behaviour and fate of organic contaminants during sewage treatment and in sewage sludges. Science of the Total Environment 185, 3–26. https://doi.org/10.1016/0048-9697(96)05039-5

Ros, O., Vallejo, A., Olivares, M., Etxebarria, N., Prieto, A., 2016. Determination of endocrine disrupting compounds in fish liver, brain, and muscle using focused ultrasound solid–liquid extraction and dispersive solid phase extraction as clean-up strategy. Anal Bioanal Chem 408, 5689–5700. https://doi.org/10.1007/s00216-016-9697-3

Rowell D L, 1994. Soil science: Methods & applications. John Wiley & Sons, Ltd. https://doi.org/10.1002/JSFA.2740660423

Ruta, J., Boccard, J., Cabooter, D., Rudaz, S., Desmet, G., Veuthey, J.L., Guillarme, D., 2012. Method development for pharmaceutics: Some solutions for tuning selectivity in reversed phase and hydrophilic interaction liquid chromatography. J Pharm Biomed Anal 63, 95–105. https://doi.org/10.1016/j.jpba.2012.01.019

Rwagitinywa, J., Sommet, A., Palmaro, A., Montastruc, J.-L., Lapeyre-Mestre, M., 2018. Utilization and costs of HIV antiretroviral drugs in Europe during the last ten years: Impact of generic antiretroviral drugs on cost reduction. Health Policy (New York) 122, 237–242. https://doi.org/10.1016/j.healthpol.2018.01.002

Sabljic, A., GUsten, H., Verhaar, H., Hermens, J., 1994. QSAR MODELLING OF SOIL SORPTION. IMPROVEMENTS AND SYSTEMATICS OF log K, vs. log Kow CORRELATIONS. Chemosphere 31, 4489–4514.

Saccà, M.L., Accinelli, C., Fick, J., Lindberg, R., Olsen, B., 2009. Environmental fate of the antiviral drug Tamiflu in two aquatic ecosystems. Chemosphere 75, 28–33. https://doi.org/10.1016/j.chemosphere.2008.11.060

Saito-Shida, S., Hamasaka, T., Nemoto, S., Akiyama, H., 2018. Multiresidue determination of pesticides in tea by liquid chromatography-high-resolution mass spectrometry: Comparison between Orbitrap and time-of-flight mass analyzers. Food Chem 256, 140–148. https://doi.org/10.1016/j.foodchem.2018.02.123

Sallach, J.B., Bartelt-Hunt, S.L., Snow, D.D., Li, X., Hodges, L., 2018. Uptake of antibiotics and their toxicity to lettuce following routine irrigation with contaminated water in different soil types. Environ Eng Sci 35, 887–896. https://doi.org/10.1089/ees.2017.0376

SANTE/11813/2017, 2018. ANALYTICAL QUALITY CONTROL AND METHOD VALIDATION PROCEDURES FOR PESTICIDE RESIDUES ANALYSIS.

Santiago, S., Roll, D.M., Ray, C., Williams, C., Moravcik, P., Knopf, A., 2016. Effects of soil moisture depletion on vegetable crop uptake of pharmaceuticals and personal care products (PPCPs). Environmental Science and Pollution Research 23, 20257–20268. https://doi.org/10.1007/s11356-016-7194-z

Sauvêtre, A., May, R., Harpaintner, R., Poschenrieder, C., Schröder, P., 2018. Metabolism of carbamazepine in plant roots and endophytic rhizobacteria isolated from Phragmites australis. J Hazard Mater 342, 85–95. https://doi.org/10.1016/j.jhazmat.2017.08.006

Schaffer, M., Boxberger, N., Börnick, H., Licha, T., Worch, E., 2012. Sorption influenced transport of ionizable pharmaceuticals onto a natural sandy aquifer sediment at different pH. Chemosphere 87, 513–520. https://doi.org/10.1016/J.CHEMOSPHERE.2011.12.053

Schantz, M.M., 2006. Pressurized liquid extraction in environmental analysis. Anal Bioanal Chem 386, 1043–1047. https://doi.org/10.1007/s00216-006-0648-2

Schnoor, J.L., Licht, L.A., McCUTCHEON, S.C., Wolfe, N.L., Carreira, L.H., 1995. Phytoremediation of Organic and Nutrient Contaminants. Environ Sci Technol 29, 318–323. https://doi.org/10.1021/es00007a002

Schoeman, C., Dlamini, M., Okonkwo, O.J., 2017. The impact of a Wastewater Treatment Works in Southern Gauteng, South Africa on efavirenz and nevirapine discharges into the aquatic environment. Emerg Contam 3, 95–106. https://doi.org/10.1016/j.emcon.2017.09.001

Shamshina, J.L., Cojocaru, O.A., Kelley, S.P., Bica, K., Wallace, S.P., Gurau, G., Rogers, R.D., 2017. Acyclovir as an Ionic Liquid Cation or Anion Can Improve Aqueous Solubility. ACS Omega 2, 3483–3493. https://doi.org/10.1021/acsomega.7b00554

Sharma, P., Poustie, A., Verburg, P., Pagilla, K., Yang, Y., Hanigan, D., 2020. Trace organic contaminants in field-scale cultivated alfalfa, soil, and pore water after 10 years of irrigation with reclaimed wastewater. Science of the Total Environment 744, 140698. https://doi.org/10.1016/j.scitotenv.2020.140698

Sheludko, Y., Volk, J., Brandt, W., Warzecha, H., 2020. Expanding the diversity of plant monoterpenoid indole alkaloids employing human cytochrome P450 3A4. ChemBioChem 1–6. https://doi.org/10.1002/cbic.202000020

Shi, Q., Xiong, Y., Kaur, P., Sy, N.D., Gan, J., 2022. Contaminants of emerging concerns in recycled water: Fate and risks in agroecosystems. Science of the Total Environment 814, 152527. https://doi.org/10.1016/j.scitotenv.2021.152527

Shon, H.K., Vigneswaran, S., Snyder, S.A., 2006. Effluent organic matter (EfOM) in wastewater: Constituents, effects, and treatment. Crit Rev Environ Sci Technol. https://doi.org/10.1080/10643380600580011

Sibeko, P., Naicker, D., Mdluli, P.S., Madikizela, L.M., 2019. Naproxen, ibuprofen, and diclofenac residues in river water, sediments and Eichhornia crassipes of Mbokodweni river in South Africa: An initial screening. Environ Forensics 20, 129–138. https://doi.org/10.1080/15275922.2019.1597780

Simiele, M., Ariaudo, A., De Nicolò, A., Favata, F., Ferrante, M., Carcieri, C., Bonora, S., Di Perri, G., D'Avolio, A., 2017. UPLC–MS/MS method for the simultaneous quantification of three new antiretroviral drugs, dolutegravir, elvitegravir and rilpivirine, and other thirteen antiretroviral agents plus cobicistat and ritonavir boosters in human plasma. J Pharm Biomed Anal 138, 223–230. https://doi.org/10.1016/j.jpba.2017.02.002

Singh, L., Bell, T.G., Yousif, M., Kramvis, A., 2019. Response of hepatitis B virus to antiretroviral treatment containing lamivudine in HBsAg-positive and HBsAg-negative HIV-positive South African adults. J Med Virol 91, 758–764. https://doi.org/10.1002/jmv.25375

Sinha, V.R., Monika, Trehan, A., Kumar, M., Singh, S., Bhinge, J.R., 2007. Stress studies on acyclovir. J Chromatogr Sci 45, 319–324. https://doi.org/10.1093/chromsci/45.6.319

Södertröm, H., Järhult, J.D., Olsen, B., Lindberg, R.H., Tanaka, H., Fick, J., 2009. Detection of the antiviral drug Oseltamivir in aquatic environments. PLoS One 4, 6–9. https://doi.org/10.1371/journal.pone.0006064

Stacia R, W.-U., Divina A, N., Lisa, Z., Diana S, A., 2014. Assessing antibiotic sorption in soil: A literature review and new case studies on sulfonamides and macrolides. Chem Cent J. https://doi.org/10.1186/1752-153X-8-5

Steckel, A., Schlosser, G., 2019. An organic chemist's guide to electrospray mass spectrometric structure elucidation. Molecules 24, 1–11. https://doi.org/10.3390/molecules24030611

Straub, J.O., 2017. Combined environmental risk assessment for the antiviral pharmaceuticals ganciclovir and valganciclovir in Europe. Environ Toxicol Chem 36, 2205–2216. https://doi.org/10.1002/etc.3758

Strauch, S., Jantratid, E., Dressman, J.B., Junginger, H.E., Kopp, S., Midha, K.K., Shah, V.P., Stavchansky, S., Barends, D.M., 2011. Biowaiver Monographs for Immediate Release Solid Oral Dosage Forms : Lamivudine 100, 2054–2063. https://doi.org/10.1002/jps

Sun, C., Dudley, S., McGinnis, M., Trumble, J., Gan, J., 2019. Acetaminophen detoxification in cucumber plants via induction of glutathione S-transferases. Science of the Total Environment 649, 431–439. https://doi.org/10.1016/j.scitotenv.2018.08.346

Sun, C., Dudley, S., Trumble, J., Gan, J., 2018. Pharmaceutical and personal care products-induced stress symptoms and detoxification mechanisms in cucumber plants. Environmental Pollution 234, 39–47. https://doi.org/10.1016/j.envpol.2017.11.041

Survival Gardner, 2015. Water Hyacinth – Water Weed or Livestock Feed? | Survival Gardener [WWW Document]. URL https://survivalgardener.com/2015/03/water-hyacinth-water-weed-or-livestock-feed/ (accessed 8.17.22).

Susantakumar, P., Gaur, A., Sharma, P., 2011. Comparative pharmacokinetics, safety and tolerability evaluation of acyclovir ir 800 mg tablet in healthy indian adult volunteers under fasting and non-fasting conditions. J Bioequivalence Bioavailab 3, 128–138. https://doi.org/10.4172/jbb.1000073

Tadić, Đ., Matamoros, V., Bayona, J.M., 2019. Simultaneous determination of multiclass antibiotics and their metabolites in four types of field-grown vegetables. Anal Bioanal Chem 411, 5209–5222. https://doi.org/10.1007/s00216-019-01895-y

Tan, A., Fanaras, J.C., 2019. Use of high-pH (basic/alkaline) mobile phases for LC–MS or LC–MS/MS bioanalysis. Biomedical Chromatography 33, 1–15. https://doi.org/10.1002/bmc.4409

Tasho, R.P., Cho, J.Y., 2016. Veterinary antibiotics in animal waste, its distribution in soil and uptake by plants: A review. Science of The Total Environment 563–564, 366–376. https://doi.org/10.1016/J.SCITOTENV.2016.04.140

Tchobanoglous, G., Burton, F.D., Eddy, M.S., 2003. Wastewater Engineering: Treatment & Re use. Mc Graw Hill, Boston.

Teo, H.L., Wong, L., Liu, Q., Teo, T.L., Lee, T.K., Lee, H.K., 2016. Simple and accurate measurement of carbamazepine in surface water by use of porous membrane-protected micro-solid-phase extraction coupled with isotope dilution mass spectrometry. Anal Chim Acta 912, 49–57. https://doi.org/10.1016/j.aca.2016.01.028

Thestar, 2018. Guidelines on Use of Antiretroviral Drugs for Treating and Preventing HIV in Kenya.

Thiele-Bruhn, S., Seibicke, T., H-R, S., Leinweber, P., 2004. Sorption of Sulfonamide Pharmaceutical Antibiotics on Whole Soils and Particle-Size Fractions. J Environ Qual 1342, 1331–1342.

Thompson, M., Ellison, S.L.R., Fajgelj, A., Willetts, P., Wood, R., 1999. Harmonised guidelines for the use of recovery information in analytical measurement (Technical Report), Pure and Applied Chemistry. https://doi.org/10.1351/pac199971020337

Tian, R., Zhang, R., Uddin, M., Qiao, X., Chen, J., Gu, G., 2019. Uptake and biotransformation of clarithromycin and sulfadiazine in lettuce. Environmental Pollution 247, 1134–1142. https://doi.org/10.1016/j.envpol.2019.02.009

Trapp, S., 2000. Modelling uptake into roots and subsequent translocation of neutral and ionisable organic compounds. Pest Manag Sci 56, 767–778. https://doi.org/10.1002/1526-4998(200009)56:9<767::AID-PS198>3.0.CO;2-Q

Ul'yanovskii, N. V., Kosyakov, D.S., Sypalov, S.A., Varsegov, I.S., Shavrina, I.S., Lebedev, A.T., 2022. Antiviral drug Umifenovir (Arbidol) in municipal wastewater during the COVID-19 pandemic: Estimated levels and transformation. Science of the Total Environment 805, 150380. https://doi.org/10.1016/j.scitotenv.2021.150380

United Nation, 2015. THE 17 GOALS | Sustainable Development [WWW Document]. URL https://sdgs.un.org/goals (accessed 9.5.22).

UNU-INWEH, 2019. UN: Rising reuse of wastewater in forecast but world lacks data on 'massive potential resource' – UNU-INWEH [WWW Document]. United Nations University Institute for Water,Environment and Health. URL https://inweh.unu.edu/un-rising-reuse-of-wastewater-in-forecast-but-world-lacks-data-on-massive-potential-resource/ (accessed 6.2.22).

US Environmental Protection Agency, 2011. Exposure Factors Handbook. U.S. Environmental Protection Agency EPA/600/R-, 1–1466. https://doi.org/EPA/600/R-090/052F

US EPA, 2012. US EPA; Estimation Program Interface (EPI) Suite. Ver 4.1 Nov,2012 [WWW Document]. URL https://www.epa.gov/oppt/exposure/pubs/episuitedl.htm

Vaclavik, L., Krynitsky, A.J., Rader, J.I., 2014. Mass spectrometric analysis of pharmaceutical adulterants in products labeled as botanical dietary supplements or herbal remedies: A review. Anal Bioanal Chem 406, 6767–6790. https://doi.org/10.1007/s00216-014-8159-z

Voisin, A., Thienpont, A., Héroguez, V., 2012. Separation study of organic bases on new polymeric stationary phases under basic conditions. Eur Polym J 48, 228–234. https://doi.org/10.1016/j.eurpolymj.2011.11.007

Von Sperling, M., 2015. Wastewater Characteristics, Treatment and Disposal, Water Intelligence Online. https://doi.org/10.2166/9781780402086

Wang, C., Yu, S., Zhang, Y., Zhang, M., Lv, L., Huang, C., Li, X., Li, J., Zhang, Z., 2019. Viral quasispecies of hepatitis B virus in patients with YMDD mutation and lamivudine resistance may not predict the efficacy of lamivudine/adefovir rescue therapy. Exp Ther Med 2473–2484. https://doi.org/10.3892/etm.2019.7255

Wang, W.L., Wu, Q.Y., Wang, Z.M., Niu, L.X., Wang, C., Sun, M.C., Hu, H.Y., 2015. Adsorption removal of antiviral drug oseltamivir and its metabolite oseltamivir carboxylate by

carbon nanotubes: Effects of carbon nanotube properties and media. J Environ Manage 162, 326–333. https://doi.org/10.1016/j.jenvman.2015.07.043

Wauchope, R.D., Yeh, S., Linders, J.B.H.J., Kloskowski, R., Tanaka, K., Rubin, B., Katayama, A., Kördel, W., Gerstl, Z., Lane, M., Unsworth, J.B., 2002. Pesticide soil sorption parameters: theory, measurement, uses, limitations and reliability. Pest Manag Sci 58, 419–445. https://doi.org/10.1002/PS.489

Webb, K., Bristow, T., Sargent, M., 2004. Methodology for Accurate Mass Measurement of Small Molecules Best Practice Guide.

Wegst-Uhrich, S.R., Navarro, D.A.G., Zimmerman, L., Aga, D.S., 2014. Assessing antibiotic sorption in soil: A literature review and new case studies on sulfonamides and macrolides. Chem Cent J 8, 1–12. https://doi.org/10.1186/1752-153X-8-5

Wilkinson, J., Boxall, A., Al-khazrajy, O.S.A., Wilkinson, J.L., Boxall, A.B.A., Kolpin, D.W., Leung, K.M.Y., Lai, R.W.S., Wong, D., Ntchantcho, R., Pizarro, J., Ifo, S.A., Wilson, P., Mart, J., Otamonga, J., Pot, J., Udikovic-kolic, N., Milakovic, M., Fatta-kassinos, D., Echeverr, S., Garric, J., Chaumot, A., Gibba, P., Kunchulia, I., Seidensticker, S., Lyberatos, G., 2022. Pharmaceutical pollution of the world's rivers. https://doi.org/10.1073/pnas.2113947119/-/DCSupplemental.Published

Williams, M., Martin, S., Kookana, R.S., 2015a. Sorption and plant uptake of pharmaceuticals from an artificially contaminated soil amended with biochars. Plant and Soil 2015 395:1 395, 75–86. https://doi.org/10.1007/S11104-015-2421-9

Williams, M., Martín, S., Kookana, R.S., 2015b. Sorption and plant uptake of Pharmaceuticals from an artificially contaminated soil amended with biochars Author (s): Mike Williams , Sheridan Martin and Rai S . Kookana Published by : Springer Stable URL : https://www.jstor.org/stable/43872461 Sorption 395, 75–86.

Wood, T.P., Du Preez, C., Steenkamp, A., Duvenage, C., Rohwer, E.R., 2017. Database-driven screening of South African surface water and the targeted detection of pharmaceuticals using liquid chromatography - High resolution mass spectrometry. Environmental Pollution 230, 453–462. https://doi.org/10.1016/j.envpol.2017.06.043

Wu, X., Conkle, J.L., Gan, J., 2012. Multi-residue determination of pharmaceutical and personal care products in vegetables. J Chromatogr A 1254, 78–86. https://doi.org/10.1016/j.chroma.2012.07.041

Wu, X., Dodgen, L.K., Conkle, J.L., Gan, J., 2015. Plant uptake of pharmaceutical and personal care products from recycled water and biosolids: a review. Science of The Total Environment 536, 655–666. https://doi.org/10.1016/J.SCITOTENV.2015.07.129

Wu, X., Fu, Q., Gan, J., 2016. Metabolism of pharmaceutical and personal care products by carrot cell cultures. Environmental Pollution 211. https://doi.org/10.1016/j.envpol.2015.12.050

Wu, Y., Trejo, H.X., Chen, G., Li, S., 2021. Phytoremediation of contaminants of emerging concern from soil with industrial hemp (Cannabis sativa L.): a review. Environment, Development and Sustainability 2021 23:10 23, 14405–14435. https://doi.org/10.1007/S10668-021-01289-0

Wu, Y., Yang, J., Duan, C., Chu, L., Chen, S., Qiao, S., Li, X., Deng, H., 2018. Simultaneous determination of antiretroviral drugs in human hair with liquid chromatography-electrospray ionization-tandem mass spectrometry. J Chromatogr B Analyt Technol Biomed Life Sci 1083, 209–221. https://doi.org/10.1016/j.jchromb.2018.03.021

Xu, Y., Yuan, Z., Ni, B.J., 2017. Biotransformation of acyclovir by an enriched nitrifying culture. Chemosphere 170, 25–32. https://doi.org/10.1016/j.chemosphere.2016.12.014

Yan, C., Nie, M., Yang, Y., Zhou, J., Liu, M., Baalousha, M., Lead, J.R., 2015. Effect of colloids on the occurrence, distribution and photolysis of emerging organic contaminants in wastewaters. J Hazard Mater 299, 241–248. https://doi.org/10.1016/j.jhazmat.2015.06.022

Yang, Y., Fu, J., Peng, H., Hou, L., Liu, M., Zhou, J.L., 2011. Occurrence and phase distribution of selected pharmaceuticals in the Yangtze Estuary and its coastal zone. J Hazard Mater 190, 588–596. https://doi.org/10.1016/j.jhazmat.2011.03.092

Yee, J., Preuss, C. V, 2022. Efavirenz - StatPearls - NCBI Bookshelf [WWW Document]. Naational Library of Medicine. URL https://www.ncbi.nlm.nih.gov/books/NBK542316/ (accessed 6.19.22).

Zhang, C., Barron, L., Sturzenbaum, S., 2021. The transportation, transformation and (bio)accumulation of pharmaceuticals in the terrestrial ecosystem. Science of the Total Environment 781, 146684. https://doi.org/10.1016/j.scitotenv.2021.146684

Zhang, D.Q., Hua, T., Gersberg, R.M., Zhu, J., Ng, W.J., Tan, S.K., 2012. Fate of diclofenac in wetland mesocosms planted with Scirpus validus. Ecol Eng 49, 59–64. https://doi.org/10.1016/j.ecoleng.2012.08.018

Zhou, C., Chen, J., Xie, Q., Wei, X., Zhang, Y. nan, Fu, Z., 2015. Photolysis of three antiviral drugs acyclovir, zidovudine and lamivudine in surface freshwater and seawater. Chemosphere 138, 792–797. https://doi.org/10.1016/j.chemosphere.2015.08.033